

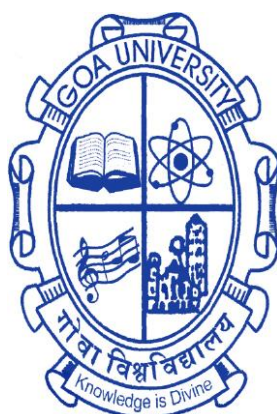
**SYNTHESIS OF SMALL ORGANIC FLUORESCENT
MOLECULES AND USE THEM FOR FLUOROGENIC AND
CHROMOGENIC ION SENSING**

A THESIS SUBMITTED IN PARTIAL FULFILLMENT FOR THE DEGREE OF

DOCTOR OF PHILOSOPHY

IN THE SCHOOL OF CHEMICAL SCIENCES

GOA UNIVERSITY



By

Ms. GEETA ANANT ZALMI

SCHOOL OF CHEMICAL SCIENCES

GOA UNIVERSITY

TALEIGAO PLATEAU, GOA

MARCH 2023

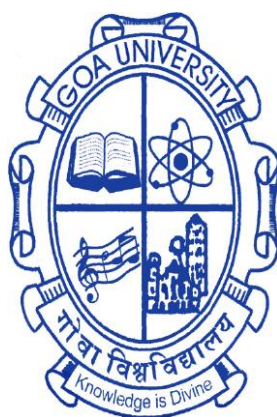
**SYNTHESIS OF SMALL ORGANIC FLUORESCENT
MOLECULES AND USE THEM FOR FLUOROGENIC AND
CHROMOGENIC ION SENSING**

A THESIS SUBMITTED IN PARTIAL FULFILLMENT FOR THE DEGREE OF

DOCTOR OF PHILOSOPHY

IN THE SCHOOL OF CHEMICAL SCIENCES

GOA UNIVERSITY



By

Ms. GEETA ANANT ZALMI

SCHOOL OF CHEMICAL SCIENCES

GOA UNIVERSITY

TALEIGAO PLATEAU, GOA

MARCH 2023

DECLARATION

I, Ms. Geeta Anant Zalmi hereby declare that this thesis represents work which has been carried out by me and that it has not been submitted, either in part or full, to any other University or Institution for the award of any research degree.

Place: Taleigao Plateau

Date:

Ms. Geeta Anant Zalmi
Research Scholar
School of Chemical Sciences
Goa University, Goa

CERTIFICATE

I, hereby declare that the above declaration of the candidate, Ms. Geeta Anant Zalmi is true and the work carried out under my supervision

Prof. S. V. Bhosale
Research guide
School of Chemical Sciences
Goa University, Goa

ACKNOWLEDGEMENT

On the successful completion of my thesis, I have achieved a milestone in my life not only because of my hard work, but the credit goes to all people who made me today what I am. Thus, I feel happy and contented to take this opportunity to write this note of thanks and express my gratitude to all who have helped me through this worthy journey.

This long journey has remained a period of intense learning for me on a scientific as well as personal front. First and foremost, I would like to express my sincere gratitude and special appreciation to my Ph.D. supervisor **Prof. Sheshanath V. Bhosale**, for his constant support and encouragement throughout my research work in to the field of Supramolecular Chemistry. I acknowledge his help and guidance to improve myself as an individual. He is a tremendous mentor and has guided me through his philosophical ideas, expertise and immense knowledge in the field.

I extend my sincere gratitude to my subject experts, **Prof. Vidhyadatta M. Shet. Verenkar** and **Dr. Sandesh T. Bugde**, for their time-to-time assistance and questions during the DRC's and for their valuable suggestions that helped me to progress in my research work.

I express my kind gratitude to **Prof. H. Menon** (Vice-Chancellor, Goa University) and **Prof. V.S. Nadkarni** (Registrar, Goa University), **Prof. Varun Sahni** (Former Vice-Chancellor, Goa University) and **Prof. Y.V. Reddy** (Former Registrar, Goa University), for providing necessary support and permissions to conduct my research work. I am thankful to **Prof. V. M. S. Verenkar** (Dean, SCS, Goa University), **Prof. S. N. Dhuri** (Vice-Dean Academics, SCS, Goa University), **Dr. Bidhan A. Shinkre** (Vice-Dean Research, SCS, Goa University) for providing all the necessary facilities for my research work.

I take this opportunity to thank all my teachers and faculty members of School of Chemical Sciences **Prof. S. G. Tilve**, **Prof. R. N. Shirsat** and **Prof. B. R. Srinivasan** for their encouragement and support. I would also like to thank **Dr. Sandesh Bugde**, **Dr. Mahesh Majik**, **Dr. Rupesh Patre**, **Dr. Vinod Mandrekar**, **Dr. Rohan Kunkalekar**, **Dr. Pranay Morajkar**, **Dr. Prachi Torney**, **Dr. Prajesh Volvoikar**, **Dr. Hari Kadam**, **Dr. Rupesh Kunkalkar**, **Dr. Vishnu Chari**, **Dr. Diptesh Naik**, **Dr. Digamber Porob**, **Dr. Savita Kundaikar**, **Dr. Kanchanmala Deshpande**, **Dr. Shrikant Naik**, **Dr. Kiran Dhavaskar** for their timely motivation, help and constant support. A special thanks goes out to **Dr. Sidhanath V. Bhosale** (CSIR-IICT, Hyderabad) his knowledge and ingenuity is something I will always keep aspiring to carryout

high-level research. I wish to thank my collaborator **Prof. Prabhat K. Singh** for giving wonderful opportunity for writing book chapter.

I am thankful to Goa university for providing the research studentship and The University Grants Commission (UGC), New Delhi for providing me financial support that enabled me to complete my Ph.D. studies successfully.

I take this opportunity to thank our Principal Madam **Prof. Vrinda Borkar, Dr. Bhanudas R. Naik and Dr. Sonia B. Parsekar** for their constant support, motivation and encouragement.

I express my earnest gratitude to **Sandesh B. Dessai** (Librarian, Goa University), **Dr. V. Gopakumar** (Former Librarian, Goa University) and other library staff members, Goa University for providing me with the required learning tools related to my research work. I sincerely appreciate the assistance of Mr. Pravin Mishal and Mr. **Vibhav Marshalkar** in regard to library matters.

I am thankful to all the non-teaching staff, **Mrs. Shital Palkar, Mr. Gaurav Kinlekar, Mr. Mehul Shirodkar, Mr. Yoganand Kholkar, Mr. Kiran Dabolkar, Late Rohidas Naik, Mr. Rayappa Harijan, Mr. Deepak Chari, Mr. Kishor Govekar, Mr. Nikhil Pednekar, Mr. Kirtesh Sawant Mr. Rudraunsh Mahale, Mr. Prajyot Chari, and Mr. Jaykant Nair** for their assistance. I extend my kind gratitude to the administrative staff of Goa University, especially to **Mr. Umakant Sawant, Mr. Kalpesh Dhuri, Mrs. Sneha Haldankar, Mr. Agostinho Rodrigues** for their timely help and cooperation.

I would like to acknowledge **Dr. Chandan Naik, Dr. Rahul Kerkar, Dr. Pratik Asogekar, Dr. Abhijeet Shetgaonkar, Mr. Ketan Mandrekar, Dr. Sarvesh Harmalkar, Dr. Prajyoti Gauns Dessai, Dr. Apurva Narvekar, Dr. Megha Deshpande, Dr. Sudesh Morajkar, Dr. Pooja Bhargao, Dr. Kedar Narvekar, Dr. Vishal Pawar** for their help during my research work. I would like to thank all my fellow research mates **Mr. Akshay Salkar, Dr. Amarja Naik, Ms. Neha Parsekar, Ms. Lima Rodrigues, Ms. Seneca Costa, Ms. Luann D'souza, Ms. Mangala Sawal, Ms. Sanjali Navlekar, Ms. Nikita Harmalkar, Mr. Pritesh Khobrekar, Mr. Leo D'souza, Ms. Siddhi Salgaonkar, Mr. Nitesh Venji, Samantha Da Costa, Sarvesha Shetgaonkar, Gayatri Kotkar** for their kind help during my university days and for making this journey knowledgeable and fun-filled

This success and wonderful journey in to research would not have been completed without the help and support of my brilliant lab mates. I express my gratitude to all my group members

Mr. Dinesh Nadimetla, Ratan W. Jadhav, Mr. Vishal More, Mr. Kerba More, Mr. Vilas Gawade, Mr. Harshad Mirgane, and Ms. Pooja Shreechippa for their timely help and support.

The final and the most awaited acknowledgements to my parents *Mr. Anant Shiva Zalmi* and *Mrs. Anandi Anant Zalmi* for their countless blessings, unconditional love, support and encouragement. Sincere gratitude to my grandfather Late *Mr. Shiva Mukund Zalmi*, you will always be remembered and have a special place in my heart. My sincere gratitude to my uncle *Mr. Mukund Shiva Jalmi, Balaji Shiva Jalmi, Mr. Dinesh Shiva Zalmi* without you, this journey was almost impossible. I thank my grandmother *Radha Shiva Zalmi* my sisters *Ms. Teena Anant Jalmi, Smita Anant Jalmi*, and my beloved brother *Mr. Yogesh Anant Zalmi* for their love, support and blessings. I also thank all my cousins *Vividha M. Zalmi, Manju Sushant Jalmi, Krupali Nitesh Gaunkar, Deepti T. Jalmi, Akshay M. Jalmi, Dishant B. Jalmi, Ishita B. Jalmi, Sani D. Jalmi, Diti D. Jalmi*, for their constant support and love. A special thank you to my best friend *Mr. Manguesh Kanolkar* for extremely building up the moral support. You are world to me and I owe you all everything. You are all inspiration to me, thank you for being part of my life.

Finally, the blessings from the almighty are always needed, thank you "Lord Ganesh" and "Shree Sateri Gavi Zalmi Purush" for surrounding me with good teachers, good friends and finally good human beings every day with kind words and actions.

Ms. Geeta Anant Zalmi

Research Scholar

*Only family makes you who
you are and who you aren't*

Dedicated to my beloved father

Anant S. Zalmi

mother

Anandi A. Zalmi

and brother

Yogesh A. Zalmi

Contents

List of Abbreviations	i
List of Schemes	iii
List of Tables	iii
List of Figures.....	iv
Synopsis.....	xi

Chapter 1	Introduction and Literature Survey		
1.1	General Introduction	5
1.2	Organic fluorescent molecule for sensing of alkali metals (Na ⁺ , K ⁺ , Ca ²⁺ , Li ⁺)	8
1.3	Fluorescent Molecules for Toxic Cation Sensing	9
1.4	Fluorescent Molecules for Anion Sensing	17
1.5	Fluorescent Molecules for Neutral Molecule	20
1.6	Fluorescent Molecules for Temperature sensing, pH sensing And Viscosity Sensing	25
1.7	Conclusion and Future Outlook	36
1.8	References	38
Chapter 2	A Receptor Based on Diphenylaniline Donor Connected with Difuran and Pyridine as Acceptors: Synthesis, Crystal Structure and Selective detection of Iron (Fe³⁺) ion.	49
2.1	Introduction	50
2.2	Experimental details	53
2.2.1.	Materials and Chemicals	53
2.2.2.	Synthetic route for synthesis of 1 4-(2,6-di(furan-2-yl)pyridin-4-yl)- <i>N,N</i> -diphenylaniline (DFPDA) 1	54
2.2.3	Synthesis of (<i>E</i>)-3-(4-(diphenylamino)phenyl)-1-(furan-2-yl)prop-2-en-1-one 4	54
2.2.4	Synthesis of 1-(2-(furan-2-yl)-2-oxoethyl)pyridin-1-ium 5	55
2.2.5	Synthesis of 4-(2,6-di(furan-2-yl) pyridin-4-yl)- <i>N,N</i> -diphenylaniline (DFPDA) 1	55
2.3	Characterization	56
2.3.1	¹ H NMR spectra of (<i>E</i>)-3-(4-(diphenylamino)phenyl)-1-(furan-2-yl)prop-2-en-1-one 4	56
2.3.2	¹³ C NMR spectra of (<i>E</i>)-3-(4-(diphenylamino)phenyl)-1-(furan-2-yl)prop-2-en-1-one 4	57

2.3.3	¹ H NMR spectra of 4-(2,6-di(furan-2-yl)pyridin-4-yl)- <i>N,N</i> -diphenylaniline (DFPDA 1)	58
2.3.4	ESI- mass analysis of 4-(2,6-di(furan-2-yl)pyridin-4-yl)- <i>N,N</i> -diphenylaniline (DFPDA 1)	58
2.4	Crystal study	59
2.4.1	Crystal study of intermediate (E)-3-(4-(diphenylamino)phenyl)-1-(furan-2-yl)prop-2-en-1-one 4	60
2.4.2	Crystal study of the compound 4-(2,6-di(furan-2-yl)pyridin-4-yl)- <i>N,N</i> -diphenylaniline DFPDA 1	61
2.5	Results and Discussion	64
2.5.1	Absorption and Emission study in different solvent	64
2.5.2	Sensing performance of receptor DFPDA 1	66
2.5.3	UV-Vis absorption study	67
2.5.4	Fluorescence emission study	67
2.5.5	Stoichiometry analysis and Binding constant	68
2.5.6	Reversibility and reusability	69
2.5.7	Competitive study	70
2.6	Conclusion	71
2.7	References	72
Chapter 3	Synthesis, characterization and application of dipyridine based fluorescent sensing a platform for recognition of Cu²⁺ ion in aqueous medium.	76
3.1	Introduction	77
3.2	Experimental	80
3.2.1	Materials and Chemicals	80
3.2.2	Synthetic route for synthesis of (<i>N,N</i> -diphenyl-4-(6-(thiophen-2-yl)-[2,2'-bipyridin]-4-yl)aniline DTBPA 1	81

3.2.3	Synthesis of (<i>E</i>)-3-(4-(diphenylamino)phenyl)-1-(thiophene-2-yl)prop-2-en-1-one (4)	81
3.2.4	Synthesis of 1-(2-(furan-2-yl)-2-oxoethyl)pyridin-1-ium (5)	82
3.2.5	Synthesis of probe (<i>N,N</i> -diphenyl-4-(6-(thiophen-2-yl)-[2,2'-bipyridin]-4-yl)aniline DTBPA 1)	82
3.3	Characterization	83
3.3.1	¹ H NMR spectra of 4 (<i>E</i>)-3-(4-(diphenylamino)phenyl)-1-(thiophen-2-yl)prop-2-en-1-one	83
3.3.2	¹³ C NMR spectra of 4 (<i>E</i>)-3-(4-(diphenylamino)phenyl)-1-(thiophen-2-yl)prop-2-en-1-one	84
3.3.3	¹ H NMR spectra of DTBPA 1 (<i>N,N</i> -diphenyl-4-(6-(thiophen-2-yl)-[2,2'-bipyridin]-4-yl)aniline)	84
3.3.4	¹³ C NMR spectra of DTBPA 1 (<i>N,N</i> -diphenyl-4-(6-(thiophen-2-yl)-[2,2'-bipyridin]-4-yl)aniline)	85
3.3.5	ESI- mass for DTBPA 1 (<i>N,N</i> -diphenyl-4-(6-(thiophen-2-yl)-[2,2'-bipyridin]-4-yl)aniline)	85
3.4	Crystal Study	86
3.4.1	Preparation of Crystal (<i>N,N</i> -diphenyl-4-(6-thiophene-2-yl)-[2,2'-bipyridin]-4-yl)aniline DTBPA 1)	86
3.5	Results and Discussion	88
3.5.1	Solvent study	88
3.5.2	Solvatochromic study	89
3.5.3	Sensing performance	89
3.5.4	UV-Vis absorption study	91
3.5.5	Fluorescence emission study	92
3.5.6	Competitive Study	94

3.5.7	Stoichiometry and Binding constant	95
3.5.8	Binding Mechanism	95
3.7	Density Functional Theory Study (DFT)	97
3.8	Practical Application	99
3.8.1	Water Analysis	99
3.9	Conclusion	100
3.10	References	101
Chapter 4	Aggregation induced emission-based material for selective and sensitive recognition of cyanide anion in solution and biological assay	106
4.1	Introduction	107
4.2	Experimental	109
4.2.1	Chemicals and Methods	109
4.2.2	Schematic pathway for synthesis of probe 1	110
4.2.3	Synthesis of 1-(4-bromophenyl)-1,2,2-triphenylethene (4)	110
4.2.4	Synthesis of 5-(4-(1,2,2-triphenylvinyl)phenyl)thiophene-2-carbaldehyde (6)	111
4.2.5	Synthesis of ethyl 2-cyano-3-(5-(4-(1,2,2-triphenylvinyl)phenyl)thiophen-2-yl)acrylate (1)	112
4.3	Characterization	113
4.3.1	¹ H NMR spectrum of 5-(4-(1,2,2-triphenylvinyl)phenyl) thiophene-2-carbaldehyde (3)	113
4.3.2	¹ H NMR ethyl-2-cyano-3-(5-(4-(1,2,2-triphenylvinyl)phenyl)thiophen-2-yl)acrylate (1)	114
4.3.3	¹³ C NMR spectrum ethyl-2-cyano-3-(5-(4-(1,2,2-triphenylvinyl)phenyl)thiophen-2-yl)acrylate (1).	115
4.3.4	¹³ C DEPT spectrum ethyl-2-cyano-3-(5-(4-(1,2,2-triphenylvinyl)phenyl)thiophen-2-yl)acrylate (1).	116

4.3.5	ESI mass of ethyl-2-cyano-3-(5-(4-(1,2,2-triphenylvinyl)phenyl)thiophen-2-yl)acrylate (1)	116
4.3.6	¹³ C NMR spectral changes observed with the addition of CN ⁻ anion to probe 1 in CDCl ₃ without addition of CN ⁻ and without addition of CN ⁻	117
4.4	Results and Discussion	117
4.4.1	Mechanochromic study	117
4.4.2	Solvent study	120
4.4.3	Aggregation induced emission (AIE) study	121
4.4.4	Sensing performance	124
4.4.5	UV-Vis study	125
4.4.6	Fluorescence emission study	126
4.4.7	Stoichiometry and binding constant	126
4.4.8	Limit of detection	128
4.4.9	The mechanism of CN ⁻ detection by ¹ H NMR Study	129
4.5	Density Functional Theoretical Calculations (DFT)	130
4.6	Competitive Study	133
4.7	Practical applications	134
4.7.1	Test Strip sensing	134
4.7.2	Application in cell imaging cell toxicity study	135
4.7.3	Food Assay	136
4.8	Comparison table for various fluorescent molecule for CN ⁻ sensing	143
4.9	Conclusion	144
4.10	References	145

Chapter 5	Synthesis of 1-(p-tolyl)-4,9-dihydro-3Hpyrido[3,4-<i>b</i>]indole an organic fluorescent receptor for selective sensing of Fluoride and Cyanide anion	152
5.1	Introduction	153
5.2	Experimental	155
	5.2.1 Methods and Materials	155
	5.2.2 Synthetic Route for synthesis of 1-(p-tolyl)-4,9-dihydro-3Hpyrido[3,4- <i>b</i>]indole	155
5.3	Characterization	156
	5.3.1 ¹ H NMR spectra of receptor 1 1-(p-tolyl)-4,9-dihydro-3Hpyrido[3,4- <i>b</i>]indole	156
	5.3.2 ¹³ C NMR spectra of receptor 1 1-(p-tolyl)-4,9-dihydro-3Hpyrido[3,4- <i>b</i>]indole	157
	5.3.3 HRMS positive mode for receptor 1 1-(p-tolyl)-4,9-dihydro-3Hpyrido[3,4- <i>b</i>]indole	157
5.4	Results and Discussion	158
	5.4.1 Solvent study	158
	5.4.2 Sensing Performance	159
	5.4.3 Absorption and fluorescence emission with various anions	160
	5.4.4 Absorption and Fluorescence titration study of CN ⁻ anion	161
	5.4.5 Absorption and fluorescence titration study for F ⁻ anion	164
5.5	Limit of Detection for CN ⁻ anion	165
5.6	Limit of detection for F ⁻ anion	165
5.7	Conclusion	165
5.8	References	166
Chapter 6	Conclusion and Future perspective	169

6.1	Conclusion	169
Appendices		174
Appendix I:	List of Publications	174
Appendix II:	List of Conferences/ Symposia/ Workshop	176

List of Abbreviation

AIE	Aggregation induced Emission
AIEgens	Aggregation-induced emission luminogens
PET	Photoinduced Electron Transfer
CHEF	Chelation induced Enhancement Fluorescence
ICT	Intramolecular charge transfer
FRET	Fluorescence resonance electron transfer
ACQ	Aggregation caused Quenching
PL	Photoluminescence
UV-Vis	UV-Visible
ESI-MS	Electron spray ionization mass spectroscopy
CV	Cyclic voltammetry
DLS	Dynamic light scattering
SEM	Scanning electron microscopy
TBA	Tetrabutylammonium salt
TD-DFT	Time-dependent density functional theory
ΔE_{act}	Activation energy
μM	Micromolar
mM	Milimolar
nM	Nanomolar
eV	Electron volt
nm	Nanometer
LOD	Limit of Detection
MOF	Metal–organic frameworks

FMO	Frontier Molecular Orbital
HOMO	Highest occupied molecular orbital
LUMO	Lowest unoccupied molecular orbital
Pd(PPh ₃) ₄	Palladium-tetrakis(triphenylphosphine)
TFA	Trifluoroacetic acid
THF	Tetrahydrofuran
TEA	Triethylamine
dsDNA	Double-stranded deoxyribonucleic acid
ssDNA	Single-stranded deoxyribonucleic acid
TPE	Tetraphenylethylene
NDI	Naphthalenediimides
DTBPA	<i>N,N</i> -diphenyl-4-(6-(thiophen-2-yl)-[2,2'-bipyridin]-4-yl)aniline
DFPDA	4-(2,6-di(furan-2-yl)pyridin-4-yl)- <i>N,N</i> -diphenylaniline
AcOH	Acetic acid
DMSO	Dimethyl sulfoxide
ACN	Acetonitrile
MeOH	Methanol
DCM	Dichloromethane
CHCl ₃	Choloform (trichloromethane)
BODIPY	Boron-Dipyrromethene
IR	Infra-red
NMR	Nuclear Magnetic Resonance
DEPT	Distortionless Enhancement by Polarization Transfer
TMS	Tetramethylsilane

TEACN	Tetraethylammonium Cyanide
DFT	Density Functional Theory
WHO	World Health Organization
EPA	Environmental Protection Agency
TLC	Thin Layer Chromatography
FITC	Fluorescein isothiocyanate
MTT	3-[4,5-dimethylthiazol-2-yl]-2,5 diphenyl tetrazolium bromide
HPS	Hexaphenylsilole
n-BuLi	n-butyllithium

List of Schemes

Chapter 2	Scheme 2.1. Schematic pathway for synthesis of receptor 1 4- (2,6-di(furan-2-yl)pyridin-4-yl)- <i>N,N</i> -diphenylaniline (DFPDA) 1	54
Chapter 3	Scheme 3.1. Synthetic route of receptor (<i>N,N</i> -diphenyl-4-(6- (thiophen-2-yl)-[2,2'-bipyridin]-4-yl)aniline (DTBPA) 1	81
Chapter 4	Scheme 4.1. Schematic pathway for synthesis of 1	110
	Scheme 4.2. Schematic pathway for synthesis of 1-(4- bromophenyl)-1,2,2-triphenylethene (4)	110
	Scheme 4.3. Schematic pathway for synthesis of 5-(4-(1,2,2- triphenylvinyl)phenyl)thiophene-2-carbaldehyde (6)	111
	Scheme 4.4. Schematic pathway synthesis of ethyl 2-cyano-3- (5-(4-(1,2,2-triphenylvinyl)phenyl)thiophen-2-yl)acrylate (1)	112
Chapter 5	Scheme 5.1. Schematic pathway for synthesis of compound 1 1-(<i>p</i> -tolyl)-4,9-dihydro-3 <i>H</i> pyrido[3,4- <i>b</i>]indole.	155

List of Tables

Chapter 2	Table 2.1. Crystal data and details of refinements for 4	60
	Table 2.2. Crystal data and details of refinements for DFPDA 1	61
Chapter 3	Table 3. 1. Crystal data and details of refinements for probe 1	86
	Table 3. 2: Conformational analysis of DTBPA 1 + Cu ²⁺	98
	Table 3. 3. Results represents the real sample analysis for probe DTBPA 1	100
Chapter 4	Table 4.1. Calculated values for HOMO and LUMO with and without addition of CN ⁻	132
	Table 4.2: Calculated TD-DFT excitation properties of probe 1 and 1:CN⁻	137
	Table 4.3. Frontier molecular orbitals of probe 1 and 1+CN⁻ - with energy in eV	138

Table 4.4. Comparison of CN ⁻ sensing with literature.	143
--	-------	-----

List of Figures

Chapter 1	Figure 1.1. Components of fluorescent chemosensor.	3
	Figure 1.2. Common structures of crown ethers.	7
	Figure 1.3. Schematic pathway for binding of K ⁺ ion by using fluorescent BODIPY receptor with crown ether	7
	Figure 1.4. NDI core substituted aza-crown ether for sensing of Ca ²⁺ , K ⁺ , and Na ⁺ ion.	8
	Figure 1.5. (a) Organic fluorescent crown ether for Li ⁺ and Ca ²⁺ sensing (b) absorption spectra with addition of Li ⁺ (c) emission spectral changes with Li ⁺ addition.	8
	Figure 1.6. Carbazole based fluorescent molecule for arsenic detection.	11
	Figure 1.7. Schematic pathway for synthesis of TPE-Cy receptor for As ³⁺ sensing.	11
	Figure 1.8. Representative chemical structures of the fluorescent material for Cd ²⁺ sensing.	12
	Figure 1.9. Conjugated polymer for sensing of Pd ²⁺	13
	Figure 1.10. TPE based phosphate monoester for sensing of Pb ²⁺	14
	Figure 1.11. Schematic illustration for coordination of Hg ²⁺ to TPE-Py.	15
	Figure 1.12. Schematic illustration for sensing mechanism by deprotection upon addition of Hg ²⁺	16
	Figure 1.13. Chemical structures of barbituric acid derivatives namely M1 , M2 , M3 with triphenylamine, carbazole, anthracene, respectively used for mercury sensing.	17
	Figure 1.14. Structure of fluorescent molecules for sensing of F ⁻ ion.	19
	Figure 1.15. BODIPY fluorescent probe for F ⁻ and CN ⁻	19

ion sensing.		
Figure 1.16. Structure of the Naphthaliimide functionalized imidazole.	20
Figure 1.17. Classification of carbohydrates.	22
Figure 1.18. Schematic representation for binding interaction with glucose.	23
Figure 1.19. Derivatives of guanidine and boronic acid substituted anthracene derivative.	24
Figure 1.20. The picture represents the Boron-Doped Graphene Quantum Dots (BGQDs). (b) shows the aggregation induced emission interaction between the BGQDs and glucose resulting into enhancement in fluorescence.	25
Figure 1.21. Schematic illustration of polymeric elastic ELP-40 derivatized with tetraphenylethylene molecule for temperature sensing.	27
Figure 1.22. A) A diagrammatic representation of the self-assembly and fabrication for TRP NPs. B) A photoluminescence emission spectrum of the TRF NPs at temperature range from 25 °C to 65 °C. C) A plot represents ratio reversibility by successive heating and cooling of TRF NPs.	28
Figure 1.23. Schematic illustration showing mechanism of pH change response of TPE-Cy . (A) A confocal images of TPE-Cy on Hela cells at 405 nm and B) confocal image at 488 nm C) merged confocal image of panel A and B, D) a confocal image merged from field image the (bright C). (E) represents the emission spectra for TPE-Cy at various pH and buffer ranges in the presence of 1,2-dioleoyl-glycero-3-phosphocholine (DOPC). (F) A plot PL intensity versus pH of solution at 489 and 615nm respectively.	30
Figure 1.24. A) Absorption spectra of the compound at three different pH. (Inset represents the protonation and	31

	deprotonation sensing mechanism for compound 3 at 50µmol/L and B) The representation of confocal images at different pH buffers on incubation of HeLa cells at 50µmol/L compound.	
	Figure 1.25. Mechanism of protonation-deprotonation for Py-TPE receptor (1 &2). B) Photographs under UV light illumination ($\lambda_{ex}=365nm$) of receptor Py-TPE (1 and 2) (0.5µM) in presence and absence of TFA(2µM) at room temperature in different solvent system. 32
	Figure 1.26. Emission spectra recorded upon addition of TFA and TEA in 1 (1×10^{-5} M) in DMF ($\lambda_{ex} = 365$ nm). B) A plot of reversibility study performed at 534 nm (fluorescence intensity vs. number repeated cycles) upon addition of TFA and TEA. c) Cell imaging application imaged under Confocal fluorescence microscope of Py-TPE receptor with($5\mu gmL^{-1}$) for PC-3 cells treated for 2 hours at different pH condition. 33
	Figure 1.27. Structure of the carbazole styryl fluorescent molecular rotors. 34
	Figure 1.28. Schematic pathway for viscosity sensing by using TPAEQ 35
	Figure 1.29. The chemical structure if different AIE active styryl quinones. 36
Chapter 2		
	Figure 2.1. Organic fluorescent molecules for sensing of Fe^{3+} metal ion labelled as T1 , T2 and T3 51
	Figure 2.2. Structure of the synthesized organic charge transfer molecules TPETPy and TPE2TPy 52
	Figure 2.3. Represents 1H NMR spectra of (<i>E</i>)-3-(4-(diphenylamino)phenyl)-1-(furan-2-yl)prop-2-en-1-one 4 56
	Figure 2.4. ^{13}C NMR spectra of the intermediate (<i>E</i>)-3-(4-(diphenylamino)phenyl)-1-(furan-2-yl)prop-2-en-1-one 4 57
	Figure 2.5. 1H NMR spectra of 4-(2,6-di(furan-2- 57

yl)pyridin-4-yl)- <i>N,N</i> -diphenylaniline (DFPDA) 1	
Figure 2.6. ¹³ C NMR spectra of 4-(2,6-di(furan-2-yl)pyridin-4-yl)- <i>N,N</i> -diphenylaniline (DFPDA) 1 58
Figure 2.7. ESI- mass analysis of 4-(2,6-di(furan-2-yl)pyridin-4-yl)- <i>N,N</i> -diphenylaniline (DFPDA) 1 58
Figure 2.8. Crystal structure of the (<i>E</i>)-3-(4-(diphenylamino)phenyl)-1-(furan-2-yl)prop-2-en-1-one 4 62
Figure 2.9. Crystal structure of 4-(2,6-di(furan-2-yl)pyridin-4-yl)- <i>N,N</i> -diphenylaniline (DFPDA) 1 63
Figure 2. 10. Packing in (<i>E</i>)-3-(4-(diphenylamino)phenyl)-1-(furan-2-yl)prop-2-en-1-one (4) due to C-H- π intermolecular H-bonding interactions separated by distance 2.718 Å. 63
Figure 2. 11. Packing in 4-(2,6-di(furan-2-yl)pyridin-4-yl)- <i>N,N</i> -diphenylaniline (DFPDA) 1 due to C-H- π intermolecular and H-bonding interactions separated by distance 3.383 Å leading to a helical structure. 64
Figure 2.12. Solvent study performed for the (DFPDA) 1 (a) UV-Vis plot recorded in various organic solvents such as DMSO, acetonitrile (ACN), Chloroform (CHCl ₃), H ₂ O, hexane, methanol (MeOH), THF. (b) The emission spectrum recorded for the receptor 1 in organic solvents. 65
Figure 2. 13. (a) Image shows naked eye detection of Fe ³⁺ metal ion in presence over other cations such as Cd ²⁺ , Fe ³⁺ , Cu ²⁺ , K ⁺ , Ba ²⁺ , Co ²⁺ , Mn ²⁺ , Ni ²⁺ , Hg ²⁺ , Al ³⁺ , Pb ²⁺ , Zn ²⁺ , Ca ²⁺ , Fe ²⁺ . (b) image shows the fluorescence colour change with the addition of Fe ³⁺ over other cations 66
Figure 2. 14. (a) UV-Vis absorption spectra of 1 (2.5×10 ⁻⁵ M) in presence of different cations and (b) absorption spectra with incremental addition of Fe ³⁺ (0-2.5equiv.), 1.37×10 ⁻⁵ M) in DMSO 67
Figure 2. 15. (a) Fluorescence emission spectra of 1 (2.5×10 ⁻⁵ M) in presence of different cations (2.5×10 ⁻³ M) 68

	and ($\lambda_{\text{ex}} = 350 \text{ nm}$, excitation and emission slit = 5nm) and	
	(b) Emission spectra with the incremental addition of Fe^{3+} from (0-2.5 equiv. of $1.37 \times 10^{-5} \text{ M}$) in DMSO ($\lambda_{\text{ex}} = 350 \text{ nm}$, excitation slit = 10 nm, emission slit = 2.5nm)	
	Figure 2.16. (a) The plot of Job's plot represents stoichiometry of the complex to be DFPDA 1: Fe^{3+} (2:1) and 69
	(b) Benesi–Hildebrand plot of probe DFPDA 1 with Fe^{3+} ion in DMSO with the binding constant observed to be $3.75 \times 10^{-8} \text{ M}$.	
	Figure 2. 17. (a) The plot representing fluorescence change intensity for the DFPDA 1 as depicted (blank 1, 2 vial addition of Fe^{3+} , 3 vial addition of NaOH to the solution containing Fe^{3+}), 70
	(b) The fluorescence color change observed at 365nm upon addition of Fe^{3+} and NaOH (inset photograph). (c) represents the number of reversible cycles with addition of Fe^{3+} ion and NaOH to the solution of the DFPDA 1.	
	Figure 2. 18. The graph represents competitive reaction between receptor DFPDA 1 and Fe^{3+} (1 equiv.) with DFPDA 1 in presence of interfering cations (1equiv.) at 357nm. Blue bar represents DFPDA 1 with other cation and red bar represents DFPDA 1+ other cations + Fe^{3+} ion 71
Chapter 3	Figure 3.1. Structures of organic fluorescent molecule for sensing of Cu^{2+} ions. 79
	Figure 3. 2. ^1H NMR spectra of 4 (<i>E</i>)-3-(4-(diphenylamino)phenyl)-1-(thiophen-2-yl)prop-2-en-1-one. 83
	Figure 3. 3. ^{13}C NMR spectra of 4 (<i>E</i>)-3-(4-(diphenylamino)phenyl)-1-(thiophen-2-yl)prop-2-en-1-one 84
	Figure 3. 4. ^1H NMR spectra of DTBPA 1 (<i>N,N</i> -diphenyl-4-(6-(thiophen-2-yl)-[2,2'-bipyridin]-4-yl)aniline 84
	Figure 3. 5. ^{13}C NMR spectra of DTBPA 1 (<i>N,N</i> -diphenyl-4-(6-(thiophen-2-yl)-[2,2'-bipyridin]-4-yl)aniline. 85
	Figure 3. 6. ESI- mass for DTBPA 1 (<i>N,N</i> -diphenyl-4-(6-(thiophen-2-yl)-[2,2'-bipyridin]-4-yl)aniline 85

	Figure 3. 7. Crystal structure of DTBPA 1 compound.	87
	Figure 3. 8. (a) Absorption spectra recorded for DTBPA 1 receptor in different solvents to study the solvatochromic effect (b) The emission plot for DTBPA 1 receptor in different solvents	90
	Figure 3. 9. The sensing performance for DTBPA 1 over different cations representing the quenching of fluorescence upon addition of Cu^{2+} ion	91
	Figure 3. 10. (a) Plot representing the absorption change upon addition of different metal ions Cu^{2+} , Fe^{3+} , Fe^{2+} , Hg^{2+} , Pb^{2+} , Ni^{2+} , Zn^{2+} , Mn^{2+} , Co^{2+} , Al^{3+} , Ca^{2+} , Ba^{2+} , Cd^{2+} , K^{+} . (b) UV-Vis absorption titration for the DTBPA 1 with incremental addition (0 – 2 equivalent)	92
	Figure 3. 11. (a) Plot representing the emission intensity upon addition of different metal ions Cu^{2+} , Fe^{3+} , Fe^{2+} , Hg^{2+} , Pb^{2+} , Ni^{2+} , Zn^{2+} , Mn^{2+} , Co^{2+} , Al^{3+} , Ca^{2+} , Ba^{2+} , Cd^{2+} , K^{+} . (b) Fluorescence titration for the DTBPA 1 with incremental addition (0 – 2 equivalent)	93
	Figure 3. 12. Competitive study performed for the DTBPA 1 in presence of cations (1+M represents different cations added to DTBPA 1 while 1+M+ Cu^{2+} indicates the different cation with addition of Cu^{2+} ion.	95
	Figure 3. 13. (a) Jobs Plot for the DTBPA 1 with copper complexation in 2:1 ratio. (b) Benesi Hildebrand plot for DTBPA 1	96
	Figure 3. 14. Mechanistic pathway for binding of Cu^{2+} with DTBPA 1 receptor	96
	Figure 3. 15. DFT study performed for DTBPA 1 probe on Gaussian 16 <i>ab initio</i> /DFT quantum chemical simulation.	97
Chapter 4	Figure 4. 1. ^1H NMR spectrum of 5-(4-(1,2,2-triphenylvinyl)phenyl) thiophene-2-carbaldehyde (3)	113
	Figure 4.2. ^1H NMR spectrum for ethyl-2-cyano-3-(5-(4-(1,2,2-triphenylvinyl)phenyl)thiophen-2-yl)acrylate (1)	114

Figure 4.3. ^{13}C NMR spectrum ethyl-2-cyano-3-(5-(4-(1,2,2-triphenylvinyl)phenyl)thiophen-2-yl)acrylate (1)	115
Figure 4.4. ^{13}C DEPT spectrum ethyl-2-cyano-3-(5-(4-(1,2,2-triphenylvinyl)phenyl)thiophen-2-yl)acrylate (1)	116
Figure 4.5. ESI mass of ethyl-2-cyano-3-(5-(4-(1,2,2-triphenylvinyl)phenyl)thiophen-2-yl)acrylate (1)	116
Figure 4.6. ^{13}C NMR spectral changes observed with the addition of CN^- anion to probe 1 in CDCl_3 (a) without addition of CN^- (b) without addition of CN^-	117
Figure 4.7 (a). Photograph representing the color changes upon grinding fuming and heating. b) represents the fluorescence emission recorded for compound upon grinding fuming and heating.	119
Figure 4.8. Solvent study performed for the compound 1 in ACN, THF and DMSO (a) Absorption spectra (b) Emission spectra	121
Figure 4.9. Representative examples for AIE and ACQ (a) and (b); ACQ phenomenon) Hexaphenylsilole an example of AIE phenomenon.	23
Figure 4.10. Aggregation induced emission study performed for the compound 1 in which (a) represents formation of aggregate as the water fraction is increased from 0 to 99%. (b) the solution after addition were place under UV light illumination.	124
Figure 4.11. (a) Photograph of solution containing compound 1 with addition of various anions the color change was observed for solution with the addition of cyanide. (b) The fluorescence color change from yellow resulting in to quenching of fluorescence with the addition of CN^-	125
Figure 4.12. (a) UV-Vis absorption spectra recorded with the addition of various anions (b) UV-Vis absorption titration performed with the incremental addition of CN^- anion (0-4 equiv.)	127

Figure 4.13. (a) Plot representing the quenching of fluorescence with the addition of CN^- in presence over other anions (b) Emission titration performed with incremental addition of CN^- (0-4equiv.)	128
Figure. 4.14. (a) the Jobs plot representing 1:1 stoichiometry (b) Benesi-Hildebrand plot for receptor 1 with CN^-	129
Figure 4.15. Emission spectra with incremental addition of CN^- (0-4 equiv.) with limit of detection plot (right)	129
Figure 4.16. ^1H NMR study performed for the probe 1 (a) without addition of CN^- (labelled as \mathbf{H}_1) (b) represents the chemical shift with addition of CN^- (labelled as \mathbf{H}_2).	130
Figure 4.17. Represents the optimized geometries of the structure without and with presence of CN^-	131
Figure 4.18. Cyclic voltammogram in presence and absence of CN^- added to probe 1	132
Figure 4.19. Competitive study performed for the probe with addition of various anion along with CN^- anion.	133
Figure 4.20. Test strip representing the color change with the addition of various anions observed under (a) day light (b) under UV light at 365nm	134
Figure 4.21. MTT Assay performed for probe 1 to determine the toxicity.	135
Figure 4.22. Cell imaging study performed for probe 1. (a) HeLa Cells focussed under bright field (b) no fluorescence observed in HeLa cells without incubation with probe 1 under FITC filter. (c) image depicts the HeLa cells incubated with probe 1 under bright field (d) image depicts the HeLa cells incubated with probe 1 under showing green fluorescence in FITC filter. (e) image capture under bright field with addition of CN^- when cells incubated with probe 1. (f) HeLa Cells placed under FITC filter with addition of CN^-	136

	Figure 4.23. The receptor 1 was utilized for detection of CN^- in food analysis.	137
	Figure 4.24. Theoretical UV-vis absorption spectra of probe 1	142
	Figure 4.25. Theoretical UV-vis absorption spectra of probe 1 : CN^-	142
Chapter 5	Figure 5.1. ^1H NMR spectra of receptor 1 1-(p-tolyl)-4,9-dihydro-3 <i>H</i> pyrido[3,4- <i>b</i>]indole.	156
	Figure 5.2. ^{13}C NMR spectra of receptor 1 1-(p-tolyl)-4,9-dihydro-3 <i>H</i> pyrido[3,4- <i>b</i>]indole.	157
	Figure 5.3. HRMS positive mode for receptor 1 1-(p-tolyl)-4,9-dihydro-3 <i>H</i> pyrido[3,4- <i>b</i>]indole.	157
	Figure 5.4. Solvatochromism study for receptor 1 in various solvents (a) Absorption spectra (b) Emission spectra.	159
	Figure 5.5. Photograph exhibiting fluorescence color change with addition of Fluoride anion in presence over other anions such as (F^- , Cl^- , NO_3^- , Br^- , I^- , HSO_4^- , HPO_4^{2-} , OAc^- , CN^-) in solution containing receptor 1 1-(p-tolyl)-4,9-dihydro-3 <i>H</i> pyrido[3,4- <i>b</i>]indole.	160
	Figure 5.6. (a) The plot represents the absorption spectra in presence of various anions such as F^- , Cl^- , NO_3^- , Br^- , I^- , HSO_4^- , HPO_4^{2-} , OAc^- , CN^- . (b) Absorption titration performed for probe 1 with addition of 10 equivalent of Fluoride anion.	162
	Figure 5.7. (a) Emission spectra recorded for the receptor 1 in presence various anions (b) Fluorescence titration performed for receptor 1 in presence of CN^- (0 to 10 equivalent.).	163
	Figure 5.8. (a) Emission spectra recorded for the receptor 1 in presence various anions (b) fluorescence titration performed for receptor 1 in presence of fluoride (0 to 2 equivalent).	164

Synopsis

SYNTHESIS OF SMALL ORGANIC FLUORESCENT MOLECULES AND USE THEM FOR FLUOROGENIC AND CHROMOGENIC ION SENSING

ABSTRACT:

Organic fluorescent molecules have shown tremendous application in various fields such as pharmacology, environmental, biology and physiology. The fluorescent chemo sensor was developed in 1970 and 1980s and over the last few decades the field has grown and thousands of research groups all around the world working on the fluorescent molecules and have developed new modified strategies for various application especially in sensing. Fluorescent chemo sensor approach has gained lot of attention in sensing of various analytes such as cations, anions, and neutral molecules. Chemosensors are molecular device/structure (organic or inorganic) that are used for sensing of particular analyte by producing detectable signal or color change in the solution. Herein we have developed different organic fluorescent molecules with aggregation induced emission property for sensing of various cation and anions. However, the molecules can be also used for detecting various physiological parameters such as temperature, pH and viscosity. The synthesized molecules were successfully characterized by nuclear magnetic resonance (NMR), CHN-Elemental analysis, ESI-Mass spectrometry, UV-Vis Spectroscopy (UV-Vis.), Photoluminescence Spectrometer (PL), Single crystal X-ray Diffraction (SXR). The binding constant was calculated by using Benesi-Hildebrand Plot while stoichiometry was determined by Jobs Plot.

THESIS OBJECTIVES

Objective of my thesis is

1. Synthesis and characterization of small organic fluorescent molecule and use them for sensing of various cations, anions and neutral molecules.
2. Synthesis of diphenyl aniline derivative containing difuran and pyridine as acceptor for sensing of Fe^{3+} metal ion.
3. Synthesis of organic fluorescent molecule diphenyl aniline derivative containing dipyridine and thiophene as acceptor for sensing of Cu^{2+} metal ion.
4. Aggregation induced emission molecule for sensing of cyanide anion.
5. Synthesis of 1-(*p*-tolyl)-4,9-dihydro-3*H*-pyrido[3,4-*b*] indole an organic fluorescent receptor for selective sensing of fluoride anion

Thesis organization: The following thesis entitle on “SYNTHESIS OF SMALL ORGANIC FLUORESCENT MOLECULES FOR FLUOROGENIC AND CHROMOGENIC ION SENSING” is divided into VI chapters

Chapter 1

Introduction and literature review

Chapter 2

A receptor based on diphenylaniline donor connected with difuran and pyridine as acceptors: synthesis, crystal structure and selective detection of iron (Fe^{3+}) ion

Chapter 3

Synthesis, characterization and application of dipyridine based fluorescent sensing a platform for recognition of Cu^{2+} ion in aqueous medium

Chapter 4

Aggregation induced emission-based material for selective and sensitive recognition of cyanide

anion in solution and biological assay

Chapter 5

1-(*p*-tolyl)-4,9-dihydro-3*H*-pyrido[3,4-*b*] indole an Organic Fluorescent Receptor for Selective Sensing of Fluoride and Cyanide anion

Chapter 6. Conclusion and future perspective

Highlights to organized chapters

Chapter 1. INTRODUCTION AND LIETRATURE REVIEW

Fluorescent Chemosensor are the molecular devices which comprises of donor and binding unit connected via spacer group are called as fluorescent chemosensor. In 1867 F. Goppelsroder developed the first fluorescent Chemosensors for determination of Al^{3+} forming the strong chelate with compound morin as shown in **Scheme 1**. Later the field expanded its application in sensing for detection of various ions including several neutral molecules. In 1980 de Silva and Czarnik explored the field of sensing and scope of applicability of the fluorescent molecules in various fields for sensing of biologically and environmentally important analytes.^{1,2} The detection mechanism of several analyte follows different photophysical mechanism such as photoinduced electron transfer (PET)³, Chelation induced enhanced fluorescence (CHEF)⁴, aggregation induced emission (AIE)^{5,6}, intramolecular charge transfer (ICT)^{7,8}.

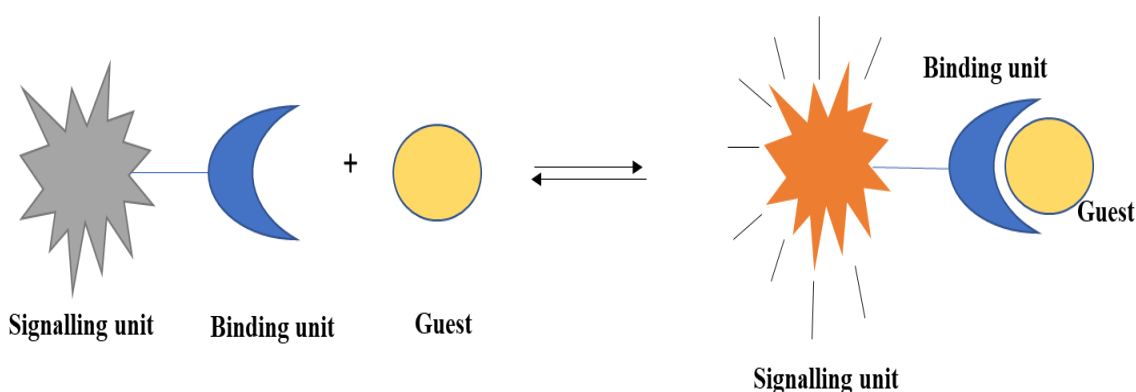
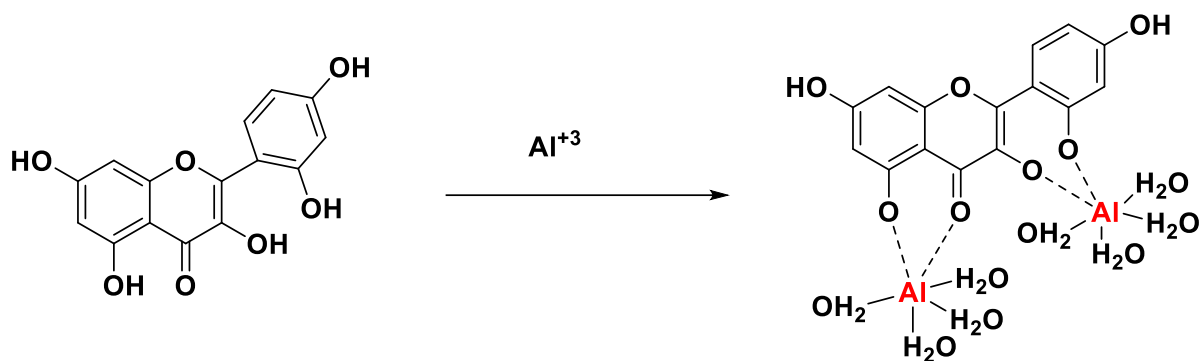


Figure 1. Schematic representation of binding components of fluorescent chemosensor by host-guest interaction.

Fluorescent chemo sensor is not only used in the field of sensing application but are used in other fields such as biology, environmental science, physiology, medical science and forensic science. However now a day this field has shown tremendous application in biological cell imaging. Here in are some examples of fluorescent molecules used for sensing of cations

anions and neutral analyte.⁹⁻¹²



Scheme 1. Schematic representation for the first fluorescent molecule for sensing of Al^{3+} .

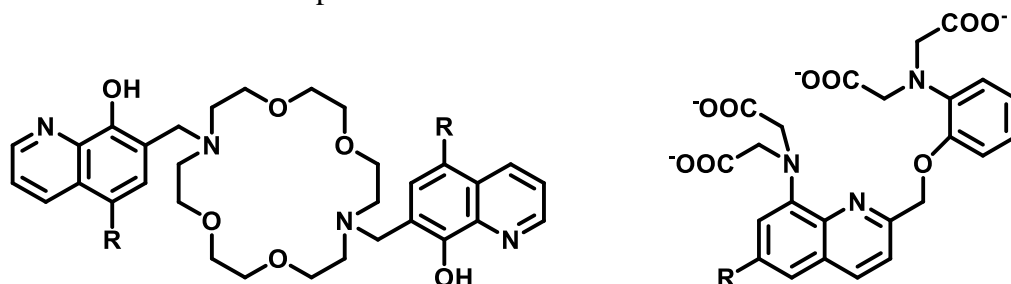


Figure 2. Fluorescent molecules used for sensing of cation.

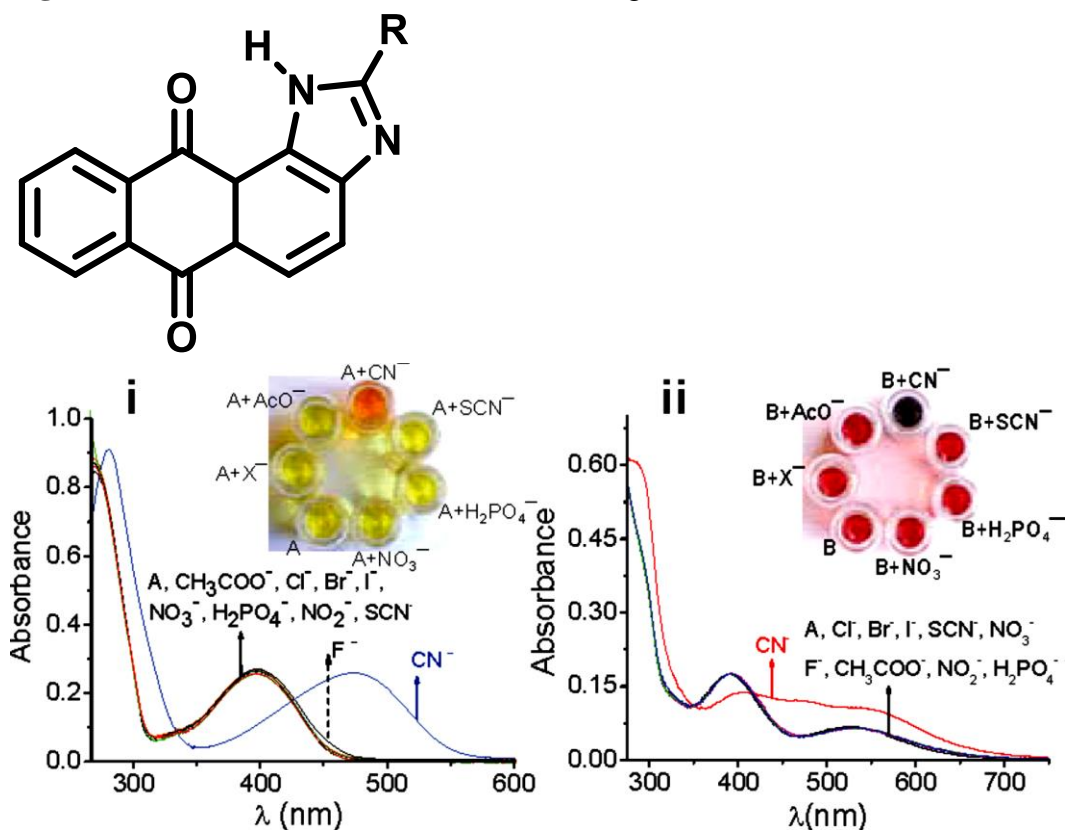
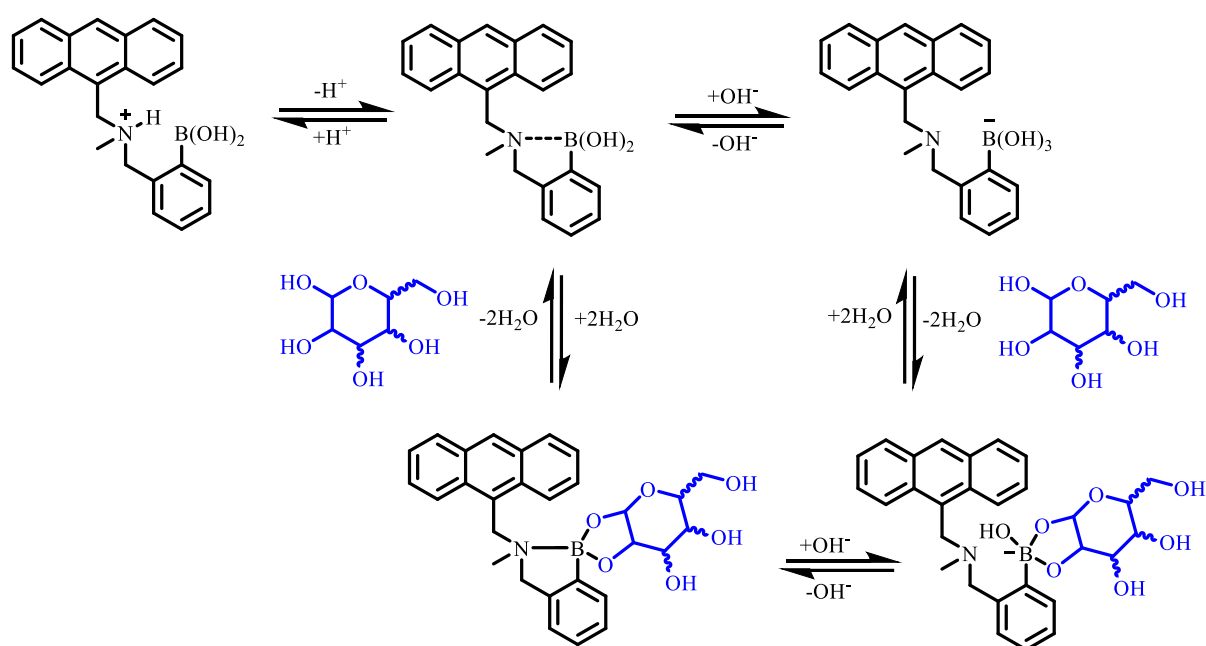


Figure 3. Organic fluorescent molecule for anion sensing.

Several cations and anions having toxic and harmful effect contaminating the various resources such as water and food sources leading harmful effect on human health and environment. Therefore, there is need of developing the methods which can be used for detection of such harmful pollutants. There are several instrumental techniques available to determine the cations and other species such as atomic absorption spectroscopy, inductively coupled plasma spectroscopy but due to their high sophistication, expensive and difficult to handle, time consuming. Over other instrumental techniques fluorescent chemosensor are more advantageous as it is easy to handle, cost effective, sensitive, selective and naked eye detection is possible.^{13,14,15}



Scheme 2. Schematic pathway for sensing of neutral molecule for glucose sensing. From the above literature synthesis of various organic fluorescent molecule for sensing application was carried out. The synthesized fluorescent molecule was used for cation and anion sensing by non-covalent coordinate metal interaction and hydrogen bond interaction between analyte and fluorescent receptor.

Chapter 2:

As per the literature study I have synthesized organic fluorescent molecules for sensing cations¹⁶. Herein in the molecule was synthesized with the receptor based on diphenylaniline as donor and heterocyclic core containing dipyrindine and thiophene system. This molecule was successfully synthesized by aldol condensation followed by Michael addition to give the final product with 57% yield. The molecule was characterized by ¹HNMR, ¹³C NMR, infrared (IR), ESI Mass, CHN-analysis and Single Crystal X-ray Diffraction (SXRD). further its

photophysical studies were studied by UV-Vis absorption spectrophotometry and Emission study by fluorescence spectrophotometer. Initially the molecule was studied for solvatochromic effect (solvent study) using different solvent systems such as Dimethyl sulphoxide (DMSO), Chloroform (CHCl₃), Acetonitrile (ACN), Water (H₂O), tetrahydrofuran (THF). After solvent study the molecule was further utilized for sensing application. It was observed that the molecule was highly selective and sensitive towards iron (Fe³⁺) metal ion in presence over other cations such as Cu²⁺, K⁺, Cd²⁺, Co²⁺, Mn²⁺, Ni²⁺, Ba²⁺, Hg²⁺, Al³⁺, Pb²⁺, Zn²⁺, Ca²⁺, Fe²⁺. Receptor 1 was characterized for its photophysical changes upon addition of Fe³⁺ metal ion by UV visible and fluorescence study. Reversibility study was performed using sodium hydroxide strong base which removes breaks the interaction between the receptor and Fe³⁺ metal ion precipitating out as Fe(OH)₃ which suggested that the molecule was reversible for three cycles. The limit of detection was found to be 52nM. The binding constant was calculated by Benesi-Hildebrand Plot which was observed to be 3.75X10⁻⁵M.

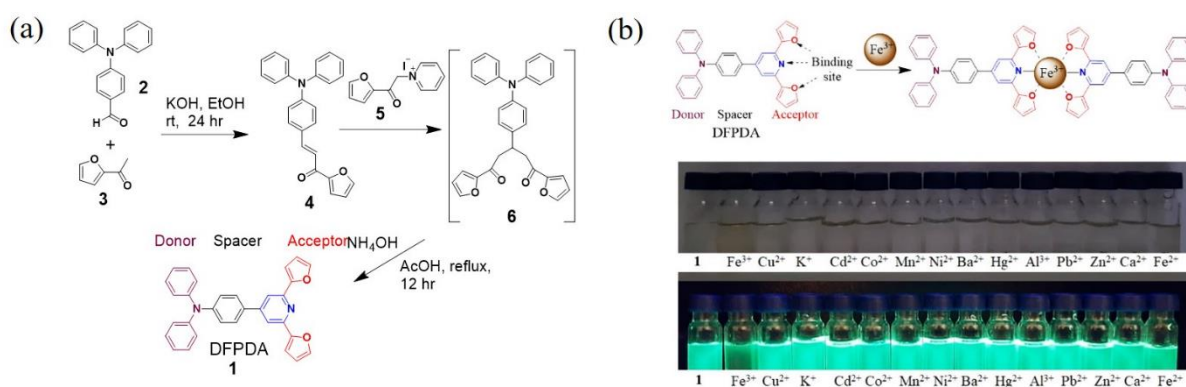


Figure 4. (a) Synthetic pathway for synthesis of the receptor 1 (DFPDA) used for sensing of Fe³⁺ metal ion. (b) sensing performance of the receptor 1 performed and observed in naked eye and at 365 nm and also represent the

Chapter 3:

The second derivative was synthesized by similar synthetic approach but the derivative comprised of diphenyl as donor and with dipyridine and thiophene heterocore^{17,18,19}. This all derivatives were synthesized with different heterocycle on order to study its selectivity towards different cations. However, the receptor showed good selectivity towards copper ion (Cu²⁺) ion in presence over other cations. The molecule was characterized by ¹HNMR, ¹³C NMR, infrared (IR), ESI Mass, CHN-analysis. After characterization the further receptor studies were performed on UV-Vis and emission studies. The fluorescence and absorption studies showed that the molecule was highly selective towards Cu²⁺ ion. The receptor interaction with Cu²⁺ ion was further characterized by density functional theory studies. The receptor 1 was employed for practical application in water analysis. The calculated limit of detection was 0.78μM and the binding constant was noted to be 1.13x 10⁶ M⁻¹. The crystal structure studies were done for

the receptor **1** by SXRD.

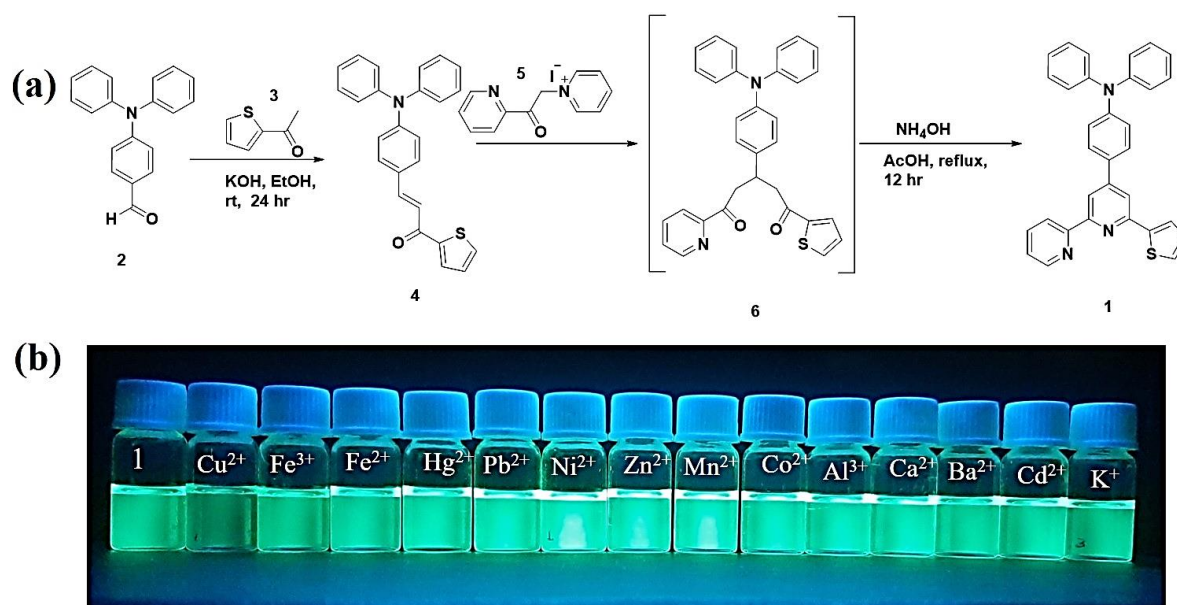


Figure 5. (a) Synthetic route proposed for synthesis of receptor **1**. (b) Sensing performance study observed under 365 nm with series of various cations which shows good selectivity towards Cu^{2+} ion.

Chapter 4:

There are several fluorescent molecules which usually follows aggregation caused quenching phenomenon. Herein I have synthesized fluorescent receptor which is based aggregation induced emission phenomenon which was developed by Tang and group in 2001 to overcome the problem of Aggregation caused quenching. Herein by using the AIE phenomenon I developed tetraphenylethene based molecule for sensing application. The receptor molecule ethyl(Z)-2-cyano-3-(5-(4-(1,2,2-triphenylvinyl)phenyl)thiophen-2-yl)acrylate **1** was synthesized via three steps as shown in **Figure 6** below. The molecule consists of vinylidene bond formed by simple Knoevenagel condensation. The receptor molecule composed of TPE as donor thiophene connected to vinylidene bond acting as receptor. the receptor **1** showed high selectivity towards CN^- anion. The selectivity study was performed in presence over other anions. The molecule also showed good mechanochromic effect study upon applying mechanical stress of grinding, fuming with acetone solvent and heating at high temperature. The interaction of between the cyanide anion and the receptor takes place by nucleophilic substitution react at vinylic bond which was confirmed by ^1H NMR titration study. Further the molecule was used for test strip and food analysis. For food analysis I focussed on the sample such as potatoes, almonds and sweet potato. Biological cell imaging is another application performed for the synthesized molecule which shows that the molecule can also be used as an

excellent fluorescent marker. The detection limit found to be 67 nM which is much lower than the provided by environmental protection agency (1.6 μ M).

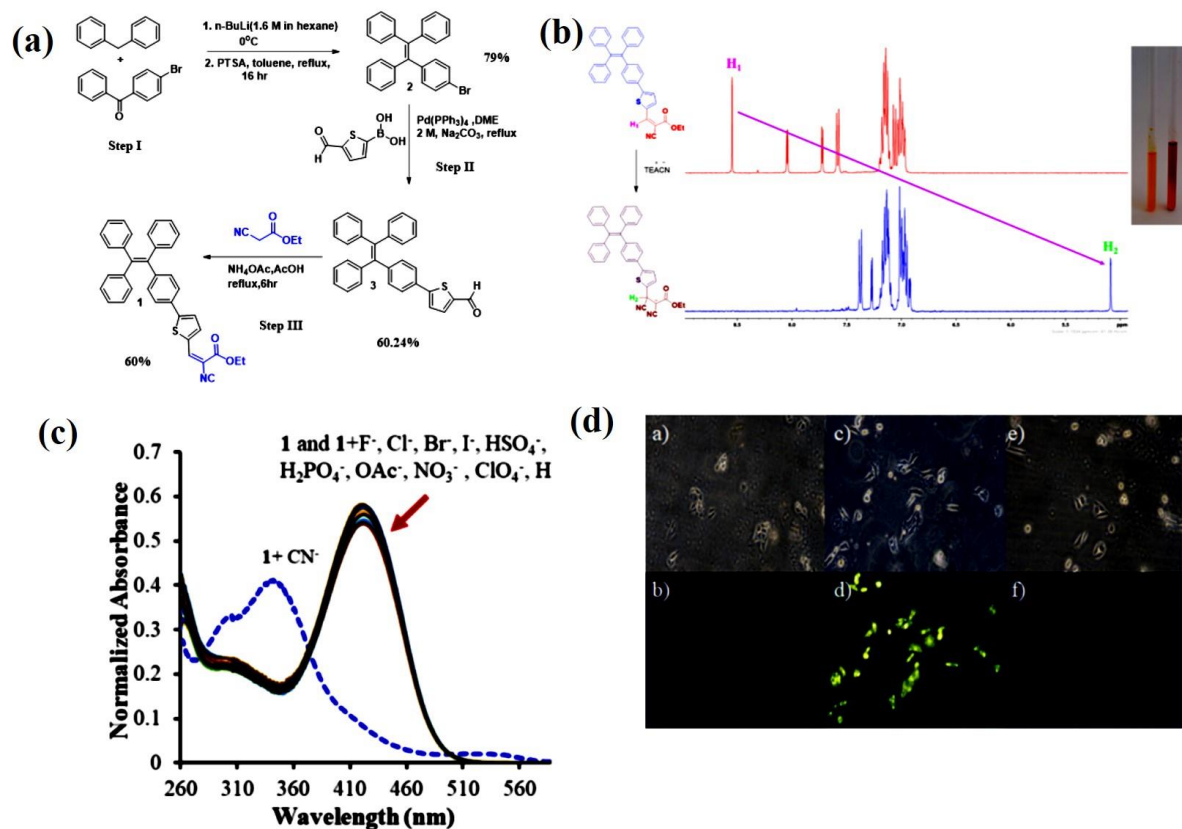


Figure 6. (a) Synthetic sequence for synthesis of receptor **1**. (b) ¹H NMR titration study performed for the receptor **1** in presence of CN⁻ and absence of CN⁻. (c) UV-Vis absorption spectra for receptor **1** upon addition of various anions. (d) Represents the biological cell imaging application.

Chapter 5:

Here I have synthesized another molecule for fluorescent sensing application. The molecule was synthesized by simple aromatization and oxidation in presence DMSO, HCl and I₂ to give 1-(*p*-tolyl)-4,9-dihydro-3*H*-pyrido[3,4-*b*] indole. The fluorescent sensing takes place by simple hydrogen bond interaction between the indole moiety with anion. This receptor was highly sensitive and selective towards fluoride anion in presence over other anions. The molecule was successfully synthesized from reported literature, characterized by ¹H NMR, ¹³C NMR, and by high resolution mass spectrometry. The receptor shows fluorescence quenching when fluoride is added this quenching mainly due to deprotonation of the proton present on the indole.

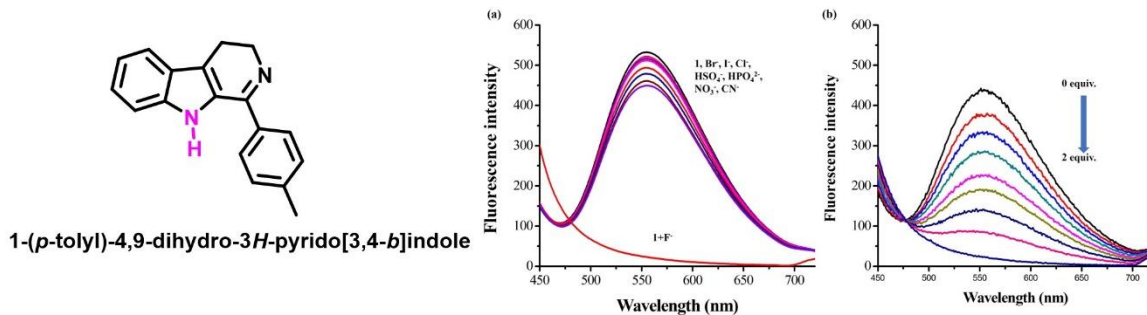


Figure 7. Structure of receptor 1-(*p*-tolyl)-4,9-dihydro-3*H*-pyrido[3,4-*b*]indole. (b) UV-Vis spectra recorded for receptor in presence of various anions. (c) sensing performance study which shows high selectivity towards F^- anion.

Chapter 6: Conclusion and future perspective

In conclusion, the molecule 4-(2,6-difuran-2-yl)pyridine-4-yl)-*N,N*-diphenyl aniline was synthesized and characterized by 1H NMR, ^{13}C NMR ESI-Mass, SXRD. The receptor was used for selective and sensitive detection of Fe^{3+} ion sensing. the sensing performance study was carried out for selectivity towards various cations which was then further characterized by UV-Vis spectroscopy and fluorescence study. The receptor showed detection limit to be 52nM. the reversibility study performance exhibited that the receptor was reversible for 3 cycles.

Another similar derivative was synthesized by same synthetic approach via aldol condensation followed by Michael addition reaction to give *N,N*-diphenyl-4-(6-(thiophen-2-yl)-[2,2'-bipyridine]-4-yl)aniline. This derivative consists of two pyridine moieties with one thiophene forming the heterocyclic core which can be used for sensing application. The molecule is successfully characterized and was found to be highly selective towards Cu^{2+} ion. The sensing performance showed that the receptor shows the quenching of fluorescence. The UV-Vis absorption recorded clearly shows the change in absorption intensity when Cu^{2+} ion is added while other cation there was no change observed in absorption. This was further confirmed by fluorescence study which showed clear quenching of fluorescence. The receptor used for practical application in water analysis. the limit of detection for the receptor was observed to be $0.78\mu M$.

A receptor molecule was synthesized based on Aggregation induced emission (AIE) phenomenon. The AIE activity was first introduced in 2001 by Tang and group which abnormal phenomenon developed to overcome the effect of aggregation caused quenching (ACQ). There

are several derivatives which shows AIE phenomenon such as hexaphenylsilole (HPS)²⁰, tetraphenylethylene (TPE)^{21,22}. Herein the molecule was synthesized by using TPE as a donor moiety which showed excellent aggregation induced emission property in THF/water fraction. The synthesized molecule consists of vinylic double bond connected via thiophene as a spacer to TPE donor. Mechanochromic study was performed for the receptor by employing mechanical stress such as grinding, heating and fuming. In order to study sensing performance initially solvent study was carried out. Further the molecule was utilized for sensing performance towards various anions. The receptor showed high selectivity towards CN⁻ anions over other anions such as F⁻, Cl⁻, I⁻, Br⁻, NO₃⁻, HPO₄²⁻, OAc⁻, HCO₃⁻. The mechanism involved behind the detection for cyanide anion is nucleophilic substitution reaction taking place at vinylic bond of the molecule. To confirm the selectivity competitive study and ¹H NMR titration study was performed. Fluorescent molecule showed its applicability in food sample analysis for qualitative determination of CN⁻ in food sample. While further the molecule was used for biological cell imaging application. The detection limit was observed to be 67nM.

Synthesized and characterized new indole based fluorescent molecule for fluoride sensing application. The mechanism of binding is just hydrogen bond interaction between H bond of indole to give HF₂⁻ complex. The absorption and fluorescence studies showed clear difference in absorption and emission properties upon addition of F⁻ anion over other anions.

Thus, I conclude that these organic fluorescent molecules were designed, synthesized and characterized for selective and sensitive detection of cations and anion. In future these fluorescent molecules can be further utilized as good fluorescent marker and for drug delivery system.

References:

- (1) De Silva, A. P.; Gunaratne, H. Q. N.; Gunnlaugsson, T.; Huxley, A. J. M.; McCoy, C. P.; Rademacher, J. T.; Rice, T. E. Signaling Recognition Events with Fluorescent Sensors and Switches. *Chem. Rev.* 1997, 97 (5), 1515–1566. <https://doi.org/10.1021/cr960386p>.
- (2) Czarnik, A. W. Chemical Communication in Water Using Fluorescent Chemosensors. *Acc. Chem. Res.* 1994, 27 (10), 302–308. <https://doi.org/10.1021/ar00046a003>.
- (3) Daly, B.; Ling, J.; De Silva, A. P. Current Developments in Fluorescent PET (Photoinduced Electron Transfer) Sensors and Switches. *Chem. Soc. Rev.* 2015, 44 (13), 4203–4211. <https://doi.org/10.1039/c4cs00334a>.
- (4) Hong, Y.; Chen, S.; Wai, C.; Leung, T.; Wing, J.; Lam, Y.; Liu, J.; Tseng, N.; Tsz, R.; Kwok, K.; Yu, Y.; Wang, Z.; Tang, B. Z. Fluorogenic Zn (II) and Chromogenic Fe (II) Sensors Based on Terpyridine-Substituted Tetraphenylethenes with Aggregation-Induced Emission Characteristics. 2011, No. Ii, 3411–3418.
- (5) Hong, Y.; Lam, J. W. Y.; Tang, B. Z. Aggregation-Induced Emission. *Chem. Soc. Rev.* 2011, 40 (11), 5361–5388. <https://doi.org/10.1039/c1cs15113d>.
- (6) Zhao, Z.; He, B.; Tang, B. Z. Aggregation-Induced Emission of Siloles. *Chem. Sci.* 2015, 6 (10), 5347–5365. <https://doi.org/10.1039/c5sc01946j>.
- (7) Hamasaki, K.; Ikeda, H.; Nakamura, A.; Ueno, A.; Toda, F.; Suzuki, I.; Osa, T. Fluorescent Sensors of Molecular Recognition. Modified Cyclodextrins Capable of Exhibiting Guest-Responsive Twisted Intramolecular Charge Transfer Fluorescence. *J. Am. Chem. Soc.* 1993, 115 (12), 5035–5040. <https://doi.org/10.1021/ja00065a012>.
- (8) Sauer, M. Single-Molecule-Sensitive Fluorescent Sensors Based on Photoinduced Intramolecular Charge Transfer. 2003, 1790–1793. <https://doi.org/10.1002/anie.200201611>.
- (9) Bhosale, S. V.; Bhosale, S. V.; Kalyankar, M. B.; Langford, S. J. A Core-Substituted Naphthalene Diimide Fluoride Sensor. *Org. Lett.* 2009, 11 (23), 5418–5421. <https://doi.org/10.1021/ol9022722>.
- (10) Yu, Z.; Jiang, N.; Kazarian, S. G.; Tasoglu, S.; Yetisen, A. K. Progress in Biomedical Engineering Progress in Biomedical Engineering. 2021.
- (11) James, T. D.; Sandanayake, K. R. A. S.; Shinkai, S. Saccharide Sensing with Molecular

-
- Receptors Based on Boronic Acid.
- (12) James, T. D.; Sandanayake, K. R. A. S. Novel Photoinduced Electron-Transfer Sensor for Saccharides Based on the Interaction of Boronic Acid and Amine. 1994, 477–478.
 - (13) Wu, D.; Sedgwick, A. C.; Gunnlaugsson, T.; Akkaya, E. U.; Yoon, J.; James, T. D. Fluorescent Chemosensors: The Past, Present and Future. *Chem. Soc. Rev.* 2017, 46 (23), 7105–7123. <https://doi.org/10.1039/c7cs00240h>.
 - (14) H Kara, O. A. M. A. *New Trends in Fluorescence Spectroscopy*; 2001; Vol. 1.
 - (15) Basabe-Desmonts, L.; Müller, T. J. J.; Crego-Calama, M. Design of Fluorescent Materials for Chemical Sensing. *Chem. Soc. Rev.* 2007, 36 (6), 993–1017. <https://doi.org/10.1039/b609548h>.
 - (16) Zhou, G.; Zhang, X.; Ni, X. Tuning the Amphiphilicity of Terpyridine-Based Fluorescent Probe in Water: Assembly and Disassembly-Controlled Hg²⁺ Sensing, Removal, and Adsorption of H₂S. *J. Hazard. Mater.* 2019, No. September, 121474. <https://doi.org/10.1016/j.jhazmat.2019.121474>.
 - (17) Wang, H.; Wu, S. Sensors and Actuators B: Chemical A Pyrene-Based Highly Selective Turn-on Fluorescent Sensor for Copper (II) Ions and Its Application in Living Cell Imaging. *Sensors Actuators B. Chem.* 2013, 181, 743–748. <https://doi.org/10.1016/j.snb.2013.01.054>.
 - (18) Kwok, R. T. K.; Leung, C. W. T.; Lam, J. W. Y.; Tang, B. Z. Biosensing by Luminogens with Aggregation-Induced Emission Characteristics. *Chem. Soc. Rev.* 2015, 44 (13), 4228–4238. <https://doi.org/10.1039/c4cs00325j>.
 - (19) Edition, I. *Chemie*. <https://doi.org/10.1002/anie.202000845>.
 - (20) Zhao, Z.; Zhang, H.; Lam, J. W. Y.; Tang, B. Z. Aggregation-Induced Emission: New Vistas at the Aggregate Level. *Angew. Chemie - Int. Ed.* 2020, 59 (25), 9888–9907. <https://doi.org/10.1002/anie.201916729>.
 - (21) Gao, M.; Tang, B. Z. Fluorescent Sensors Based on Aggregation-Induced Emission: Recent Advances and Perspectives. *ACS Sensors* 2017, 2 (10), 1382–1399. <https://doi.org/10.1021/acssensors.7b00551>.
 - (22) Saha, S.; Ghosh, A.; Mahato, P.; Mishra, S.; Mishra, S. K.; Suresh, E.; Das, S.; Das, A. Specific Recognition and Sensing of CN⁻ in Sodium Cyanide Solution. *Org. Lett.* 2010, 12 (15), 3406–3409. <https://doi.org/10.1021/ol101281x>.

CHAPTER 1

Chapter 1

1.1. Introduction

Now a days, for the development and betterment of the whole world new strategies and technologies are being employed. But at present it is observed that in the name of development and advancement there is lot of destruction and pollution is going on [1,2]. These destructions have led to loss of various natural habitat, pollution of natural resources such as soil pollution, water pollution and so on harming the whole environmental resources as well as in turn harmful for human health. The reason behind the cause is due to destroying the environment, infrastructure, employing the new methodologies for agricultural development, release of toxic pollutants in natural water bodies, deforestation, mining and so on. These all activities led to the toxification of resources available on the earth [3]. Considering these facts there is need of detecting and remediation to overcome the various problems or challenges faced by mankind. Therefore, the various fields such as physical analysis, chemical analysis and biological studies play the major role to overcome the problem and find the solution. Learning from the recent studies showed tremendous growth in the field of science to overcome the problems.

The Chemistry field has gain lot of attention of many scientists to overcome the pollution caused by aforementioned sources such as industrialization which is considered as one of the major causes of pollution of various water bodies [4]. In chemistry now a days “Supramolecular Chemistry” has drawn attention of many researchers. Supramolecular chemistry is the branch of chemistry that deals with formation of new structure by non-covalent interactions such as electrostatic interaction, hydrogen bonding, van der Waals forces, π - π interactions, metal coordination.[5] The field of supramolecular chemistry was first introduced by Jean Marie Lehn. He termed the supramolecular chemistry as the “*chemistry beyond the molecule*” [6]. In addition, Sir Donald J. Cram (host-guest Chemistry) and Sir Charles Pedersen (synthesis of crown ether for specific interaction of high selectivity) [7,8]. They received Nobel Prize in

chemistry in the year 1987 [9]. Supramolecular chemistry usually composed of molecular self-assembly, molecular folding, molecular recognition, host guest chemistry, mechanically-interlocked architecture, and dynamic covalent chemistry. Amongst all these fields host guest chemistry is considered as one of the best approaches for detection and remediation of various pollutants/analyte. Further in host guest chemistry chemosensor is another field which is used for sensing of various essential, non-essential, neutral and toxic analyte from the system [10]. Chemosensors is a molecular device consisting of binding site, spacer, and fluorophore unit, which are also termed are receptor or probe. These chemosensors usually shows the fluorescence phenomenon accordingly it is also termed as fluorescent chemosensor/ fluorescent probe. **Figure 1.1.** The fluorescent molecule has wide application in various field such as biomedical application, biological fluorescent marker, optoelectronics, forensic sciences, food industry and sensing application [11,12].

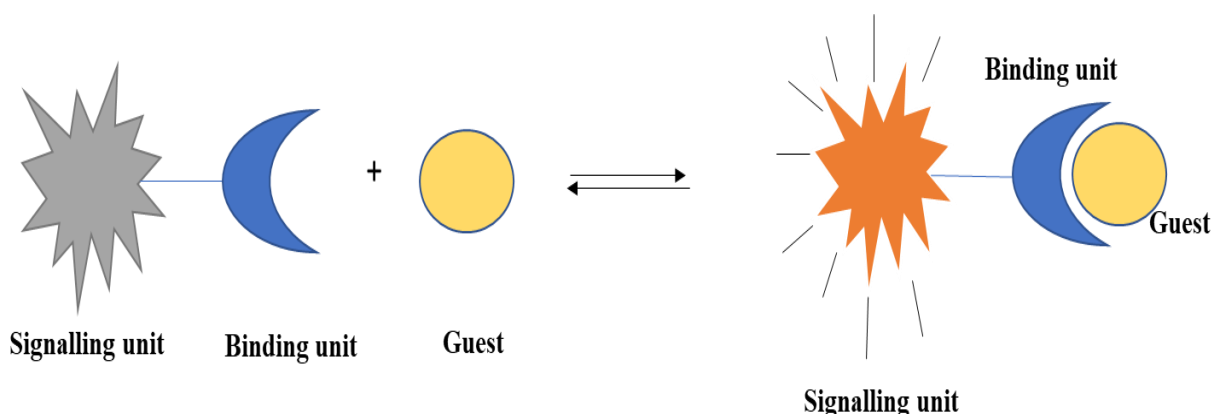


Figure 1.1. Components of fluorescent chemosensor

However, we are more interested in application of synthesis of organic fluorescent molecule and use them for sensing application for various cations, anions and neutral molecules. Although there are various instrumental techniques being employed for determination of various analyte species. But fluorescent molecules due to its high sensitivity, high selectivity, detection limit, hand-held method and naked eye detection is possible. Few fluorescent molecules can be synthesized by simple synthetic approach using cost effective reagents. There

is no use of highly sophisticated instrument required for sensing application therefore, fluorescent sensing is considered as major focus of many scientists and the field has explored its application in various fields of scientific technology [13].

F. Goppelsroder developed the first fluorescent chemosensor in 1867 which is based on strong interaction between the morin ligand and aluminium ion (Al^{3+}). This resulted into birth and development of analytical chemistry in the field of sensing application [14,15]. Later de Silva and Czarnik explored the field of sensing application. Now a days many researchers are focusing on sensing of various anions, neutral molecules as well as these fluorescent molecules can be utilized for determination of intracellular pH, temperature and viscosity. Along with the sensing application the field has shown the rapid advancement in biological imaging application. The detection of analyte by fluorescent sensor is carried out by various photophysical phenomenon such as photoinduced electron transfer [16], chelation induced enhanced fluorescence (CHEF) [17], aggregation induced electron transfer (AIE) [18,19], intramolecular charge transfer (ICT) [20,21]. The aforementioned photophysical processes mainly occurs by various when the analyte and fluorescent molecule interaction takes place by hydrogen bond interaction, metal coordination, van der Waals interaction, nucleophilic substitution reaction and protection deprotection mechanism [22]. Herein are few examples of various organic fluorescent molecules that can be used for sensing of cation, anions, neutral molecules, pH, temperature and viscosity.

Various analytes especially anions and cations are essential as well as measured harmful for human health, which enters in to the environment by illegal activities or negligence. This led to contamination of water resources and affects the food chain. All over the countries Europe India, Africa, South America and China water pollution is the major problem. Different cations such as Al^{3+} , Cr^{3+} , Cd^{2+} , Co^{2+} , Mg^{2+} , Hg^{2+} , Sb^{3+} , CN^- , F^- , Br^- , Cl^- , As^{3+} , As^{5+} , Cu^{2+} enter in to the water bodies due to industrialization. Few metal ions play very crucial role in biological

and physiological processes occurring in nature which includes alkaline metal ion such as sodium (Na^+), Calcium (Ca^{2+}), potassium (K^+), copper (Cu^{2+}), Zinc (Zn^{2+}), Magnesium (Mg^{2+}) however few are toxic which includes lead (Pb^{2+}), Cadmium (Cd^{2+}), mercury (Hg^{2+}), Arsenic (As^{3+}). There are different instrumental techniques such as electro analytical methods, atomic absorption spectroscopy (AAS) [23], inductively coupled plasma mass spectrometry (ICP-MS) [24], colorimetric methods that can be used for detection of this toxic pollutants. Due to high sophistication, expensive, difficult to handle, time consuming analysis hence amongst all those techniques fluorescent sensing is considered as most convenient method for sensing application as it is fast, low cost of instrumentation, cost effective, simple and easy to handle, and naked eye detection. There are number of fluorescent dyes such tetraphenylethylene (TPE) [25], naphthalene-diimide (NDI) [26], carbon dots (CQ-D) [27,28], Schiff's bases [29,30,31], conjugated polymer, various metal organic framework (MOFs) [32], pyrene [33], coumarin substituted derivatives and so on [34].

1.2. Fluorescent molecules for sensing essential cations (Na^+ , K^+ , Ca^{2+})

The cations are very important and great interest to many scientists in various field such as chemists, biologist, environmentalist and for clinical biochemist. There are different metal ions such as that essential and involved in biological processes. Sodium, potassium magnesium and calcium are considered the essential elements which are involved in muscle contraction, cell activity regulation, many nerve transmission impulses, enzyme activation, blood pressure regulation in the body, pH and various ionic concentration are governed by this element. All these elements in excessive dosage leads to different health disease and hampers various biological activities. Analytical techniques available for detection of cation includes flame photometry, atomic absorption spectrometry, neutron activation analysis, ion selective electrode, electron probe analysis. But these techniques due to high sophistication, expensive and large amount of sample is requirement instrumental methods is now replaced with another

method extensively used now a days is the method of fluorescent sensor. Fluorescent sensing offers more advantages over other instrumental methods in terms of high selectivity, rapid response time, naked eye detection high sensitivity and lowest limit of detection [35,36]. Crown ethers are the basic scaffold used for capturing the alkali metal ions such as Li^+ , Na^+ , K^+ , Ca^{2+} and Mg^+ . Crown ether was first discovered by Charles Pederson in 1967 along with DuPont [37]. The Crown ether was synthesized while preparing the complexing agent for divalent cation. His approach was to use catechol groups with hydroxyl on each molecule which led to formation of byproduct complex with K^+ ion. Some common structures of crown ether **Figure 1.2.** [38,39].

Muller *et al.* developed red to near infra-red (NIR)-emitting **BODIPY** fluorophore for potassium sensing. Most of the time crown ethers, cryptands have shown wide application in sensing of K^+ and Ca^{2+} . Crown ethers shows selectivity depending upon the core/cavity size of crown ether. In this work **BODIPY** is functionalized with crown ether which showed high selectivity towards K^+ ion. Initially the molecule appears to be non-fluorescent while upon addition of K^+ the molecule showed turn ON fluorescence. The binding mechanism is as represented in **Figure 1.3.** below [40].

Another core substituted naphthalidiimide system functionalized with crown ether was synthesized by Cox and co-workers. In their work two new NDI functionalized with aza-15-crown-5 ether (**NDI 5**) other NDI was functionalized with aza-18-crown-6 ether (**NDI 6**). The two functionalized **NDI** were successfully investigated for sensing of alkali metals, to study its photophysical properties and binding mechanism. the molecule **NDI 5** showed high selectivity towards Ca^{2+} ion while **NDI 6** showed excellent selectivity towards Na^+ and K^+ ions. From this it concluded that by differing the size of the crown ether the optical properties and selectivity with different alkali metal ion can be tuned successfully. the structures of the compounds are as shown in **Figure 1.4.** below [41].

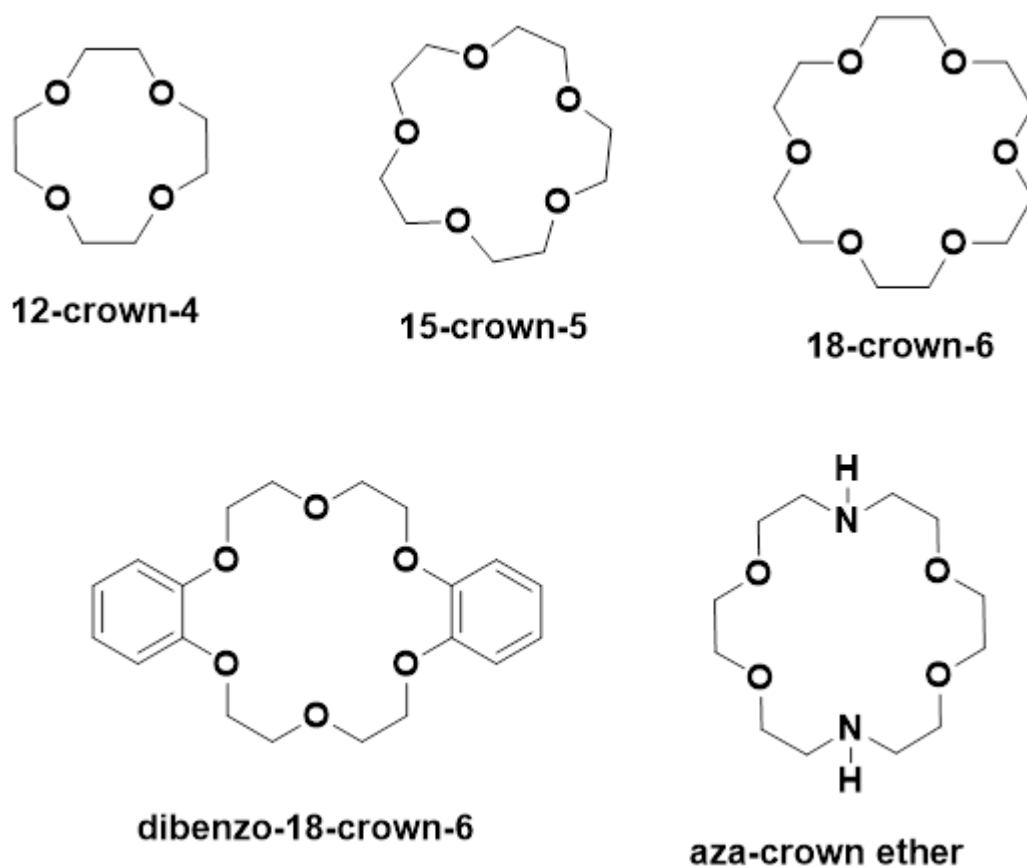


Figure 1.2. Common structures of crown ethers

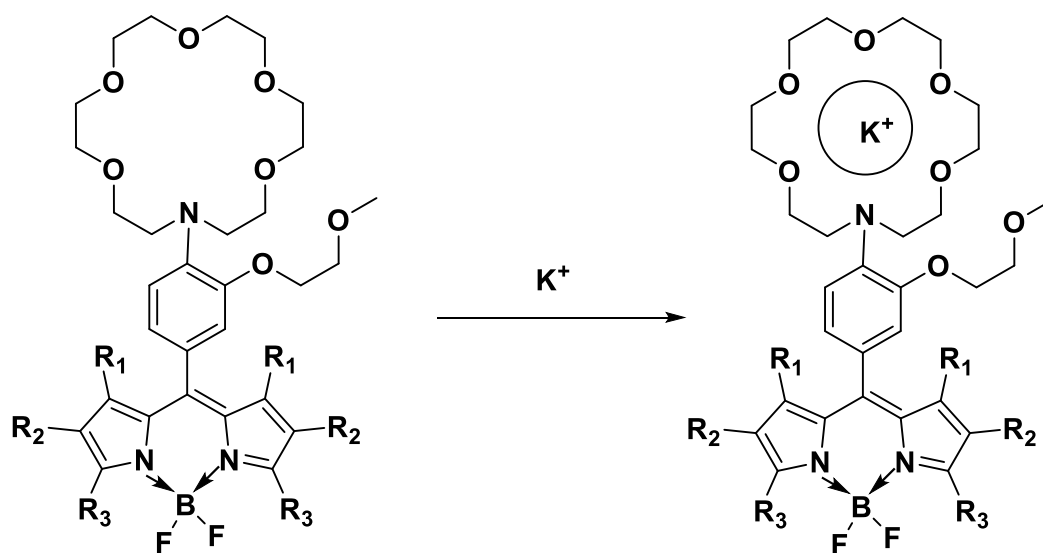


Figure 1.3. Schematic pathway for binding of K^+ ion by using fluorescent BODIPY receptor with crown ether.

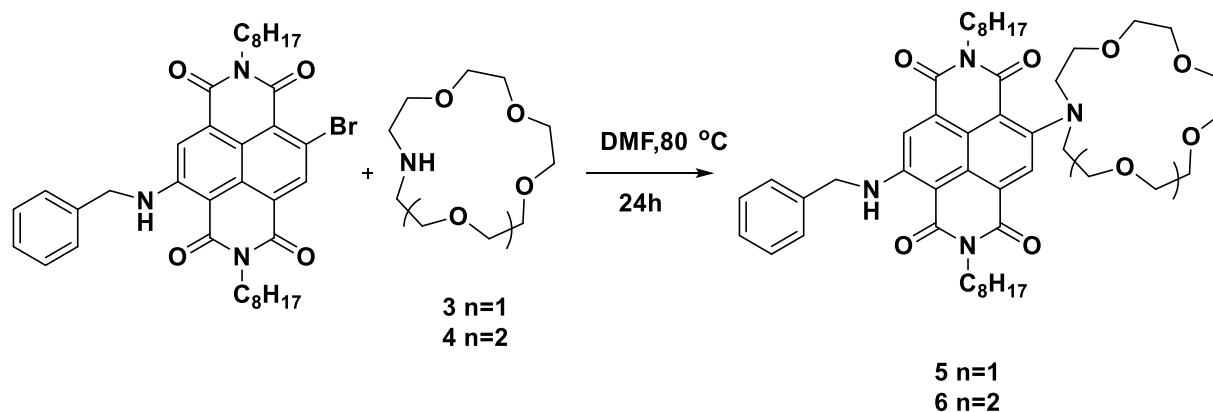


Figure 1.4. NDI-core substituted aza-crown ether for sensing of Ca^{2+} , K^+ , and Na^+ ion.

Functionalized crown ethers are not only used for Na^+ and K^+ ion sensing but the molecules can be also used for sensing of Li^+ ion in aqueous environment. It very important to detect the Li^+ in aqueous solution as the heavy dosage may led to various neurological disorders such as depression. Herein Hangarge and group designed aza-12-crown-4 ether substituted to NDI core that is successfully used for sensing of Li^+ ion. The structure for the synthesized NDI (**NDI-12-C-4**) based sensor as shown in **Figure 1.5.** with observed spectral and color changes with the addition of Li^+ ion **Figure 1.5. (b) and (c)** [42,43,44].

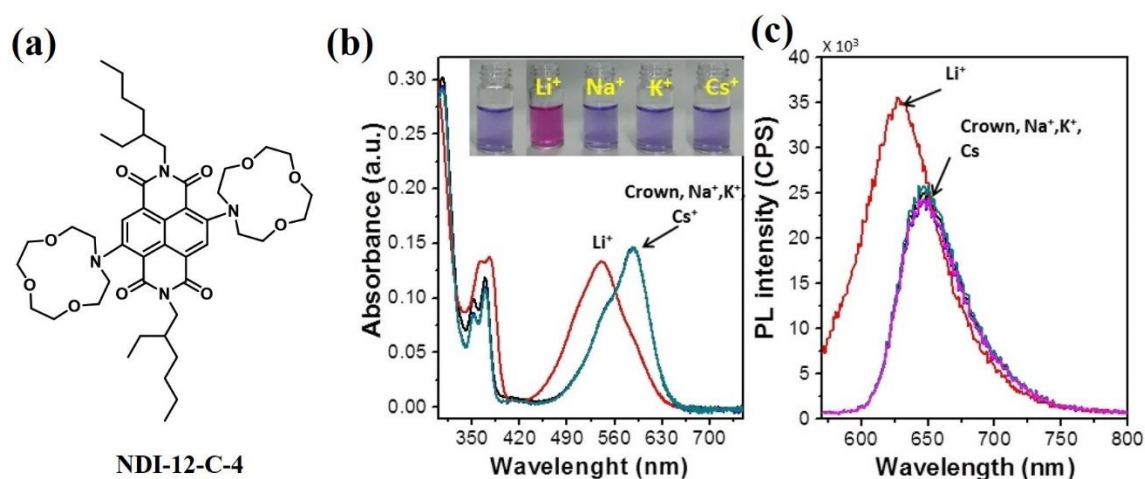


Figure 1.5. (a) Organic fluorescent crown ether for Li^+ and Ca^{2+} sensing (b) absorption spectra with addition of Li^+ and (c) Emission spectral changes with Li^+ addition.

1.3. Fluorescent molecules for toxic cation sensing

Various biological and physiological processes in body and in all other life forms are governed by metal ion hence are considered very important topic on interest on many researchers. Metal ions essentially participate in various biochemical processes such as metal transportations in the body, energy conversion and metabolic activities. Excess of metal ion in the body may lead to serious health issue and restrict the various biological metabolism [45]. Hence there is need of monitoring, study its distribution in the individual system such as various cells and tissues in living organisms. On the earth crust there are several essential (Na^+ , K^+ , Ca^{2+} , Zn^{2+} and Mg^{2+} , Fe^{2+}) and nonessential metal ions/toxic metal ions (Hg^{2+} , Pd^{2+} , Pb^{2+} , Cu^{2+} , As^{3+} , Cr^{3+}) and anions (F^- , Cl^- , CN^- , Br^-) [46].

There are several instrumental methods available to detect the metal ions such as atomic absorption spectroscopy (AAS), atomic emission spectroscopy (AES), ICP-MS etc. But due to high sophistication, cost and difficult to handle limits its application in sensing. However, over various instrumental techniques organic fluorescent material has gained greater advantage due to its high selectivity, sensitivity, high fluorescence quantum yield, easy synthesis methods, handheld method. From environmental and biological significance perspective detection of metal ions is very important with lowest detection limit which is successfully achieved by the using organic fluorescent derivative. Therefore, organic fluorescent molecules found to be promising platform for sensing of various analytes and other fields. Different fluorescent molecules for sensing of toxic cations are introduced such as sensing of arsenic, lead, mercury, cadmium, palladium by using aggregation induced emission phenomenon (AIE) [47]. Herein are some examples of various fluorescent material for sensing of toxic pollutants.

Arsenic (As) is the most toxic species and found especially in ground water leading to serious health issue which is responsible for breaking of DNA, induces the increase in cellular level of nitric oxide and superoxide, and affecting phosphorylation with proteins. The permissible limit

of arsenic in water is 10ppb as prescribed by World Health Organization (WHO) but contamination level is increasing day by day [48,49]. There are several instrumental methods for analysis of As^{3+} content in water such as AAS, AES, ICP-MS, and AFS however, fluorescent method has proved to be excellent approach due to its rapid analysis, low cost, easy synthesis method, high selectivity and sensitivity [50,51].

Tian and coworkers designed and synthesized AIE active molecule by reacting 3,5-dibromobenzaldehyde with (9-phenyl-9H-carbazol-3-yl)boronic acid *via* Suzuki coupling reaction in single step. In this material carbazole acts as molecular rotor which is combined with cysteine that can be used for sensing of As^{3+} in aqueous medium. The observed binding mode of arsenic with receptor was via chelation with the thiol group of the cysteine. The fluorescence response towards various cations such as As^{3+} , Ni^{2+} , Mn^{2+} , Co^{2+} , Pb^{2+} , Cd^{2+} , Cu^{2+} , Al^{3+} , Hg^{2+} , Fe^{3+} , Cr^{3+} and Fe^{3+} were performed in order to check the selectivity. The enhancement in fluorescence was observed with addition of As^{3+} over other competing cations [52]. **Figure 1.6.**

Another cysteine functionalized AIE active TPE derivative was introduced by Beglan and coworkers for detection of As^{3+} in aqueous medium. The schematic pathway for synthesis of derivative as shown in **Figure 1.7.** The synthesized molecule consists of cysteine with thiol acting as a binding site for As^{3+} (As-S) bond. For this receptor basic binding mode is via three thiol groups of cysteine that binds with As^{3+} forming trigonal pyramidal geometry (As-(Cys-TPE)₃). Due to π - π stacking interaction of TPE results in to turn on fluorescence with addition of As^{3+} [53].

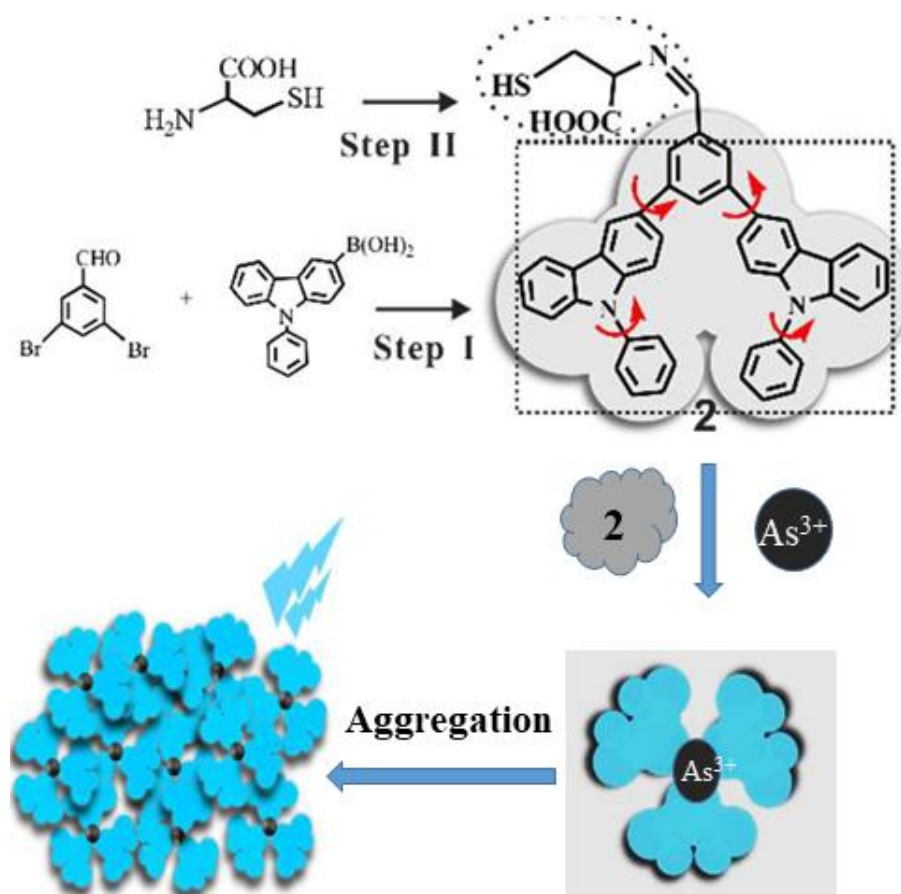


Figure 1.6. Carbazole based fluorescent molecule for arsenic detection.

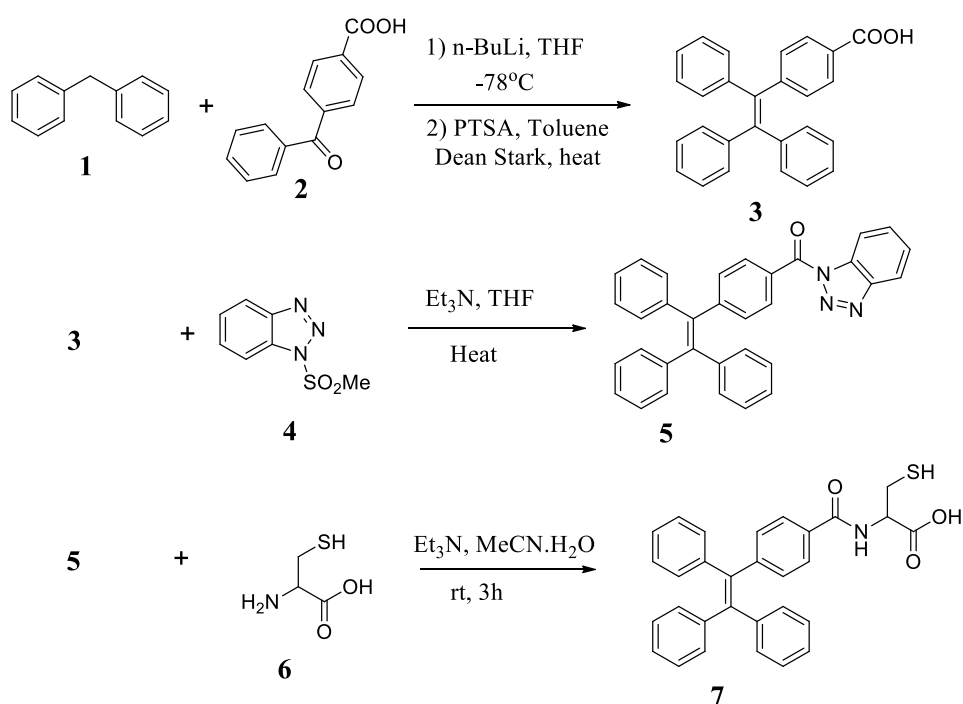


Figure 1.7. Schematic pathway for synthesis of TPE-Cy receptor for As^{3+} sensing.

Cadmium is another toxic pollutant which needs to be detected from an environmental aspect. In the last 10 decades, there have been a number of sensors devised for the sensing of cadmium. Recently, Li et al. synthesized a Y-shaped AIE active molecule for the sensing of Cd^{2+} and Fe^{3+} metal ions in an aqueous medium. The Y-shaped dimb exhibits a turn ON fluorescence response towards Cd^{2+} while quenching of fluorescence was observed with the addition of Fe^{3+} metal ion [54]. **Figure 1.8.**

Zhang and co-workers synthesized another AIE active fluorescent material for turn ON sensing of Cd^{2+} . The molecule consists of a triazole-bridged cyclodextrin (CD) connected to a TPE molecule with excellent AIE active properties, exhibiting a $0.01\ \mu\text{M}$ detection limit. Palladium gained wide importance in the petroleum and chemical industry, but in addition, it has detrimental harmful effects on human health, the environment, and various biological systems. With this respect, the sensing of Pd^{2+} is very important, which can be detected by using a non-destructive and less expensive method, i.e. by utilizing a fluorescent material [55]. Herein, Liu et al. synthesized a conjugated polymer α,ω -diene by using an acyclic diene metathesis approach (ADMET).

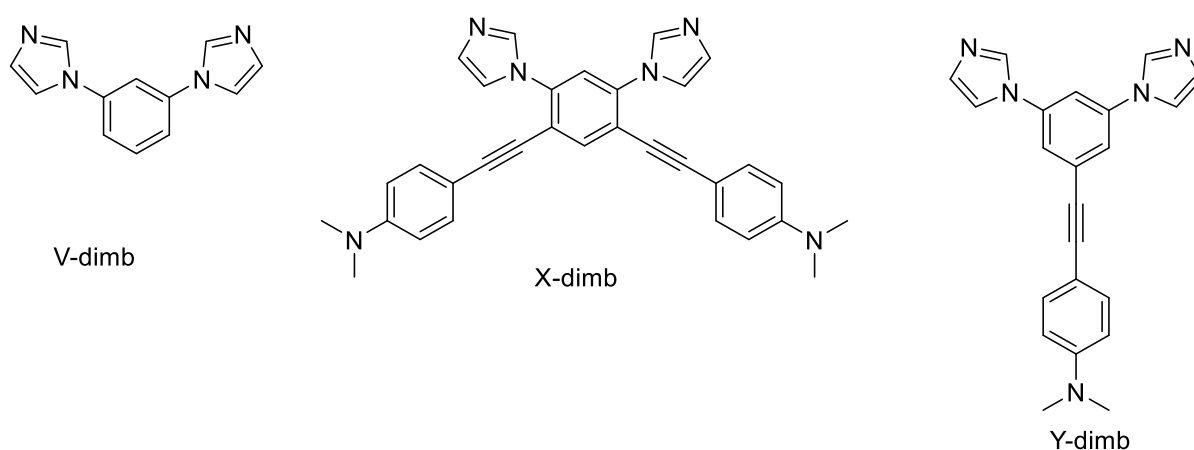


Figure 1.8. Representative chemical structures of the fluorescent material for Cd^{2+} sensing.

The synthesis approach is very simple by linking two diene monomer M1 (1,2-diphenyl-1,2-bis(4-vinylphenyl) ethane) (DBVE) and 4,4-(2,2-diphenylethene-1,1-diyl)bis-(vinylbenzene) (DDBV) connected to AIE active TPE moiety via two different modes. Further in order to increase the solubility it was functionalized with other three comonomer units (M2) such as 1,9-decadiene (C10) linear alkene, 2,7-divinyl-9,9-di-noctylfluorene (Flu) and 1,4-dihexyl-2,5-divinylbenzene (Ben). Dynamic fluorescence quenching was observed with the addition of Pd²⁺ which thus proved to be effectively used for environmental sensing of Pd²⁺ successfully [56]. **Figure 1.9.** In addition, Mukherjee and co-workers developed mono-pyridine substituted triarylethene derivative for detection of Pd²⁺ [57].

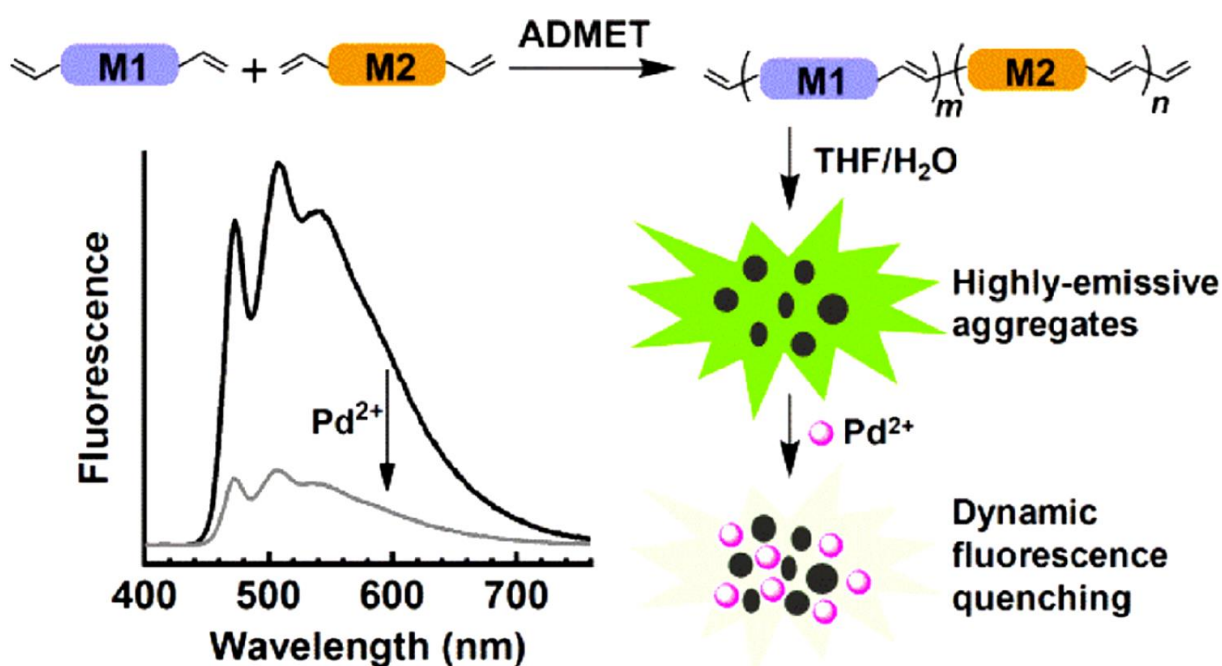


Figure 1.9. Conjugated polymer for sensing of Pd²⁺.

Lead (Pb) is another toxic component and detrimental to human health in addition Pb^{2+} and its derivatives are also considered extremely toxic has cumulative effect especially on children's health [58]. Herein turn on and turn off sensing strategy is applied for detecting Pb^{2+} ion one of the best examples is TPE based fluorescent chemodosimeter synthesized by Khandre et.al for selective detection of Pb^{2+} . The chemodosimeter consists of tetraphenylethene phosphate monoester residues that exhibit strong affinity towards Pb^{2+} at 95% water :THF fraction by turn on strategy with lowest detection limit of 10ppb [59]. **Figure 1.10.**

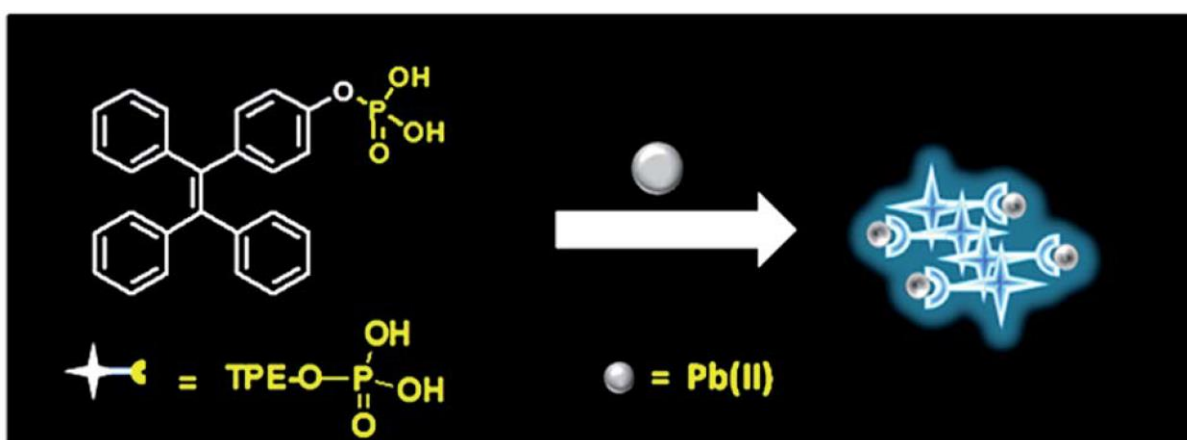


Figure 1.10. TPE based phosphate monoester for sensing of Pb^{2+} .

Soils and water are heavily polluted by toxic element such as lead and mercury which have potential negative and harmful effect on environment and human health. Mercury is widely spread in various water bodies due to industrialization and new agricultural practices. Mercury has a major impact on the immune, endocrine, and nervous systems. Methyl mercury is a potent neurotoxin that causes serious damage to the central nervous system and damages several parts of the body [60,61]. Huang et al. worked on a tetra pyridyl TPE AIE active molecule for the selective and sensitive detection of Hg^{2+} ions. However, the same tetra pyridyl probe was used for H^+ sensing and for sensing of intracellular pH by fluorescence cell imaging. The molecule showed excellent AIE activity with a turn ON fluorescence towards Hg^{2+} . The compound was weakly emissive but as the concentration of Hg^{2+} ions increased, there was a significant increase in the fluorescence.

intensity. It is interpreted that the 4 pyridyl groups shows coordinate interaction. Further HSO_4^- addition leads to enhancement of fluorescence as shown in **Figure 1.11**. below [63].

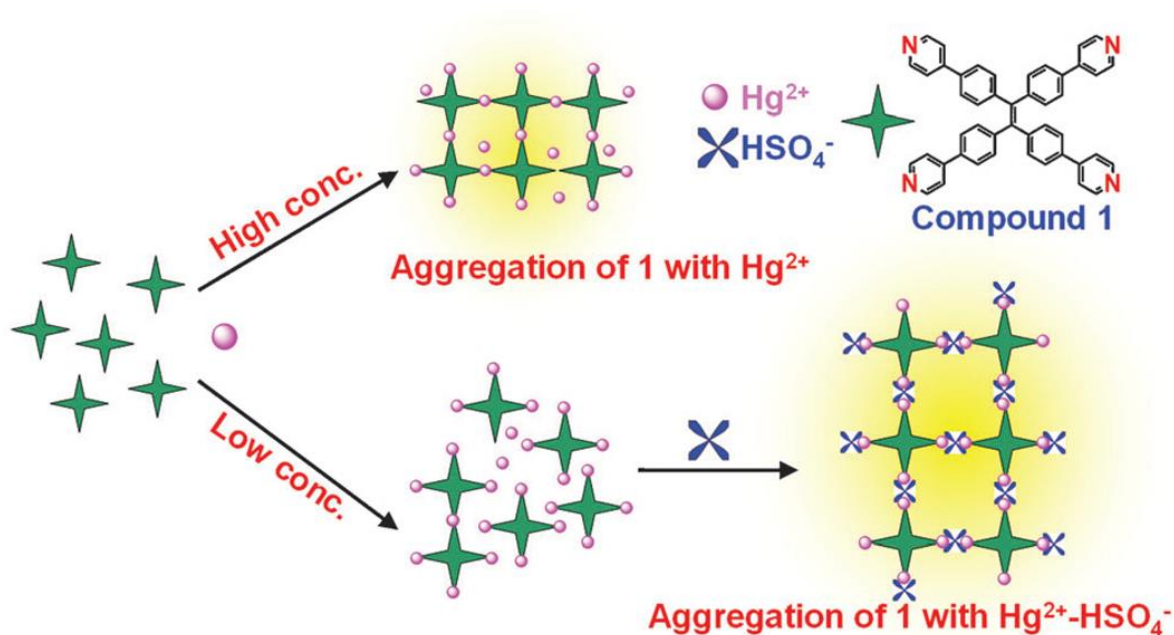


Figure 1.11. Schematic illustration for coordination of Hg^{2+} to TPE-Py.

Ruan et.al designed a novel AIEgens comprising of two thioketal moieties (*p*-DTPES and *m*-DTPES) for sensing of Hg^{2+} ions which undergoes via deprotection reaction as represented in **Figure 1.12**. The luminescence properties change especially the color change was observed from sky blue to yellow green upon addition of Hg^{2+} ion which was also observed through naked eye. Further the probe was successfully employed for real practical application in determining mercury ion in water sample [64].

Shi *et al.* synthesized three a simple derivative namely **M1** with triphenylamine, as donor moiety and barbituric acid as acceptor species by Knoevenagel reaction exhibited excellent aggregation induced emission enhancement (AIEE) characteristics in a THF- H_2O . It was observed that probe showed excellent selectivity towards Hg^{2+} ions. Herein there is interaction between Hg^{2+} ion with thymine like groups in **M1** leading to enhancement in fluorescence [65].

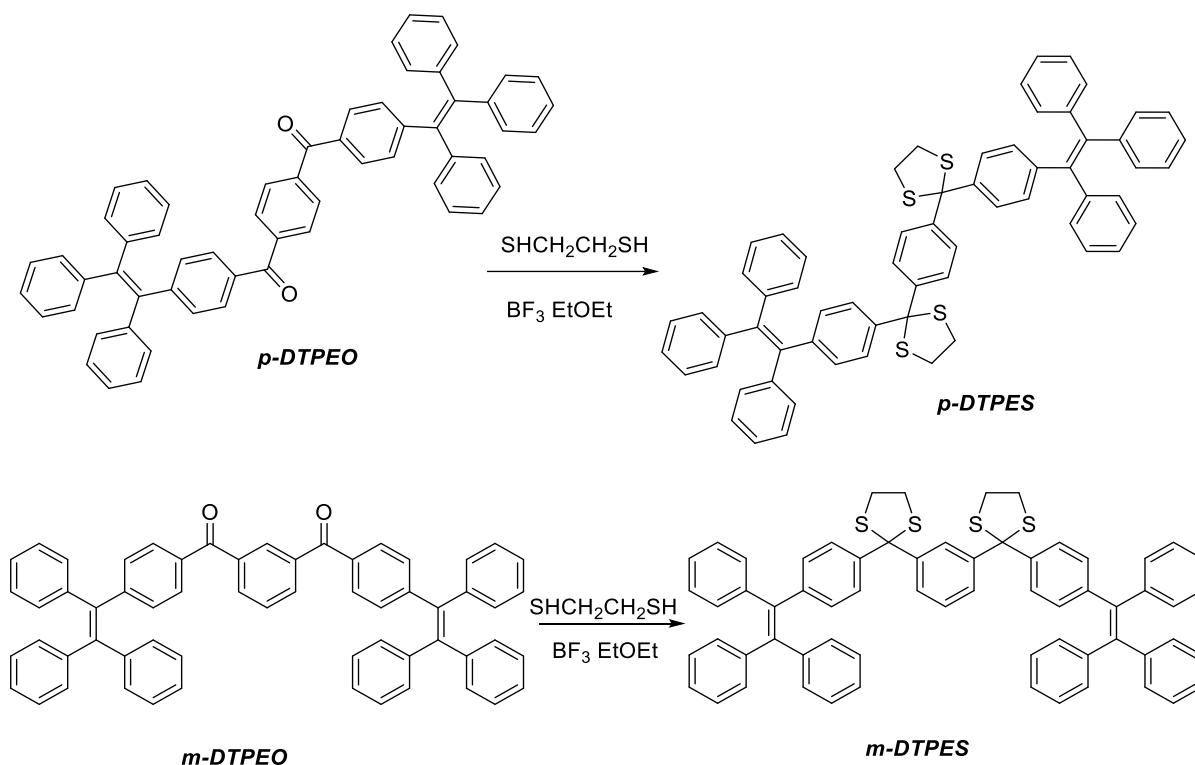


Figure 1.12. Schematic illustration for sensing mechanism by deprotection upon addition of Hg²⁺.

In another example Kala and colleague developed similar carbazole derivative of barbituric acid based AIE active derivative found to be highly selective and sensitive towards detection of Hg²⁺ ion **M2** [66]. Wherein Wang and co-workers designed anthracene derivative which acts as donor and barbituric acid as acceptor by forming mercury (II) barbiturate coordination polymer **M3**. The barbituric acid plays important role in supramolecular chemistry to afford Hg²⁺ mediated supramolecular self-assemblies. Thus, the fluorescent molecules have wide application in detecting the toxic ions from environmental system [67] **Figure 1.13.**

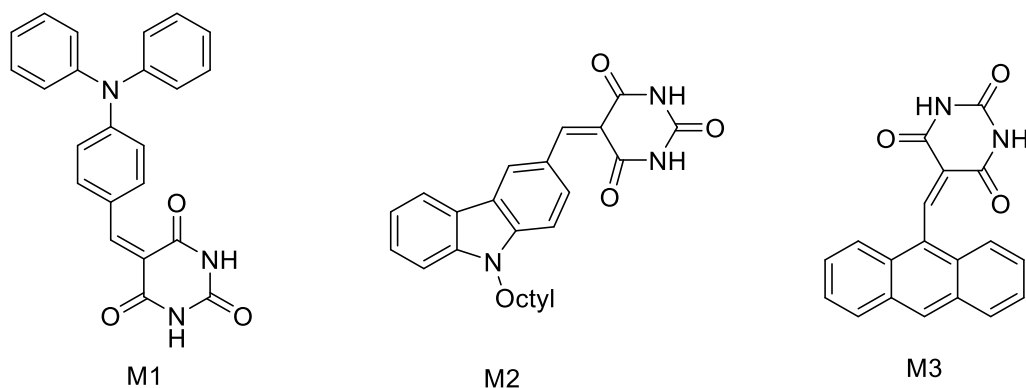


Figure 1.13. Chemical structures of barbituric acid derivatives namely **M1**, **M2**, **M3** with triphenylamine, carbazole, anthracene, respectively used for mercury sensing.

1.4. Fluorescent molecules for sensing of anions

Now a days it very much needed to develop the method for recognizing and sensing of environmentally and biological analytes and considered important field in chemical sensor. This is because various biological, chemical and physiological processes are governed by different analyte/ species such as anions and cations. Anions play very important role in chemical biological aspect such as F^- , Cl^- , Br^- , I^- , HCO_3^{2-} , HPO_4^{2-} , OAC^- , CN^- , NO_3^- , HSO_4^- . Amongst various anions F^- and CN^- are the most commonly recognized and investigated. Fluoride with highest charge density, small ionic radii, hard Lewis basic nature led to design of fluorescent receptor which focuses on host/guest chemistry in the field of supramolecular chemistry. Fluoride sensing can be achieved by protonation and deprotonation mechanism, deprotection mechanism, hydrogen bond interaction. While the cyanide sensing can be achieved by hydrogen bond interaction, or via substitution reaction. Herein few examples discussed for sensing of anion [68].

Chen and co-workers synthesized turn on fluorescent probe based on difluoro boron dipyrromethene (**BODIPY**) dye conjugated with hydrazone (**BDBH**) for selective and sensitive detection of fluoride anion. The receptor **BDBH** [**S1**] consists of N-H group which act as binding site for Fluoride. When tetra butyl ammonium salt of F^- anion was added to the

solution containing receptor **BDBH** the solution shows “turn on” fluorescence. This occurs via deprotonation of N-H proton with the incremental addition of F^- [69].

Another example of fluoride sensing which clearly exhibit the protonation and deprotonation sequence for sensing of fluoride anion. Herein Nadimetla *et.al.* synthesized TPE cyclic urea based fluorescent molecule for sensing of fluoride anion. In their work TPE is used as the donor moiety with cyclic urea contain NH protons are used as receptor species. [S2] The fluorescent molecule shows fluorescence quenching with addition of F^- anion [70]. However, our group recently studied that OH^- containing receptors are also susceptible for sensing of fluoride by deprotonation reaction via proton abstraction from the hydroxyl group. The molecule was synthesized by using quinoxaline as donor and Schiff's base as receptor contain OH^- group. [S3] The molecule showed good AIE phenomenon when F^- anion was added to the receptor solution complete quenching of fluorescence was observed. The F^- anion interacts with hydrogen of hydroxyl group in receptor by deprotecting and resulting in to formation of HF_2^- complex which was confirmed by 1H NMR study. From 1H NMR data it is confirmed that the hydroxyl hydrogen peak appearing at 13.5 disappear completely with the appearance of triplet in the region of 15.85 ppm to 16.6 ppm [71]. The structures of the compounds are shown in **Figure 1.14**.

In addition to fluoride anion, cyanide is one of the most toxic and caused terrific effect on human health and environment. Therefore, it is very crucial to detect the F^- and CN^- ion below its detection limit. Usually, the mechanism involved for sensing application goes via hydrogen bonding but other approach that is more prominent for cyanide sensing is via anion induced reaction finally resulting in to formation of new compound. Based on this criteria Borah and co-workers developed BODIPY based fluorescent molecule for selective sensing of F^- and CN^- ion reaction mechanism as shown in **Figure 1.15**. below [72].

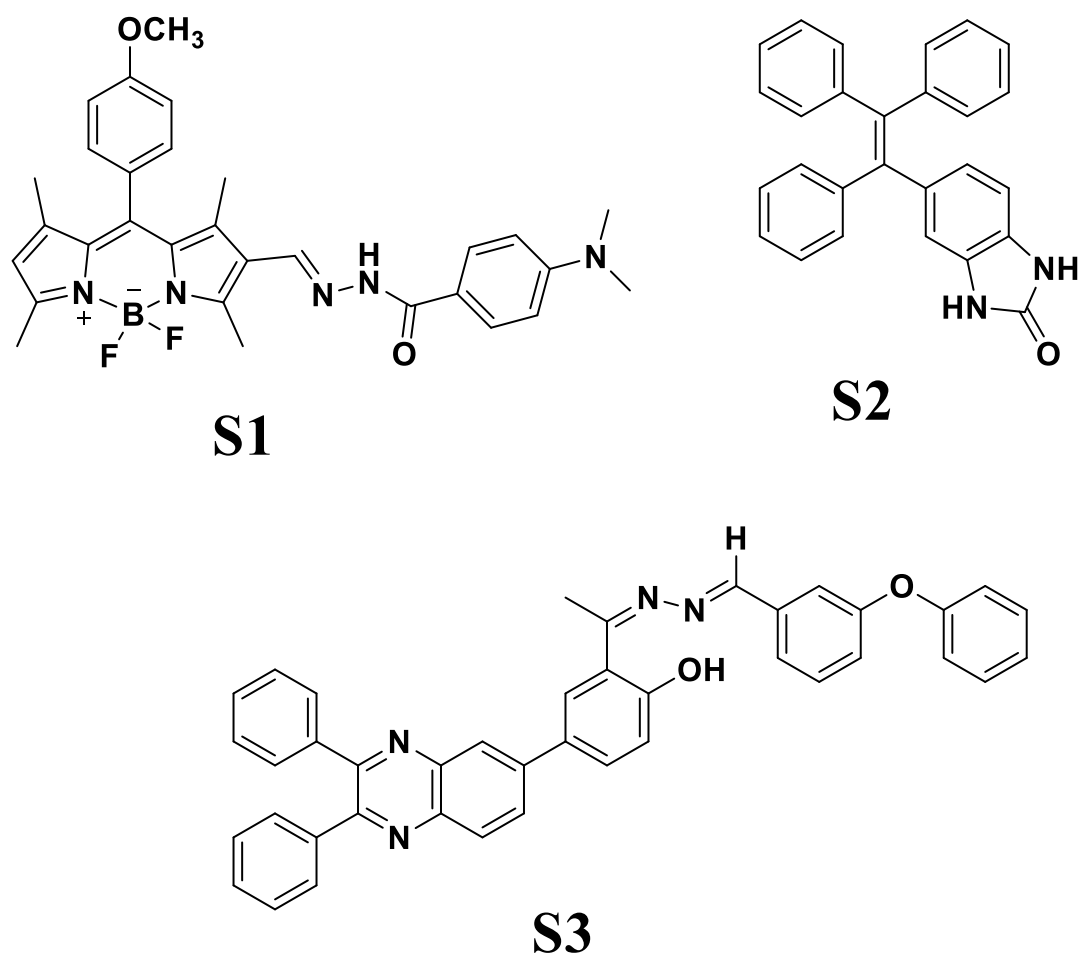


Figure 1.14. Structure of fluorescent molecules for sensing of F^- ion.

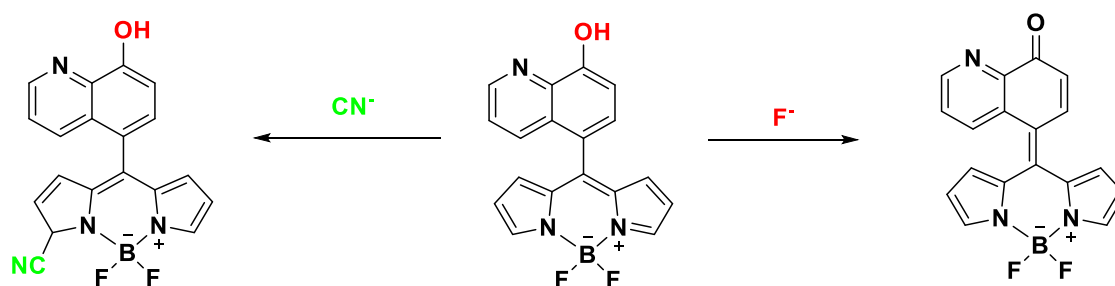


Figure 1.15. BODIPY fluorescent probe for F^- and CN^- ion sensing

Kim *et.al* synthesized naphthaliimide derivative with imidazole receptor moiety for sensing of CN^- and F^- ion. The fluorescent molecule was synthesized by linking naphthaliimide unit and benzimidazole moiety connected through phenyl as a spacer **Figure 1.16**. The binding with CN^- and F^- was successfully examined by UV-Vis absorption, fluorescence emission study and ^1H NMR studies. When CN^- and F^- anion was added to the solution of the probe changes the color from yellow to reddish orange. The observed color change as well as photophysical change was due to deprotonation of N-H of the imidazole moiety which is actually recognition unit of the synthesized probe [73].

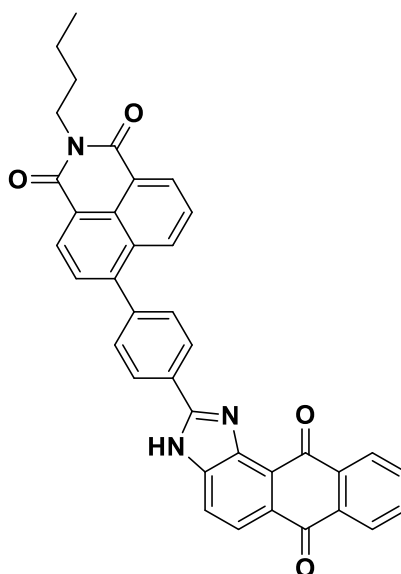


Figure 1.16. Structure of the Naphthaliimide functionalized imidazole.

1.5. Fluorescent molecules for sensing of neutral molecules/ biomolecules

Carbohydrates—fiber, starches and sugars are essential food nutrients that turn into glucose as a source of energy for body functioning [74]. Glucose and other saccharides are the class of compounds belonging to carbohydrates which are considered very important for daily life, for example, glucose, fructose, and other saccharides. Classification of different carbohydrates as represented in **Figure 1.17**. [75]. As said carbohydrates are not only essential nutrients but high levels of the carbohydrate may result in serious health issues. One major health problem is blood sugar level widely known as “Diabetes” [76,77]. After meals, carbohydrates are broken

down into glucose causing the blood sugar level to increase resulting in the production of insulin, a hormone that allows the body to use that as energy or storage. Further the continuous increase in the blood sugar level resulting to decrease in the production of insulin commonly known to be insulin resistance. Therefore, there is a need of determining the blood glucose level and control the level of sugar in the body reducing the health effect. [78,79]

Diabetes or Diabetes Mellitus is a metabolic disorder resulting in to increase in a high level of blood sugar further creating other health complications such as cardiovascular diseases, chronic kidney diseases and stroke. It is considered one of the leading causes of death all over the world [80,81]. According to recent reports from the International Diabetes Federation increase in the diabetes has resulted in the greatest burden on the individual and government sector all over the world. Therefore, there is a need of developing efficient methods for diagnosis and further treatment of the patients. The earliest detection of diabetes helps to improve the life for individual safety and health and plays crucial role in order to initiate the treatment for the individual safety and health. Monitoring of blood glucose concentration plays a significant role that helps in the diagnosis and prevention of diabetes. The commonly employed method for glucose sensing is the use of an electrochemical sensor. First the enzymatic glucose with glucose oxidase immobilization works on the catalytic oxidation of glucose in presence of oxygen as a mediator. Secondly, nonenzymatic glucose sensor which is stable but needs to overcome the higher overpotential of glucose oxidation [82].

Looking into the significance of glucose sensing, very few reports are available that cover insight into this concept. Many scientists explored the field such as electrochemical sensors for glucose determination, fluorescence method, Raman spectroscopy, IR-spectroscopy and so on. However, this book chapter provides an overview of various sensing methods and different strategies with the advancement in technologies for glucose monitoring [83].

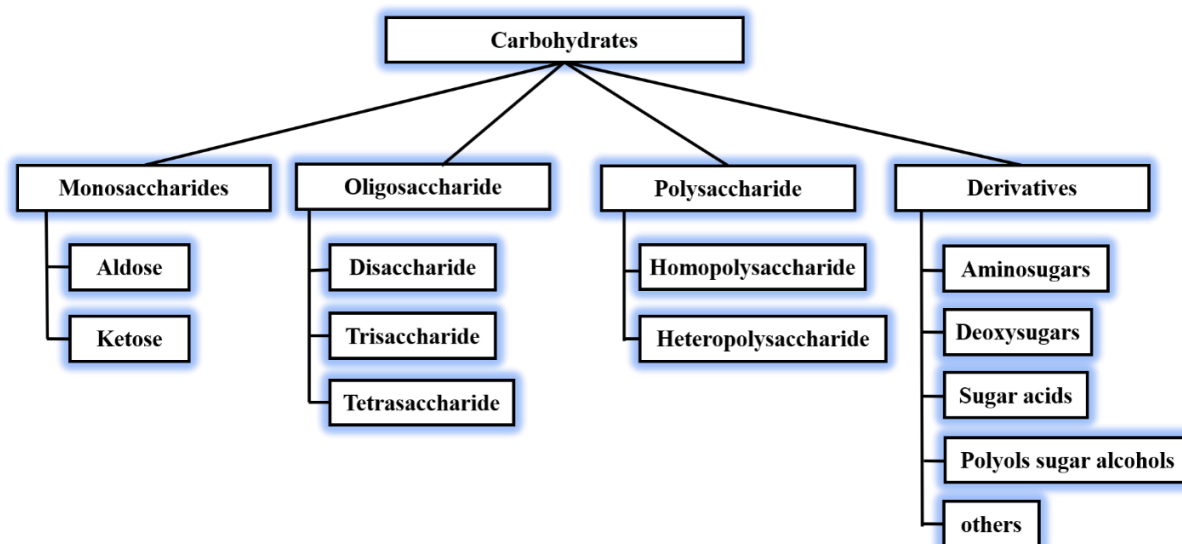


Figure 1.17. Classification of carbohydrates

There are many organic fluorescent molecules for the detection of neutral molecules using boronic acid through covalent interaction as it has excellent hydrogen bond formation capacity in aqueous media. The Shinkai and coworkers instigated the boronic acid compound for the effective detection of the glucose for the first time [84]. But few boronic acid functionalized receptor lacks electronic charges which tend to interact with neutral molecule and an important factor is pH which plays an important role as the saccharide and boronic acid forms the complex at high pH by forming the boronate anion therefore to overcome the disadvantage James *et al.* modified and synthesized a novel photoinduced electron transfer fluorescent sensor based functionalized with boronic acid and amine for saccharide detection. In this work, compound **II** doesn't inhibit the photoinduced electron transfer (PET) quenching process though having boronic-amine interaction but compound **III** contains the separated amine from boronic acid at very high pH so fluorescence got quenched. While the interaction of saccharide inhibited the electron transfer process resulted in high fluorescence in compounds **IV** and **V**. The schematic presentation for binding of D-glucose as shown in **Figure 1.18**. [85,86].

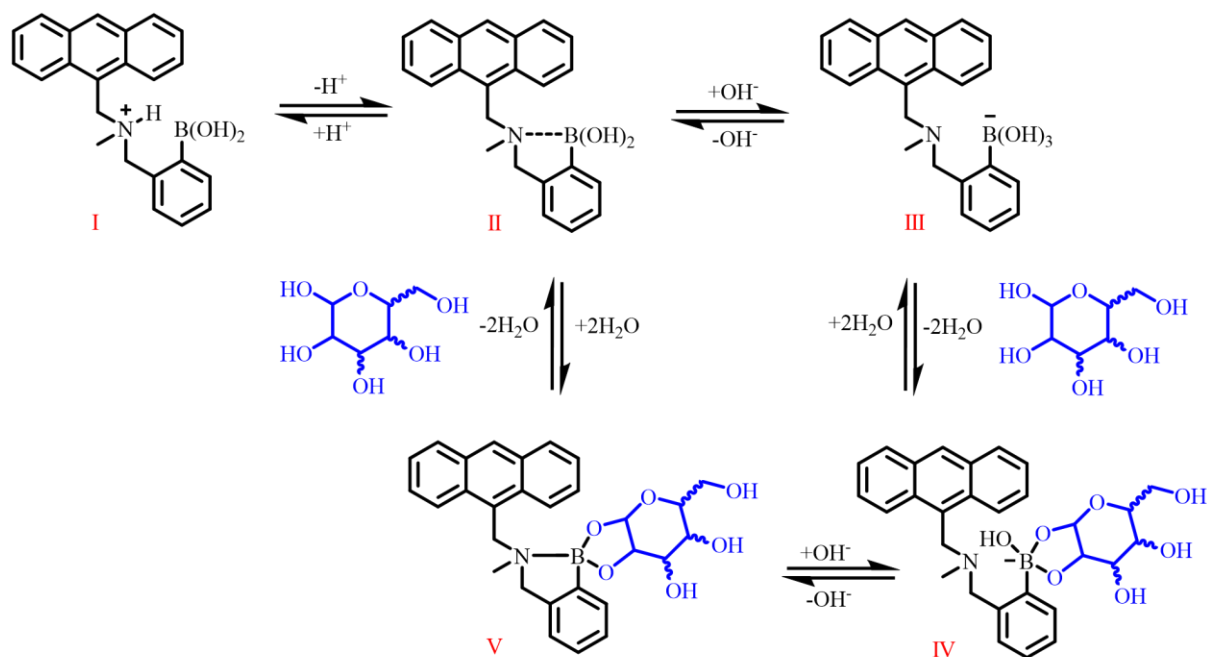


Figure 1.18. Schematic representation for binding interaction with glucose.

Yang and co-worker designed another fluorescent molecule that is combined with boronic acid and a guanidium recognition site onto the anthracene derivative. This molecule shows the reversible formation of cyclic ester and strong interaction between the guanidium moiety and carboxylate. Further, the fluorescence experiments were conducted by using simple anthracene substituted with guanidine and anthracene with boronic acid as the control compound to study the effect of saccharides on the receptor. It is observed that the control compound substituted with guanidine did not exhibit any change in fluorescence upon addition of glucarate, upon addition of the glucarate to anthracene substituted to only boronic acid with glucarate addition showed a change in fluorescence however the magnitude was smaller. The receptor with two different binding sites showed a prominent response to spectral change upon the addition of D-glucarate. As shown in **Figure 1.19**, different derivatives of anthracene are substituted with guanidine and boronic acid (**1**, **2**, **3**). This change is mainly due to the boronic acid and guanidium-specific binding site on the anthracene derivative with two binding modes as appropriate linker length and excellent rigidity. This rigidity is mainly due to the glucarate binds more strongly with glucuronic acid indicating that both the carboxylates are involved in

binding via interaction with guanidium chain [87,88].

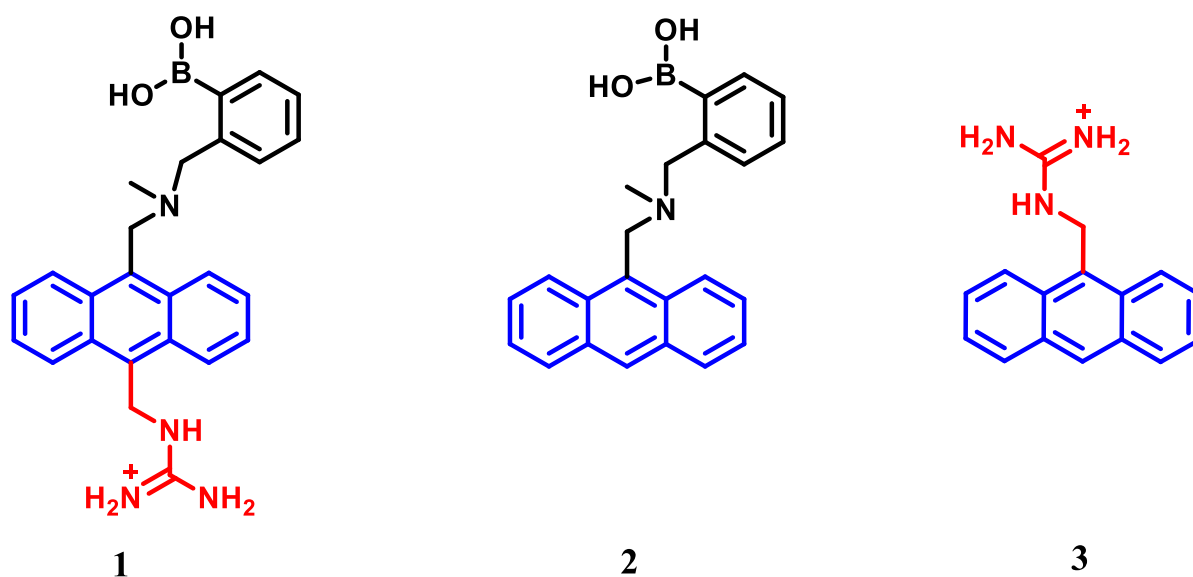


Figure 1.19. Derivatives of guanidine and boronic acid substituted anthracene derivative

Zhang and group for the first time successfully designed the boron doped graphene quantum dot which operates on the abnormal mechanism known as aggregation induced emission process. Thus by using the concept of aggregate formation and intramolecular rotations giving reproducible enhancement in fluorescence which was first time observed in graphene quantum dots which is well explained in this work. A hydrothermal approach was utilized for preparing the Boron doped graphene quantum dot (**BGQDs**). The boronic acid functionalization on the **BGQDs** facilitates the use of the quantum dot glucose detection. Since the glucose consists of the cis diol units which easily get coordinated with boronic acid group. Upon binding of diol to boronic acid group on the functionalized graphene quantum dot it forms the rigid BGQD-glucose aggregate, thus restricting the free rotation resulting in to enhancement of fluorescence intensity **Figure 1.20**. From this it is revealed that the boron doped quantum dot is highly specific and sensitive for detection of glucose over other saccharides such as fructose, galactose and mannose. In conclusion the doped boron atom on to the GQDs which creates the new platform which has great scientific importance [89,90].

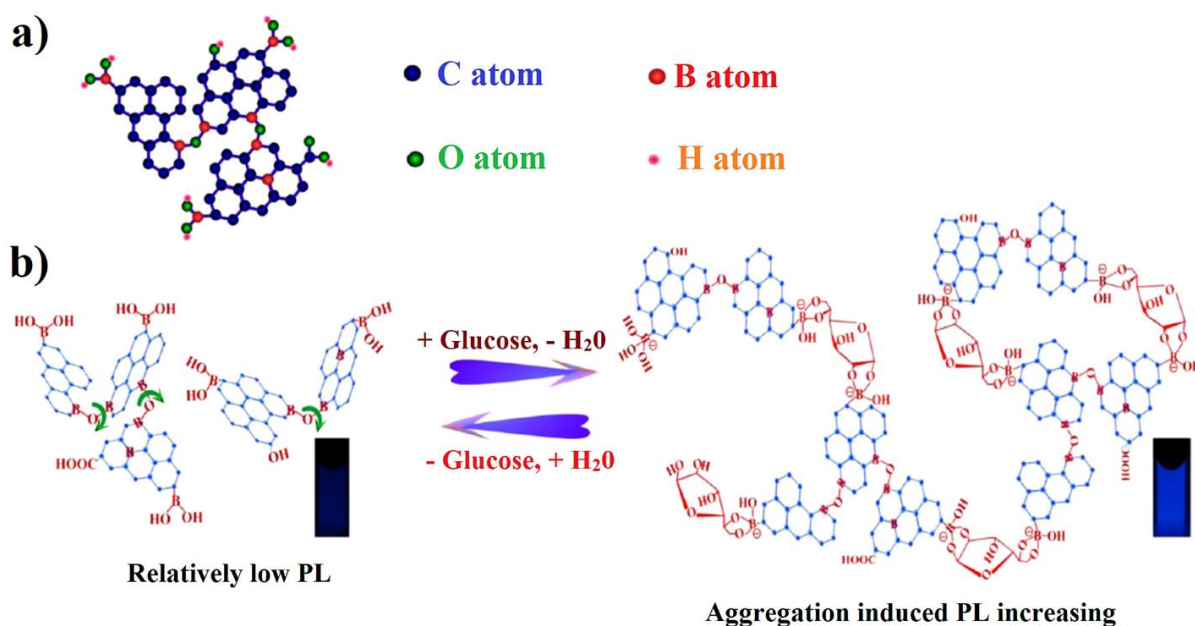


Figure 1.20. The picture represents the Boron-Doped Graphene Quantum Dots (BGQDs). (b) shows the aggregation induced emission interaction between the BGQDs and glucose resulting into enhancement in fluorescence.

1.6. Organic fluorescent molecules for Temperature, pH and Viscosity sensing

Temperature, pH, and viscosity are the important fundamental physiological parameters and gained enormous attention due to its wide biomedical application. Recently the molecular sensor is used extensively for change in behavior for external stimuli such as light, temperature, pH and viscosity. Broad range of biological activities especially biological reactions which include enzyme activity, gene expression, energy metabolism and cell division in living cell organelle [91]. Abnormal changes in pH, temperature results in to various cellular microenvironment to dysfunction. It is difficult to measure the temperature pH and viscosity of the small confined individual cell, however there are several conventional methods to detect the parameters. Therefore, fluorescent molecules have shown promising results and increasing demand for biological due to its high selectivity, spatial resolution and rapid response time. However accurate sensing of the pH, temperature and viscosity in individual cells still

remaining challenging [92].

From last past few years, number of fluorescent materials have been developed for thermosensitive, pH sensitive and viscosity sensing but still it is difficult to characterize these parameters and has certain limitations such as lack of hydrophilic nature, leakage of cell, poor structural stability and biotoxicity. Therefore, to overcome these problems fluorescent material with polymeric materials were designed and synthesized to employ for monitoring the insight in to temperature, pH and viscosity measurement intracellular in live cell. The polymeric fluorescent material comprises of thermo-responsive unit and conventional fluorescent moiety. Herein few examples for selective and sensitive sensing of intracellular temperature, pH, and viscosity sensing. The polymeric organic fluorescent material with aggregation induced emission has gained lot of attention. Herein Chen and co-worker designed and constructed thermos-responsive elastin like polypeptide (ELPs) connected with TPE used for temperature sensing. The synthesized derivative consists of val-pro-gly-xaa-gly (VPGXG) pentapeptide the guest residue X represents any amino acid other than proline. It was noted that with change in amino acid the ELPs shows tunable change with respect temperature change from between 0°C to 100°C. **Figure 1.21.** The photophysical properties of ELPs40-TPE and ELPs40 were studied by measuring absorption and emission spectra. The ELPs-40 with TPE showed excellent aggregation induced emission properties. Further the ELPs40-TPE was investigated for temperature sensing property and it was observed that the molecule showed gradual decrease in fluorescence intensity as the temperature increases from 5°C from 25°C to 50°C with excellent linear regression coefficient of 0.9953. The reversible nature of ELPs40-TPE was observed by decreasing and increasing the temperature. It noted that the molecule shows decrease in fluorescence intensity while fluorescence slowly reappears as the temperature turns back to 25°C [93].

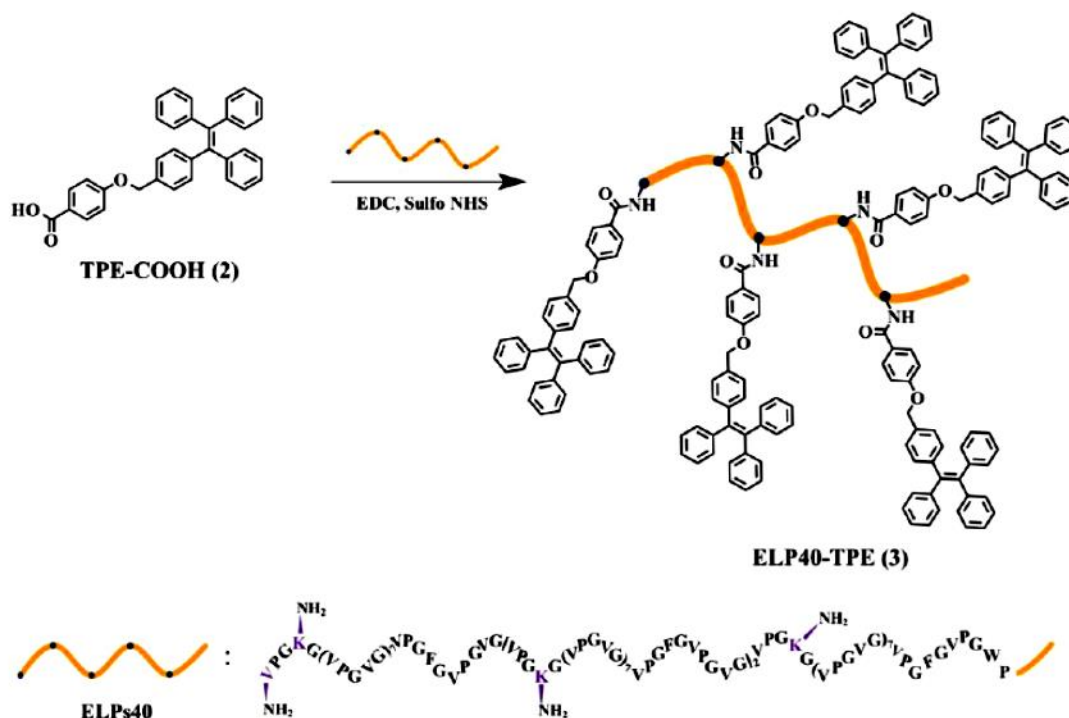


Figure 1.21. Schematic illustration of polymeric elastic ELP-40 derivatized with tetraphenylethylene molecule for temperature sensing.

Wang *et.al* synthesized long-term cellular tracing TPE-based AIE active polymer which can be employed as temperature-sensitive fluorescent organic nanoparticle with aggregation-induced emission [94]. This temperature-sensitive organic nanoparticle with the AIE effect was synthesized with tetraphenylethylene based poly(*N*-isopropylacrylamide) (TPE-PNIPAM) via atom transfer radical polymerization (ATRP). The obtained TPE-PNIPAM shows good AIE characteristics in water which self-assembles into nanoparticle [95,96].

A donor- π -acceptor luminogen, 2-([1,1'-biphenyl]-4-yl)-3-(4-((*E*)-4-diphenylamino) styryl) phenyl) fumaronitrile (TBB) ratiometric organic fluorescent thermometer was synthesized by Meng *et.al* based on TICT near-infrared for intracellular temperature sensing. The TBB was designed by encapsulating NIR fluorophore TBB and Rhodamine 110 dyes into an amphiphilic polymer matrix F127 to yield TBB&R110@F127 nanoparticle (TRF NPs) which showed excellent temperature response in the temperature range of 25°C to 65°C and good aggregation induced emission.

Since the TRF NPs has reversible temperature sensing nature and therefore it is employed for intracellular temperature sensing application with temperature change from 25°C to 53°C. It is observed that the emission decrease as the temperature increases at 680 nm while emission intensity remains unchanged at 520 nm. The stability and reversibility studies were performed for TRF NPs with heating and cooling cycles from 25°C to 65°C which remained constant throughout the analysis indicating the excellent stability [97]. **Figure 1.22.**

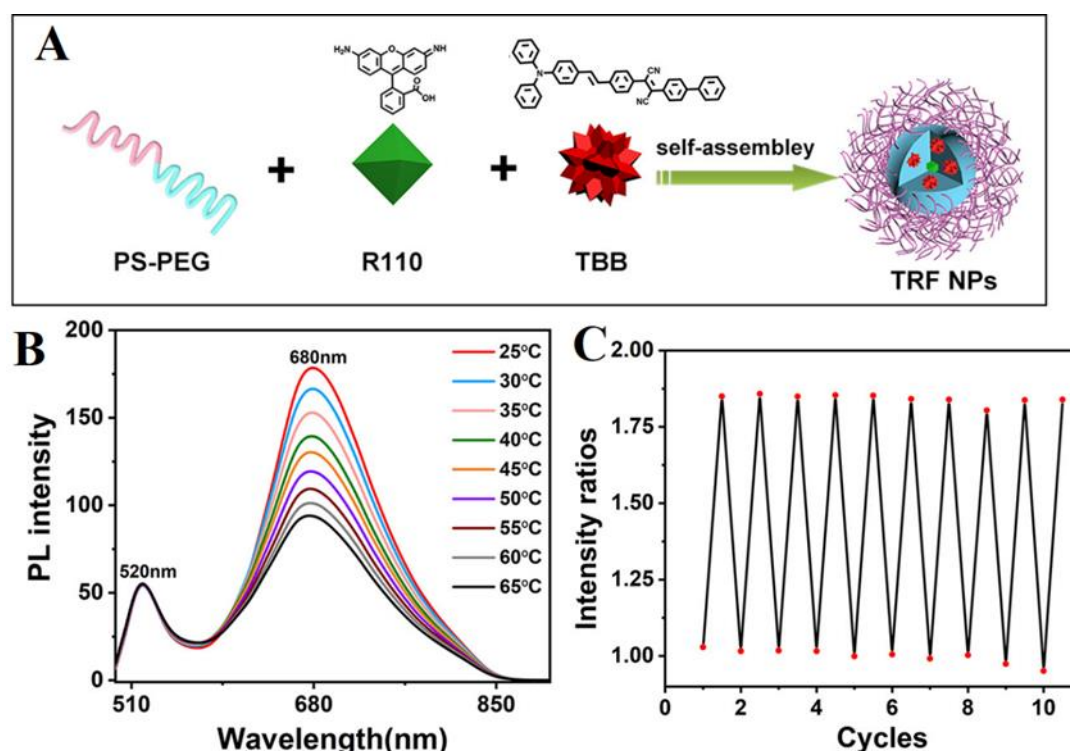


Figure 1.22. A) A diagrammatic representation of the self-assembly and fabrication for TRP NPs. B) A photoluminescence emission spectrum of the TRF NPs at temperature range from 25 °C to 65 °C. C) A plot represents ratio reversibility by successive heating and cooling of TRF NPs.

pH is another physiological parameter that is important for maintaining various biological, chemical and environmental process. Therefore, it is very important for accurately measuring the pH. The pH of blood and intracellular fluid is 7.35-7.45. Most of the time frequently pH electrode is used for pH determination due to certain drawbacks such as rigid design,

mechanical fragility and temperature dependent response. However, the pH electrode has limited applications, therefore to overcome the problem optical pH sensing has explored wide application in various field. Optical properties can be well performed with absorption and fluorescence study which shows distinct changes upon protonation and deprotonation at different pH values. Many organic florescent molecules have been employed so far for intracellular pH determination but these fluorescent molecules usually exhibit single fluorescence intensity variation as the pH changes however, sometimes it shows toxicity with non-specific binding site and requires other source to transfer in the cell for intracellular determination of pH [98].

An AIE active hemi cyanine fluorogen red/emissive fluorescent molecule was designed by Chen and co-workers deigned with sensing range by switch + knob effect. The red emissive zwitterionic dye hemi cyanine dye composed of TPE and N-alkylated indolium moiety (TPE-Cy). The molecule showed excellent photophysical property along with high sensitivity towards H^+/OH^- . TPE-Cy can sense the pH in the wide range of pH by exhibiting different color change and emission intensity. It was observed that as the pH range changes for pH 5-7 moderate red emission was observed while at pH 7-10 weak emission in addition as the pH increases form 10-14 strong blue emission was observed. This present study on the fluorescence molecule helps to design various fluorescent material for pH sensing. the synthesized dye exhibited excellent biocompatible and cell permeability making the dye promising for intracellular detection of pH in wide range of physiological pH from acidic to basic with intense red to blue emission. Thus, the use of the TPE-Cy for intracellular pH sensing was monitored by confocal microscopy, radiometric analysis and flow cytometry **Figure 1.23**. [99, 100].

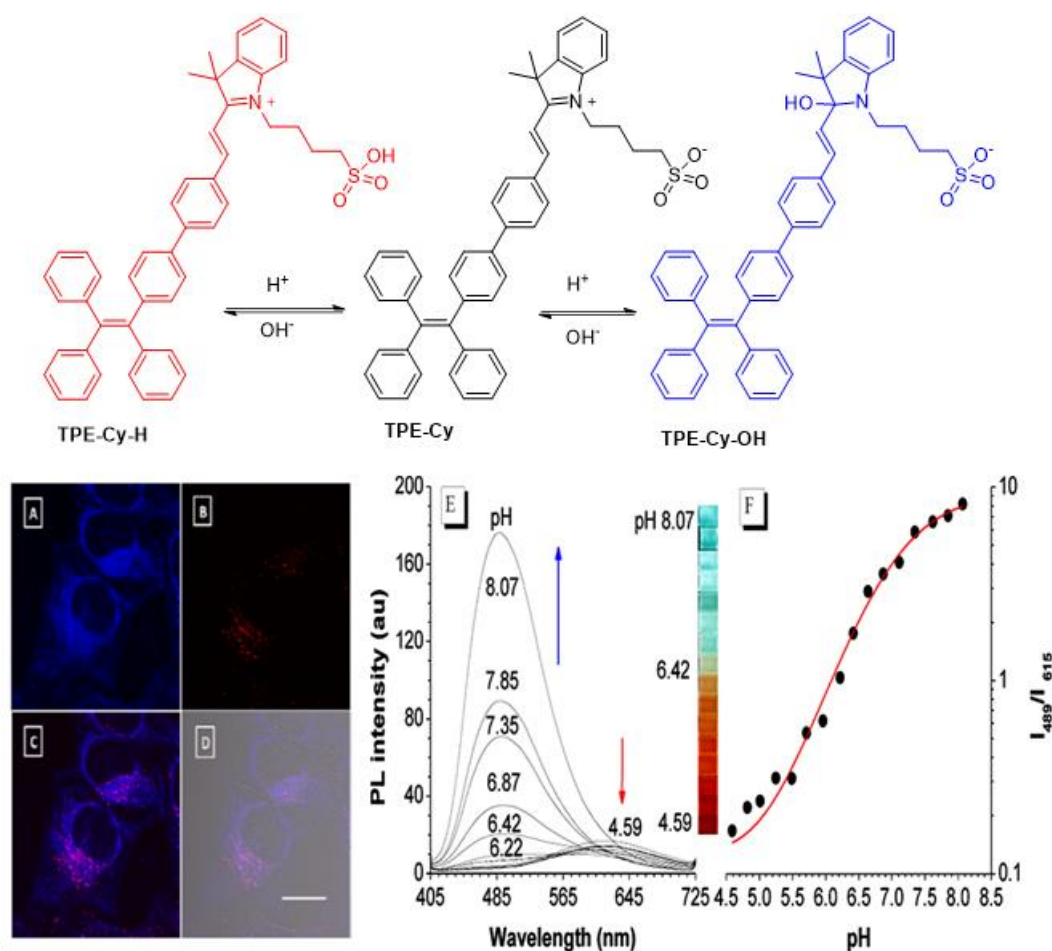


Figure 1.23. Schematic illustration showing mechanism of pH change response of **TPE-Cy**. **(A)** Confocal images of TPE-Cy on HeLa cells at 405 nm and **(B)** confocal image at 488 nm **(C)** merged confocal image of panel A and B, **(D)** a confocal image merged from field image the (bright C). **(E)** Represents the emission spectra for TPE-Cy at various pH and buffer ranges in the presence of 1,2-dioleoyl-glycero-3-phosphocholine (DOPC). **(F)** A plot PL intensity versus pH of solution at 489 and 615 nm respectively.

An aggregation-induced emission luminogen of 2-(5-(4-carboxyphenyl)-2-hydroxyphenyl) benzothiazole was designed and synthesized Li and co-workers. The luminescence properties in different solvents were investigated for compound. Variation in emission properties arises from the prototropic equilibrium in various solvents and this tunability is based on the excited state intramolecular proton transfer and restriction of intramolecular rotations in addition this also resulted in to reversible acid/base switched yellow cyan emission. The proposed

mechanism states that the photophysical luminescence properties are influenced by protonation and deprotonation reaction. The synthesized benzothiazole compound was used for fluorescence imaging and for studying the intracellular pH sensing using HeLa cells. **Figure 1.24.** [101].

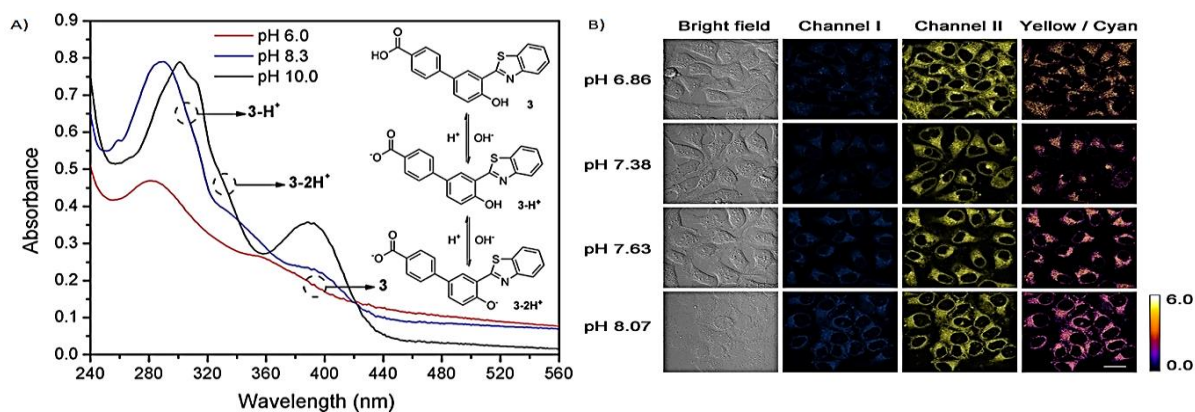


Figure 1.24. A) Absorption spectra of the compound at three different pH. (Inset represents the protonation and deprotonation sensing mechanism for compound **3** at 50 μ mol/L and B) The representation of confocal images at different pH buffers on incubation of HeLa cells at 50 μ mol/L compound.

A series of 4-*N,N*-dimethylaminoaniline salicylaldehyde Schiff base AIE active derivative (DAS) was synthesized Qi feng and group. the compound showed good aggregation induced emission property along with high fluorescence quantum yield in aggregated state. The pH dependent properties indicates that the series of compound prepped has potential application in pH sensing. Fluorescence changes were observed at different pH ranging from 2.0 to 10.0. it is observed that the compound exhibited strong fluorescence in alkaline condition and different fluorescence in acidic condition [102].

A pyridyl functionalized tetraphenylethene ratiometric fluorescent (Py-TPE) was developed by Bhosale *et.al* for intracellular pH sensing. The synthesized probe was used as reversible probe for sensing acid/ base in solution as well as in live cells. Its photophysical properties such as absorption, emission and naked eye detection was performed in different solvent such as

(MeOH, DMF, CHCl_3). Upon protonation and deprotonation distinct color change was observed under naked eye using Py-TPE probe. The observed color change was from light yellow to green in acidic condition trifluoroacetic acid (TFA) but when triethylamine (TEA) was added the colour of the solution reverse back to yellow in DMF, Methanol and chloroform **Figure 1.25**. In addition, the molecule was successfully employed for detection of intracellular pH in live cell which was performed by recording the confocal images under confocal laser microscopy at different pH (at pH 3, pH 7, and pH 9). **Figure 1.26**. [62].

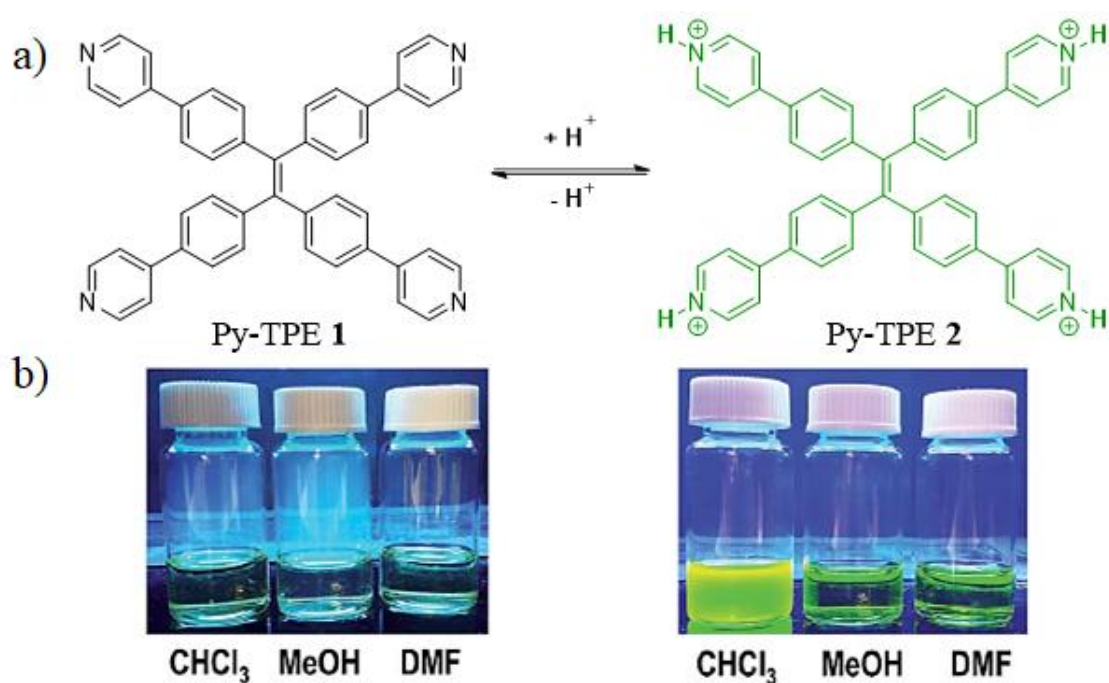


Figure 1.25. Mechanism of protonation-deprotonation for Py-TPE receptor (1 & 2). B) Photographs under UV light illumination ($\lambda_{\text{ex}}=365\text{nm}$) of receptor Py-TPE (1 and 2) ($0.5\mu\text{M}$) in presence and absence of TFA($2\mu\text{M}$) at room temperature in different solvent system.

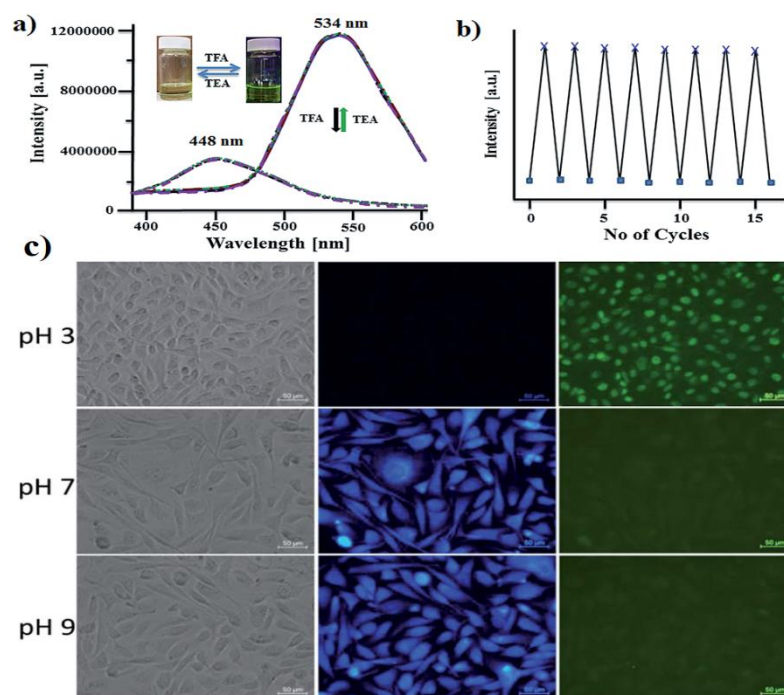


Figure 1.26. Emission spectra recorded upon addition of TFA and TEA in **1** (1×10^{-5} M) in DMF ($\lambda_{\text{ex}} = 365$ nm). B) A plot of reversibility study performed at 534 nm (fluorescence intensity vs. number repeated cycles) upon addition of TFA and TEA. c) Cell imaging application imaged under Confocal fluorescence microscope of Py-TPE receptor with ($5 \mu\text{g mL}^{-1}$) for PC-3 cells treated for 2 hours at different pH condition.

Beside the temperature and pH another parameter that is considered as an important factor in intercellular processes is viscosity which can be monitored by using fluorescent material. The viscosity of cell membrane and cytoplasmic viscosity can be monitored from cellular level to organism level which helps to detect various diseases. There are number of conventional methods for determining the viscosity but at cellular level it is very difficult to employ the capillary viscometer or rotational viscometer for intracellular viscosity measurement. Therefore, one of the best approaches is the use of molecular rotors and fluorescent material such as AIE active materials and dyes [103,104,105]. A viscosity dependent fluorescent emission and quantum yield can be used for better characterization which is described by Forster Hoffmann Equation [106].

$$\Phi_f = Z \eta^\alpha$$

Where Z and α are constants

η = viscosity

Fluorescence quantum Φ_f and life time τ_f can be solved for molecular rotors by using Hoffmann Forster equation [107].

Herein the carbazole styryl based fluorescent molecular rotors (FMR) was developed by Kumbhar and coworkers which are functionalized with different functional groups at C=C bond. Depending upon change in the chemical functionality the fluorescent properties of the molecular rotor's changes. These derivatives are highly responsive to viscous medium in which low viscous medium shows free rotation of C=C bond but as the viscosity of the solution increases there is restriction of free rotation along the C=C bonds. The chemical structures are as represented below in **Figure 1.27**. [108].

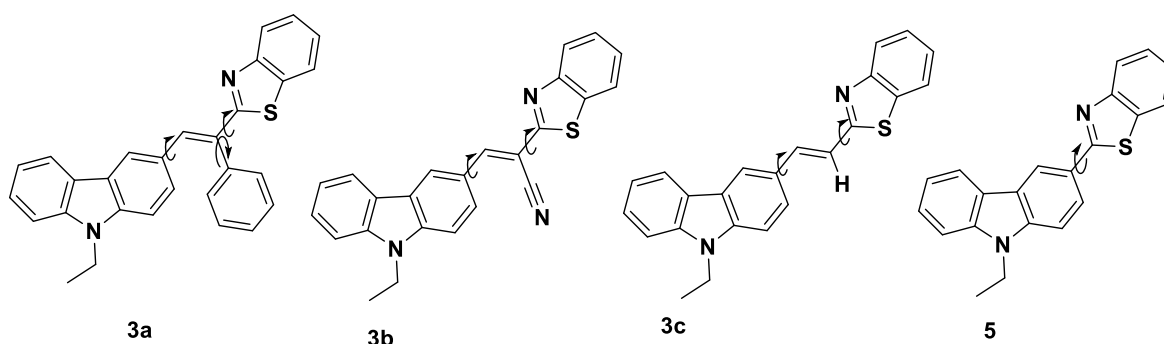


Figure 1.27. Structure of the carbazole styryl fluorescent molecular rotors.

Derivatives of Binol are considered an important fluorescent material for viscosity sensing herein Yang et.al. synthesized Binol derivative by using axially chiral 1,1-binaphthol (BINOL) and 1,4-dihydropyridine and axially chiral 1,4-dihydropyridine derivative [(R)-/(S)-2] with AIE was designed. This fluorescent material shows excellent application in chiral recognition and very useful in fluorescence imaging. Viscosity dependent behavior was investigated for the [(R)-/(S)-2] by adding glycerol to the solution. It is observed that as the fraction of glycerol

increases from 0% to 80% emission intensity gradually increases for [(R)-/(S)-2] [109]. In addition, Chen and coworkers developed TPE-Cy fluorescent material that has excellent AIE active property and used for mapping viscosity in live cell. In this study the fluorescence intensity increases as the viscosity increases which was performed by using the glycerol and ethylene glycol. Viscosity measurement is not only important for living cell measurement but also an important quality parameter in fluid drinks. Food spoilage in most of the cases are indicated by the viscosity of that liquid [110]. Herein Xu et.al. developed new infrared fluorophore based on tetranitrile anthracene (TPAEQ) to determine the viscosity.

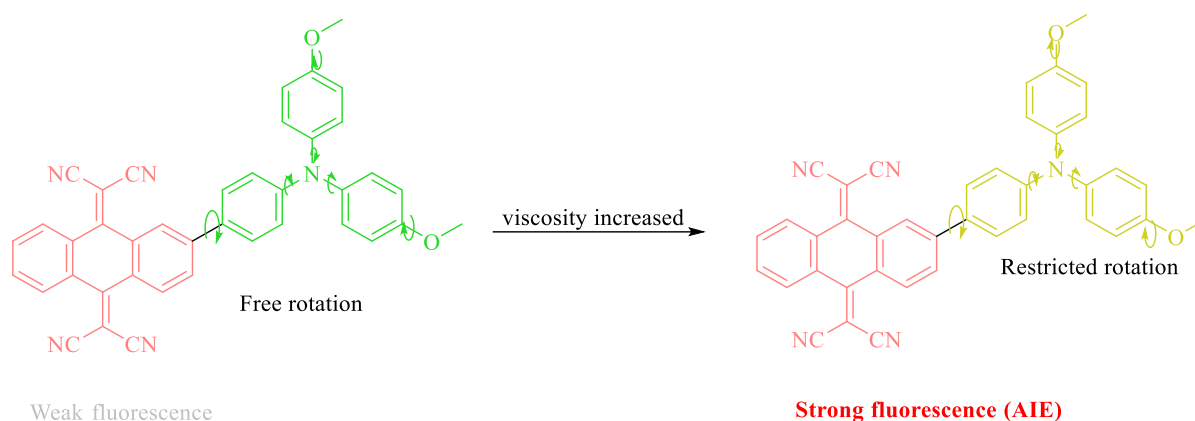


Figure 1.28. Schematic pathway for viscosity sensing by using TPAEQ

This fluorescent molecule consists of triphenylamine ether as donor while anthraquinone diamino nitrile as acceptor moiety. **Figure 1.28.** The dialkyl ether and triphenylamine exhibit free rotation in low viscous medium while as the viscosity increases intramolecular rotations of the molecule is restricted which results in to enhancement in fluorescence intensity. This fluorescent probe was utilized for monitoring the spoilage of fluid drinks by measuring the viscosity. In this study various fluid drinks were selected such as fruit juice, Kaman juice, jasmine tea juice, pear juice, sea buckthorn juice, Jam, liquor and milk. To all these fluids food thickeners such as sodium carboxymethylcellulose pectin and Xanthan gum was added and emission properties were studied. It was observed that as the concentration of food thickeners increases fluorescence intensity increases [111]. An AIE active styryl quinone fluorophores

were designed by Dou and coworkers. This styryl quinone molecule display strong fluorescence in solid state while exhibit poor fluorescence in organic solvents. The chemical structures of the molecules are shown below in **Figure 1.29**. this molecule showed excellent AIE active property hence these derivatives are used for biological application for viscosity and pH sensing [112].

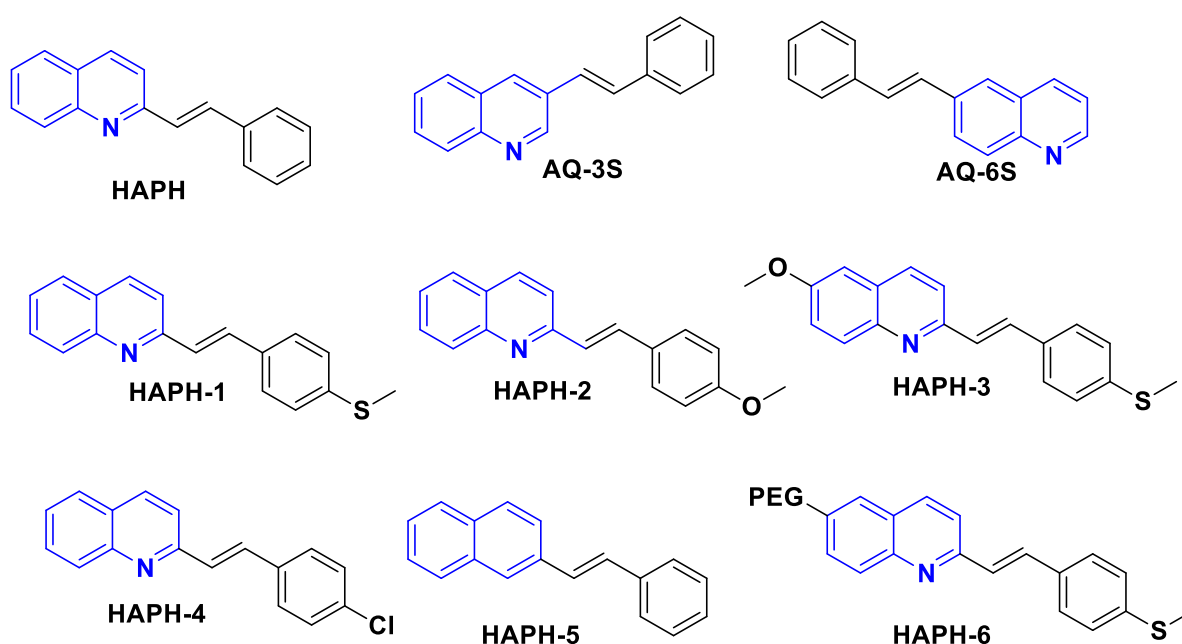


Figure 1.29. The chemical structure of different AIE active styryl quinones.

1.7. Conclusion and Future outlook

In this, chapter I have introduced to the field of supramolecular chemistry and how supramolecular chemistry can be used for chemical sensing application in order to sense various essential, non-essential as well at the toxic ions. In this I have also introduced briefly about the aggregation induced emission phenomenon and how the phenomenon drives towards the sensing application. The various organic fluorescent molecule consists of donor acceptor moiety that can be utilized not only for sensing application but can be utilized for various other application in different field of science and technology. The fluorescent molecule shows wide

application for biological cell imaging application, in drug delivery system, forensic science, food industry for detection of toxic contaminants, for determination of pesticides and so on.

Different organic fluorescent molecules have been described such as TPE based, pyrene, NDI, organic dyes and AIE active metal organic frameworks (MOFs) etc. for detection of environmental toxic pollutants such as CN^- , Hg^{2+} , Cu^{2+} , Pb^{2+} , Sb^{3+} , Pd^{2+} , Cd^{2+} , F^- , NO_3^- , As^{3+} , hydrazine. These organic fluorescent molecules are not only used for sensing of toxic pollutants but can be successfully utilized for sensing of intracellular pH, temperature, and viscosity measurement. In addition, the fluorescent molecule has shown extended application in the field of theranostic application for drug delivery system.

This chapter also explores about the various fluorescent molecules for biomolecules (neutral) sensing. Different optical methods were developed for glucose sensing most common methods are by using boronic acid, concanavalin A-based molecules, enzyme-based glucose sensor carbon dot functionalized glucose sensor, polymer-based glucose sensor and other spectroscopic methods are also available for glucose sensing such as Infrared Raman and Photoacoustic spectroscopy. In this I have briefly described various organic fluorescent molecules for glucose sensing with the most possible binding mode of glucose to the receptor moiety that is used for sensing application.

From thorough literature we designed different fluorescent molecule for sensing of various analyte using the host guest chemistry in the field of supramolecular chemistry. Thus, from these it can be concluded that in future if we modify these fluorescent molecules by functionalizing its application can be extended further in various other field of scientific technology and development. There is still need of developing various optical methods for sensing of analytes by employing simple and easy methods for synthesis and detection over wide range of instrumental methods. This will help many researchers to develop new strategies and new scope in the development of research in sensing.

1.8. References

- (1) Samal, A.; Pradhan, B. B. Impact of Industrialization on the Environment. *Int. J. Psychosoc. Rehabil.* **2019**, *23* (6), 292–298. <https://doi.org/10.37200/IJPR/V23I6/PR190769>.
- (2) Ahmed, F.; Ali, I.; Kousar, S.; Ahmed, S. The Environmental Impact of Industrialization and Foreign Direct Investment: Empirical Evidence from Asia-Pacific Region. *Environ. Sci. Pollut. Res.* **2022**, *29* (20), 29778–29792. <https://doi.org/10.1007/s11356-021-17560-w>.
- (3) Mudu, P.; Terracin, B.; Martuzzi, M. Human Health in Areas with Industrial Contamination. **2014**, 380.
- (4) Hernández, F.; Bakker, J.; Bijlsma, L.; de Boer, J.; Botero-Coy, A. M.; Bruinen de Bruin, Y.; Fischer, S.; Hollender, J.; Kasprzyk-Hordern, B.; Lamoree, M.; López, F. J.; Laak, T. L. te.; van Leerdam, J. A.; Sancho, J. V.; Schymanski, E. L.; de Voogt, P.; Hogendoorn, E. A. The Role of Analytical Chemistry in Exposure Science: Focus on the Aquatic Environment. *Chemosphere* **2019**, *222*, 564–583. <https://doi.org/10.1016/j.chemosphere.2019.01.118>.
- (5) Kolesnichenko, I. V.; Anslyn, E. V. Practical Applications of Supramolecular Chemistry. *Chem. Soc. Rev.* **2017**, *46* (9), 2385–2390. <https://doi.org/10.1039/c7cs00078b>.
- (6) Lehn, J. M. Supramolecular Chemistry Opening Lecture. *J. Coord. Chem.* **1992**, *27* (1–3), 3–6. <https://doi.org/10.1080/00958979209407941>.
- (7) Lehn, J. M. Supramolecular Chemistry: From Molecular Information towards Self-Organization and Complex Matter. *Reports Prog. Phys.* **2004**, *67* (3), 249–265. <https://doi.org/10.1088/0034-4885/67/3/R02>.
- (8) Huang, F.; Anslyn, E. V. Introduction: Supramolecular Chemistry. *Chem. Rev.* **2015**, *115* (15), 6999. <https://doi.org/10.1021/acs.chemrev.5b00352>.
- (9) Izatt, R. M. Charles J. Pedersen's Legacy to Chemistry. *Chem. Soc. Rev.* **2017**, *46* (9), 2380–2384. <https://doi.org/10.1039/c7cs00128b>.
- (10) De Silva, A. P.; Gunaratne, H. Q. N.; Gunnlaugsson, T.; Huxley, A. J. M.; McCoy, C. P.; Rademacher, J. T.; Rice, T. E. Signaling Recognition Events with Fluorescent Sensors and Switches. *Chem. Rev.* **1997**, *97* (5), 1515–1566. <https://doi.org/10.1021/cr960386p>.
- (11) Czarnik, A. W. Chemical Communication in Water Using Fluorescent Chemosensors.

- Acc. Chem. Res.* **1994**, 27 (10), 302–308. <https://doi.org/10.1021/ar00046a003>.
- (12) Daly, B.; Ling, J.; De Silva, A. P. Current Developments in Fluorescent PET (Photoinduced Electron Transfer) Sensors and Switches. *Chem. Soc. Rev.* **2015**, 44 (13), 4203–4211. <https://doi.org/10.1039/c4cs00334a>.
- (13) Guo, C.; Sedgwick, A. C.; Hirao, T.; Sessler, J. L. Supramolecular Fluorescent Sensors: An Historical Overview and Update. *Coord. Chem. Rev.* **2021**, 427, 213560. <https://doi.org/10.1016/j.ccr.2020.213560>.
- (14) Wu, D.; Sedgwick, A. C.; Gunnlaugsson, T.; Akkaya, E. U.; Yoon, J.; James, T. D. Fluorescent Chemosensors: The Past, Present and Future. *Chem. Soc. Rev.* **2017**, 46 (23), 7105–7123. <https://doi.org/10.1039/c7cs00240h>.
- (15) Saari, L. A.; Seitz, W. R. Immobilized Morin as Fluorescence Sensor for Determination of Aluminum(III). *Anal. Chem.* **1983**, 55 (4), 667–670. <https://doi.org/10.1021/ac00255a020>.
- (16) Sadamoto, R.; Tomioka, N.; Aida, T. Photoinduced Electron Transfer Reactions through Dendrimer Architecture. *J. Am. Chem. Soc.* **1996**, 118 (16), 3978–3979. <https://doi.org/10.1021/ja952855v>.
- (17) Akkaya, E. U.; Huston, M. E.; Czarnik, A. W. Chelation-Enhanced Fluorescence of Anthrylazamacrocyclic Conjugate Probes in Aqueous Solution. *J. Am. Chem. Soc.* **1990**, 112 (9), 3590–3593. <https://doi.org/10.1021/ja00165a051>.
- (18) Würthner, F. Aggregation-Induced Emission (AIE): A Historical Perspective. *Angew. Chemie - Int. Ed.* **2020**, 59 (34), 14192–14196. <https://doi.org/10.1002/anie.202007525>.
- (19) Hong, Y.; Lam, J. W. Y.; Tang, B. Z. Aggregation-Induced Emission. *Chem. Soc. Rev.* **2011**, 40 (11), 5361–5388. <https://doi.org/10.1039/c1cs15113d>.
- (20) Sasaki, S.; Drummen, G. P. C.; Konishi, G. I. Recent Advances in Twisted Intramolecular Charge Transfer (TICT) Fluorescence and Related Phenomena in Materials Chemistry. *J. Mater. Chem. C* **2016**, 4 (14), 2731–2743. <https://doi.org/10.1039/c5tc03933a>.
- (21) Slama-Schwok, A.; Blanchard-Desce, M.; Lehn, J. M. Intramolecular Charge Transfer in Donor-Acceptor Molecules. *J. Phys. Chem.* **1990**, 94 (10), 3894–3902. <https://doi.org/10.1021/j100373a007>.
- (22) Ma, X.; Zhao, Y. Biomedical Applications of Supramolecular Systems Based on Host-Guest Interactions. *Chem. Rev.* **2015**, 115 (15), 7794–7839. <https://doi.org/10.1021/cr500392w>.
- (23) Lagalante, A. F. Atomic Absorption Spectroscopy: A Tutorial Review. *Appl. Spectrosc.*

- Rev.* **2004**, *34* (3), 173–189. <https://doi.org/10.1081/asr-100100844>.
- (24) Niu, H.; Houk, R. S. Review Houk Ion Extraction in ICPMS. *Spectrochim. Acta B* **2002**, *51*, 37.
- (25) La, D. D.; Bhosale, S. V.; Jones, L. A.; Bhosale, S. V. Tetraphenylethylene-Based AIE-Active Probes for Sensing Applications. *ACS Appl. Mater. Interfaces* **2018**, *10* (15), 12189–12216. <https://doi.org/10.1021/acsami.7b12320>.
- (26) Basak, S.; Nandi, N.; Paul, S.; Banerjee, A. Luminescent Naphthalene Diimide-Based Peptide in Aqueous Medium and in Solid State: Rewritable Fluorescent Color Code. *ACS Omega* **2018**, *3* (2), 2174–2182. <https://doi.org/10.1021/acsomega.7b01813>.
- (27) Pandit, S.; Behera, P.; Sahoo, J.; De, M. In Situ Synthesis of Amino Acid Functionalized Carbon Dots with Tunable Properties and Their Biological Applications. *ACS Appl. Bio Mater.* **2019**, *2* (8), 3393–3403. <https://doi.org/10.1021/acsabm.9b00374>.
- (28) Jadhav, R. W.; Khobrekar, P. P.; Bugde, S. T.; Bhosale, S. V. Nanoarchitectonics of Neomycin-Derived Fluorescent Carbon Dots for Selective Detection of Fe³⁺ Ions. *Anal. Methods* **2022**, *14* (34), 3289–3298. <https://doi.org/10.1039/d2ay01040b>.
- (29) Yadav, R.; Rai, A.; Sonkar, A. K.; Rai, V.; Gupta, S. C.; Mishra, L. A Viscochromic, Mechanochromic, and Unsymmetrical Azine for Selective Detection of Al³⁺ and Cu²⁺ Ions and Its Mitotracking Studies. *New J. Chem.* **2019**, *43* (18), 7109–7119. <https://doi.org/10.1039/c8nj06413j>.
- (30) Kalia, S.; Kumar, A.; Munjal, N.; Prasad, N. Synthesis of Ferrites Using Various Parts of Plants: A Mini Review. *J. Phys. Conf. Ser.* **2021**, *1964* (3). <https://doi.org/10.1088/1742-6596/1964/3/032003>.
- (31) Liu, Y.; Ren, D.; Zhang, J.; Li, H.; Yang, X. F. A Fluorescent Probe for Hydrazine Based on a Newly Developed 1-Indanone-Fused Coumarin Scaffold. *Dye. Pigment.* **2019**, *162*, 112–119. <https://doi.org/10.1016/j.dyepig.2018.10.012>.
- (32) Zhu, X. D.; Zhang, K.; Wang, Y.; Long, W. W.; Sa, R. J.; Liu, T. F.; Lü, J. Fluorescent Metal-Organic Framework (MOF) as a Highly Sensitive and Quickly Responsive Chemical Sensor for the Detection of Antibiotics in Simulated Wastewater. *Inorg. Chem.* **2018**, *57* (3), 1060–1065. <https://doi.org/10.1021/acs.inorgchem.7b02471>.
- (33) Venkatesan, P.; Wu, S. P. A Turn-on Fluorescent Pyrene-Based Chemosensor for Cu(II) with Live Cell Application. *RSC Adv.* **2015**, *5* (53), 42591–42596. <https://doi.org/10.1039/c5ra05440k>.
- (34) Cao, D.; Liu, Z.; Verwilt, P.; Koo, S.; Jangjili, P.; Kim, J. S.; Lin, W. Coumarin-Based Small-Molecule Fluorescent Chemosensors. *Chem. Rev.* **2019**, *119* (18), 10403–10519.

- <https://doi.org/10.1021/acs.chemrev.9b00145>.
- (35) Valeur, B.; Leray, I. Design Principles of Fluorescent Molecular Sensors for Cation Recognition. *Coord. Chem. Rev.* **2000**, *205* (1), 3–40. [https://doi.org/10.1016/s0010-8545\(00\)00246-0](https://doi.org/10.1016/s0010-8545(00)00246-0).
- (36) Chen, Z.; Tan, L.; Hu, L.; Luan, Y. Superior Fluorescent Probe for Detection of Potassium Ion. *Talanta* **2015**, *144*, 247–251. <https://doi.org/10.1016/j.talanta.2015.06.015>.
- (37) Pedersen, C. J. Cyclic Polyethers and Their Complexes. *J. Am. Chem. Soc.* **1967**, *2* (11), 7017–7036.
- (38) Pedersen, C. J. The Discovery of Crown Ethers (Noble Lecture). *Angew. Chemie Int. Ed. English* **1988**, *27* (8), 1021–1027. <https://doi.org/10.1002/anie.198810211>.
- (39) Gokel, G. W.; Leevy, W. M.; Weber, M. E. Crown Ethers: Sensors for Ions and Molecular Scaffolds for Materials and Biological Models. *Chem. Rev.* **2004**, *104* (5), 2723–2750. <https://doi.org/10.1021/cr020080k>.
- (40) Müller, B. J.; Borisov, S. M.; Klimant, I. Red- to NIR-Emitting, BODIPY-Based, K⁺-Selective Fluoroionophores and Sensing Materials. *Adv. Funct. Mater.* **2016**, *26* (42), 7697–7707. <https://doi.org/10.1002/adfm.201603822>.
- (41) Cox, R. P.; Sandanayake, S.; Scarborough, D. L. A.; Izgorodina, E. I.; Langford, S. J.; Bell, T. D. M. Investigation of Cation Binding and Sensing by New Crown Ether Core Substituted Naphthalene Diimide Systems. *New J. Chem.* **2019**, *43* (4), 2011–2018. <https://doi.org/10.1039/C8NJ05666H>.
- (42) Bhosale, S. V.; Al Kobaisi, M.; Jadhav, R. W.; Morajkar, P. P.; Jones, L. A.; George, S. Naphthalene Diimides: Perspectives and Promise. *Chem. Soc. Rev.* **2021**, *50* (17), 9845–9998. <https://doi.org/10.1039/d0cs00239a>.
- (43) Kobaisi, M. Al; Bhosale, S. V.; Latham, K.; Raynor, A. M.; Bhosale, S. V. Functional Naphthalene Diimides: Synthesis, Properties, and Applications. *Chem. Rev.* **2016**, *116* (19), 11685–11796. <https://doi.org/10.1021/acs.chemrev.6b00160>.
- (44) Hangarge, R. V.; La, D. D.; Boguslavsky, M.; Jones, L. A.; Kim, Y. S.; Bhosale, S. V. An Aza-12-Crown-4 Ether-Substituted Naphthalene Diimide Chemosensor for the Detection of Lithium Ion. *ChemistrySelect* **2017**, *2* (35), 11487–11491. <https://doi.org/10.1002/slct.201702085>.
- (45) Evans, A. E. V; Mateo-sagasta, J.; Qadir, M.; Boelee, E.; Ippolito, A. ScienceDirect Agricultural Water Pollution : Key Knowledge Gaps and Research Needs \$. *Curr. Opin. Environ. Sustain.* **2019**, *36*, 20–27. <https://doi.org/10.1016/j.cosust.2018.10.003>.

- (46) Yang, X.; Chen, X.; Lu, X.; Yan, C.; Xu, Y.; Hang, X.; Qu, J.; Liu, R. A Highly Selective and Sensitive Fluorescent Chemosensor for Detection of CN^- , SO_3^{2-} and Fe^{3+} Based on Aggregation-Induced Emission. *J. Mater. Chem. C* **2016**, *4* (2), 383–390. <https://doi.org/10.1039/c5tc02865e>.
- (47) Ding, D.; Li, K.; Liu, B.; Tang, B. Z. Bioprobes Based on AIE Fluorogens. *Acc. Chem. Res.* **2013**, *46* (11), 2441–2453. <https://doi.org/10.1021/ar3003464>.
- (48) Edmunds, W. M.; Ahmed, K. M.; Whitehead, P. G. A Review of Arsenic and Its Impacts in Groundwater of the Ganges-Brahmaputra-Meghna Delta, Bangladesh. *Environ. Sci. Process. Impacts* **2015**, *17* (6), 1032–1046. <https://doi.org/10.1039/c4em00673a>.
- (49) Zhang, Q.; Minami, H.; Inoue, S.; Atsuya, I. Differential Determination of Trace Amounts of Arsenic (III) and Arsenic (V) in Seawater by Solid Sampling Atomic Absorption Spectrometry after Preconcentration by Coprecipitation with a Nickel – Pyrrolidine Dithiocarbamate Complex. **2004**, *508*, 99–105. <https://doi.org/10.1016/j.aca.2003.11.053>.
- (50) Klaue, B.; Blum, J. D. Trace Analyses of Arsenic in Drinking Water by Inductively Coupled Plasma Mass Spectrometry : High Resolution versus Hydride Generation Spectrometer (ICPMS) Was Applied to the Determination Chloride Interference , the Accompanying Reduction In. **1999**, *71* (7), 1408–1414.
- (51) Cai, Y. Speciation and Analysis of Mercury , Arsenic , and Selenium by Atomic Fluorescence Spectrometry. **2000**, *19* (1), 62–66.
- (52) Tian, X.; Chen, L.; Li, Y.; Yang, C.; Nie, Y.; Zhou, C.; Wang, Y. Design and Synthesis of a Molecule with Aggregation-Induced Emission Effects and Its Application in the Detection of Arsenite in Groundwater. *J. Mater. Chem. C* **2017**, *5* (15), 3669–3672. <https://doi.org/10.1039/C7TC00363C>.
- (53) V. A.; Baglan, M. Selective and Sensitive Turn-on Fluorescent Sensing of Arsenite Based on Cysteine Fused Tetraphenylethene with AIE Characteristics in Aqueous Media \ddagger . **2013**, 5325–5327. <https://doi.org/10.1039/c3cc42238k>.
- (54) Li, C.; Gao, C.; Lan, J.; You, J.; Gao, G. Biomolecular Chemistry. **2014**, 9524–9527. <https://doi.org/10.1039/c4ob01635a>.
- (55) Zhang, L.; Hu, W.; Yu, L.; Wang, Y. Click Synthesis of a Novel Triazole Bridged AIE Active Cyclodextrin Probe for Specific Detection of Cd^{2+} . *Chem. Commun.* **2015**, *51* (20), 4298–4301. <https://doi.org/10.1039/c4cc09769f>.
- (56) Liu, X.; Chen, T.; Yu, F.; Shang, Y.; Meng, X.; Chen, Z. R. AIE-Active Random Conjugated Copolymers Synthesized by ADMET Polymerization as a Fluorescent

- Probe Specific for Palladium Detection. *Macromolecules* **2020**, *53* (4), 1224–1232. <https://doi.org/10.1021/acs.macromol.0c00042>.
- (57) Mukherjee, A.; Chakravarty, M. Regioisomeric Monopyridine-Functionalized Triarylethene: Small AIEgens with Isomeric Effect and an Efficient Platform for the Selective and Sensitive Detection of Pd²⁺ and Fe³⁺. *New J. Chem.* **2020**, *44* (16), 6173–6181. <https://doi.org/10.1039/d0nj00306a>.
- (58) Needleman, H. Lead Poisoning. *Annu. Rev. Med.* **2004**, *55* (1), 209–222. <https://doi.org/10.1146/annurev.med.55.091902.103653>.
- (59) Khandare, D. G.; Joshi, H.; Banerjee, M.; Majik, M. S.; Chatterjee, A. An Aggregation-Induced Emission Based Turn-on Fluorescent Chemodosimeter for the Selective Detection of Pb²⁺ Ions. *RSC Adv.* **2014**, *4* (87), 47076–47080. <https://doi.org/10.1039/c4ra09451d>.
- (60) Donzelli, G.; Carducci, A.; Llopis-Gonzalez, A.; Verani, M.; Llopis-Morales, A.; Cioni, L.; Morales-Suárez-varela, M. The Association between Lead and Attention-Deficit/Hyperactivity Disorder: A Systematic Review. *Int. J. Environ. Res. Public Health* **2019**, *16* (3), 1–14. <https://doi.org/10.3390/ijerph16030382>.
- (61) Zhou, R.; Li, B.; Wu, N.; Gao, G.; You, J.; Lan, J. Cyclen-Functionalized Perylenebisimides as Sensitive and Selective Fluorescent Sensors for Pb²⁺ in Aqueous Solution. *Chem. Commun.* **2011**, *47* (23), 6668–6670. <https://doi.org/10.1039/c1cc11200g>.
- (62) Rananaware, A.; Bhosale, R. S.; Patil, H.; Al Kobaisi, M.; Abraham, A.; Shukla, R.; Bhosale, S. V.; Bhosale, S. V. Precise Aggregation-Induced Emission Enhancement via H⁺ Sensing and Its Use in Ratiometric Detection of Intracellular pH Values. *RSC Adv.* **2014**, *4* (103), 59078–59082. <https://doi.org/10.1039/c4ra10511g>.
- (63) Huang, G.; Zhang, G.; Zhang, D. Turn-on of the Fluorescence of Tetra(4-Pyridylphenyl)Ethylene by the Synergistic Interactions of Mercury(II) Cation and Hydrogen Sulfate Anion. *Chem. Commun.* **2012**, *48* (60), 7504–7506. <https://doi.org/10.1039/c2cc32504g>.
- (64) Ruan, Z.; Shan, Y.; Gong, Y.; Wang, C.; Ye, F.; Qiu, Y.; Liang, Z.; Li, Z. Novel AIE-Active Ratiometric Fluorescent Probes for Mercury(II) Based on the Hg²⁺-Promoted Deprotection of Thioketal, and Good Mechanochromic Properties. *J. Mater. Chem. C* **2018**, *6* (4), 773–780. <https://doi.org/10.1039/c7tc04712f>.
- (65) Shi, W.; Zhao, S.; Su, Y.; Hui, Y.; Xie, Z. Barbituric Acid-Triphenylamine Adduct as an AIEE-Type Molecule and Optical Probe for Mercury(II). *New J. Chem.* **2016**, *40* (9),

- 7814–7820. <https://doi.org/10.1039/c6nj00894a>.
- (66) Kala, K.; Manoj, N. A Carbazole Based “Turn on” Fluorescent Sensor for Selective Detection of Hg^{2+} in an Aqueous Medium. *RSC Adv.* **2016**, *6* (27), 22615–22619. <https://doi.org/10.1039/c5ra27530j>.
- (67) Wang, J.; Zhang, L.; Qi, Q.; Li, S.; Jiang, Y. Specific Ratiometric Fluorescent Sensing of Hg^{2+} via the Formation of Mercury(II) Barbiturate Coordination Polymers. *Anal. Methods* **2013**, *5* (3), 608–611. <https://doi.org/10.1039/c2ay26389k>.
- (68) Zhou, Y.; Zhang, J. F.; Yoon, J. Fluorescence and Colorimetric Chemosensors for Fluoride-Ion Detection. *Chem. Rev.* **2014**, *114* (10), 5511–5571. <https://doi.org/10.1021/cr400352m>.
- (69) Chen, X.; Liu, Y. C.; Bai, J.; Fang, H.; Wu, F. Y.; Xiao, Q. A “Turn-on” Fluorescent Probe Based on BODIPY Dyes for Highly Selective Detection of Fluoride Ions. *Dye. Pigment.* **2021**, *190* (January), 109347. <https://doi.org/10.1016/j.dyepig.2021.109347>.
- (70) Nadimetla, D. N.; Zalmi, G. A.; Bhosale, S. V. An AIE-Active Tetraphenylethylene-Based Cyclic Urea as a Selective and Efficient Optical and Colorimetric Chemosensor for Fluoride Ions. *ChemistrySelect* **2020**, *5* (28), 8566–8571. <https://doi.org/10.1002/slct.202002126>.
- (71) Zalmi, G. A.; Jadhav, S. E.; Mirgane, H. A.; Madje, B. R.; Bhosale, S. V. A Phenolic Schiff Based AIE-Active Quinoxaline-Based Receptor for Selective Sensing of Fluoride Ions. *ChemistrySelect* **2023**, *8* (5). <https://doi.org/10.1002/slct.202203380>.
- (72) Borah, J.; Hazarika, U. N.; Khakhlary, P. Extending the Chemistry of Reaction between BODIPY and Cyanide Ions: An Application in Selective Sensing of Fluoride and Cyanide Ions. *ACS Omega* **2022**, *7* (50), 46234–46240. <https://doi.org/10.1021/acsomega.2c04422>.
- (73) Kim, M.; Mergu, N.; Son, Y. A. Imidazole-Containing Ratiometric Receptor for the Selective and Sensitive Detection of Cyanide and Fluoride via Deprotonation and a Receptor-Anion Ensemble for Cu^{2+} Sensing. *J. Lumin.* **2018**, *204* (July), 244–252. <https://doi.org/10.1016/j.jlumin.2018.08.021>.
- (74) Hans Englyst, carbohydrates N.; Hudson, G. J. The Classification and Measurement of Dietary. *Food Chemisrry* **1996**, *57* (1), 15–21.
- (75) Asp, N. G. Dietary Carbohydrates: Classification by Chemistry and Physiology. *Food Chem.* **1996**, *57* (1), 9–14. [https://doi.org/10.1016/0308-8146\(96\)00055-6](https://doi.org/10.1016/0308-8146(96)00055-6).
- (76) Kolterman, O.; Reaven, G. M.; Olefsky, J. M. Insulin Binding in Chemical Diabetes: Relationship to Plasma Insulin Levels and Insulin Sensitivity. *Clin. Res.* **1977**, *25* (2).

- (77) Ip, M.; Mokhlesi, B. Sleep and Glucose Intolerance/Diabetes Mellitus. *Sleep Med. Clin.* **2007**, 2 (1), 19–29. <https://doi.org/10.1016/j.jsmc.2006.12.002>.
- (78) Palmer, J. P.; Asplin, C. M.; Clemons, P.; Lyen, K.; Tatpati, O.; Raghu, P. K.; Paquette, T. L. Insulin Antibodies in Insulin-Dependent Diabetics before Insulin Treatment. *Science (80-.)*. **1983**, 222 (4630), 1337–1339. <https://doi.org/10.1126/science.6362005>.
- (79) Hugoson, A.; Thorstensson, H.; Faltt, H.; Kuylenstierna, J. Periodontal Conditions in Insulin-dependent Diabetics. *J. Clin. Periodontol.* **1989**, 16 (4), 215–223. <https://doi.org/10.1111/j.1600-051X.1989.tb01644.x>.
- (80) Van Raalte, D. H.; Diamant, M.; Ouwens, D. M.; Ijzerman, R. G.; Linssen, M. M. L.; Guigas, B.; Eringa, E. C.; Serné, E. H. Glucocorticoid Treatment Impairs Microvascular Function in Healthy Men in Association with Its Adverse Effects on Glucose Metabolism and Blood Pressure: A Randomised Controlled Trial. *Diabetologia* **2013**, 56 (11), 2383–2391. <https://doi.org/10.1007/s00125-013-3016-8>.
- (81) James, T. D.; Samankumara Sandanayake, K. R. A.; Iguchi, R.; Shinkai, S. Novel Saccharide-Photoinduced Electron Transfer Sensors Based on the Interaction of Boronic Acid and Amine. *J. Am. Chem. Soc.* **1995**, 117 (35), 8982–8987. <https://doi.org/10.1021/ja00140a013>.
- (82) Faghihi, T.; Radfar, M.; Barmal, M.; Amini, P.; Qorbani, M.; Abdollahi, M.; Larijani, B. A Randomized, Placebo-Controlled Trial of Selenium Supplementation in Patients with Type 2 Diabetes: Effects on Glucose Homeostasis, Oxidative Stress, and Lipid Profile. *Am. J. Ther.* **2014**, 21 (6), 491–495. <https://doi.org/10.1097/MJT.0b013e318269175f>.
- (83) Lobnik, A.; Turel, M.; Urek, Š. K. Optical Chemical Sensors : Design and Applications, Advances in Chemical Sensors, Prof. Wen Wang. **2012**, 4–28.
- (84) James, T. D.; Sandanayake, K. R. A. S. Novel Photoinduced Electron-Transfer Sensor for Saccharides Based on the Interaction of Boronic Acid and Amine. **1994**, 477–478.
- (85) James, T. D.; Sandanayake, K. R. A. S.; Shinkai, S. REVINS Saccharide Sensing with Molecular Receptors Based on Boronic Acid.
- (86) Sandanayake, K. R.. A. S.; Imazu, S.; James T.D.; Mikani M.; and Shinkai S. Molecular fluorescence sensor for saccharides based on amino coumarin. *Chemistry Letters*. **1995**, 2, 139-140. <https://doi.org/10.1246/cl.1995.139>.
- (87) Yang, W.; Yan, J.; Fang, H.; Wang, B. The First Fluorescent Sensor for D-Glucarate Based on the Cooperative Action of Boronic Acid and Guanidinium Groups. *Chem. Commun.* **2003**, 6, 792–793. <https://doi.org/10.1039/b300098b>.

- (88) Fang, H.; Kaur, G.; Wang, B. Progress in Boronic Acid-Based Fluorescent Glucose Sensors. *J. Fluoresc.* **2004**, *14* (5), 481–489. <https://doi.org/10.1023/B:JOFL.0000039336.51399.3b>.
- (89) Zhang, L.; Zhang, Z. Y.; Liang, R. P.; Li, Y. H.; Qiu, J. D. Boron-Doped Graphene Quantum Dots for Selective Glucose Sensing Based on the “Abnormal” Aggregation-Induced Photoluminescence Enhancement. *Anal. Chem.* **2014**, *86* (9), 4423–4430. <https://doi.org/10.1021/ac500289c>.
- (90) Zhai, H.; Bai, Y.; Wang, H.; Qin, J.; Liu, H.; Feng, F. Development of a Novel Fluorescence Ratiometric Glucose Sensor Based on Carbon Dots and a Potential Fluorophore: M -Dihydroxybenzene. *Anal. Methods* **2018**, *10* (45), 5380–5386. <https://doi.org/10.1039/c8ay01821a>.
- (91) Mazza, M. M. A.; Raymo, F. M. Structural Designs for Ratiometric Temperature Sensing with Organic Fluorophores. *J. Mater. Chem. C* **2019**, *7* (18), 5333–5342. <https://doi.org/10.1039/c9tc00993k>.
- (92) Shi, P.; Deng, D.; He, C.; Ji, L.; Duan, Y.; Han, T.; Suo, B.; Zou, W. Mechanochromic Luminescent Materials with Aggregation-Induced Emission: Mechanism Study and Application for Pressure Measuring and Mechanical Printing. *Dye. Pigment.* **2020**, *173* (September 2019), 107884. <https://doi.org/10.1016/j.dyepig.2019.107884>.
- (93) Chen, Z.; Ding, Z.; Zhang, G.; Tian, L.; Zhang, X. Construction of Thermo-Responsive Elastin-like Polypeptides (ELPs)-Aggregation-Induced-Emission (AIE) Conjugates for Temperature Sensing. *Molecules* **2018**, *23* (7). <https://doi.org/10.3390/molecules23071725>.
- (94) Wang, Z.; Yong, T. Y.; Wan, J.; Li, Z. H.; Zhao, H.; Zhao, Y.; Gan, L.; Yang, X. L.; Xu, H. B.; Zhang, C. Temperature-Sensitive Fluorescent Organic Nanoparticles with Aggregation-Induced Emission for Long-Term Cellular Tracing. *ACS Appl. Mater. Interfaces* **2015**, *7* (5), 3420–3425. <https://doi.org/10.1021/am509161y>.
- (95) Yallapu, M. M.; Jaggi, M.; Chauhan, S. C. Design and Engineering of Nanogels for Cancer Treatment. *Drug Discov. Today* **2011**, *16* (9–10), 457–463. <https://doi.org/10.1016/j.drudis.2011.03.004>.
- (96) Saunders, B. R.; Laajam, N.; Daly, E.; Teow, S.; Hu, X.; Stepto, R. Microgels: From Responsive Polymer Colloids to Biomaterials. *Adv. Colloid Interface Sci.* **2009**, *147–148* (C), 251–262. <https://doi.org/10.1016/j.cis.2008.08.008>.
- (97) Meng, L.; Jiang, S.; Song, M.; Yan, F.; Zhang, W.; Xu, B.; Tian, W. TICT-Based Near-Infrared Ratiometric Organic Fluorescent Thermometer for Intracellular Temperature

- Sensing. *ACS Appl. Mater. Interfaces* **2020**, *12* (24), 26842–26851. <https://doi.org/10.1021/acsami.0c03714>.
- (98) Shamsipur, M.; Barati, A.; Nematifar, Z. Fluorescent PH Nanosensors: Design Strategies and Applications. *J. Photochem. Photobiol. C Photochem. Rev.* **2019**, *39*, 76–141. <https://doi.org/10.1016/j.jphotochemrev.2019.03.001>.
- (99) Chen, S.; Liu, J.; Liu, Y.; Su, H.; Hong, Y.; Jim, C. K. W.; Kwok, R. T. K.; Zhao, N.; Qin, W.; Lam, J. W. Y.; Wong, K. S.; Tang, B. Z. An AIE-Active Hemicyanine Fluorogen with Stimuli-Responsive Red/Blue Emission: Extending the PH Sensing Range by “Switch + Knob” Effect. *Chem. Sci.* **2012**, *3* (6), 1804–1809. <https://doi.org/10.1039/c2sc01108e>.
- (100) Chen, S.; Hong, Y.; Liu, Y.; Liu, J.; Leung, C. W. T.; Li, M.; Kwok, R. T. K.; Zhao, E.; Lam, J. W. Y.; Yu, Y.; Tang, B. Z. Full-Range Intracellular PH Sensing by an Aggregation-Induced Emission-Active Two-Channel Ratiometric Fluorogen. *J. Am. Chem. Soc.* **2013**, *135* (13), 4926–4929. <https://doi.org/10.1021/ja400337p>.
- (101) Li, K.; Feng, Q.; Niu, G.; Zhang, W.; Li, Y.; Kang, M.; Xu, K.; He, J.; Hou, H.; Tang, B. Z. Benzothiazole-Based AIEgen with Tunable Excited-State Intramolecular Proton Transfer and Restricted Intramolecular Rotation Processes for Highly Sensitive Physiological PH Sensing. *ACS Sensors* **2018**, *3* (5), 920–928. <https://doi.org/10.1021/acssensors.7b00820>.
- (102) Feng, Q.; Li, Y.; Wang, L.; Li, C.; Wang, J.; Liu, Y.; Li, K.; Hou, H. Multiple-Color Aggregation-Induced Emission (AIE) Molecules as Chemodosimeters for PH Sensing. *Chem. Commun.* **2016**, *52* (15), 3123–3126. <https://doi.org/10.1039/c5cc10423h>.
- (103) Luby-Phelps, K. Cytoarchitecture and Physical Properties of Cytoplasm: Volume, Viscosity, Diffusion, Intracellular Surface Area. *Int. Rev. Cytol.* **1999**, *192*, 189–221. [https://doi.org/10.1016/s0074-7696\(08\)60527-6](https://doi.org/10.1016/s0074-7696(08)60527-6).
- (104) Harkness, J. The Viscosity of Human Blood Plasma; Its Measurement in Health and Disease. *Biorheology* **1971**, *8* (3), 171–193. <https://doi.org/10.3233/BIR-1971-83-408>.
- (105) Yang, Z.; Fan, J.; Peng, X. Fluorescence Ratiometry and Fluorescence Lifetime (FLIM) Imaging: Dual Mode Imaging Cellular Viscosity by a Single Molecular Rotor. *2011 Funct. Opt. Imaging, FOI 2011* **2011**, 6626–6635. <https://doi.org/10.1109/FOI.2011.6154843>.
- (106) Luby-Phelps, K.; Mujumdar, S.; Mujumdar, R. B.; Ernst, L. A.; Galbraith, W.; Waggoner, A. S. A Novel Fluorescence Ratiometric Method Confirms the Low Solvent Viscosity of the Cytoplasm. *Biophys. J.* **1993**, *65* (1), 236–242.

- [https://doi.org/10.1016/S0006-3495\(93\)81075-0](https://doi.org/10.1016/S0006-3495(93)81075-0).
- (107) Haidekker, M. A.; Brady, T. P.; Chalian, S. H.; Akers, W.; Lichlyter, D.; Theodorakis, E. A. Hydrophilic Molecular Rotor Derivatives - Synthesis and Characterization. *Bioorg. Chem.* **2004**, *32* (4), 274–289. <https://doi.org/10.1016/j.bioorg.2004.04.002>.
- (108) Kumbhar, H. S.; Deshpande, S. S.; Shankarling, G. S. Aggregation Induced Emission (AIE) Active Carbazole Styryl Fluorescent Molecular Rotor as Viscosity Sensor. *ChemistrySelect* **2016**, *1* (9), 2058–2064. <https://doi.org/10.1002/slct.201600001>.
- (109) Yang, Z.; Huo, Y.; Liu, Y.; Du, G.; Zhang, W.; Zhou, L.; Zhan, L.; Ren, X.; Duan, W.; Gong, S. Axially Chiral 1,4-Dihydropyridine Derivatives: Aggregation-Induced Emission in Exciplexes and Application as Viscosity Probes. *RSC Adv.* **2019**, *9* (55), 32219–32225. <https://doi.org/10.1039/c9ra06553a>.
- (110) Chen, S.; Hong, Y.; Zeng, Y.; Sun, Q.; Liu, Y.; Zhao, E.; Bai, G.; Qu, J.; Hao, J.; Tang, B. Z. Mapping Live Cell Viscosity with an Aggregation-Induced Emission Fluorogen by Means of Two-Photon Fluorescence Lifetime Imaging. *Chem. - A Eur. J.* **2015**, *21* (11), 4315–4320. <https://doi.org/10.1002/chem.201405658>.
- (111) Xu, L.; Ni, L.; Zeng, F.; Wu, S. Tetranitrile-Anthracene as a Probe for Fluorescence Detection of Viscosity in Fluid Drinks: Via Aggregation-Induced Emission. *Analyst* **2020**, *145* (3), 844–850. <https://doi.org/10.1039/c9an02157d>.
- (112) Dou, Y.; Liu, J.; Zhang, F.; Cai, C.; Zhu, Q.; Kenry. 2-Styrylquinoline-Based Two-Photon AIEgens for Dual Monitoring of pH and Viscosity in Living Cells. *J. Mater. Chem. B* **2019**, *7* (48), 7771–7775. <https://doi.org/10.1039/c9tb02036e>.

CHAPTER 2

CHAPTER 2

2.1. Introduction

Many biochemical and physiological processes are governed by various transition metal ions in which iron (Fe^{3+}) plays very crucial role maintaining the life organism. Iron acts as an important catalyst and helps in electron transfer in various oxidoreductase catalysis, oxygen metabolism [1]. Although the iron has several advantages but overdose as well as deficiency may result into health problems such as hypoferremia and hyperferremia. Iron deficiency may also lead to various disorder such as diabetes, anaemia, and kidney failure. In human body spleen and liver are richest source of Fe^{3+} ion [2]. Nearly 4gm of iron is present in the well-nourished body with 70% in haemoglobin (Hgb) and 25% as the storage protein. Due to severe diseases, there is need of maintaining the level of Fe^{3+} ion in body. Many vegetables such as spinach, fruits are rich source of Fe^{3+} ion, therefore person with the deficiency doctors recommends maintaining the diet by providing the natural sources or by giving iron rich supplements [3].

In environment iron (Fe^{3+}) enters by various events such as weathering, industrial waste or corrosion of metals which results in change in taste of water as well as subsequent bacterial proliferation. Detection of iron is not only important with respect to environmental monitoring but also important for biomedical application. There are different instrumental methods that are employed for determination of Fe^{3+} metal ion in the system such as atomic absorption spectrometry, various spectrophotometric methods, and electrochemical methods. Since the instrumental methods are time consuming, expensive, and highly sophisticated, simple methods are more preferred [4,5,6,7].

Fluorescent Chemosensors with donor acceptor system has extended application. Many research groups have developed different fluorescent material for sensing of Fe^{3+} metal ions.

Various organic fluorescent molecules such as rhodamine [8,9], pyrene [10], TPE [11,12], coumarin [13], naphthalenediimide (NDI) [14], triphenylamine derivative [15], carbazole [16], anthracene, naphthalene [17,18], terpyridine appended polymers etc. [19]. Zhang and co-workers developed novel organic charge transfer fluorescent molecule with donor and acceptor for sensing of Fe^{3+} ion. A series of new charge transfer organic molecules **T1**, **T2**, and **T3** were synthesized that are highly specific and selective to Fe^{3+} metal ion undergoes quenching phenomenon in presence of Fe^{3+} by the formation of complex between charge transfer molecule and metal ion [20]. as shown in **Figure 2.1** Herein another terpyridine based molecule was synthesized by Hong *et.al* for sensing application and it was noted that the molecules showed excellent selectivity towards Zn^{2+} ion. It consists of donor tetraphenylethylene (TPE) connected to three pyridine moieties **TPETPy** and **TPE2TPy**. The molecules effectively demonstrate a good example for sensing of Zn^{2+} ions leading to metal to ligand charge transfer experiencing the quenching of fluorescence [21]. The structures are as given in **Figure 2.2**

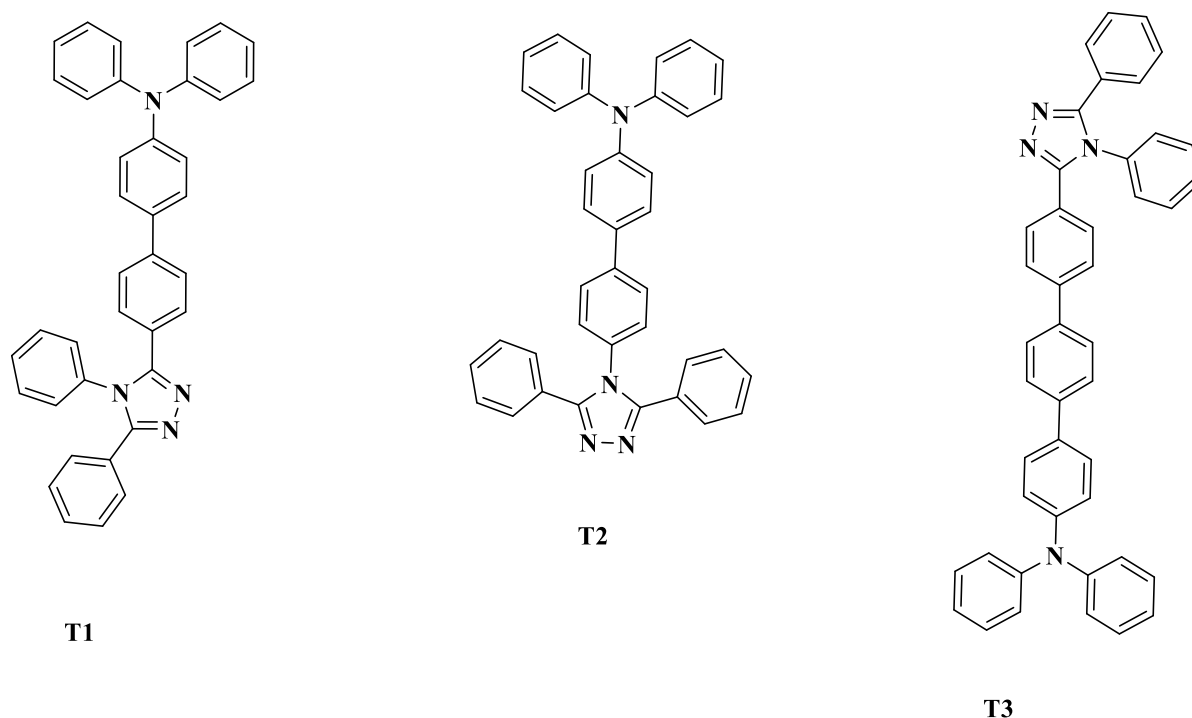


Figure 2.1. Organic fluorescent molecules for sensing of Fe^{3+} metal ion labelled as **T1**, **T2** and **T3**.

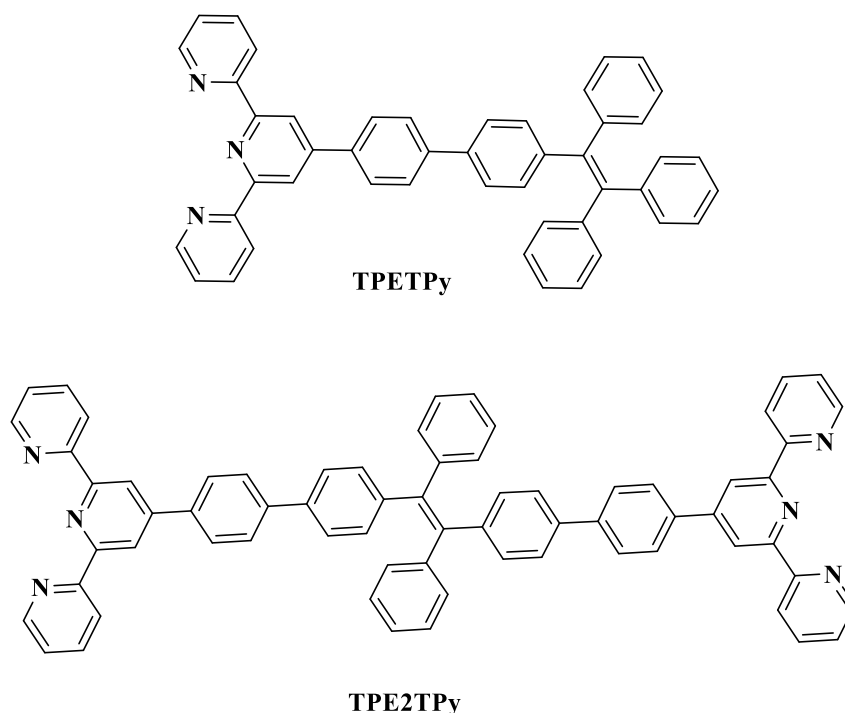


Figure 2.2. Structure of the synthesized organic charge transfer molecules **TPETPy** and **TPE2TPy**.

From the thorough literature and present scenario, the metal ion detection mainly occurs by a co-ordinate interaction between the receptor and the metal ion [22,23,24]. Herein our group developed donor acceptor receptor based on diphenylamine donor and heterocyclic core as receptor with nitrogen(N), and dithiophene moiety. The synthesis of this heterocyclic core 4-(2,6-di(thiophen-2-yl)-*N,N*-diphenylaniline (**DTPDA 1**) involves simple aldol condensation in presence of potassium hydroxide (KOH) in ethanol solvent at room temperature to give α,β -unsaturated ketone. Further undergoes Michael addition reaction with pyridinium salt in presence of ammonium hydroxide and acetic acid for 12 hours in refluxing condition to yield the receptor **DTPDA 1**. Nandre and group used these fluorescent molecules for sensing of iron (Fe^{3+}) and lead (Pb^{2+}) metal ion [25]. Recently Nadimetla developed another molecule by replacing the diphenyl donor moiety with AIE active tetraphenylethylene molecule and it was observed that the molecule was highly selective to Cu^{2+} ion [26]. The molecule was synthesized by using the above mentioned synthetic procedure. These molecules consists of TPE as a donor

and acceptor as heterocyclic core consisting of thiophene and dipyridine moiety. However, it was observed that the molecule showed excellent selectivity towards Cu^{2+} ion in presence over other metal ion such as Fe^{3+} , Fe^{2+} , Hg^{2+} , Pb^{2+} , Ni^{2+} , Al^{3+} , Mn^{2+} , Co^{2+} , Zn^{2+} , Ca^{2+} . Thus, from this deeper understanding it is observed that mechanistic coordination of metal ion differs as the heterocyclic core moiety changes. Therefore, we decided to further design more derivative and investigate its selectivity towards different metal ions. Herein we have synthesized another diphenyl derivative by employing the procedure given in the literature [27,28,29,30] via Krohnke pyridine synthesis method. Certainly the synthesized derivative 4-(2,6-di(furan-2-yl)pyridin-4-yl)-*N,N*-diphenylaniline (**DFPDA 1**) containing difuran and pyridine moiety with diphenyl aniline as donor moiety. The study of molecule was focuses more on its selectivity towards various cations. From the thorough investigation it was observed that this derivative was highly selective towards Fe^{3+} metal ion. Detailed selectivity study of the receptor (**DFPDA 1**) is discussed in this chapter.

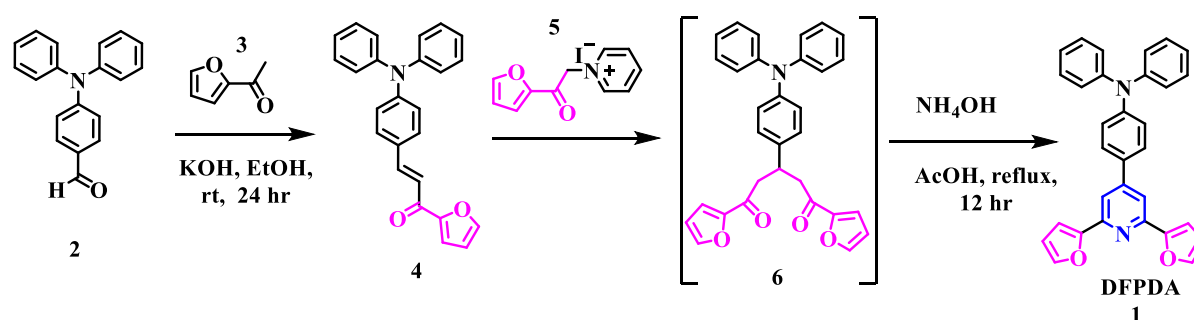
2.2 Experimental

2.2.1. Materials and chemicals

The receptor was synthesized using following chemical such as diphenylaniline aldehyde was purchased from TCI chemical, ammonium acetate, acetic acid, potassium hydroxide, ethanol and ammonium hydroxide. Further various cations (Fe^{3+} , Cu^{2+} , K^+ , Cd^{2+} , Co^{2+} , Mn^{2+} , Ni^{2+} , Ba^{2+} , Hg^{2+} , Al^{3+} , Pb^{2+} , Zn^{2+} , Ca^{2+} , Fe^{2+} salt, dimethyl sulfoxide (DMSO) were purchased from Sigma-Aldrich and TCI. After successful synthesis the compound was purified by column chromatography using 10% ethyl acetate and pet ether solvent. The purified compound was further characterized by recording ^1H NMR spectrum on 400 MHz and ^{13}C NMR using 100 MHz Bruker spectrometer using Tetramethylsilane (TMS) as an internal standard and CDCl_3 -*d* and $\text{DMSO-}d_6$ as a deuterated solvent. Mass spectrometric data were obtained by positive electron spray ionization (ESI-MS) technique on an Agilent Technologies 1100 Series (Agilent

Chemistation Software) mass spectrometer. IR spectra were recorded on a Perkin Elmer FT-IR 400 spectrometer. UV-vis absorption spectra were recorded by UV-vis-1800 Shimadzu spectrophotometer and fluorescence emission measured on RF-6000 (Shimadzu, Japan) Spectro-fluorophotometer.

2.2.2. Synthetic route for synthesis of receptor **1** 4-(2,6-di(furan-2-yl)pyridin-4-yl)-*N,N*-diphenylaniline (**DFPDA**) **1**



Scheme 2.1. Schematic pathway for synthesis of receptor **1** 4-(2,6-di(furan-2-yl)pyridin-4-yl)-*N,N*-diphenylaniline (**DFPDA**) **1**.

2.2.3. Synthesis of (*E*)-3-(4-(diphenylamino)phenyl)-1-(furan-2-yl)prop-2-en-1-one **4**

2-acetyl furan **3** (0.20 gm, 0.002 mol) was added to 4-(diphenylamino) benzaldehyde **2** (0.5 gm, 0.002 mol) in 15ml ethanol. To the above reaction mixture 5% potassium hydroxide (0.5 gm in 10ml) was added slowly. The reaction mixture was allowed to stir at room temperature for 24 hours. Yellow precipitate formed was filtered and washed with cold water, and recrystallized from ethanol gives **4** (0.36 gm, 51.64%). Melting point 162°C. Elemental analysis: C₂₅H₁₉NO₂ Calculated. (%): C, 82.17; H, 5.24; N, 3.83. Found (%): C, 82.24; H, 5.28; N, 3.90. IR (cm⁻¹): 3152, 3055, 3027, 2631, 1658, 1578, 1503, 1485, 1324, 1048, 753, 704. ¹H NMR (400 MHz, CDCl₃) δ ppm: 6.60 (m, *J*=1.6 Hz, 1H), 7.05 (d, *J*=8.4 Hz, 2H), 7.17 (m, 6H), 7.36 (m, 6H), 7.52 (d, *J*=8.4 Hz, 2H), 7.65(s, 1H), 7.88 (d, *J*=1.6 Hz, 1H); ¹³C NMR (100 MHz,

CDCl₃) δ ppm: 178.1, 154.0, 150.3, 146.8, 146.3, 143.8, 129.9, 129.5, 127.7, 125.5, 124.2, 121.5, 118.5, 117.0, 112.5. ESI-MS calculated. 365.14 (M)⁺, obs. 366.3 (M+1)⁺.

2.2.4. Synthesis of 1-(2-(furan-2-yl)-2-oxoethyl)pyridin-1-ium (5) iodide

To a mixture of 2-acetyl furan (2.2 gm, 0.02 mol) and Iodine (5.05 gm, 0.02 mol) 25ml of pyridine was added and reaction mixture was refluxed for 3 hours. After completion of reaction allow the reaction mixture to cool at 20° C. The precipitate formed was filtered and washed thoroughly with cold pyridine which was then used for next reaction without purification (Yield: 1.168 gm, 73%).

2.2.5. Synthesis of 4-(2,6-di(furan-2-yl) pyridin-4-yl)-*N,N*-diphenylaniline (DFPDA) 1

A mixture of (4) (0.300 gm, 0.001 mol) and (5) (2.1 gm, 0.007 mol) was heated under reflux. To these 4 ml of ammonium hydroxide and 10 ml of acetic acid was added slowly. The reaction mixture was kept under reflux at 90°C for 12 hours. The reaction mixture was allowed to come to room temperature and after cooling 30 ml of cold distilled water was added. The precipitate formed was washed thoroughly with cold methanol dried and purified by column chromatography. The final product obtained was brown solid 1.3 gm (57% yield). Elemental analysis: C₃₁H₂₂N₂O₂ Calculated (%): C, 81.92; H, 4.88; N, 6.16; Found (%): C, 81.38; H, 4.96; N, 6.23. IR (cm⁻¹): 3441, 3063, 2961, 2849, 1583, 1484, 1427, 1322, 1269, 1175, 1090, 1025, 803, 755, 695, 619. ¹H NMR (400 MHz, CDCl₃) δ (ppm): 6.48-6.49 (dd, *J*=4 Hz, 2H), 7.03 (t, *J*=7.4 Hz, 2H), 7.10 (m, 3H), 7.14 (m, 2H), 7.25-7.19 (t, *J*=8.4 Hz, 4H), 7.4 (m, 2H), 7.57 (d, *J*=8.4 Hz, 2H), 7.70 (s, 2H). ¹³C NMR (100 MHz, CDCl₃) δ ppm: 153.2, 149.5, 149.1, 147.6, 147.2, 147.0, 143.4, 138.5, 138.4, 130.9, 129.7, 129.4, 129.0, 127.8, 126.3, 125.1, 125, 124.4, 123.9, 123.6, 122.8, 119.3, 119, 114.2, 112.1, 109.74. ESI-MS: Calculated. 454.168 (M)⁺, obs. 455.100 (M+1)⁺.

2.3. Characterization

After the successful synthesis and purification, the structural characterization of the molecule was done by different techniques such as ^1H NMR, ^{13}C NMR, elemental analysis, Single crystal X-ray Diffraction, ESI-Mass, and Infra-red spectroscopy. Further its photophysical properties were investigated by using UV-Vis and Spectrofluorometer. From above analysis the molecule was successfully characterized, and the final product formed has the molecular structure as synthesized by the applied synthetic procedure. The characterization data is represented as follows:

2.3.1. ^1H NMR spectra of (*E*)-3-(4-(diphenylamino)phenyl)-1-(furan-2-yl)prop-2-en-1-one **4**

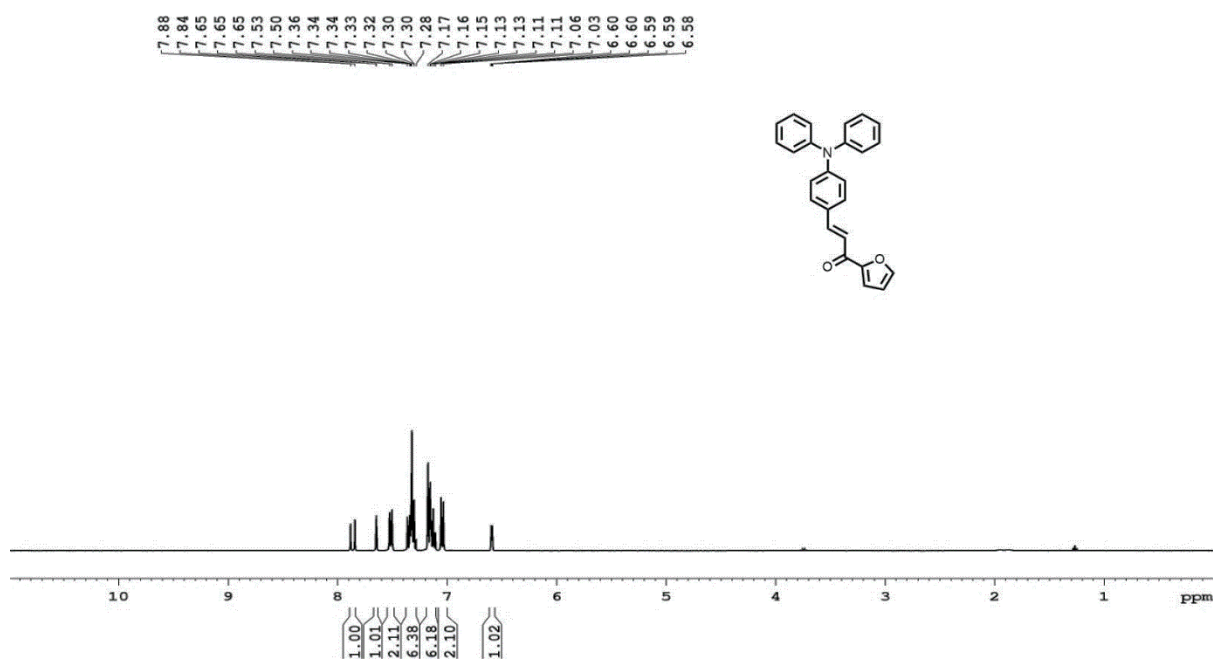


Figure 2.3. Represents ^1H NMR spectrum of (*E*)-3-(4-(diphenylamino)phenyl)-1-(furan-2-yl)prop-2-en-1-one **4**

2.3.2. ^{13}C NMR spectrum of (*E*)-3-(4-(diphenylamino)phenyl)-1-(furan-2-yl)prop-2-en-1-one
4.

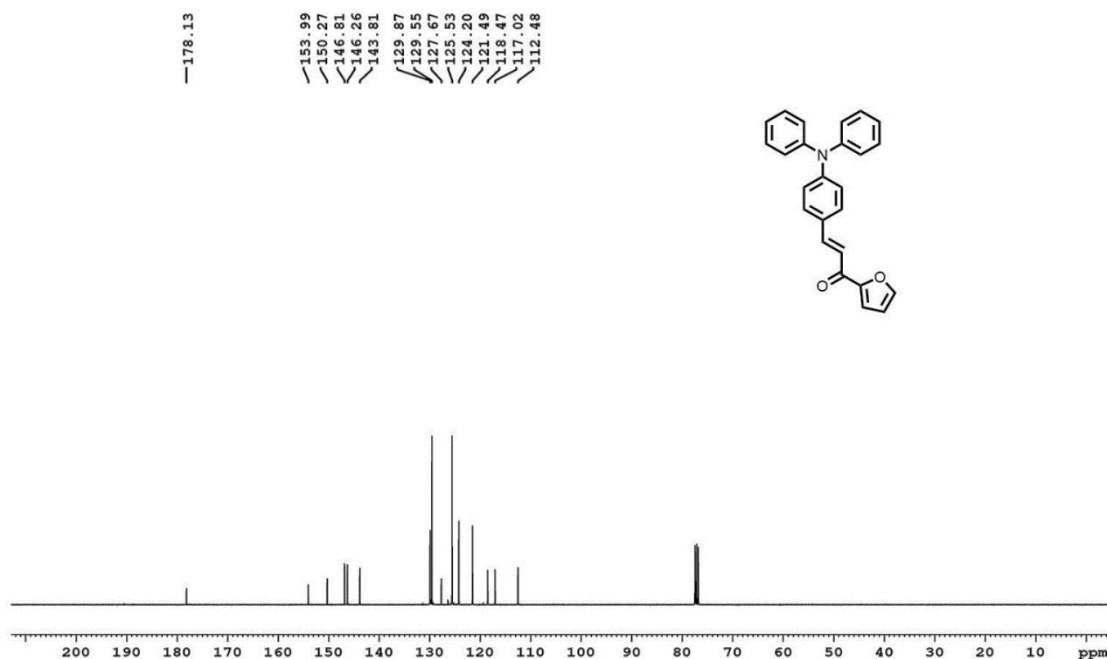


Figure 2.4. ^{13}C NMR spectrum of the intermediate (*E*)-3-(4-(diphenylamino)phenyl)-1-(furan-2-yl)prop-2-en-1-one **4**.

2.3.3. ^1H NMR spectrum of 4-(2,6-di(furan-2-yl)pyridin-4-yl)-*N,N*-diphenylaniline (**DFPDA**)
1

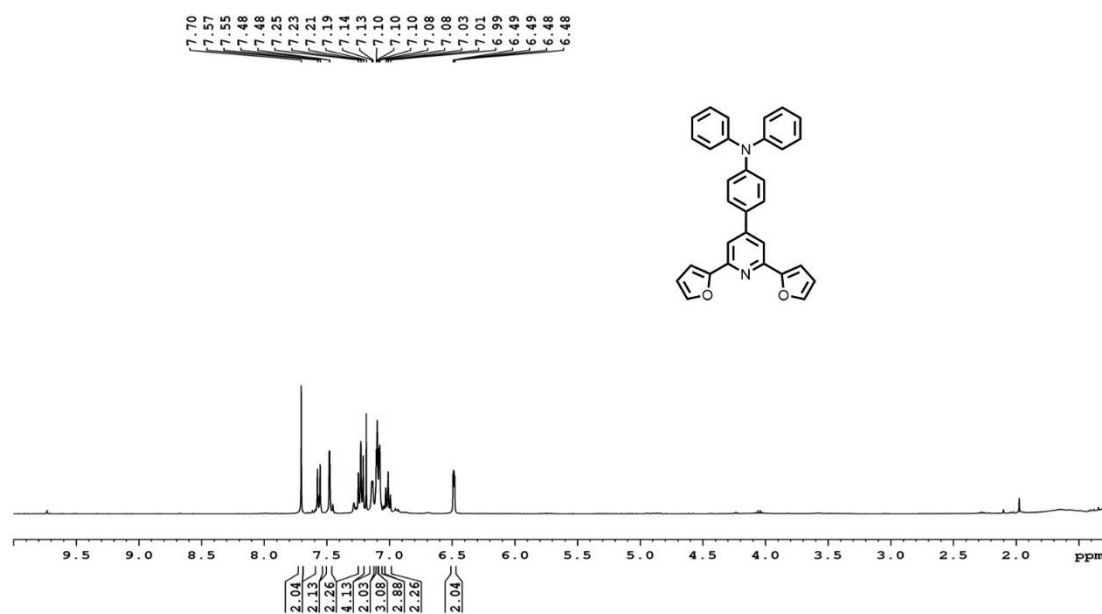


Figure 2.5. ^1H NMR spectrum of 4-(2,6-di(furan-2-yl)pyridin-4-yl)-*N,N*-diphenylaniline **DFPDA**

(DFPDA) 1**2.3.4. ¹³C NMR spectrum of 4-(2,6-di(furan-2-yl)pyridin-4-yl)-*N,N*-diphenylaniline (DFPDA)**

1

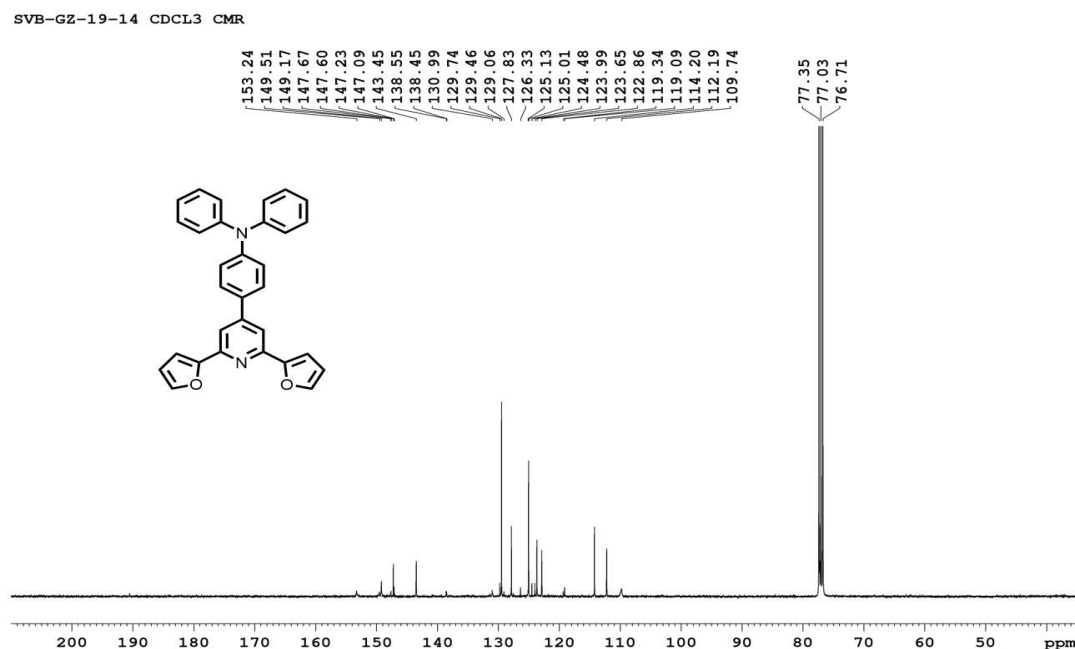


Figure 2.6. ¹³C NMR spectrum of 4-(2,6-di(furan-2-yl)pyridin-4-yl)-*N,N*-diphenylaniline (DFPDA) 1

2.3.4. ESI- mass analysis of 4-(2,6-di(furan-2-yl)pyridin-4-yl)-*N,N*-diphenylaniline (DFPDA)

1

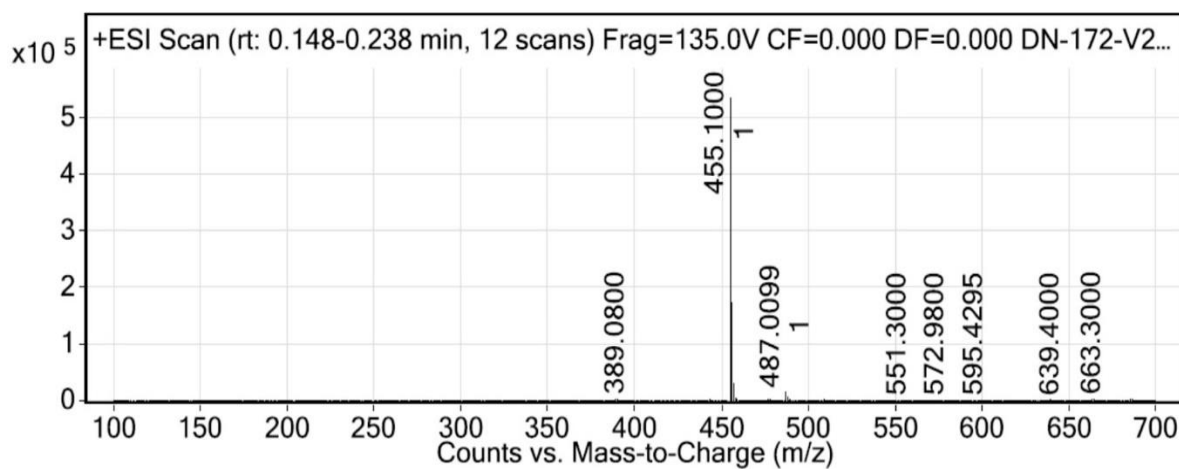


Figure 2.7. ESI-Mass analysis of 4-(2,6-di(furan-2-yl)pyridin-4-yl)-*N,N*-diphenylaniline (DFPDA) 1

2.4. Crystal study

2.4.1. Crystal study of intermediate 4

(*E*)-3-(4-(diphenylamino)phenyl)-1-(furan-2-yl)prop-2-en-1-one **4**: The crystal of intermediate and final product was successfully grown in chloroform:methanol solution by diffusion process for 8 days. The compound intermediate (*E*)-3-(4-(diphenylamino)phenyl)-1-(furan-2-yl)prop-2-en-1-one crystallizes in monoclinic space group $P2_1/c$ $Z=4$. The following technical details are discussed as below. The crystal was analyzed using Bruker D8 Quest Eco X-ray diffractometer. The analysis was performed at room temperature using monochromator ($\text{MoK}\alpha=0.7107 \text{ \AA}$). For integrating frames, the program suite APEX3 (Version 2018.1), to perform absorption correction and determine the unit cell. The non-hydrogen atoms are refined anisotropically. The H atoms attached to the aromatic ring were introduced in the calculated positions and included in the refinement by riding on their respective parent C atoms. The compound forms one dimensional structure forming intermolecular hydrogen C-H- π interaction with 2.718 \AA separation. **Figure 2.10.**

2.4.2. Crystal study of the compound 4-(2,6-di(furan-2-yl)pyridin-4-yl)-*N,N*-diphenylaniline **DFPDA 1**

The receptor **DFPDA 1** compound was crystallized in chloroform: methanol by diffusion method. The prepared crystal was found to monoclinic space group $P2_1/c$ $Z=4$. The crystal structure of the compound was characterized by using Bruker D8 Quest Eco X-ray diffractometer. The technical data was collected at room temperature using ($\text{MoK}\alpha=0.7107 \text{ \AA}$) monochromatic radiations. In order to determine the absorption and correction and unit cell program suite APEX3 (Version 2018.1) was used. Thus, by using SHELXS the consequent structures were solved. Herein all non-hydrogen atoms are anisotropically refined. The aromatic hydrogens are introduced on the calculated positions and riding on the respective carbon atoms. From the packing interactions as shown in **Figure 2.11.** it is very clear that the

crystal represents 1 dimensional network resulting in to C-H- π interaction with 3.383 Å helical structure. The crystallographic data for compound (E)-3-(4-(diphenylamino)phenyl)-1-(furan-2-yl)prop-2-en-1-one **4** and 4-(2,6-di(furan-2-yl)pyridin-4-yl)-*N,N*-diphenylaniline (**DFPDA**) **1** are reported. **Figure 2.8.** and **Figure 2.9** The data have been submitted in the Cambridge crystallographic data centre with CCDC numbers 2149520 and 2149521, respectively.

Table 2.1. Crystal data and details of refinements for **4**

Empirical formula	C ₂₅ H ₁₉ NO ₂
Formula weight	365.43
Crystal system	Monoclinic
Space group	<i>P2₁/c</i>
a (Å)	11.2990(5)
b (Å)	10.2751(5)
c (Å)	16.5433(7)
α (°)	90°
β (°)	98.4830(1)
γ (°)	90°
Volume (Å ³)	1899.64(15)
Temperature	293 (2)K
F(000)	768
θ rang(deg)	2.85 to 28.14
μ (mm ⁻¹)	0.081
Collected reflections	23205
Independent reflections	4700
Final R indices R ₁	0.0618
[I > 2 sigma (I)] wR ₂	0.1501

R indices (all data)	R ₁ =0.0826
	wR ₂ = 0.1612
Goodness of fit	1.073
CCDC number	2149520

Crystal study of 4-(2,6-di(furan-2-yl)pyridin-4-yl)-*N,N*-diphenylaniline (**DFPDA 1**)

Table 2.2. Crystal data and details of refinements for **DFPDA 1**

Empirical formula	C ₃₁ H ₂₂ N ₂ O ₂
Formula weight	454.53
Crystal system	Monoclinic
Space group	<i>P</i> 2 ₁ / <i>c</i>
a (Å)	15.2782(6)
b (Å)	8.4305(3)
c (Å)	18.5467(7)
α (°)	90 ⁰
β (°)	101.928 ⁰
γ (°)	90 ⁰
Volume (Å ³)	2337.29(15)
Temperature	293 (2) K
F(000)	952
θ rang(deg)	2.77 to 26.69
μ(mm-1)	0.081
Collected reflections	33674
Independent reflections	5806
Final R indices R ₁	0.0580

[I >2 sigma (I)] wR ₂	0.1099
R indices (all data)	R1 =0.1265
	wR ₂ = 0.1406
Goodness of fit	1.038
CCDC number	2149521

Crystal Structure of intermediate (*E*)-3-(4-(diphenylamino)phenyl)-1-(furan-2-yl)prop-2-en-1-one 4

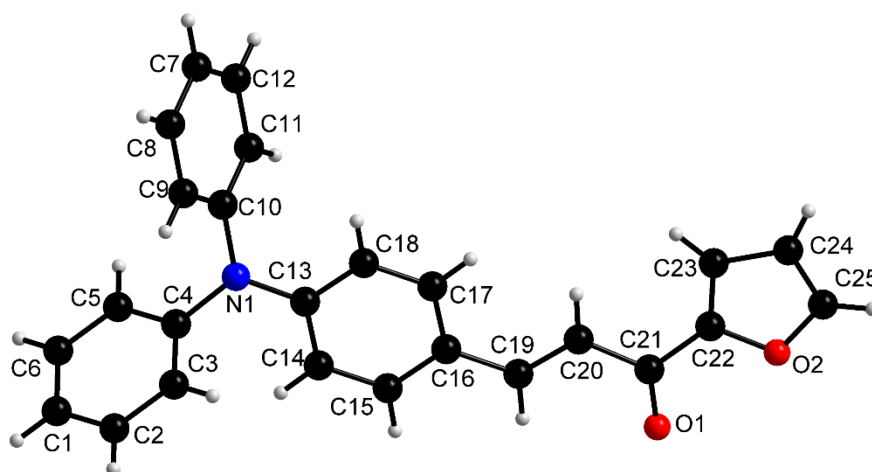


Figure 2. 8. Crystal structure of the (*E*)-3-(4-(diphenylamino)phenyl)-1-(furan-2-yl)prop-2-en-1-one 4

Crystal structure of 4-(2,6-di(furan-2-yl)pyridin-4-yl)-*N,N*-diphenylaniline (**DFPDA**) **1**

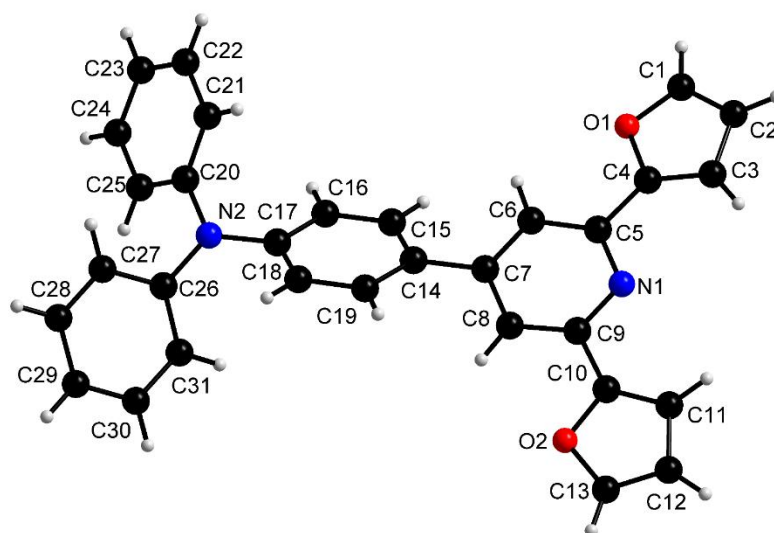


Figure 2.9. Crystal structure of 4-(2,6-di(furan-2-yl)pyridin-4-yl)-*N,N*-diphenylaniline (**DFPDA**) **1**

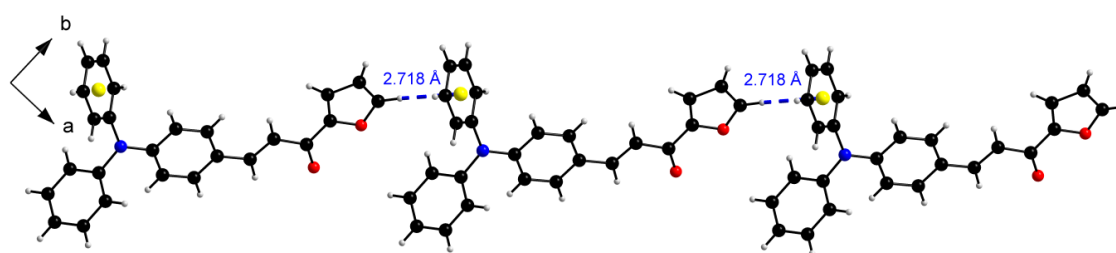


Figure 2.10. Packing in (*E*)-3-(4-(diphenylamino)phenyl)-1-(furan-2-yl)prop-2-en-1-one (**4**) due to C-H- π intermolecular H-bonding interactions separated by distance 2.718 Å.

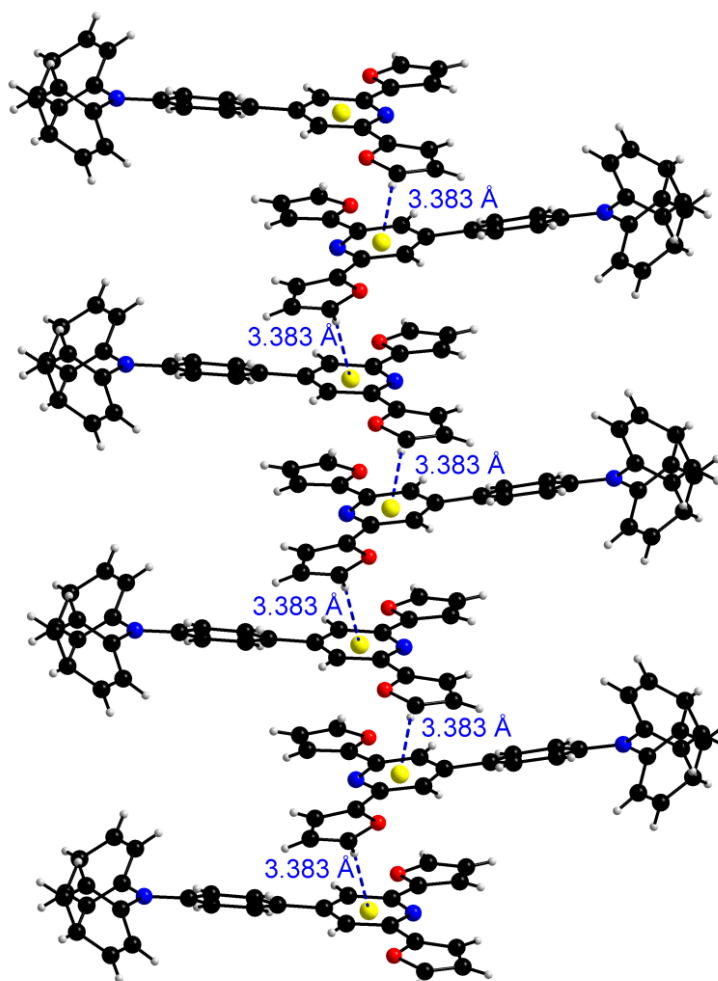


Figure 2. 11. Packing in 4-(2,6-di(furan-2-yl)pyridin-4-yl)-*N,N*-diphenylaniline (**DFPDA**) **1** due to C-H- π -intermolecular and H-bonding interactions separated by distance 3.383 Å leading to a helical structure.

2.5. Results and discussion

2.5.1 Absorption and emission study in different solvent

The molecule 4-(2,6-di(furan-2-yl)pyridin-4-yl)-*N,N*-diphenylaniline (**DFPDA**) **1** was successfully synthesized and structure was characterized by various techniques as discussed above in the chapter. Further we investigated receptor **1** to study its photophysical properties and its application in sensing of various analytes. Before sensing application, we performed the solvent study to study its solvatochromic effect or to study the effect of various organic solvents. It was observed that our molecule was soluble in various organic solvent and insoluble

in water. Therefore, we performed the solvent analysis in different organic solvents such as DMSO, acetonitrile (ACN), Chloroform (CHCl_3), water (H_2O), hexane, methanol (MeOH) tetrahydrofuran (THF). The absorption spectrum was recorded for each solvent as shown in

Figure 2.12.

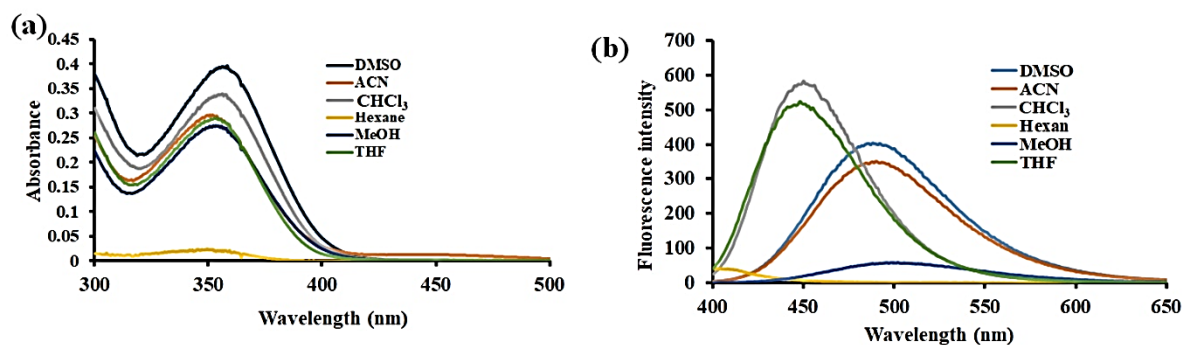


Figure 2.12. Solvent study performed for the (DFPDA) **1** (a) UV-Vis plot recorded in various organic solvents such as DMSO, acetonitrile (ACN), Chloroform (CHCl_3), H_2O , hexane, methanol (MeOH), THF. (b) The emission spectrum recorded for the receptor **1** in organic solvents.

From solvent study we observed that DMSO is good solvent for further analysis as it shows appreciable shift in absorption as well as in the emission. Hence for further analysis of sensing application we have chosen DMSO as solvent. In solvent study investigation it is observed that as shown in **Figure 2.12. (a)** THF and CHCl_3 shows blue shift in emission while DMSO and ACN showed red shift in emission. We also observed that when receptor **1** was studied in hexane there was no emission band observed, in plot **Figure 2.12. (b)** there was quenching in fluorescence observed. From this it is noted that good absorption and emission band was observed for DMSO solvent compared to other solvent. Hence the reason for using DMSO as solvent for further analysis.

2.5.2. Sensing performance of receptor 1

After the solvent study we performed the selectivity study of the receptor **DFPDA 1** towards various cations such as Cd^{2+} , Fe^{3+} , Cu^{2+} , K^+ , Ba^{2+} , Co^{2+} , Mn^{2+} , Ni^{2+} , Hg^{2+} , Al^{3+} , Pb^{2+} , Zn^{2+} , Ca^{2+} , Fe^{2+} by a naked eye detection as well as under UV light illumination at 365 nm. The solution of receptor **1** was prepared ($50\mu\text{L } 2.5 \times 10^{-5}\text{M}$) in DMSO solvent. To this solution a series of cations in its chloride and sulphate salts of were added (1.5 equiv). Upon addition of various cations the change in color under day light **Figure 2.13. (a)** as well as under UV-Vis (365 nm) light were monitored as illustrated in **Figure 2.13. (b)** respectively. The obtained results shows that under day light receptor **1** in DMSO is colorless but with the addition of different cations only Fe^{3+} ion shows the remarkable color change in the solutions in presence over other cations. Therefore the receptor **DFPDA 1** can be used as fluorimetric and for naked eye detection of Fe^{3+} metal ion.

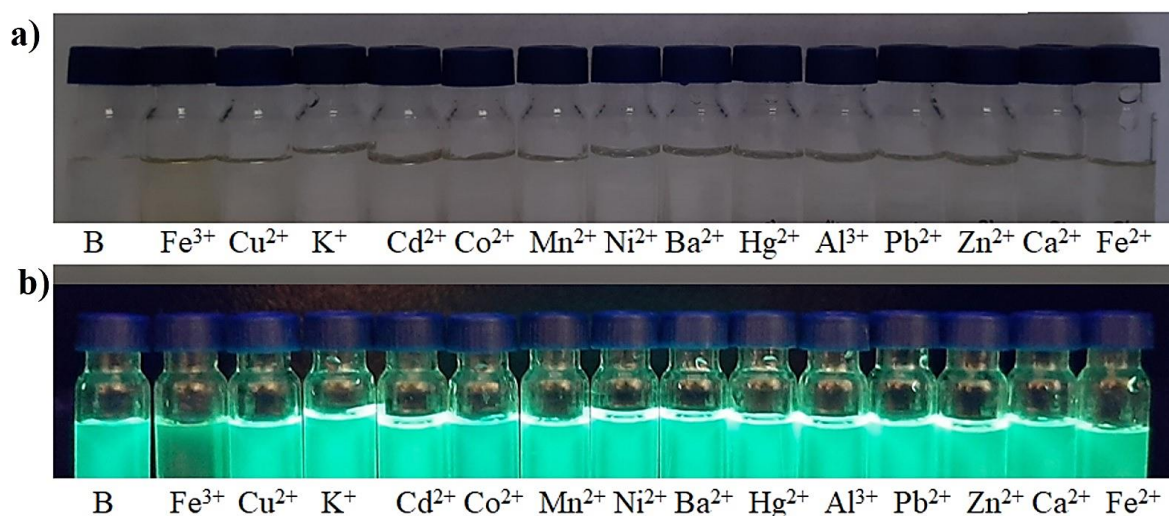


Figure 2. 13. (a) Image shows naked eye detection of Fe^{3+} metal ion in presence over other cations such as Cd^{2+} , Fe^{3+} , Cu^{2+} , K^+ , Ba^{2+} , Co^{2+} , Mn^{2+} , Ni^{2+} , Hg^{2+} , Al^{3+} , Pb^{2+} , Zn^{2+} , Ca^{2+} , Fe^{2+} . **(b)** Image shows the fluorescence colour change with the addition of Fe^{3+} over other cations.

2.5.3. UV-Vis absorption study

Furthermore, the UV-vis absorption spectra of receptor **DFPDA 1** was recorded with the addition of cations such as Cd^{2+} , Fe^{3+} , Cu^{2+} , K^+ , Ba^{2+} , Co^{2+} , Mn^{2+} , Ni^{2+} , Hg^{2+} , Al^{3+} , Pb^{2+} , Zn^{2+} ,

Ca^{2+} , Fe^{2+} as illustrated in **Figure 2.14 a**. The UV-Vis absorption spectra exhibited absorption maxima at 357 nm. The absorption at 357nm may be due to intramolecular charge transfer (ICT) effect which ultimately affect the optical and photophysical properties. There was no significant absorption change experienced with different cations but observed increase in absorption by the addition of Fe^{3+} metal ion. Thus, receptor **DFPDA 1** can be efficiently utilized for detection of Fe^{3+} with high selectivity. To get the insightful details further the UV-Vis titration was performed with incremental addition of Fe^{3+} ions as shown in **Figure 14 b**. The UV-Vis absorption changes were monitored with incremental addition of Fe^{3+} ion (0-2.5 equiv.) to **DFPDA 1** in DMSO ($1.25 \times 10^{-5}\text{M}$). It was observed that the upon incremental addition of Fe^{3+} ions to the receptor **DFPDA 1** absorption goes on increasing at 357 nm from (0-2.5 equiv.). This increase in absorption intensity is mainly due to metal to ligand charge transfer.

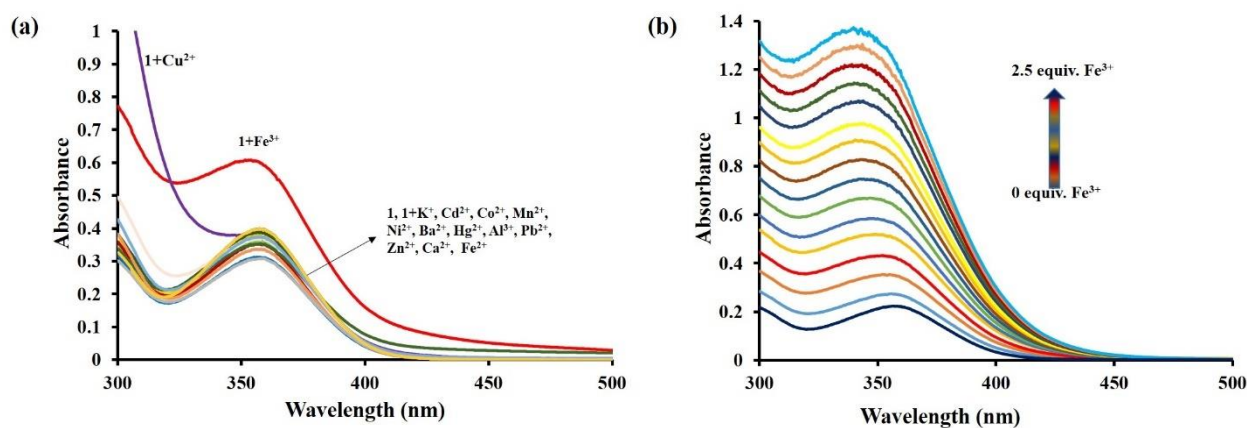


Figure 2. 14. (a) UV-Vis absorption spectra of **1** (2.5×10^{-5} M) in presence of different cations and (b) Absorption spectra with incremental addition of Fe^{3+} (0-2.5equiv.), 1.37×10^{-5} M) in DMSO.

2.5.4. Fluorescence emission study

Fluorescence emission spectral study was performed to investigate the selectivity of **DFPDA 1** towards Fe^{3+} ion in DMSO solvent. The obtained results are illustrated in **Figure 15**. As the

DFPDA 1 was excited at 350 nm exhibited the fluorescence emission band at 495 nm. Upon addition of Fe^{3+} fluorescence colour change was observed from but as incremental addition of Fe^{3+} ion there is complete quenching of fluorescence. Further to study the sensing ability of the probe **DFPDA 1** fluorescence titration was performed which showed that upon incremental addition of Fe^{3+} ion there is quenching of fluorescence observed. The fluorescence quenching is described by the donating nature of diphenyl rings which results in to participation of the electron pair present on nitrogen and difuran moiety to coordinate with Fe^{3+} . The coordination of Fe^{3+} metal ion to receptor led to quenching of fluorescence of fluorescence due to photoinduced electron transfer (PET) process. The fluorescence quenching constant was observed to be $K_{sv}=4.96 \times 10^4$.

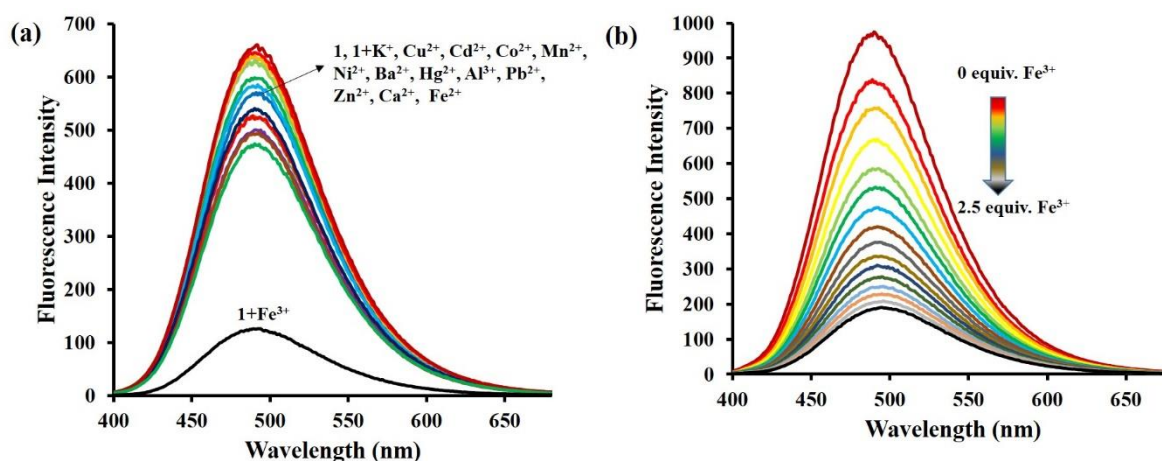


Figure 2. 15. (a) Fluorescence emission spectra of **1** (2.5×10^{-5} M) in presence of different cations (2.5×10^{-3} M) and ($\lambda_{ex} = 350$ nm, excitation and emission slit = 5nm) and (b) Emission spectra with the incremental addition of Fe^{3+} from (0-2.5 equiv. of 1.37×10^{-5} M) in DMSO ($\lambda_{ex} = 350$ nm, excitation slit = 10 nm, emission slit = 2.5nm).

2.5.5. Stoichiometry analysis and binding constant

The stoichiometry between the metal ion and receptor was investigated by Jobs method while the binding constant was determined by Benesi Hildebrand plot. The Jobs plot was determined as a function of fluorescence intensity against mole fraction $[1]/[1+\text{Fe}^{3+}]$. The stoichiometry of the complex formed between **DFPDA 1** is 2:1 complex ($1: \text{Fe}^{3+}$) as shown in **Figure 2.16. a**

the binding constant between the receptor **DFPDA 1** and metal was calculated by Benesi Hildebrand plot **Figure 2.16. b** and was found to be 3.75×10^{-8} M.

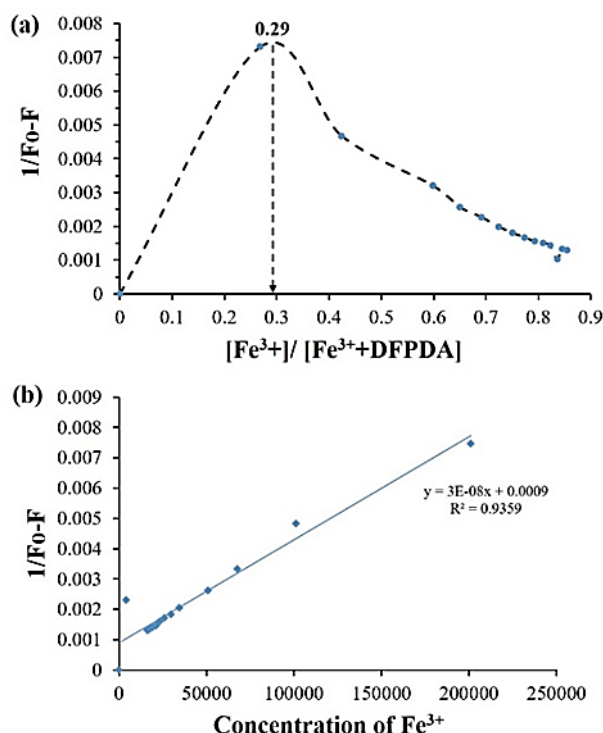


Figure 2.16. (a) The plot of Job's plot represents stoichiometry of the complex to be **DFPDA 1:Fe³⁺** (2:1) and (b) Benesi–Hildebrand plot of probe **DFPDA 1** with Fe^{3+} ion in DMSO with the binding constant observed to be 3.75×10^{-8} M.

2.5.6. Reversibility and reusability

The reversibility one of the most important characteristics that is to be analysed. A reversibility study determines for how many times/cycles one can use the same species for determination of analytical application. Therefore, there is need of studying the reversibility and reusability of the fluorescent molecule of sensing of analyte. The receptor **DFPDA 1** was further employed for reversibility and how we can reuse the following molecule for sensing of Fe^{3+} . Herein we employed simple basic chemistry. Many researchers utilized ethylenediamine for studying the reversibility. But when EDTA is used there is need of maintaining the pH of the solution. Hence

applied simple chemistry of base. We know that Fe^{3+} in basic condition precipitate as $\text{Fe}(\text{OH})_3$ therefore for reversibility we used NaOH base to break this interaction between Fe^{3+} metal and receptor and it was observed that the **DFPDA 1** showed reversible nature. After observing it under 365 nm light we recorded its absorption and fluorescence spectra at room temperature with addition of NaOH. Initially **DFPDA 1** (2.5×10^{-5} M) was taken in the cuvette in 2ml DMSO and to that 50 μL of Fe^{3+} was added and to the same solution NaOH was added. It was observed that upon addition of NaOH the fluorescence reappears where in ferric hydroxide $\text{Fe}(\text{OH})_3$ precipitates out. The solution was centrifuged, and its absorbance and fluorescence spectra were recorded. See **Figure 2.17**. thus, reversibility studies revealed that the molecule was reversible for 3 cycles.

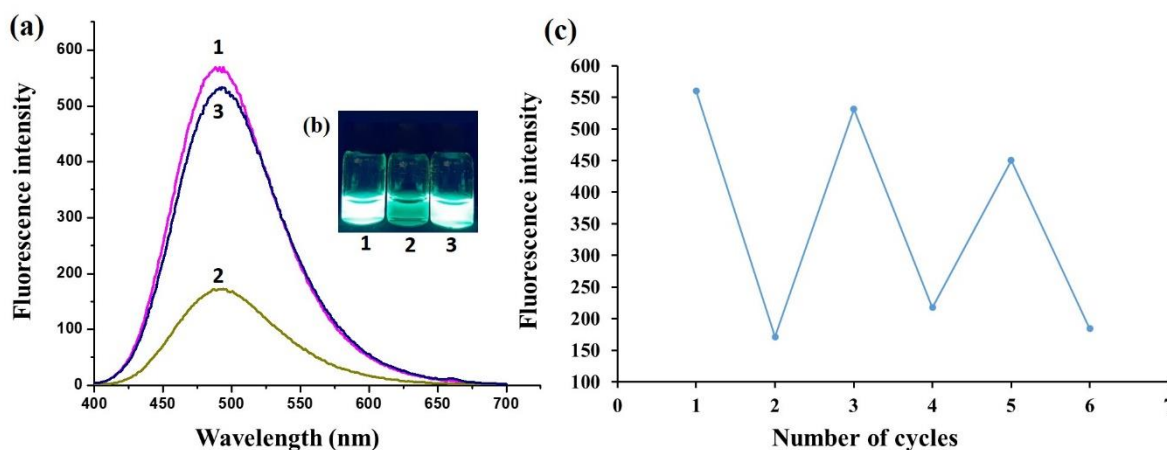


Figure 2. 17. (a) The plot representing fluorescence change intensity for the **DFPDA 1** as depicted (blank 1, 2 vial addition of Fe^{3+} , 3 vial addition of NaOH to the solution containing Fe^{3+}), (b) The fluorescence color change observed at 365 nm upon addition of Fe^{3+} and NaOH (inset photograph). (c) Represents the number of reversible cycles with addition of Fe^{3+} ion and NaOH to the solution of the **DFPDA 1**.

2.5.7. Competitive study

The competitive study was performed to study the selectivity towards various cations in presence over other competing cations. In this study we added different cations and Fe^{3+} ion to

the solution of receptor **DFPDA 1**. When cations such as Cd^{2+} , Cu^{2+} , K^+ , Ba^{2+} , Co^{2+} , Mn^{2+} , Ni^{2+} , Hg^{2+} , Al^{3+} , Pb^{2+} , Zn^{2+} , Ca^{2+} , Fe^{2+} was added there was no change in absorption intensity observed but to the same solution when we added Fe^{3+} metal ion there was increase in absorption intensity while the fluorescence intensity showed the quenching of fluorescence. Thus, it proves that in presence over other competing metal ions only Fe^{3+} shows the change in its photophysical properties as shown in **Figure 2.18**.

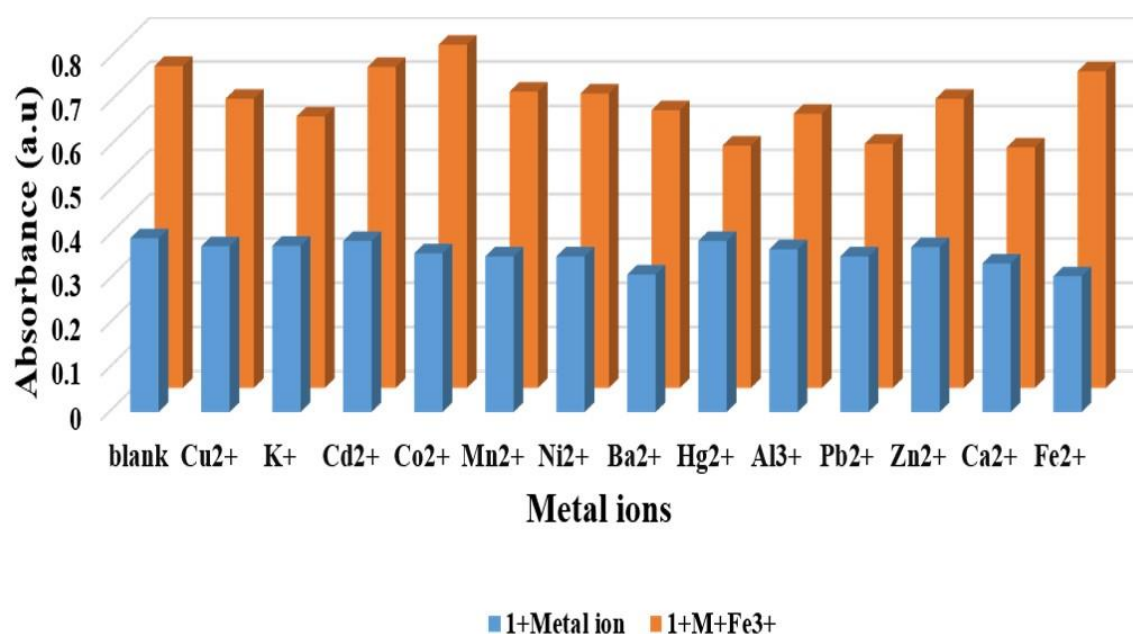


Figure 2. 18. The graph represents competitive reaction between receptor **DFPDA 1** and Fe^{3+} (1 equiv.) with **DFPDA 1** in presence of interfering cations (1equiv.) at 357 nm. Blue bar represents **DFPDA 1** with other cation and red bar represents **DFPDA 1**+ other cations + Fe^{3+} ion.

2.6. Conclusion

The fluorescent molecule 4-(2,6-di(furan-2-yl) pyridin-4-yl)-*N,N*-diphenylaniline (**DFPDA 1**) was synthesized by simple aldol condensation and further undergoes Krohnke pyridine synthesis to form the final receptor **DFPDA 1**. The synthesized probe was successfully characterized by various characterization techniques such as ^1H NMR, ^{13}C NMR, ESI-MS, elemental analysis and by single crystal XRD. The probe DFPDA was further studied for its

photophysical studies which is investigated by using UV-Vis and Fluorescence emission. The compound was utilized for fluorescent sensing application while the compound **DFPDA 1** showed excellent selectivity and sensitivity towards Fe^{3+} metal ion in presence over other cations such as Fe^{3+} , Fe^{2+} , Hg^{2+} , Pb^{2+} , Ni^{2+} , Al^{3+} , Mn^{2+} , Co^{2+} , Zn^{2+} , Ca^{2+} , Cu^{2+} . The reversibility study was performed for the receptor towards Fe^{3+} by using simple base that is sodium hydroxide. It showed reversible nature with 3 number of cycles. While the LOD and binding constant was found to be 52 nM and 3.75×10^{-8} M respectively. Therefore, it can be concluded that the probe was successfully utilized for sensing application of Fe^{3+} .

2.7. References

- (1) Cairo, G.; Pietrangelo, A. Iron Regulatory Proteins in Pathobiology. *Biochem. J.* **2000**, 352 (2), 241–250. <https://doi.org/10.1042/0264-6021:3520241>.
- (2) Liu, Y.; Shen, R.; Ru, J.; Yao, X.; Yang, Y.; Liu, H.; Tang, X.; Bai, D.; Zhang, G.; Liu, W. A Reversible Rhodamine 6G-Based Fluorescence Turn-on Probe for Fe^{3+} in Water and Its Application in Living Cell Imaging. *RSC Adv.* **2016**, 6 (113), 111754–111759. <https://doi.org/10.1039/c5ra09758d>.
- (3) Wang, Y.; Guo, R.; Hou, X.; Lei, M.; Zhou, Q.; Xu, Z. Highly Sensitive and Selective Fluorescent Probe for Detection of Fe^{3+} Based on Rhodamine Fluorophore. *J. Fluoresc.* **2019**, 29 (3), 645–652. <https://doi.org/10.1007/s10895-019-02378-0>.
- (4) He, Y. H.; Lai, J. P.; Sun, H.; Chen, Z. M.; Lan, S. A Fast, Sensitive and Stable Fluorescent Fiber-Optic Chemosensor for Quantitative Detection of Fe^{3+} in Real Water and HepG2 Living Cells. *Sensors Actuators, B Chem.* **2016**, 225, 405–412. <https://doi.org/10.1016/j.snb.2015.11.048>.
- (5) Sen, S.; Sarkar, S.; Chattopadhyay, B.; Moirangthem, A.; Basu, A.; Dhara, K.; Chattopadhyay, P. A Ratiometric Fluorescent Chemosensor for Iron: Discrimination of Fe^{2+} and Fe^{3+} and Living Cell Application. *Analyst* **2012**, 137 (14), 3335–3342. <https://doi.org/10.1039/c2an35258c>.
- (6) Bhowmick, R.; Islam, A. S. M.; Saha, U.; Suresh Kumar, G.; Ali, M. Rhodamine Based Turn-on Chemosensor for Fe^{3+} in Aqueous Medium and Interactions of Its Fe^{3+} Complex with DNA. *New J. Chem.* **2018**, 42 (5), 3435–3443. <https://doi.org/10.1039/c7nj04505k>.

- (7) Kim, Y. S.; Lee, J. J.; Lee, S. Y.; Jo, T. G.; Kim, C. A Highly Sensitive Benzimidazole-Based Chemosensor for the Colorimetric Detection of Fe(II) and Fe(III) and the Fluorometric Detection of Zn(II) in Aqueous Media. *RSC Adv.* **2016**, *6* (66), 61505–61515. <https://doi.org/10.1039/c6ra10086d>.
- (8) Chan, S.; Li, Q.; Tse, H.; Lee, A. W. M.; Mak, N. K.; Lung, H. L.; Chan, W. H. A Rhodamine-Based “off-on” Fluorescent Chemosensor for Selective Detection of Fe³⁺ in Aqueous Media and Its Application in Bioimaging. *RSC Adv.* **2016**, *6* (78), 74389–74393. <https://doi.org/10.1039/c6ra14411j>.
- (9) Kagit, R.; Yildirim, M.; Ozay, O.; Yesilot, S.; Ozay, H. Phosphazene Based Multicentered Naked-Eye Fluorescent Sensor with High Selectivity for Fe³⁺ Ions. **2014**.
- (10) Zhao, M.; Zhou, X.; Tang, J.; Deng, Z.; Xu, X.; Chen, Z.; Li, X.; Yang, L.; Ma, L. Spectrochimica Acta Part A: Molecular and Biomolecular Spectroscopy Pyrene Excimer-Based Fluorescent Sensor for Detection and Removal of Fe³⁺ and Pb²⁺ from Aqueous Solutions. *SAA* **2017**, *173*, 235–240. <https://doi.org/10.1016/j.saa.2016.09.033>.
- (11) Ye, J.; Liu, J.; Wang, Z.; Bai, Y.; Zhang, W.; He, W. A New Fe³⁺ Fluorescent Chemosensor Based on Aggregation-Induced Emission. *Tetrahedron Lett.* **2014**, *55* (27), 3688–3692. <https://doi.org/10.1016/j.tetlet.2014.05.008>.
- (12) Jia-min, C.; Jing, Z.; Zhen, Z.; Abudu-rexit, A. A Novel Colorimetric Fluorescent Probe for Fe³⁺ Based on Tetraphenylethylene-Rhodamine. *Chinese J. Anal. Chem.* **2019**, *47* (11), e19139–e19146. [https://doi.org/10.1016/S1872-2040\(19\)61196-5](https://doi.org/10.1016/S1872-2040(19)61196-5).
- (13) Yao, J.; Dou, W.; Qin, W.; Liu, W. A New Coumarin-Based Chemosensor for Fe³⁺ in Water. *Inorg. Chem. Commun.* **2009**, *12* (2), 116–118. <https://doi.org/10.1016/j.inoche.2008.11.012>.
- (14) Wang, C.; Zhang, D.; Huang, X.; Ding, P.; Wang, Z.; Zhao, Y.; Ye, Y. A Fluorescence Ratiometric Chemosensor for Fe³⁺ Based on TBET and Its Application in Living Cells. *Talanta* **2014**, *128*, 69–74. <https://doi.org/10.1016/j.talanta.2014.03.073>.
- (15) Mohanasundaram, D.; Bhaskar, R.; Lenin, N.; Nehru, K.; Rajagopal, G.; Vinoth, G.; Rajesh, J. Journal of Photochemistry & Photobiology, A: Chemistry A Simple Triphenylamine Based Turn-off Fluorescent Sensor for Copper (II) Ion Detection in Semi-Aqueous Solutions. **2022**, *427* (January).
- (16) Yang, L.; Zhu, W.; Fang, M.; Zhang, Q.; Li, C. Spectrochimica Acta Part A: Molecular and Biomolecular Spectroscopy A New Carbazole-Based Schiff-Base as Fluorescent Chemosensor for Selective Detection of Fe³⁺ and Cu²⁺. *Spectrochim. Acta Part A Mol. Biomol. Spectrosc.* **2013**, *109*, 186–192. <https://doi.org/10.1016/j.saa.2013.02.043>.

-
- (17) Yao, W.; Xu, K.; Kong, H.; Kou, L.; Zhang, Q. Novel Naphthalene-Based Fluorescent Chemosensors for Cu and Fe in Aqueous Media. **2013**, 0278. <https://doi.org/10.1080/10610278.2012.735366>.
- (18) Bhuvanesh, N.; Velmurugan, K.; Suresh, S.; Prakash, P.; John, N.; Murugan, S. Naphthalene Based Fluorescent Chemosensor for Fe²⁺ Ion Detection in Microbes and Real Water Samples. *J. Lumin.* **2017**, 188 (April), 217–222. <https://doi.org/10.1016/j.jlumin.2017.04.026>.
- (19) Tessore, F.; Roberto, D.; Ugo, R.; Pizzotti, M.; Inorganica, C.; Uni, V.; Cimaina, E.; Cnr, M.; Venezian, V. G.; Quici, S.; Cavazzini, M.; Molecolari, T.; Golgi, V. C.; Inorganica, C.; Uni, V.; Via, G.; Angelis, F. De; Molecolari, T.; Uni, V. Terpyridine Zn (II), Ru (III), and Ir (III) Complexes : The Relevant Role of the Nature of the Metal Ion and of the Ancillary Ligands on the Second-Order Nonlinear Response of Terpyridines Carrying Electron Donor or Electron Acceptor Groups. **2005**, 44 (24), 355–366.
- (20) Zhang, Z.; Li, F.; He, C.; Ma, H.; Feng, Y.; Zhang, Y.; Zhang, M. Novel Fe³⁺ Fluorescence Probe Based on the Charge-Transfer (CT) Molecules. *Sensors Actuators, B Chem.* **2018**, 255, 1878–1883. <https://doi.org/10.1016/j.snb.2017.08.211>.
- (21) Hong, Y.; Chen, S.; Wai, C.; Leung, T.; Wing, J.; Lam, Y.; Liu, J.; Tseng, N.; Tsz, R.; Kwok, K.; Yu, Y.; Wang, Z.; Tang, B. Z. Fluorogenic Zn (II) and Chromogenic Fe (II) Sensors Based on Terpyridine-Substituted Tetraphenylethenes with Aggregation-Induced Emission Characteristics. **2011**, No. Ii, 3411–3418.
- (22) Cao, X.; Li, Y.; Yu, Y.; Fu, S.; Gao, A.; Chang, X. Multifunctional Supramolecular Self-Assembly System for Colorimetric Detection of Hg²⁺, Fe³⁺, Cu²⁺ and Continuous Sensing of Volatile Acids and Organic Amine Gases. *Nanoscale* **2019**, 11 (22), 10911–10920. <https://doi.org/10.1039/c9nr01433k>.
- (23) Gao, X. X.; Zhou, X.; Ma, Y. F.; Wang, C. P.; Chu, F. X. A Fluorometric and Colorimetric Dual-Mode Sensor Based on Nitrogen and Iron Co-Doped Graphene Quantum Dots for Detection of Ferric Ions in Biological Fluids and Cellular Imaging. *New J. Chem.* **2018**, 42 (18), 14751–14756. <https://doi.org/10.1039/c8nj01805g>.
- (24) Trigo-López, M.; Muñoz, A.; Ibeas, S.; Serna, F.; García, F. C.; García, J. M. Colorimetric Detection and Determination of Fe(III), Co(II), Cu(II) and Sn(II) in Aqueous Media by Acrylic Polymers with Pendant Terpyridine Motifs. *Sensors Actuators, B Chem.* **2016**, 226, 118–126. <https://doi.org/10.1016/j.snb.2015.11.116>.
- (25) Nandre, K. P.; Puyad, A. L.; Bhosale, S. V.; Bhosale, S. V. A Novel Donor-Acceptor

- Receptor for Selective Detection of Pb²⁺ and Fe³⁺ Ions. *Talanta* **2014**, *130*, 103–107. <https://doi.org/10.1016/j.talanta.2014.06.064>.
- (26) Nadimetla, D. N.; Bhosale, S. V. Tetraphenylethylene AIEgen Bearing Thiophenylbipyridine Receptor for Selective Detection of Copper (II) Ion. **2021**, 7614–7621. <https://doi.org/10.1039/d1nj01001h>.
- (27) Zhang, X.; Shen, L. Y.; Zhang, Q. L.; Yang, X. J.; Huang, Y. L.; Redshaw, C.; Xu, H. A Simple Turn-off Schiff Base Fluorescent Sensor for Copper (II) Ion and Its Application in Water Analysis. *Molecules* **2021**, *26* (5). <https://doi.org/10.3390/molecules26051233>.
- (28) Jiang, B.; Hao, W.; Wang, X.; Shi, F.; Tu, S. Diversity-Oriented Synthesis of Krohnke Pyridines. **2009**, 846–850.
- (29) Adib, M.; Tahermansouri, H.; Koloogani, S. A.; Mohammadi, B.; Bijanzadeh, H. R. Kröhnke Pyridines: An Efficient Solvent-Free Synthesis of 2,4,6-Triarylpyridines. *Tetrahedron Lett.* **2006**, *47* (33), 5957–5960. <https://doi.org/10.1016/j.tetlet.2006.01.162>.
- (30) Kröhnke, F.; Zecher, W.; Curtze, J.; Drechsler, D.; Pflegar, K.; Schnalke, K. E.; Weis, W. Synthesis Using the Michael Addition of Phridinium Salts. *Angew. Chemie Int. Ed. English* **1962**, *1* (12), 626–632. <https://doi.org/10.1002/anie.196206261>.

CHAPTER 3

CHAPTER 3

3.1. Introduction

The fluorescent chemosensors which can detect the environmentally and biologically important metal ions such as Zn^{2+} , Fe^{3+} , Cu^{2+} , Cd^{2+} , Pb^{2+} , Hg^{2+} and As^{3+} is an important area of research interest [1]. In human body copper (Cu^{2+}) is considered as the third most essential transition metal [2]. In biological systems copper plays very important role in different physiological processes such as a cofactor in electron transfer system, catalyst in various oxidoreductase reactions and signal transduction. Due to cellular toxicity controlling the copper content in the body is extremely necessary. In case if the level of Cu^{2+} content increases in body may result in to formation of reactive oxygen species (ROS), that can harm lipids, proteins and nucleic acids. Excess amount of Cu^{2+} may result in to severe diseases such as Alzheimer, prion disease, Menkes and Wilson disease due to cellular toxicity [3,4,5]. Copper is considered most common metal pollutant due to its extensive usage. According to United State Environmental Protection Agency (EPA) permissible level of copper is 1.3 ppm [6].

Over the last few years there are several instrumental techniques have been developed for detection of copper such as atomic absorption spectroscopy, surface enhanced Raman spectroscopy, and inductively coupled plasma mass spectrometry. Since these methods are expensive, operation of the instrument is tedious and more time consuming. Thus, the fluorescent chemosensor for Cu^{2+} has gained lot of attention and its detection is of primary importance [7]. Most of the fluorescent chemosensor detect the Cu^{2+} by a fluorescence quenching process via charge transfer or energy transfer mechanism.

There are various organic fluorescent materials have been developed for selective and sensitive detection of Cu^{2+} such as coumarin derivative [8,9,10,11], rhodamine derivatives [12], triarylamine derivative [13], pyrene [14], 1,8-naphthalenediimide [15], carbazole derivative [16]. There are many more derivatives which are utilized for detection of Cu^{2+} . Thus,

introducing to few fluorescent probes that are used for detection of copper such as various functionalized organic dyes [17,18], quantum dots [19], fluorescent metal organic framework [20], Binol based derivative [21]. All this material has high photostability, biocompatibility, low photobleaching, large stokes shift and low toxicity.

Generally, the fluorescent chemical sensor for detection of Cu^{2+} and Fe^{3+} ions are designed according to their interactions usually by reaction mode which results in to formation of new product or by chelation mode which has linkers between the receptor site and fluorophore [22]. Thus, for metal cation sensing usually fluorophore can be constructed by using heteroatoms such as N, O, and S [23]. The metal cation binding to the heteroatom detection takes place via coordination which produces luminescence changes and absorption changes by various photophysical phenomenon such as photoinduced electron transfer (PET) [24,25] intramolecular charge transfer (ICT) [26,27] and energy transfer, however upon coordination there is no structural changes observed but there are spectral intensity changes [28]. Usually, this kind of response is observed with the fluorescent molecule undergoing chelation mode upon binding with metal ion. Few examples are discussed below [29,30].

Liu and co-workers derived the molecule by using naphthaliimide as chromophore for copper sensing. In this work the molecule was prepared by condensing 2-(thiophen-2-ylmethylene)hydrazine with naphthaliimide to give a simple Schiff base structure [S1]. The molecule showed excellent and promising result for sensing of Cu^{2+} ion [31]. To add on Wang *et al.* developed two photon turn on-off-on fluorescent probe for selective sensing of Cu^{2+} ion in biological cell line. The molecule is simple Schiff base synthesized by reacting 4-(diethylamino)-2-hydroxybenzaldehyde with 2,2'-((4-aminophenyl)azanediyl)bis(ethan-1-ol) in presence of catalytic amount of glacial acetic acid and ethanol refluxed for 12 hours. The molecule showed excellent application in determination of Cu^{2+} ion biological cell lines [32]. Another similar Schiffs base was designed by Hu and co-workers by using 4-*N,N'*-dihydroxy

ethyl salicylaldehyde and aniline to give π conjugated system. The Schiff base shows interaction with metal ion via hydroxy and CH=N bond in the receptor [S2] [33]. Wang *et al.* derived quinoline based fluorescent material for Cu^{2+} ion with high selectivity and sensitivity. Cu^{2+} ion probes show quenching of fluorescence due to paramagnetic behaviour [S3] [34].

Figure 3.1.

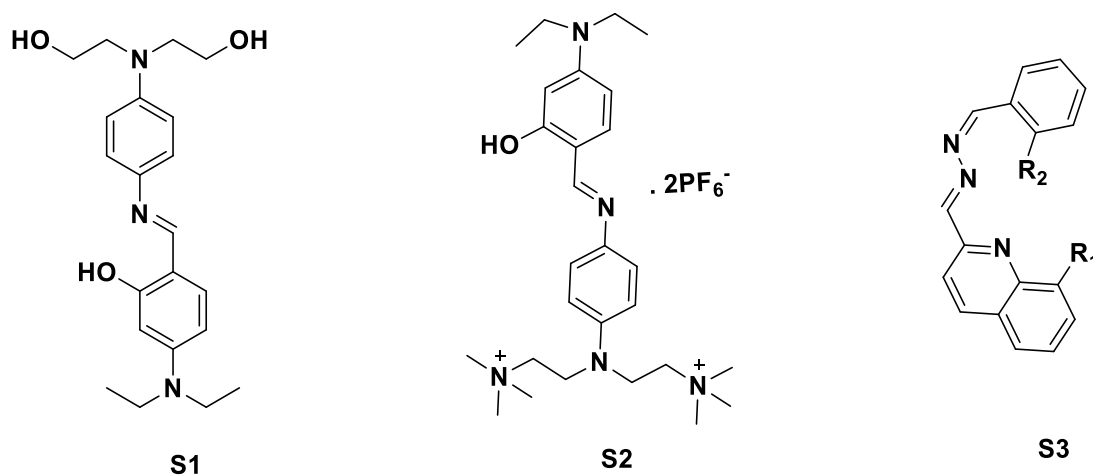


Figure 3.1. Structures of organic fluorescent molecule reported for sensing of Cu^{2+} ions.

In chapter two we have already discussed about 4-(2,6-di(furan-2-yl)pyridin-4-yl)-*N,N*-diphenylaniline [DFPDA 1] derivative which is highly selective and sensitive towards Fe^{3+} metal ion. In this regards we wanted to study the selectivity of the molecule towards various cations therefore we have derivatized the molecule by changing the difuran moiety with thiophene and dipyridine acceptor core. The molecule was successfully synthesized and characterized by ^1H NMR, ^{13}C NMR, elemental analysis, Single crystal X-ray Diffraction, and ESI-Mass. On the part of current ongoing research herein we have synthesized *N,N*-diphenyl-4-(6-thiophene-2-yl)-[2,2'-bipyridin]-4-yl)aniline [DTBPA 1] fluorescent probe which exhibits turn off fluorescence response towards Cu^{2+} metal ion. The probe [DTBPA 1] was synthesized by reacting 4-(diphenylamino)benzaldehyde with Michael salt of pyridine in presence of ammonium hydroxide and catalytic amount of acetic acid. The probe [DTBPA 1] consists of dipyridine and thiophene unit. From the earlier reported work we synthesized

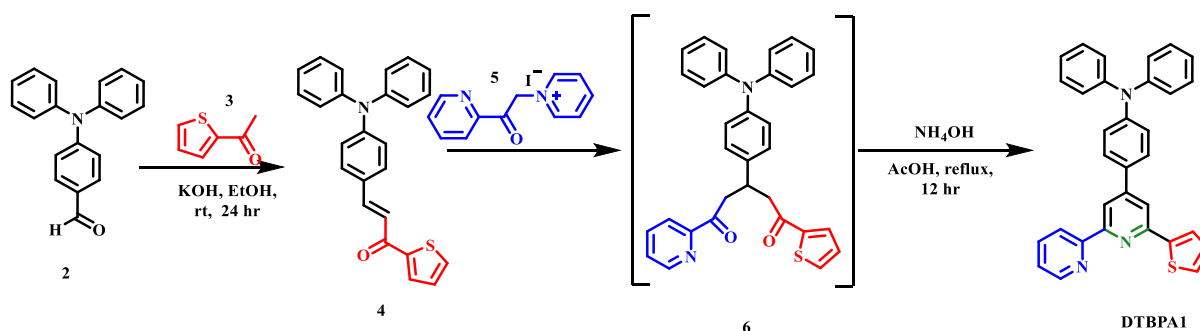
another derivative using diphenylamine as donor [35]. The probe **[DTBPA 1]** comprising of the two pyridine and thiophene unit showed good selectivity towards the Cu^{2+} ion in presence over other ions. The recognition moiety binds with Cu^{2+} ion by sharing of lone pair of the electrons present on the two nitrogens of pyridine present in the core. In addition, its optical and photophysical properties were studied by UV-Vis and fluorescence spectrofluorometer. The molecule was also used for sensing of copper in water sample. DFT study was performed to study its interaction with Cu^{2+} ion.

3.2. Experimental

3.2.1 Materials and chemicals:

The chemical requirements for synthesis of probe **DTBPA 1** are diphenyl aniline aldehyde was purchased from TCI chemical, acetyl thiophene, ammonium acetate, acetyl pyridine, acetic acid, potassium hydroxide, ethanol, and ammonium hydroxide. For sensing application various cations such as (Fe^{3+} , Cu^{2+} , K^+ , Cd^{2+} , Co^{2+} , Mn^{2+} , Ni^{2+} , Ba^{2+} , Hg^{2+} , Al^{3+} , Pb^{2+} , Zn^{2+} , Ca^{2+} , Fe^{2+} salt. Acetonitrile was used for sensing application which was purchased from Sigma-Aldrich and TCI. The synthesized compound was purified by column chromatography by using 10% ethyl acetate and pet ether solvent. After purification the compound was characterized by recording ^1H NMR 400 MHz and ^{13}C NMR using 100 MHz Bruker spectrometer using Tetramethylsilane (TMS) as an internal standard and CDCl_3 as a deuterated solvent. Mass spectrometric data were obtained by positive electron spray ionization (ESI-MS) technique on an Agilent Technologies 1100 Series (Agilent Chemstation Software) mass spectrometer. UV-Vis absorption spectra was recorded by UV-vis-1800 Shimadzu spectrophotometer. Fluorescence was measured on Cary Eclipse software on Agilent technologies spectrofluorometer.

3.2.2. Synthetic route for synthesis of (*N,N*-diphenyl-4-(6-(thiophen-2-yl)-[2,2'-bipyridin]-4-yl)aniline **DTBPA 1**



Scheme 3.1. Synthetic route of receptor (*N,N*-diphenyl-4-(6-(thiophen-2-yl)-[2,2'-bipyridin]-4-yl)aniline (**DTBPA**) **1**.

3.2.3. Synthesis of (*E*)-3-(4-(diphenylamino)phenyl)-1-(thiophene-2-yl)prop-2-en-1-one (**4**)

To the reaction mixture of 4-(diphenylamino) benzaldehyde **2** (0.20 gm, 0.002 mol) and 2-acetyl thiophene **3** (0.5 gm, 0.002 mol) in 15 ml ethanol 5% potassium hydroxide (0.5 gm dissolved in 10ml ethanol) was added dropwise over 10 min. The reaction mixture was allowed to stir at room temperature for 24 hours [36]. The orange solid product formed was filtered and washed with water which was further recrystallized using ethanol to give compound **4** (0.51 gm, 64.4%). ¹H NMR (CDCl₃, 400 MHz): δ_H 7.81 (2H, t, *J* = 10.3 Hz), 7.63 (1H, d, *J* = 3.5 Hz), 7.48 (2H, d, *J* = 8.4 Hz), 7.12 (9H, m, *J* = 7.5, 18.8 Hz), 7.02 (9H, d, *J* = 8.8 Hz) ¹³C NMR (100 MHz, CDCl₃) δ ppm: 182.057, 150.262, 146.829, 145.984, 143.904, 133.415, 131.375, 129.822, 129.557, 128.197, 127.650, 125.532, 124.202, 121.540, 118.925, 77.413, 77.095, 76.777., Elemental analysis: Calculated. (%): C, 78.71; H, 5.02; N, 3.67; Found (%): C, 78.12; H, 5.13; N, 3.45.

3.2.4. Synthesis of 1-(2-(furan-2-yl)-2-oxoethyl)pyridin-1-ium (5)

The reaction mixture containing 2-acetyl thiophene **3** (2.2 gm, 0.02 mol) and iodine (5.1 gm, 0.02 mol) mixed in 25 ml of pyridine was refluxed for 3hrs. The intermediate **5** was prepared by following reported literature [37]. Allow the reaction mixture to cool after completion the precipitate formed was filtered. The solid product formed was washed thoroughly with cold pyridine. The product formed was directly used for next step reaction without any purification. (yield: 6.02gm, 80%).

3.2.5. Synthesis of probe (N,N-diphenyl-4-(6-(thiophen-2-yl)-[2,2'-bipyridin]-4-yl)aniline DTBPA 1

The intermediate **6** was formed by refluxing the mixture of **4** (0.3 gm, 0.001 mol) and **5** (2.1 gm, 0.007 mol) in presence of ammonium hydroxide and 10ml acetic acid at 90°C for 12 hrs. The reaction completion was monitored by thin layer chromatography (TLC). After completion the reaction was allowed to cool to room temperature and add 30 ml of cold water. The solid compound formed was washed with cold methanol dried and impurities were removed by eluting on column chromatography with ethyl acetate and PET ether solvent. Greenish yellow solid was obtained. Yield (1.4gm, 58 %). ¹H NMR (CDCl₃, 400 MHz): δ_H 8.62 (1H, d, *J* = 4.6 Hz), 8.55 (1H, d, *J* = 8.2 Hz), 8.46 (1H, d, *J* = 1.8 Hz), 7.79 (2H, m, *J* = 2.9, 5.8, 5.8 Hz), 7.63 (3H, m, *J* = 2.4, 6.9, 10.0 Hz), 7.36 (1H, q, *J* = 2.0 Hz), 7.09 (9H, m, *J* = 4.4, 8.7 Hz), 7.01 (9H, t, *J* = 7.4 Hz). ¹³C NMR (100 MHz, CDCl₃) δ ppm: 154.913, 151.291, 148.7607, 147.915, 147.878, 146.295, 144.435, 135.973, 130.547, 128.386, 126.988, 126.931, 126.512, 123.847, 123.481, 122.831, 122.456, 122.034, 120.534, 115.714, 114.923, 76.307, 75.990, 75.672. ESI-MS calculated. (M)⁺, 481.16, obs. 481.61 (M+1)⁺. Elemental analysis: Calculated (%): C, 79.80; H, 4.81; N, 8.72 Found (%): C, 79.62; H, 4.79; N, 8.34.

3.3. Characterization

The molecule was successfully synthesized, purified and structural characterization was done by different techniques such as ^1H NMR, ^{13}C NMR, elemental analysis, Single crystal X-ray Diffraction, ESI-Mass. Further its photophysical properties were investigated by using UV-Vis and photoluminescence spectroscopy. From above analysis the molecule was successfully characterized, and the final product formed has the molecular structure as synthesized by the applied synthetic procedure. The characterization data is represented as follows:

3.3.1. ^1H NMR spectra of **4** (*E*)-3-(4-(diphenylamino)phenyl)-1-(thiophen-2-yl)prop-2-en-1-one.

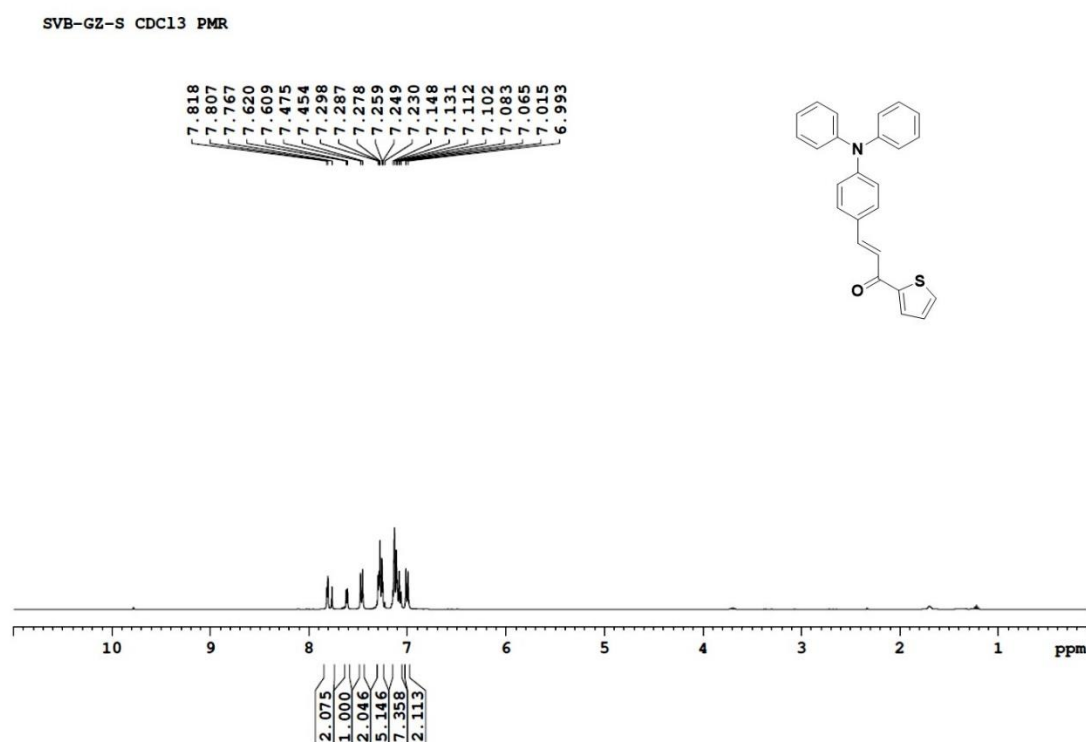


Figure 3. 2. ^1H NMR spectrum of **4** (*E*)-3-(4-(diphenylamino)phenyl)-1-(thiophen-2-yl)prop-2-en-1-one.

3.3.2. ^{13}C NMR spectrum of **4** (*E*)-3-(4-(diphenylamino)phenyl)-1-(thiophen-2-yl)prop-2-en-1-one.

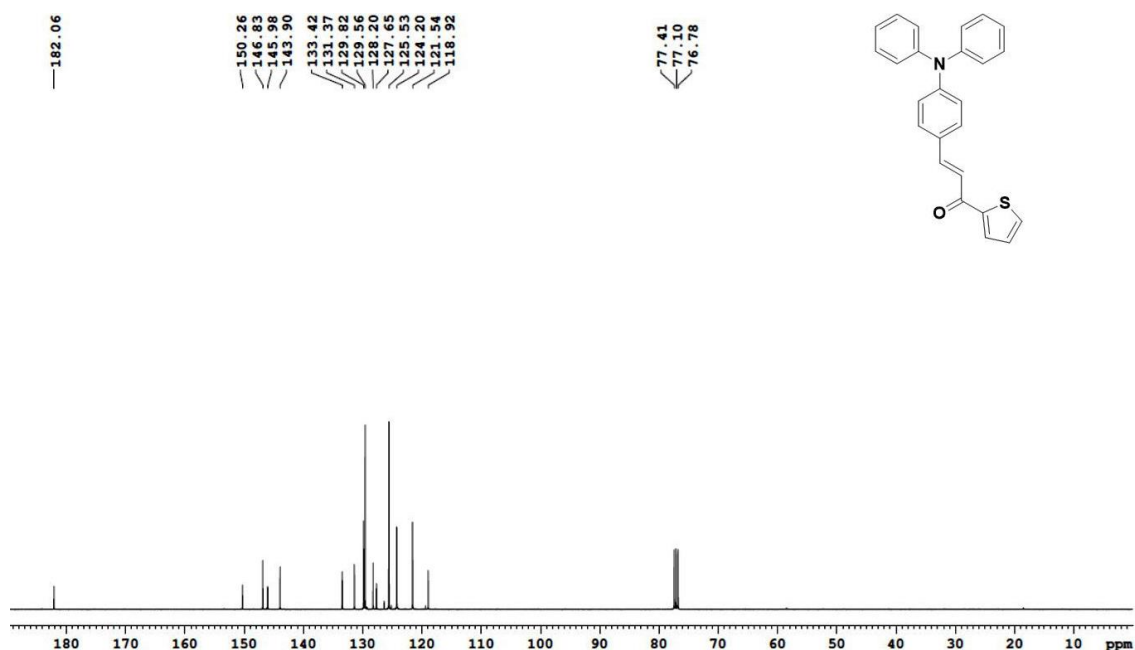


Figure 3.3. ^{13}C NMR spectrum of **4** (*E*)-3-(4-(diphenylamino)phenyl)-1-(thiophen-2-yl)prop-2-en-1-one

3.3.3. ^1H NMR spectrum of **DTBPA 1** (*N,N*-diphenyl-4-(6-(thiophen-2-yl)-[2,2'-bipyridin]-4-yl)aniline).

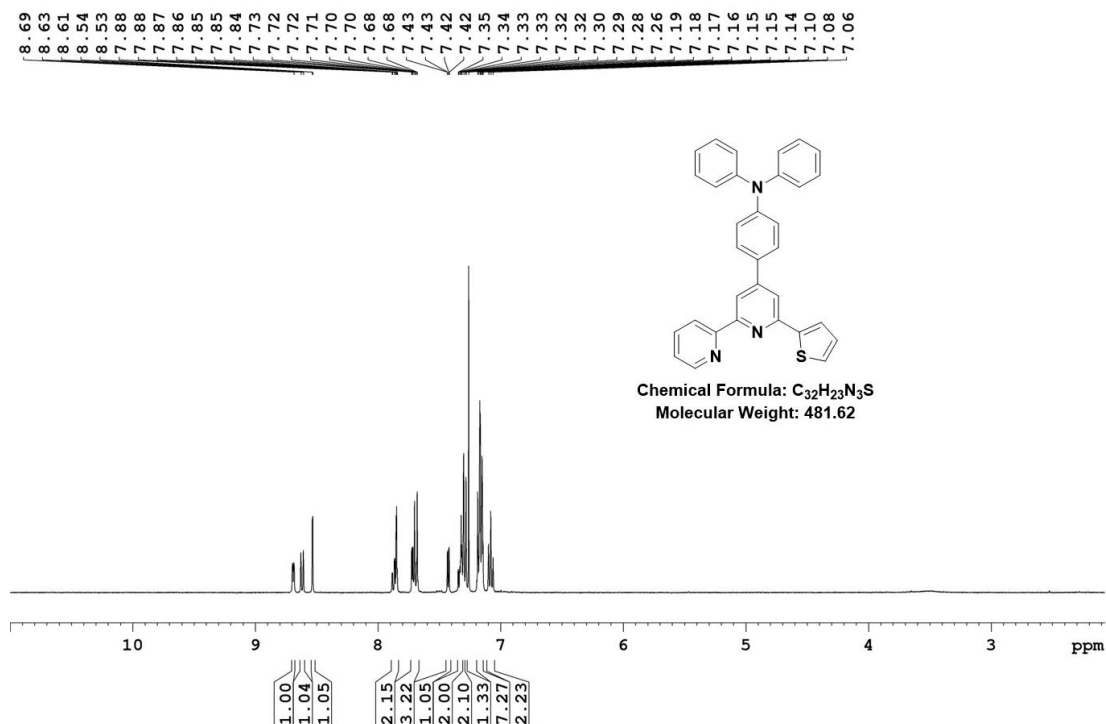


Figure 3.4. ^1H NMR spectrum of **DTBPA 1** (*N,N*-diphenyl-4-(6-(thiophen-2-yl)-[2,2'-bipyridin]-4-yl)aniline).

3.3.4. ^{13}C NMR spectrum of **DTBPA 1** (*N,N*-diphenyl-4-(6-(thiophen-2-yl)-[2,2'-bipyridin]-4-yl)aniline).

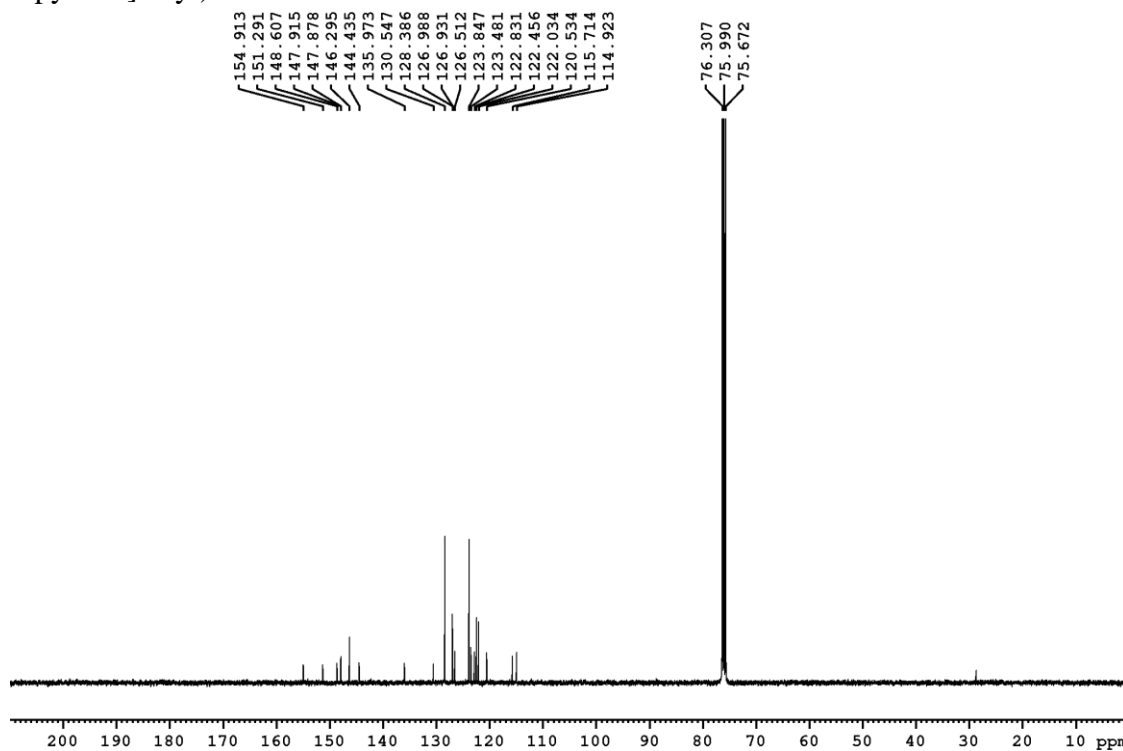


Figure 3.5. ^{13}C NMR spectrum of **DTBPA 1** (*N,N*-diphenyl-4-(6-(thiophen-2-yl)-[2,2'-bipyridin]-4-yl)aniline).

3.3.5. ESI-Mass of **DTBPA 1** (*N,N*-diphenyl-4-(6-(thiophen-2-yl)-[2,2'-bipyridin]-4-yl)aniline).

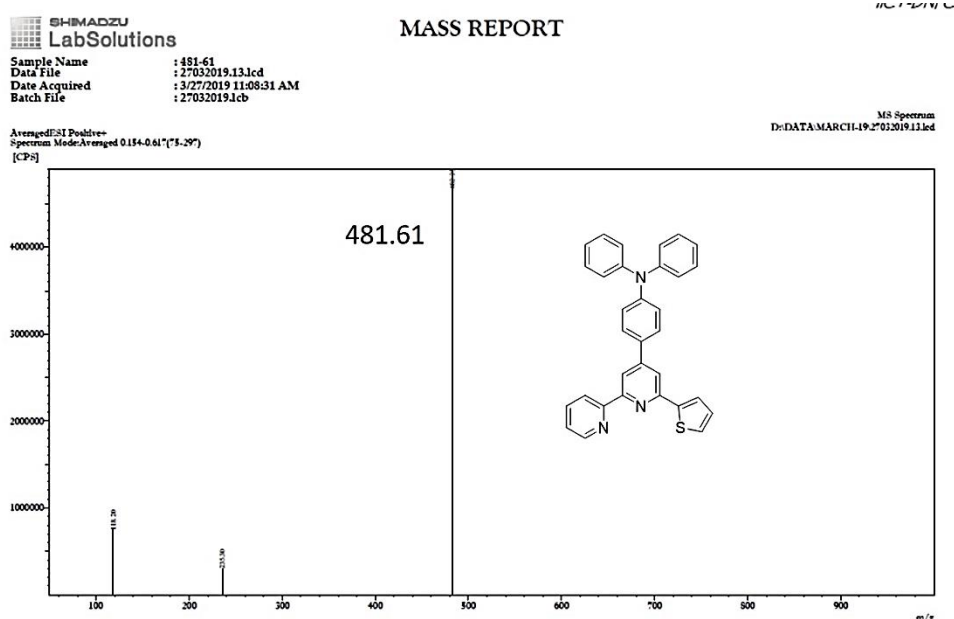


Figure 3.6. ESI- Mass for **DTBPA 1** (*N,N*-diphenyl-4-(6-(thiophen-2-yl)-[2,2'-bipyridin]-4-yl)aniline).

3.4 Crystal study

3.4.1. Preparation of crystal (*N,N*-diphenyl-4-(6-thiophene-2-yl)-[2,2'-bipyridin]-4-yl)aniline **DTBPA 1**

N,N-diphenyl-4-(6-thiophene-2-yl)-[2,2'-bipyridin]-4-yl)aniline [**DTBPA 1**] was crystallized in chloroform: methanol by diffusion method. The crystal structure of the compound was characterized by using Bruker D8 Quest Eco X-ray diffractometer. The prepared crystal represents monoclinic space group $P2_1/c$ $Z=4$. The data was collected at room temperature using ($\text{MoK}\alpha=0.7107 \text{ \AA}$) monochromatic radiations. The APEX3 (Version 2018.1) was used in order to determine the absorption correction and unit cell. The structure was resolved by using SHELX. In the structure it was found that all non-hydrogen atoms are anisotropically refined. The aromatic hydrogens are introduced on the calculated positions and riding on the respective carbon atoms. The crystallographic data for compound *N,N*-diphenyl-4-(6-thiophene-2-yl)-[2,2'-bipyridin]-4-yl)aniline **DTBPA 1** are reported in the given **Table 1** below. The data have been submitted in the Cambridge crystallographic data centre with CCDC number 2234448. The crystal structure of the probe **DTBPA 1** shown in **Figure 3.7**.

Table 3. 1. Crystal data and details of refinements for **DTBPA 1**

Empirical formula	$\text{C}_{32}\text{H}_{23}\text{N}_3\text{S}$
Formula weight (g mol^{-1})	481.59
Crystal system	Monoclinic
Space group	$P2_1/c$
a (\AA)	15.5622(10)
b (\AA)	8.5985(6)
c (\AA)	19.0719(13)
α (deg)	90
β (deg)	102.299
γ (deg)	90

Volume (Å ³)	2493.5(3)
Temperature (K)	296(2)
F(000)	1008.0
θ range (deg)	2.80 to 25.87
μ (mm ⁻¹)	0.081
Collected reflections	36219
Independent reflections	6195
Final R indices [I > 2 sigma (I)]	R1= 0.0824, wR2= 0.1613
R indices (all data)	R1= 0.2152, wR2= 0.2188
Goodness of fit	1.011
CCDC number	2234448

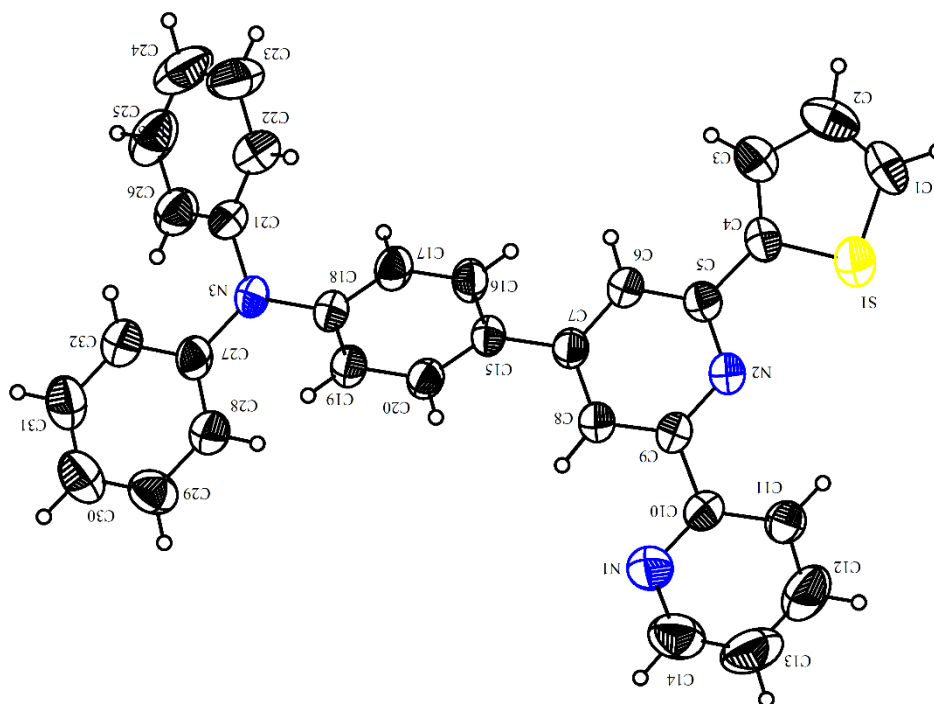


Figure 3.7. Crystal structure of probe **DTBPA 1**

3.5. Results and discussion

3.5.1. Solvent study

Solvatochromism is now a days used widely in many fields especially in chemical and biological research to understand the local polarity conformations and binding interaction with different analytes but still the phenomenon involved in solvatochromic study remains unresolved due to various interactions and dynamic processes of solute and solvent. Various industrial activities and scientific technology have focussed on synthetic dyes for optoelectronic applications and biomedical applications in the treatment of various diseases. Therefore, it is very important to study the solvent behaviours [38]. Solvent study helps to understand in detail intermolecular effects on structural modification, helps to determine the solubility as well as the polarizability effects. Solvent study also helps to determine the solute solvent hydrogen bond interaction and aggregation phenomenon can be well determined. All these different situations affect photophysical properties in terms of absorption and emission signal in terms of peak position and shape or the peak which results in to either quenching or enhancement [39]. Most of the molecular probes are highly sensitive and evident to show solvatochromic effect due to intermolecular interactions and even small changes in surrounding environment. Molecules which represent such behaviour usually undergoes charge transfer due to presence of donor and acceptor system in the chromophore. The spectral behaviour of chromophore changes as solvent interactions takes place by preferential solvation which further modifies the solute behaviour. In this regard absorption spectra are the best and simple approach for studying the transitions in the molecule which reveals the details of absorption wavelength shift of solute-solvent interaction this is termed as solvatochromism which is further determined by solute solvent interaction in ground and excited state. The energy gap of electronic state changes due to difference in the polarities of the ground and excited state of chromophore thus when the solvent polarity changes lead to stability differences in the ground and excited state. These further affects the shape, position, and intensity of absorption or

emission spectra. To study this behaviour, we performed solvent study to investigate whether DTBPA 1 shows the solvatochromic effect or not? [40,41]

3.5.2. Solvatochromic study

The probe **DTBPA 1** was successfully synthesized and characterized by ^1H NMR, ^{13}C NMR, ESI-Mass, Single crystal XRD. The optical and photophysical properties were investigated by UV-Vis and fluorescence spectrophotometry. Solubility is the most important parameter that is considered before analysis, and it was found that the probe **DTBPA 1** was completely soluble in organic solvents. The UV-Vis and fluorescence studies were performed to study its solvatochromic effect in different solvent such as dimethyl sulphoxide (DMSO), Acetonitrile (ACN), tetrahydrofuran (THF), Chloroform (CHCl_3) and water (H_2O). The probe **DTBPA 1** showed good absorption peak at 285 nm and 358 nm with strong emission at 495nm in ACN. While in DMSO and THF the absorption was observed at 285 nm and 358 nm and emission for DMSO was 498 nm but for THF emission was shifted to 448 nm. However, for CHCl_3 the emission band was observed at 448 nm with weak fluorescence intensity. But when the probe **DTBPA 1** was added in water absorption intensity was weak compared to the other organic polar aprotic solvents and the emission intensity was also weak as shown in plot **Figure 3.8**. This reveals that the probes **DTBPA 1** shows solvatochromic effect in different solvent. From the solvent study, we confirmed that DMSO as well as ACN can be used as good solvent for further analysis. But we have selected ACN for further applications.

3.5.3. Sensing Performance

Our next approach was to utilize the probe **DTBPA 1** for studying the detailed recognition of various cations such as Cu^{2+} , Fe^{3+} , Fe^{2+} , Hg^{2+} , Pb^{2+} , Ni^{2+} , Zn^{2+} , Mn^{2+} , Co^{2+} , Al^{3+} , Ca^{2+} , Ba^{2+} , Cd^{2+} , K^+ . The sensing performance for the probe was analyzed in acetonitrile solvent by placing 1mM stock solution in 2 ml of ACN. The series of solution of probe was prepared in 2 ml vials

and various cations were added (~1mM). Subsequently upon addition of different cations the vials were placed under UV light illumination at 365nm. It was observed that the green fluorescence of the probe quenches with addition of Cu^{2+} ion while there was no change in fluorescence observed for other cation. Therefore, we could conclude that the probe **DTBPA 1** has high selectivity towards Cu^{2+} ion in presence over other metal ions. While no color change was observed into visible light to the solution of probe when various cations are added. The following fluorescence change was detected as shown in **Figure 3.9**.

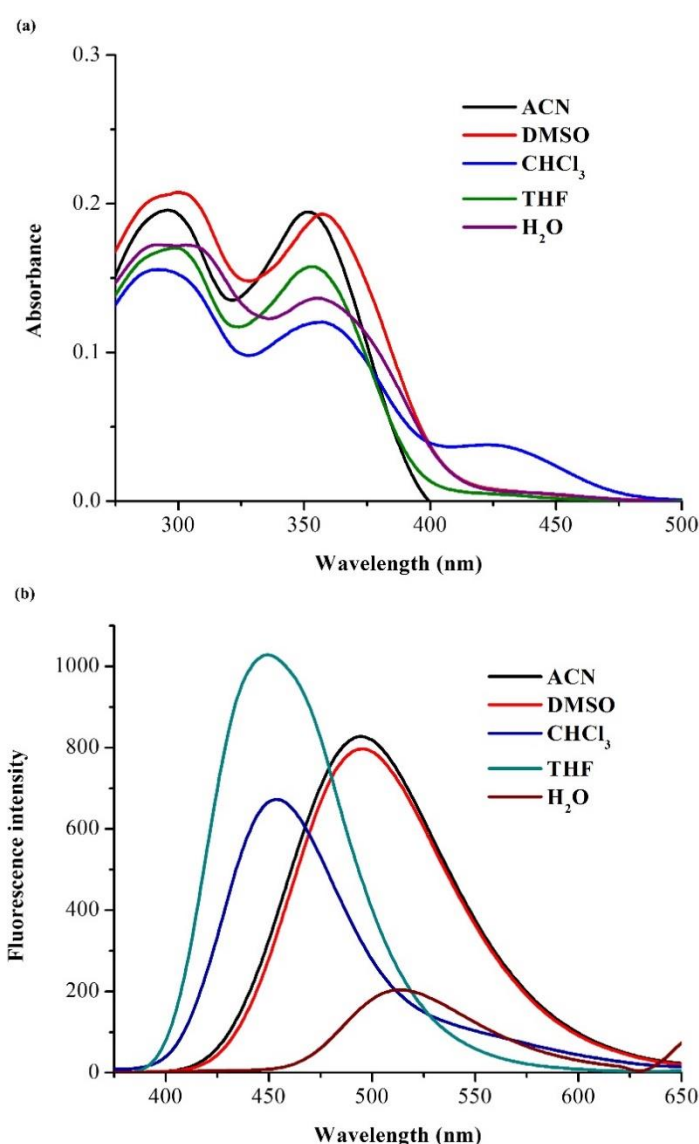


Figure 3.8. (a) Absorption spectra recorded for **DTBPA 1** probe in different solvents to study the solvatochromic effect (b) The emission plot for **DTBPA 1** probe in different solvents.



Figure 3.9. The sensing performance for **DTBPA 1** over different cations representing the quenching of fluorescence upon addition of Cu^{2+} ion.

3.5.4. UV- Vis absorption study

From the sensing performance i.e., under UV light illumination at 365 nm we confirmed that the receptor shows quenching phenomenon upon addition of Cu^{2+} ion in presence over other ions. Similarly, from the earlier reported work the core containing bipyridine and thiophene unit shows with TPE donor showed high selectivity and sensitivity towards Cu^{2+} ion [42]. Thus, from the above conclusion, we performed UV-visible studies to confirm its selectivity experimentally. To study its detecting ability towards metal ions 5 μM of the probe **DTBPA 1** solution was subjected to metal ions such as Cu^{2+} , Fe^{3+} , Fe^{2+} , Hg^{2+} , Pb^{2+} , Ni^{2+} , Zn^{2+} , Mn^{2+} , Co^{2+} , Al^{3+} , Ca^{2+} , Ba^{2+} , Cd^{2+} , K^{+} . As shown in **Figure 3.10. (a)** upon addition of different cations there was prominent change in absorption that exhibits good selectivity towards Cu^{2+} ion while there was no change in its absorption with other metal ions. The obtained results showed prominent change in its optical properties. Initially the probe **DTBPA 1** showed two clear absorption peaks at 298 nm and 358 nm but upon addition of Cu^{2+} there was disappearance of absorption peak that appeared at 358 nm with strong increase in absorption peak at 298 nm. In addition, the UV-Vis titrations studies revealed that upon incremental addition of copper from 0 to 2 equivalent absorption goes on increasing with disappearance of the peak at 358 nm and increase in absorption intensity at 298 nm **Figure 3.10. (b)** This confirms that the peak appearing at 358 nm belongs to the bipyridine and thiophene recognition unit while the peak

at 298 corresponds to the diphenyl donor unit. Therefore, upon addition of Cu^{2+} ion to the solution containing **DTBPA 1** probe there was change in absorption intensity which depicts that the bipyridine and thiophene recognition unit shows the binding to copper ion.

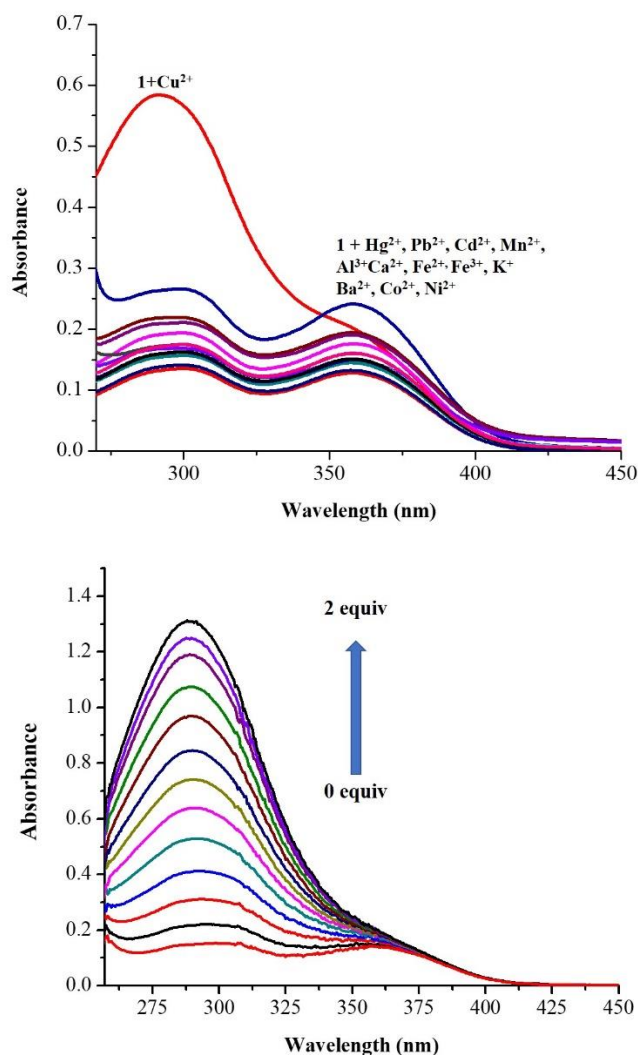


Figure 3. 10. (a) Plot representing the absorption change upon addition of different metal ions Cu^{2+} , Fe^{3+} , Fe^{2+} , Hg^{2+} , Pb^{2+} , Ni^{2+} , Zn^{2+} , Mn^{2+} , Co^{2+} , Al^{3+} , Ca^{2+} , Ba^{2+} , Cd^{2+} , K^{+} . (b) UV-Vis absorption titration for the **DTBPA 1** with incremental addition (0 – 2 equivalent)

3.5.5. Fluorescence emission study

The fluorescence studies were performed for the probe **DTBPA 1** in acetonitrile solvent upon excitation at 340 nm where the emission intensity was observed at 498 nm. As it was observed under UV light that when the different metal ions were added the prominent fluorescence

quenching was observed which was confirmed by fluorescence study. It is observed that when the different ions were added to the solution containing probe there was initially no change observed in the fluorescence intensity while upon addition of 2 equivalent of Cu^{2+} ion there was abrupt decrease in the fluorescence while there was no prominent change observed for the metal ions except Cu^{2+} . This fluorescence quenching in the molecule occurs mainly due to photon induced electron transfer (PET).

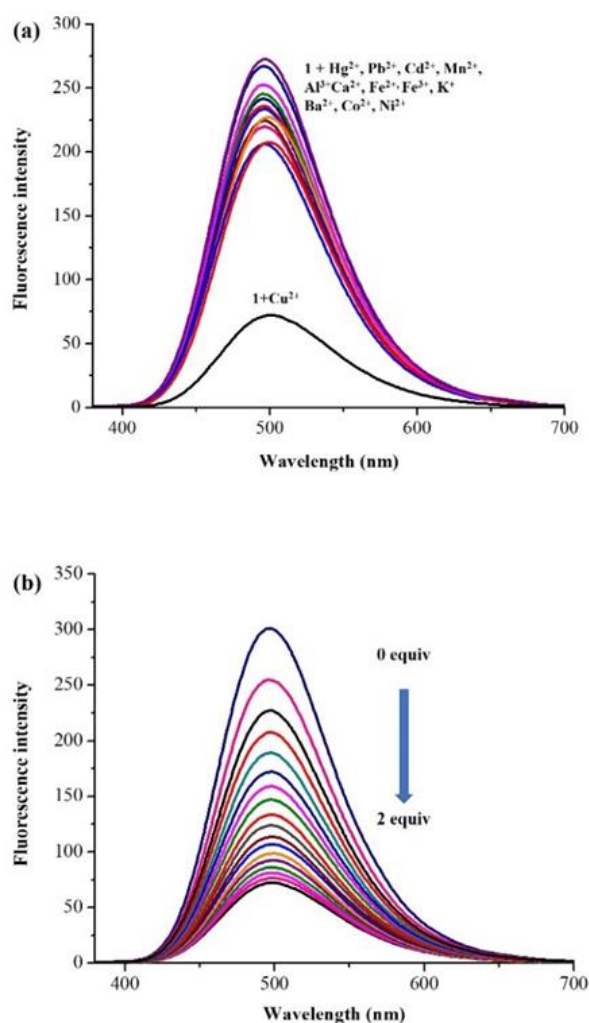


Figure 3. 11. (a) Plot representing the emission intensity upon addition of different metal ions Cu^{2+} , Fe^{3+} , Fe^{2+} , Hg^{2+} , Pb^{2+} , Ni^{2+} , Zn^{2+} , Mn^{2+} , Co^{2+} , Al^{3+} , Ca^{2+} , Ba^{2+} , Cd^{2+} , K^+ . (b) Fluorescence titration for the **DTBPA 1** with incremental addition (0 – 2 equivalent)

The lone pairs present on the pyridine are easily available for metal ion coordination. The coordination of metal ion inhibits the ICT in the probe and results into PET process which is frequently observed in many fluorophores. The emission intensity changes are represented in **Figure 3.11 (a)** with addition of various cations and **Figure 3.11 (b)** represent the the emission change with incremental addition of Cu^{2+} ion from 0 to 2 equivalent.

3.5.6. Competitive Study

From the above absorption and fluorescence studies it clear that the probe is highly selective and sensitive towards Cu^{2+} ion. But sometimes interference from other competing metal ions study is required to study the competition between the Cu^{2+} in presence over other metal ion. Herein fluorescence study was performed for determining the interference from other ionic species towards the probe **DTBPA 1**. The binding event was studied by adding different ions in the solution containing probe **DTBPA 1**. To the probe containing different cations Cu^{2+} ion was added as shown in the bar graph **Figure 3.12**. The blue bar represents the probe **DTBPA 1** and red bar represents the probe with various ion along with Cu^{2+} ion. The probe did not show any change upon addition of various cations but with the addition of Cu^{2+} ion there was decrease in fluorescence intensity observed for the probe. Thus, when the Cu^{2+} ion was added to the solution probe containing different cation there was quenching of fluorescence with decrease in fluorescence intensity. The decrease in the fluorescence intensity upon addition of Cu^{2+} ion in presence over another ion clearly depicts that the probe is highly selective towards Cu^{2+} . Thus, we could conclude the selectivity of the probe towards Cu^{2+} ion in presence over another interfering cation.

3.5.7. Stoichiometry and Binding constant

The stoichiometric analysis was performed by using Jobs method and it was observed that the molecule showed 2:1 ligand to metal complexation with the two-pyridine nitrogen. While the binding constant for the **DTBPA 1** for copper sensing was found to be $1.13 \times 10^6 \text{ M}^{-1}$. The binding constant was calculated by Benesi- Hildebrand plot. The Job stociometry 1:Cu²⁺ and binding plot is as shown in **Figure 3.13 (a)** and **(b)** respectively.

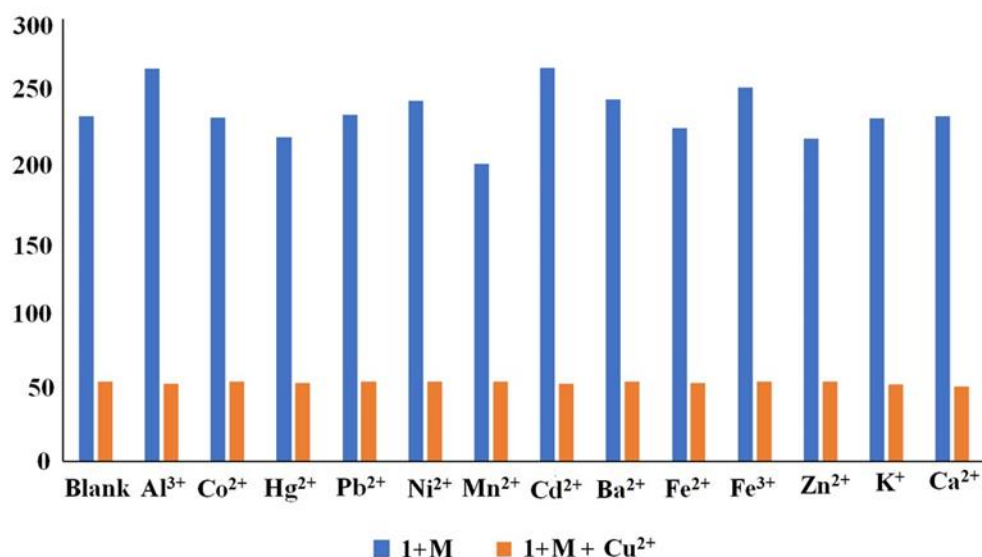


Figure 3. 12. Competitive study performed for the **DTBPA 1** in presence of cations (1+M represents different cations added to **DTBPA 1** while 1+M+ Cu²⁺ indicates the different cation with addition of Cu²⁺ ion.

3.5.8 Binding mechanism

Form the DFT study it is predicted that the molecule binds the Cu²⁺ ion by non-covalent interaction with two pyridine moieties present in the **DTBPA 1** probe. the pyridine which present in free conformation rotates in the solution when copper is added resulting in to interaction between probe and Cu²⁺ ion. The binding mechanism is as shown below in **Figure 3.14.**

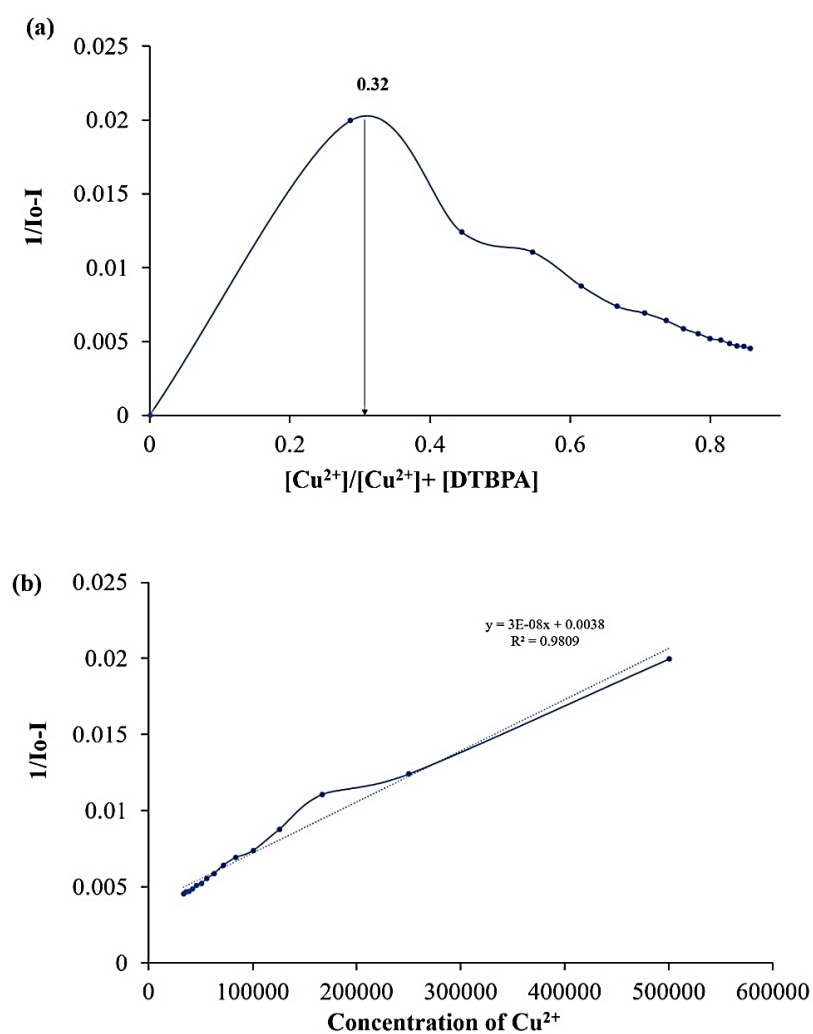


Figure 3. 13. (a) Jobs Plot for the **DTBPA 1** with copper complexation in 2:1 ratio. (b) Benesi-Hildebrand plot for **DTBPA 1**.

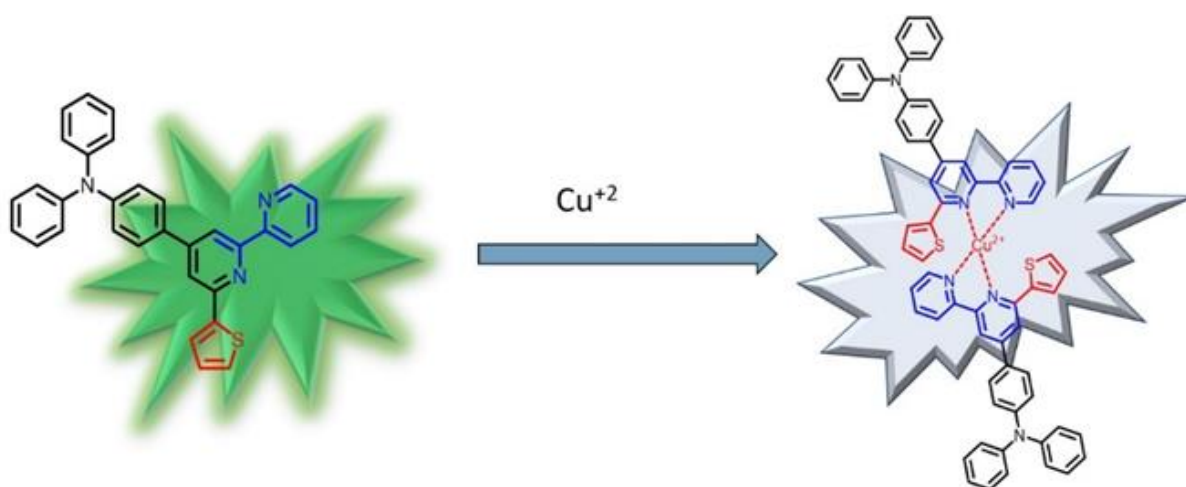


Figure 3. 14. Mechanistic pathway for binding of Cu^{2+} with **DTBPA 1** probe.

3.7. Density functional theory study (DFT)

The computational results were obtained by calculation using the Gaussian 16 *ab initio*/DFT quantum chemical simulation package [44]. The geometry optimization of all possible conformations 1C-M, 2C-M, 3C-M, 4C-M) of molecule N,N-diphenyl-4-(6-(thiophen-2-yl)-[2,2'-bipyridin]-4-yl)aniline is carried out at B3LYP/6-31+g(d) level, further to investigate their interaction with Cu^{+2} , all possible conformations of molecule after complexation with Cu^{+2} (1C-M+ Cu^{+2} , 2C-M+ Cu^{+2} , 3C-M+ Cu^{+2} , 4C-M+ Cu^{+2}) were optimized at the B3LYP/LANL2DZ/6-31+g(d) level. [45,46] **Figure 3.15.** The energies changes before and after forming complex between the **DTBPA 1** and Cu^{+2} accomplishes that the 2C-M upon interaction with Cu^{+2} forms 1C-M + Cu^{+2} , with the rotation of C-C bond connecting central and side substituted pyridine rings. Conformational analysis was performed **Table 3.2**

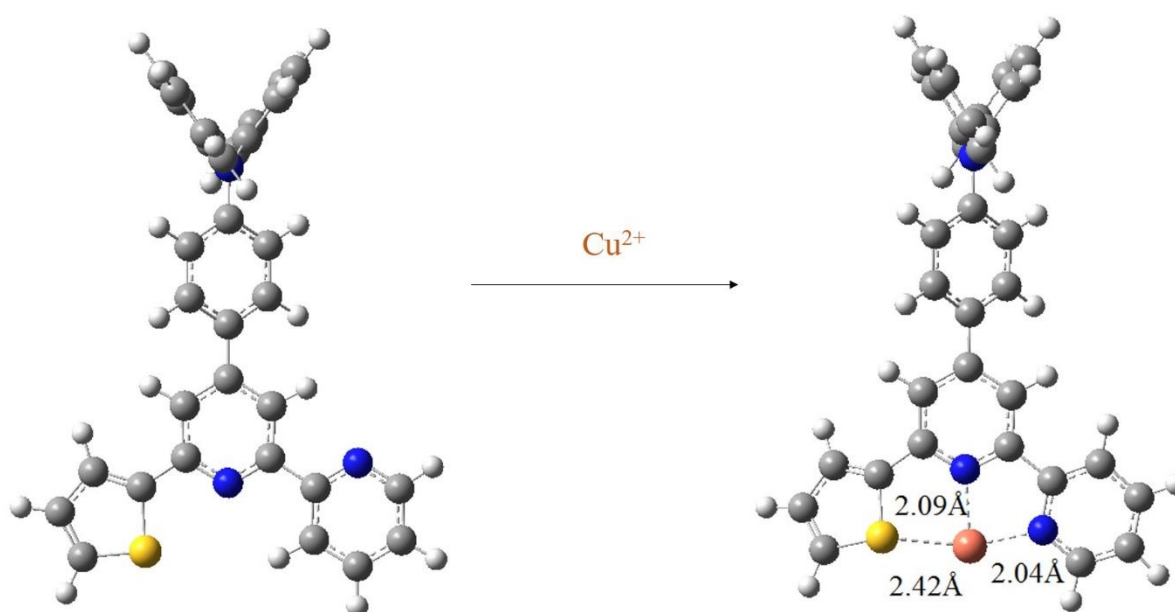
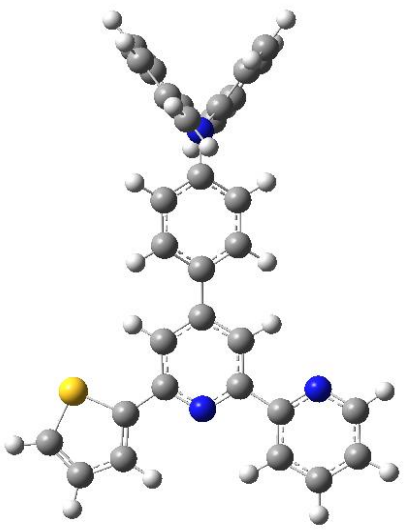
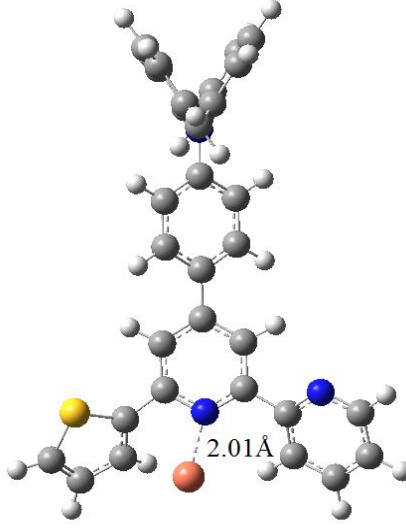
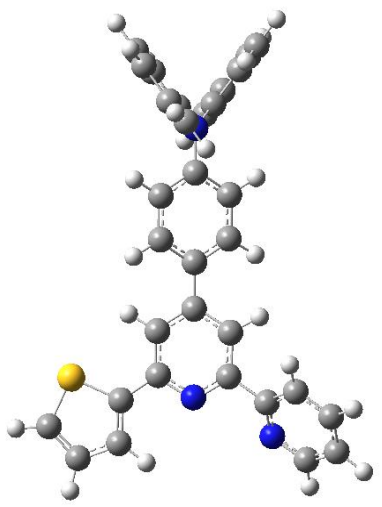
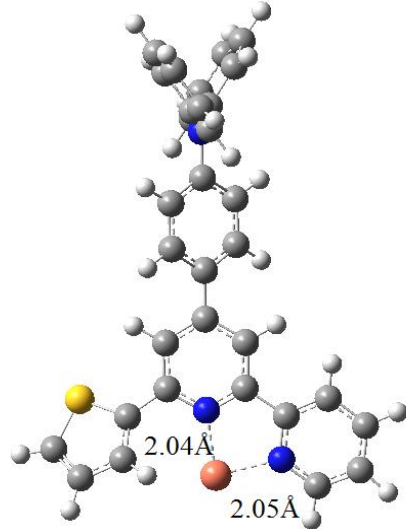


Figure 3.15. DFT study performed for **DTBPA 1** probe on Gaussian 16 *ab initio*/DFT quantum chemical simulation.

Table 3. 2. Conformational analysis of **DTBPA 1** + Cu^{2+} .

Conformations		Conformations + Cu^{2+}	
1C-M		1C-M + Cu^{2+}	
	-1126849.83 kcal/mol		-1249634.599 kcal/mol (stable)
2C-M		2C-M + Cu^{2+}	
	(stable) -1126856.069 kcal/mol		-1249613.417 kcal/mol

3C-M		3C-M + Cu ²⁺	
	-1126855.119 kcal/mol		-1249608.866 kcal/mol
4C-M		4C-M + Cu ²⁺	
	-1126849.39 kcal/mol		-1249627.477 kcal/mol

3.8. Practical application

3.8.1 Water analysis

Copper is needed in small amount (as micronutrient) but can cause problem if level is too high.

Copper can cause problem in drinking water leading to change in color of water which appears as blue green and taste of water also changes. Therefore, there is need of determination of

copper in water sample. For this purpose, we selected tap water and river water and carried out the analysis by standard addition method. The analysis and its result obtained are as follows. Herein the synthesized probe 1 was used for practical application for detecting trace amount of Cu^{2+} ion in real water sample. In this analysis two water sample were collected river water and tap water and was pre-treated before analysis. River water sample was collected from River Mandovi Goa and Drinking water was taken from the tap source. The river water was spiked with 2.5 μL of 1mM Cu^{2+} ion and tap water was spiked with 6.5 μL of 1mM Cu^{2+} ion and to the above solution 10 μL of probe was added, mix the solution thoroughly and record the emission after 5 minutes. The emission intensity was plotted against the standard plot of fluorescence intensity. Thus, the pre-spiked Cu^{2+} ion concentration could be easily detected by probe in the contaminated water sample with 98 to 104 % recovery as shown Table 3.3. below.

Sr.No	Sample	Concentration of Cu (II)ion found	Concentration of Cu (II)ion added	Recovery % RSD
1	Drinking Water	3.40×10^{-6}	3.25×10^{-6}	104.61%
2	River Water	1.23×10^{-6}	1.25×10^{-6}	98.40%

Table 3. 3. Results represents the real sample analysis for probe **DTBPA 1**

3.9. Conclusion

The molecule **DTBPA 1** was synthesized by simple aldol condensation and second step by Michael addition of pyridine salt. Further reacted to give **DTBPA 1** by Krohnke pyridine synthesis where pyridine core is formed in presence of ammonium hydroxide ammonium acetate and acetic acid under refluxing condition. The molecule **DTBPA 1** was purified column chromatography and characterized by ^1H NMR, ^{13}C NMR, elemental analysis, single crystal XRD, ESI-Mass spectrometry. After characterization the molecule was investigated for its photophysical properties which is analysed by UV-Vis and fluorescence spectroscopy and

fluorescence emission spectroscopy. The reported the fluorescent **DTBPA 1** molecule was showed good response towards Cu^{2+} ion in a solution in presence of various cations. Further the interaction of molecule to Cu^{2+} was theoretically calculated by DFT calculation which were performed by using ab initio gaussian software Gaussian 16 *ab initio*/DFT quantum chemical simulation. The detection limit of $0.789\mu\text{M}$ which is very low given by environmental protection agency EPA guidelines. The developed molecule was successfully utilized for determination of copper in water sample.

References

- (1) Wang, H.; Wu, S. Sensors and Actuators B : Chemical A Pyrene-Based Highly Selective Turn-on Fluorescent Sensor for Copper (II) Ions and Its Application in Living Cell Imaging. *Sensors Actuators B. Chem.* **2013**, *181*, 743–748. <https://doi.org/10.1016/j.snb.2013.01.054>.
- (2) Zhang, X.; Shen, L. Y.; Zhang, Q. L.; Yang, X. J.; Huang, Y. L.; Redshaw, C.; Xu, H. A Simple Turn-off Schiff Base Fluorescent Sensor for Copper (II) Ion and Its Application in Water Analysis. *Molecules* **2021**, *26* (5). <https://doi.org/10.3390/molecules26051233>.
- (3) Bandmann, O.; Weiss, K. H.; Kaler, S. G. Wilson's Disease and Other Neurological Copper Disorders. *Lancet Neurol.* **2015**, *14* (1), 103–113. [https://doi.org/10.1016/S1474-4422\(14\)70190-5](https://doi.org/10.1016/S1474-4422(14)70190-5).
- (4) Ellingsen, D. G.; Møller, L. B.; Aaseth, J. Copper. *Handb. Toxicol. Met. Fourth Ed.* **2015**, *1* (29), 765–786. <https://doi.org/10.1016/B978-0-444-59453-2.00035-4>.
- (5) Manto, M. Abnormal Copper Homeostasis: Mechanisms and Roles in Neurodegeneration. *Toxics* **2014**, *2* (2), 327–345. <https://doi.org/10.3390/toxics2020327>.
- (6) Anand, T.; Sivaraman, G.; Chellappa, D. Journal of Photochemistry and Photobiology A : Chemistry Quinazoline Copper (II) Ensemble as Turn-on Fluorescence Sensor for Cysteine and Chemodosimeter for NO. "Journal Photochem. Photobiol. A Chem. **2014**, *281*, 47–52. <https://doi.org/10.1016/j.jphotochem.2014.02.015>.
- (7) Yilmaz, I.; Cukurovali, A. Dyes and Pigments A Highly Sensitive and Selective Fluorescent Sensor for the Determination of Copper (II) Based on a Schiff Base. **2009**,

- 83, 211–217. <https://doi.org/10.1016/j.dyepig.2009.04.012>.
- (8) Wang, Y.; Hao, X.; Liang, L.; Gao, L.; Ren, X. RSC Advances. **2020**, 6109–6113. <https://doi.org/10.1039/c9ra10632d>.
- (9) Akhila, A. K.; Renuka, N. K. For Femtomolar Level Detection of Copper (II) †. **2019**, 1001–1008. <https://doi.org/10.1039/c8nj04732d>.
- (10) Yeh, J. T.; Chen, W. C.; Liu, S. R.; Wu, S. P. A Coumarin-Based Sensitive and Selective Fluorescent Sensor for Copper(II) Ions. *New J. Chem.* **2014**, 38 (9), 4434–4439. <https://doi.org/10.1039/c4nj00695j>.
- (11) Feng, S.; Gao, Q.; Gao, X.; Yin, J.; Jiao, Y. Fluorescent Sensor for Copper (II) Ions Based on Coumarin Derivative and Its Application in Cell Imaging. *Inorg. Chem. Commun.* **2019**, 102 (October 2018), 51–56. <https://doi.org/10.1016/j.inoche.2019.01.012>.
- (12) Liu, S.; Wang, Y.; Han, J. Fluorescent Chemosensors for Copper (II) Ion : Structure , Mechanism and Application. "*Journal Photochem. Photobiol. C Photochem. Rev.* **2017**, <https://doi.org/10.1016/j.jphotochemrev.2017.06.002>.
- (13) Mohanasundaram, D.; Bhaskar, R.; Lenin, N.; Nehru, K.; Rajagopal, G.; Vinoth, G.; Rajesh, J. Journal of Photochemistry & Photobiology , A : Chemistry A Simple Triphenylamine Based Turn-off Fluorescent Sensor for Copper (II) Ion Detection in Semi-Aqueous Solutions. **2022**, 427 (January).
- (14) Ghorai, A.; Mondal, J.; Manna, A. K.; Chodhury, S.; Pra, G. K. A Novel Pyrene based highly selective reversible fluorescent colorimetric sensor for rapid detection of Cu²⁺: application in bio-imaging Analytical Methods. (RSC) **2018**. <https://doi.org/10.1039/C8AY00097B>.
- (15) Fu, Y.; Pang, X.; Wang, Z.; Chai, Q.; Ye, F. Spectrochimica Acta Part A : Molecular and Biomolecular Spectroscopy A Highly Sensitive and Selective Fluorescent Probe for Determination of Cu (II) and Application in Live Cell Imaging. *Spectrochim. Acta Part A Mol. Biomol. Spectrosc.* **2019**, 208, 198–205. <https://doi.org/10.1016/j.saa.2018.10.005>.
- (16) Yang, L.; Zhu, W.; Fang, M.; Zhang, Q.; Li, C. Spectrochimica Acta Part A : Molecular and Biomolecular Spectroscopy A New Carbazole-Based Schiff-Base as Fluorescent Chemosensor for Selective Detection of Fe³⁺ and Cu²⁺. *Spectrochim. Acta Part A Mol. Biomol. Spectrosc.* **2013**, 109, 186–192. <https://doi.org/10.1016/j.saa.2013.02.043>.
- (17) Nandre, K. P.; Puyad, A. L.; Bhosale, S. V.; Bhosale, S. V. A Novel Donor-Acceptor Receptor for Selective Detection of Pb²⁺ and Fe³⁺ Ions. *Talanta* **2014**, 130, 103–107.

- <https://doi.org/10.1016/j.talanta.2014.06.064>.
- (18) Saleem, M.; Rafiq, M.; Hanif, M.; Shaheen, M. A.; Seo, S. Y. A Brief Review on Fluorescent Copper Sensor Based on Conjugated Organic Dyes; Springer US, 2018; Vol. 28. <https://doi.org/10.1007/s10895-017-2178-z>.
- (19) Wang, F.; Gu, Z.; Lei, W.; Wang, W.; Xia, X.; Hao, Q. Graphene Quantum Dots as a Fluorescent Sensing Platform for Highly Efficient Detection of Copper(II) Ions. *Sensors Actuators, B Chem.* **2014**, *190*, 516–522. <https://doi.org/10.1016/j.snb.2013.09.009>.
- (20) Xie, S.; Liu, Q.; Zhu, F.; Chen, M.; Wang, L.; Xiong, Y.; Zhu, Y.; Zheng, Y.; Chen, X. AIE-Active Metal-Organic Frameworks: Facile Preparation, Tunable Light Emission, Ultrasensitive Sensing of Copper(II) and Visual Fluorescence Detection of Glucose. *J. Mater. Chem. C* **2020**, *8* (30), 10408–10415. <https://doi.org/10.1039/d0tc00106f>.
- (21) Wang, M.; Li, K.; Hou, J.; Wu, M.; Huang, Z.; Yu, X. Anion in Water. **2012**, No. Ii.
- (22) Royzen, M.; Dai, Z.; Canary, J. W. Ratiometric Displacement Approach to Cu(II) Sensing by Fluorescence. *J. Am. Chem. Soc.* **2005**, *127* (6), 1612–1613. <https://doi.org/10.1021/ja0431051>.
- (23) Hong, Y.; Chen, S.; Wai, C.; Leung, T.; Wing, J.; Lam, Y.; Liu, J.; Tseng, N.; Tsz, R.; Kwok, K.; Yu, Y.; Wang, Z.; Tang, B. Z. Fluorogenic Zn (II) and Chromogenic Fe (II) Sensors Based on Terpyridine-Substituted Tetraphenylethenes with Aggregation-Induced Emission Characteristics. **2011**, No. Ii, 3411–3418.
- (24) Piotrowiak, P. Photoinduced Electron Transfer in Molecular Systems: Recent Developments. *Chem. Soc. Rev.* **1999**, *28* (2), 143–150. <https://doi.org/10.1039/a707029b>.
- (25) Bissell, R. A.; DE Silva, A. P.; Gunaratne, H. Q. N.; Lynch, P. L. M.; Maguire, G. E. M.; Mccoy, C. P.; Sandanayake, K. R. A. S. ChemInform Abstract: Fluorescent PET (Photoinduced Electron Transfer) Sensors. *ChemInform* **2010**, *25* (1), no-no. <https://doi.org/10.1002/chin.199401322>.
- (26) Grabowski, Z. R.; Rotkiewicz, K.; Rettig, W. Structural Changes Accompanying Intramolecular Electron Transfer: Focus on Twisted Intramolecular Charge-Transfer States and Structures. *Chem. Rev.* **2003**, *103* (10), 3899–4031. <https://doi.org/10.1021/cr940745l>.
- (27) McConnell, H. M. Intramolecular Charge Transfer in Aromatic Free Radicals. *J. Chem. Phys.* **1961**, *35* (2), 508–515. <https://doi.org/10.1063/1.1731961>.
- (28) Zhou, G.; Zhang, X.; Ni, X. Tuning the Amphiphilicity of Terpyridine-Based Fluorescent Probe in Water: Assembly and Disassembly-Controlled Hg²⁺ Sensing ,

- Removal, and Adsorption of H₂S. *J. Hazard. Mater.* **2019**, No. September, 121474. <https://doi.org/10.1016/j.jhazmat.2019.121474>.
- (29) Li, Z.; Hou, J. T.; Wang, S.; Zhu, L.; He, X.; Shen, J. Recent Advances of Luminescent Sensors for Iron and Copper: Platforms, Mechanisms, and Bio-Applications. *Coord. Chem. Rev.* **2022**, *469*, 214695. <https://doi.org/10.1016/j.ccr.2022.214695>.
- (30) Silpcharu, K.; Soonthonhut, S.; Sukwattanasinitt, M.; Rashatasakhon, P. Fluorescent Sensor for Copper(II) and Cyanide Ions via the Complexation-Decomplexation Mechanism with Di(Bissulfonamido)Spirobifluorene. *ACS Omega* **2021**, No. II. <https://doi.org/10.1021/acsomega.1c02744>.
- (31) Liu, Y. L.; Yang, L.; Li, P.; Li, S. J.; Li, L.; Pang, X. X.; Ye, F.; Fu, Y. A Novel Colorimetric and “Turn-off” Fluorescent Probe Based on Catalyzed Hydrolysis Reaction for Detection of Cu²⁺ in Real Water and in Living Cells. *Spectrochim. Acta - Part A Mol. Biomol. Spectrosc.* **2020**, *227*, 2–9. <https://doi.org/10.1016/j.saa.2019.117540>.
- (32) Wang, H.; Fang, B.; Zhou, L.; Li, D.; Kong, L.; Uvdal, K.; Hu, Z. A Reversible and Highly Selective Two-Photon Fluorescent “on-off-on” Probe for Biological Cu²⁺ Detection. *Org. Biomol. Chem.* **2018**, *16* (13), 2264–2268. <https://doi.org/10.1039/c8ob00257f>.
- (33) Hu, L.; Wang, H.; Fang, B.; Hu, Z.; Zhang, Q.; Tian, X.; Zhou, H.; Wu, J.; Tian, Y. A Reversible Two-Photon Fluorescence Probe for Cu(II) Based on Schiff-Base in HEPES Buffer and in Vivo Imaging. *Sensors Actuators, B Chem.* **2017**, *251*, 993–1000. <https://doi.org/10.1016/j.snb.2017.05.140>.
- (34) Wang, P.; Fu, J.; Yao, K.; Chang, Y.; Xu, K.; Xu, Y. A Novel Quinoline-Derived Fluorescent “Turn-on” Probe for Cu²⁺ with Highly Selectivity and Sensitivity and Its Application in Cell Imaging. *Sensors Actuators, B Chem.* **2018**, *273* (June), 1070–1076. <https://doi.org/10.1016/j.snb.2018.07.028>.
- (35) Kröhnke, F.; Zecher, W.; Curtze, J.; Drechsler, D.; Pflegar, K.; Schnalke, K. E.; Weis, W. Synthesis Using the Michael Addition of Pyridinium Salts. *Angew. Chemie Int. Ed. English* **1962**, *1* (12), 626–632. <https://doi.org/10.1002/anie.196206261>.
- (36) Kumar, K. A.; Lokeshwari, D. M. Heteroaryl Chalcones: Prominent Pharmacophores of Synthetic and Biological Interest. *IOSR J. Appl. Chem. (IOSR-JAC)* **2021**, *14* (6), 41–52. <https://doi.org/10.9790/5736-1406014152>.
- (37) Liu, B.; Bao, Y.; Du, F.; Wang, H.; Tian, J.; Bai, R. Synthesis and Characterization of a Fluorescent Polymer Containing 2,6-Bis(2-Thienyl)Pyridine Moieties as a Highly

- Efficient Sensor for Pd²⁺ Detection. *Chem. Commun.* **2011**, 47 (6), 1731–1733. <https://doi.org/10.1039/c0cc03819a>.
- (38) Marini, A.; Muñoz-Losa, A.; Biancardi, A.; Mennucci, B. What Is Solvatochromism? *J. Phys. Chem. B* **2010**, 114 (51), 17128–17135. <https://doi.org/10.1021/jp1097487>.
- (39) Nigam, S.; Rutan, S. Principles and Principles And. *Appl. Spectrosc.* **2001**, 55 (11), 362A.
- (40) Hadjmohammadi, M. R.; Chaichi, M. J.; Yousefpour, M. Solvatochromism Effect of Different Solvents on UV-Vis Spectra of Flouresceine and Its Derivatives. *Iran. J. Chem. Chem. Eng.* **2008**, 27 (4), 9–14.
- (41) Rauf, M. A.; Hisaindee, S. Studies on Solvatochromic Behavior of Dyes Using Spectral Techniques. *J. Mol. Struct.* **2013**, 1042, 45–56. <https://doi.org/10.1016/j.molstruc.2013.03.050>.
- (42) Nadimetla, D. N.; Bhosale, S. V. Tetraphenylethylene AIEgen Bearing Thiophenylbipyridine Receptor for Selective Detection of Copper (II) Ion. **2021**, 7614–7621. <https://doi.org/10.1039/d1nj01001h>.
- (43) Gaussian 16, Revision B.01 M. J. Frisch, G. W. Trucks, H. B. Schlegel, G. E. Scuseria, M. A. Robb, J. R. Cheeseman, G. Scalmani, V. Barone, G. A. Petersson, H. Nakatsuji, X. Li, M. Caricato, A. V. Marenich, J. Bloino, B. G. Janesko, R. Gomperts, B. Mennucci, H. P. Hratchian, J. V. Ortiz, A. F. Izmaylov, J. L. Sonnenberg, D. Williams-Young, F. Ding, F. Lipparini, F. Egidi, J. Goings, B. Peng, A. Petrone, T. Henderson, D. Ranasinghe, V. G. Zakrzewski, J. Gao, N. Rega, G. Zheng, W. Liang, M. Hada, M. Ehara, K. Toyota, R. Fukuda, J. Hasegawa, M. Ishida, T. Nakajima, Y. Honda, O. Kitao, H. Nakai, T. Vreven, K. Throssell, J. A. Montgomery, Jr., J. E. Peralta, F. Ogliaro, M. J. Bearpark, J. J. Heyd, E. N. Brothers, K. N. Kudin, V. N. Staroverov, T. A. Keith, R. Kobayashi, J. Normand, K. Raghavachari, A. P. Rendell, J. C. Burant, S. S. Iyengar, J. Tomasi, M. Cossi, J. M. Millam, M. Klene, C. Adamo, R. Cammi, J. W. Ochterski, R. L. Martin, K. Morokuma, O. Farkas, J. B. Foresman, and D. J. Fox, Gaussian, Inc., Wallingford CT, 2016.
- (44) Avogadro: an open-source molecular builder and visualization tool. Version 1.1.0. <http://avogadro.openmolecules.net/>
- (45) Marcus D Hanwell, Donald E Curtis, David C Lonie, Tim Vandermeersch, Eva Zurek and Geoffrey R Hutchison; "Avogadro: An advanced semantic chemical editor, visualization, and analysis platform" *Journal of Cheminformatics* 2012, 4:17.

CHAPTER 4

CHAPTER 4

4.1. Introduction

The development of fluorescent molecule as anion sensor has received incredible attention because of several application such as bioimaging and environmental detection of toxic analyte. Amongst various anions Cl^- , I^- , F^- , Br^- , HSO_4^- , H_2PO_4^- , HCO_3^- , NO_3^- , ClO_4^- cyanide anion is considered most toxic. Cyanide anion inhibits the mitochondrial electron-transport in respiratory chain upon binding with ferric form of cytochrome P450 [1]. The cyanide anions exhibit the toxic effect and cause serious health problem which damage central nervous system and living environment [2,4]. Cyanide enters the environment system by various developmental activities such as industrialization, gold mining, herbicides synthetic fiber, and electroplating technology. Usually, the cyanide enters in the drinking water due to human activities, and industrialization led to the release of cyanide anion in water bodies and has affected the food chain leading to various disease [5-12].

According to World Health Organization (WHO) The permissible amount of cyanide in water is about $1.9 \mu\text{M}$ [13]. High toxic nature that is affecting the physiological and environmental system led to the efficient detect the cyanide anion (CN^-) in the system [14]. Therefore, the development of artificial probes that have the great potential of selectively recognizing and sensing CN^- ion species [15,16]. Organic fluorescent probes are used for sensing of CN^- anion while the sensing approach is usually undergoing via cyanide complex reaction with transition metal [17], displacement reaction, electrophilic substitution reaction, [18,19,20] luminescent approach and via hydrogen bond interaction [21]. Due to poor selectivity in presence over other anions such as acetate, hydroxy and fluoride anion certainly limits its application. This problem can be overcome by nucleophilicity of CN^- ion [22].

The fluorescence method has proved to be an excellent method for the detection of cyanide with high selectivity and sensitivity. While the most common approach is by nucleophilic

addition reaction of cyanide anion over various fluorescent derivatives such as dibenzothiophene-based barbituric derivative (DTB) [23], carbazole-based sensor [24], salicylaldehyde [25], oxazine [26], pyrylium [27], acryltrizene [28], squaraine [29], trifluoroacetophenone [30], imine [31] and trifluoroacetamide [32] derivatives. So far, many scientists and researchers have developed a number of optical, colorimetric and fluorescent based sensors for cyanide anion detection [33-36]. Most of the organic fluorescent molecules are soluble in organic solvent therefore recognition of CN^- cannot be achieved in aqueous media. Hence it is very challenging to develop the fluorescent molecule that is having good solubility in water. As CN^- exists in industrial waste water and drinking water which are completely soluble and it becomes very difficult to isolate and detect by fluorescent material which are insoluble in water. Hence it is very challenging to develop sensor for CN^- ion detection in water.

Recently in 2001, Tang *et al.* reported unusual photophysical phenomenon of fluorescence termed aggregation-induced emission (AIE) [37-39]. The phenomenon states that in an organic solution the molecule does not show any emission while strong emission is observed in an aqueous solution due to the formation of aggregate [40]. The AIE phenomenon is observed due to the restriction of intramolecular rotation in the aggregates. Therefore, using the Aggregation induced emission (AIE) strategy has attracted much attention and revealed that there are very few reports on AIE active fluorescent material for CN^- ion, detection [41-45]. From thorough literature search on AIE based sensing probes for CN^- ion detection has been reported [46-48]. This, design and synthesis of AIE active material is of prime importance for CN^- ion detection in aqueous solution.

Herein, we reported simple and an effective AIE active molecular architecture **1** **Scheme 4.1**. for detection of CN^- ions. probe **1** showed highly selectivity and sensitivity towards CN^- ion in THF: H₂O ($f_{\text{water}} = 99\%$). The results are monitored by employing visual detection, UV-vis,

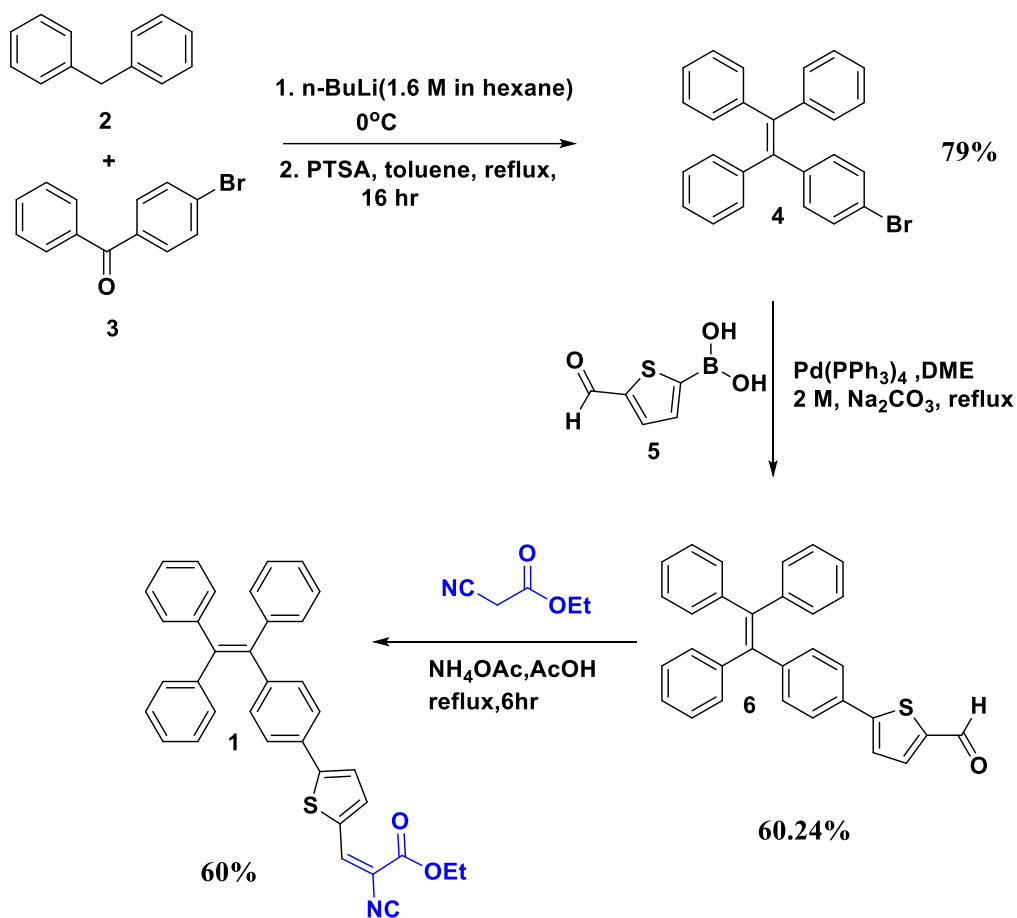
emission, ^1H NMR changes. Furthermore, probe **1** based paper strips under visible and UV light showed excellent and high sensitivity for CN^- ion detection. Moreover, it was employed successfully for CN^- ion detection in living cells with an obvious fluorescence change. The receptor **1** was utilized for detection of CN^- anion in various food samples.

4.2. Experimental

4.2.1 Chemicals and methods

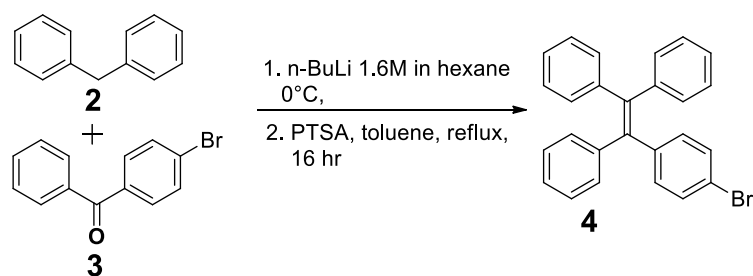
Compounds **4** and **6** were synthesized from obtained literature [49] while the probe **1** was synthesized by Knoevenagel condensation by reacting ethyl cyanoacetate and 5-(4-(1,2,2-triphenylvinyl)phenyl)thiophene-2-carbaldehyde **6**, in presence of ammonium acetate and acetic acid as solvent. For sensing performance, the analytes obtained were all tetrabutyl ammonium salt such as (I^- , F^- , Cl^- , Br^- , HSO_4^- , H_2PO_4^- , HCO_3^- , NO_3^- , ClO_4^-) and tetraethylammonium cyanide (CN^-) salt and Dimethyl sulfoxide (DMSO) solvent were purchased from Sigma-Aldrich and TCI. The synthesized compound was successfully characterized on by ^1H NMR which was recorded on 400 MHz and ^{13}C NMR using 100 MHz Bruker spectrometer by using Tetramethylsilane (TMS) as an internal standard. A deuterated solvent CDCl_3-d and $\text{DMSO}-d_6$ were used as solvent. Mass spectrometric data were obtained by positive electron spray ionization (ESI-MS) technique on an Agilent Technologies 1100 Series (Agilent Chemstation Software) mass spectrometer. IR spectra were recorded on a Perkin Elmer FT-IR 400 spectrometer. UV-vis absorption spectra were recorded by UV-vis-1800 Shimadzu spectrophotometer and fluorescence emission measured on RF-6000 (Shimadzu, Japan) Spectrofluorometer.

4.2.2. Schematic pathway for synthesis of probe 1



Scheme 4.1. Schematic pathway for synthesis of 1

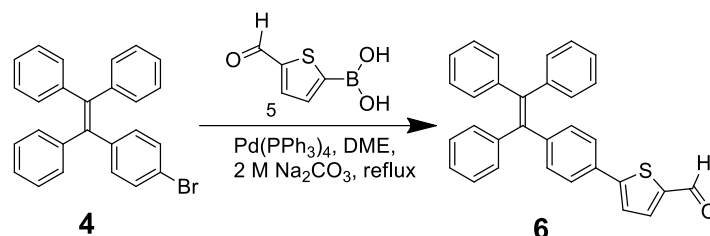
4.2.3. Synthesis of 1-(4-bromophenyl)-1,2,2-triphenylethene (4)



Scheme 4.2. Schematic pathway for synthesis of 1-(4-bromophenyl)-1,2,2-triphenylethene (4)

The compound **4** was prepared following a known literature procedure. *n*-butyl-lithium (1.6 M in hexane, 18.5 mL) was added dropwise to a solution of diphenylmethane **2** (2.0 g, 11.88 mmol) in dry THF (80 mL) at 0 °C under a nitrogen atmosphere. The following reacted mixture was kept for 2hr at the same temperature followed by addition of (4-bromophenyl)(phenyl)methanone **3** (2.48 g, 9.51 mmol) in 15 ml THF. Later the reaction mixture was allowed stir constantly at room temperature which was further monitored by TLC. After reaction completion the reaction was quenched with NH₄Cl and extraction was done with DCM (3×30 ml) dry with Na₂SO₄. Upon evaporation the crude alcohol is obtained which was then dissolved in toluene (40 ml) and PTSA (1.5 gm) was added. the reaction was further reflux for 16 hr. the toluene was evaporated and the obtained the crude solid was purified by column chromatography with *n*-hexane to give pure compound **4**. The obtained compound was white solid with 79% yield (3.08 g). Melting point: 160 °C; ¹H NMR (400 MHz, CDCl₃) δ: 7.23 (d, *J* = 9.3, 2H Hz), 7.16 - 7.10 (m, 9H), 7.05 - 7.00 (m, 6H), 6.91 (d, *J*=8.8 Hz, 2H).

4.2.4. Synthesis of 5-(4-(1,2,2-triphenylvinyl)phenyl)thiophene-2-carbaldehyde (**6**)

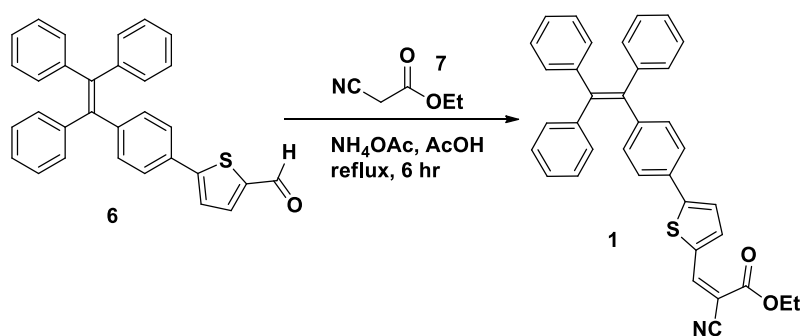


Scheme 4.3. Schematic pathway for Synthesis of 5-(4-(1,2,2-triphenylvinyl)phenyl)thiophene-2-carbaldehyde (**6**)

This compound also was prepared following a known literature procedure.¹⁸ To the solution of dimethoxyethane(DME) compound **4** was added (1.0 g, 2.4 mmol). To the same solution 2 M Na₂CO₃ (3:1, 40 mL) was added and reaction was kept under argon atmosphere followed by the addition of (5-formylthiophen-2-yl)boronic acid **5** (0.49 g, 3.16 mmol), and the reaction mixture was degassed using argon gas for 15-20 min. Followed by the addition of Pd(PPh₃)₄

(0.085 g) and the reaction mixture was refluxed for 30 hr at 90 °C. The reaction was monitored by TLC analysis. Finally, after reaction completion the reaction was quenched with water and extracted with DCM in proportion of (3×50 mL). The collected organic layer was continuously washed with water, which was dried over anhydrous sodium sulfate, and organic layer was evaporated on vacuum rotary evaporator. The obtained crude compound was purified by column chromatography, which was eluted with 8:92 Ethyl acetate and hexane to give **6** which found to be yellow solid with 60.2 % yield (0.783 g). ¹H NMR (400 MHz, CDCl₃) δ: 9.79 (s, 1H), 7.63 (d, *J* = 4.0, Hz, 1H), 7.37 - 7.33 (m, 2H), 7.27 (d, *J* = 4.2 Hz, 1H), 7.08 - 7.02 (m, 10H), 7.01 - 6.94 (m, 7H).

4.2.5 Synthesis of ethyl 2-cyano-3-(5-(4-(1,2,2-triphenylvinyl)phenyl)thiophen-2-yl)acrylate (1)



Scheme 4.4. Schematic pathway synthesis of ethyl 2-cyano-3-(5-(4-(1,2,2-triphenylvinyl)phenyl)thiophen-2-yl)acrylate (1)

5-(4-(1,2,2-triphenylviyl)phenyl)thiophen-2-carbaldehyde **6** (0.2gm, 0.37mmol) was added to a mixture of ethyl cyanoacetate **7** (0.33 gm, 2.97 mmol) in presence of ammonium acetate (15 ml) and acetic acid solvent. The reaction mixture was heated for 12 hours at 60 °C. after reaction is completed the resulting mixture was allowed to cool at room temperature and 30 ml of ice-cold water was added. The yellow precipitate was obtained which was filtered. (60%) m.p. 179 °C ¹H NMR (400 MHz, CDCl₃) δ: 8.30 (s, 1H), 7.73 (d, *J* = 4.0 Hz, 1H), 7.47 (dd,

$J = 2.1, 8.7$ Hz, 2H), 7.36 (d, $J = 4.5$ Hz, 3H), 7.28 (s, 3H), 7.18 - 7.04 (m, 17H), 4.39 (q, $J = 7.1$ Hz, 2H), 1.41 (t, $J = 7.2$ Hz, 3H); ^{13}C -NMR (100 MHz, CDCl_3 δ : 163.03, 154.5, 146.5, 143.4, 143.3, 143.2, 142.1, 139.9, 139, 134.7, 132.7, 132.1, 131.4, 131.3, 130.5, 127.9, 127.8, 127.7, 126.9, 126.7, 126.6, 126.1, 125.7, 124.1, 116.1, 97.8, 62.5, 29.7, 14.2; Elemental Analysis: $\text{C}_{36}\text{H}_{27}\text{NO}_2\text{S}$: Cal. C, 80.42; H, 5.06; N, 2.61 and Obs. C, 79.79; H, 5.13; N, 2.71.

4.3 Characterization

4.3.1. ^1H NMR spectrum of 5-(4-(1,2,2-triphenylvinyl)phenyl) thiophene-2-carbaldehyde (3)

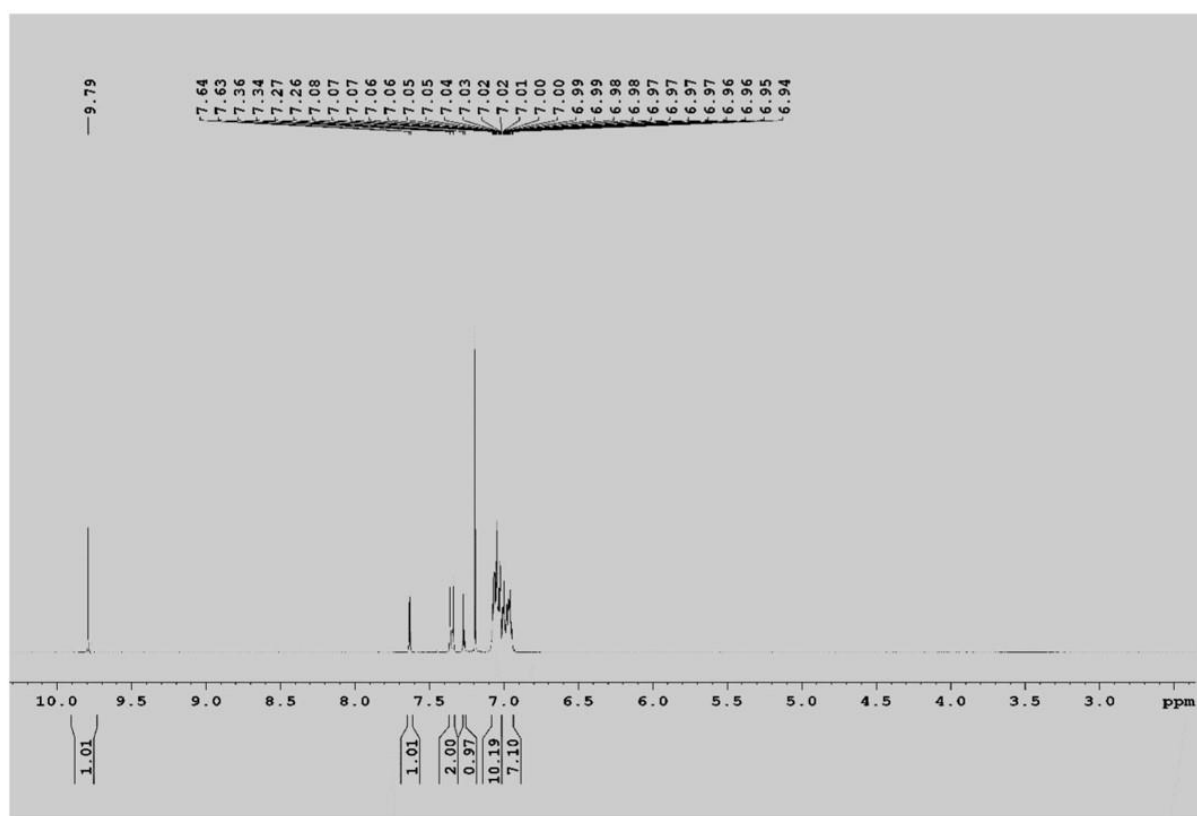


Figure 4.1. ^1H NMR spectrum of 5-(4-(1,2,2-triphenylvinyl)phenyl) thiophene-2-carbaldehyde (3)

The compound **3** and **1** was characterized successfully by ^1H NMR, ^{13}C NMR, DEPT as shown in figures below. The Carbaldehyde group appearing 9.8 ppm as shown in **Figure 4.1** completely disappears which clearly shows that the aldehyde is functionalized vinylidene bond upon Knoevenagel condensation to give ethyl-2-cyano-3-(5-(4-(1,2,2-triphenylvinyl)phenyl)thiophen-2-yl)acrylate (**1**) which was characterized successfully as shown in **Figure 4.2**

4.3.2. ^1H NMR ethyl-2-cyano-3-(5-(4-(1,2,2-triphenylvinyl)phenyl)thiophen-2-yl)acrylate (**1**).

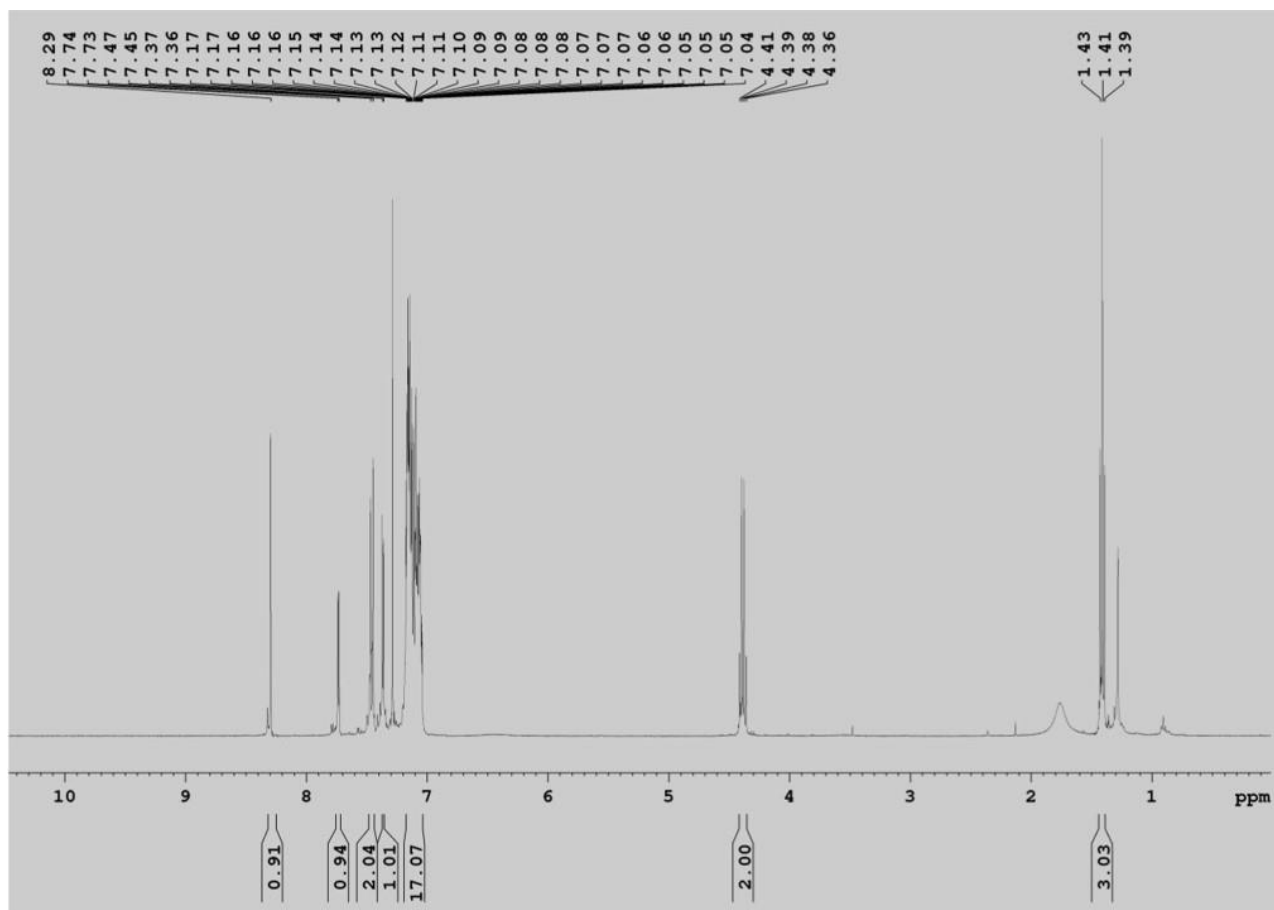


Figure 4.2. ^1H NMR spectrum for ethyl-2-cyano-3-(5-(4-(1,2,2-triphenylvinyl)phenyl)thiophen-2-yl)acrylate (**1**).

4.3.3. ^{13}C NMR spectrum ethyl-2-cyano-3-(5-(4-(1,2,2-triphenylvinyl)phenyl)thiophen-2-yl)acrylate (**1**).

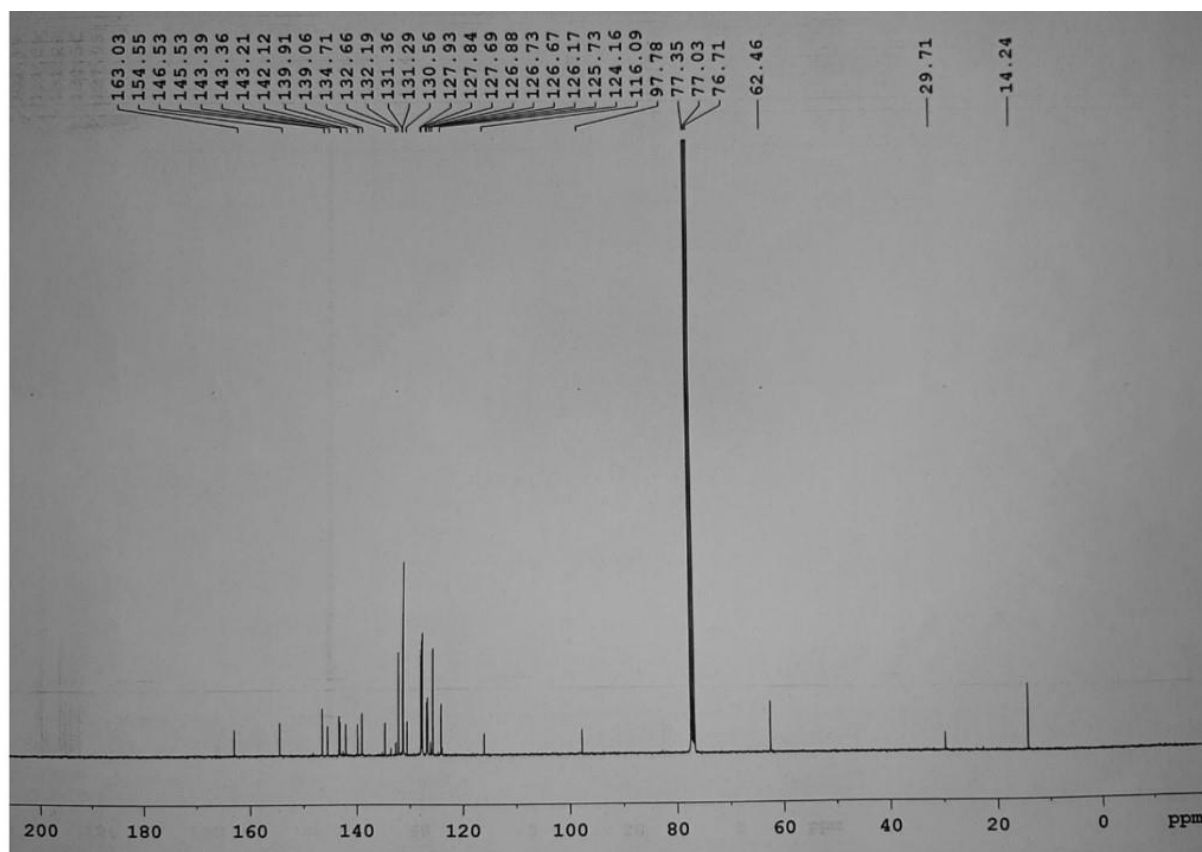
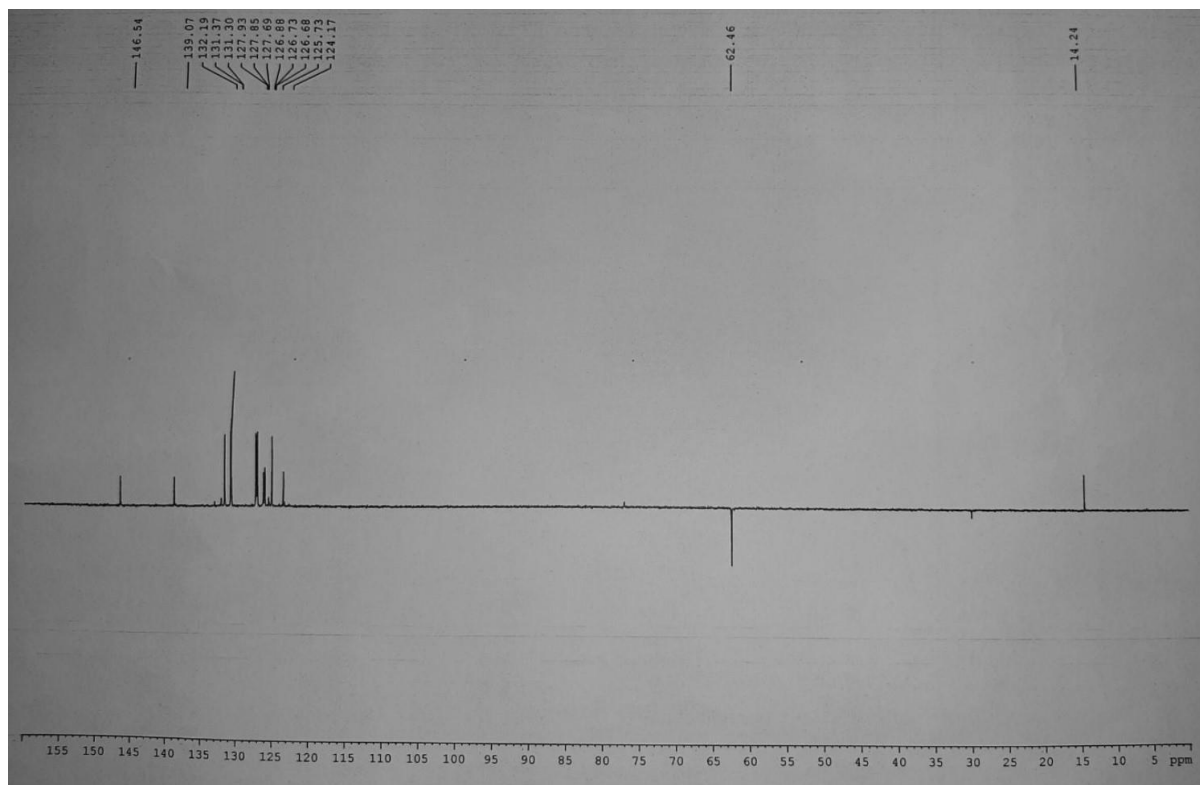
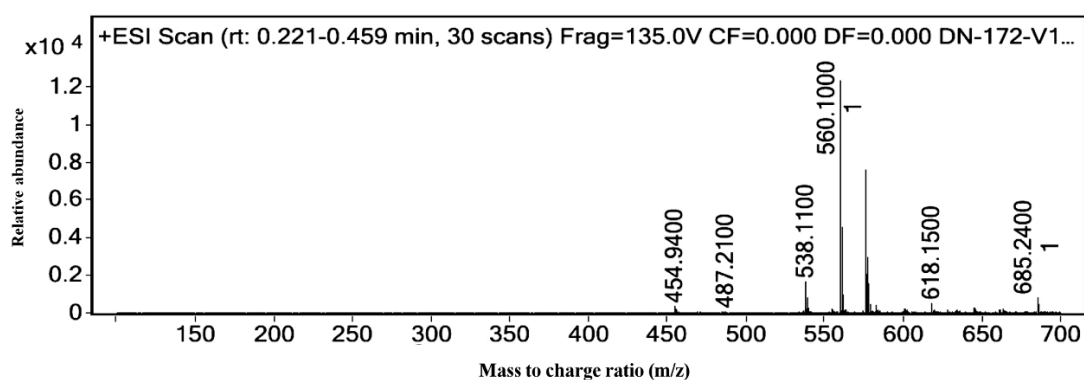


Figure 4.3. ^{13}C NMR spectrum ethyl-2-cyano-3-(5-(4-(1,2,2-triphenylvinyl)phenyl)thiophen-2-yl)acrylate (**1**).

4.3.4. ^{13}C DEPT spectrum ethyl-2-cyano-3-(5-(4-(1,2,2-triphenylvinyl)phenyl)thiophen-2-yl)acrylate (**1**).**Figure 4.4.** ^{13}C DEPT spectrum ethyl-2-cyano-3-(5-(4-(1,2,2-triphenylvinyl)phenyl)thiophen-2-yl)acrylate (**1**).**4.3.5** ESI-Mass of ethyl-2-cyano-3-(5-(4-(1,2,2-triphenylvinyl)phenyl)thiophen-2-yl)acrylate (**1**)**Figure 4.5.** ESI-Mass of ethyl-2-cyano-3-(5-(4-(1,2,2-triphenylvinyl)phenyl)thiophen-2-yl)acrylate (**1**).

4.3.6. ^{13}C NMR spectral changes observed with the addition of CN^- anion to **probe 1** in CDCl_3 (a) without addition of CN^- (b) with addition of CN^- .

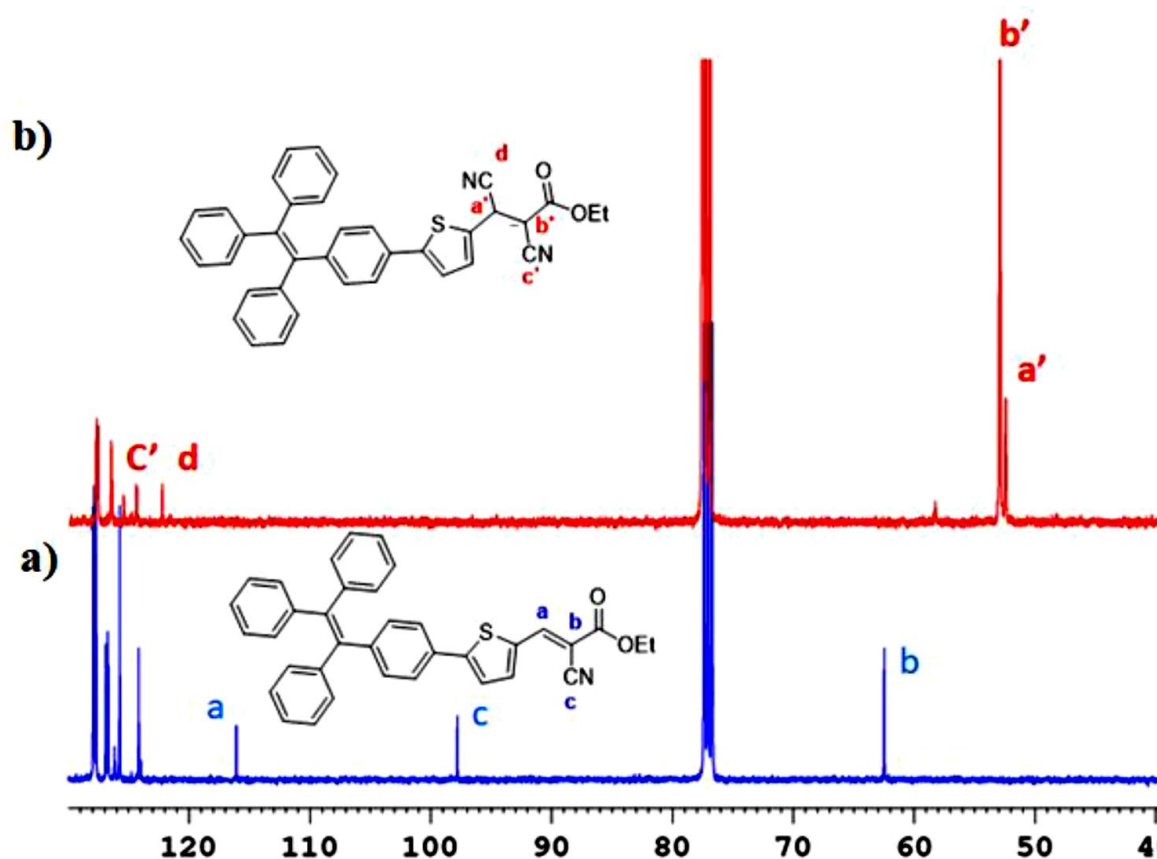


Figure 4.6. ^{13}C NMR spectral changes observed with the addition of CN^- anion to probe 1 in CDCl_3 (a) without addition of CN^- (b) with addition of CN^-

4.4 . Results and Discussion

4.4.1 Mechanochromic study

Organic Mechanochromic fluorescent materials are also known as piezo chromic material which are smart material that significantly undergoes reversible emission and color changes upon application of external stimuli such as temperature, moisture, stress, pH, and magnetic or electric field. [50] Mechanochromic behaviour has attracted great attention due to its potential application in rewritable smart materials, optical storage devices and, pressure sensor, and security ink. This smart material is also known as “stimuli-responsive materials” which are considered fourth-generation materials after synthetic polymeric material, natural material, and

artificial material which are the most developed modern technology and material science. [51, 52]. Nowadays due to excellent optical properties based on aggregation-induced emission (AIE) organic mechanochromic materials have better prospects and research value which has become a hot topic. During grinding process, the reversible phase transition from crystalline to amorphous state takes place. It is very difficult to study in detail the actual mechanism through grinding as grinding force is uncontrollable in magnitude and anisotropic in direction. However, an alternative method over the grinding method is hydrostatic pressure to study the mechanochromic behavior as hydrostatic pressure employed is controllable and direction is isotropic. There are basically four types of mechanisms followed in mechanochromic studies: intermolecular conformation change, the transformation from a locally excited state to intramolecular charge state (ICT), and intermolecular interaction change. It is predicted and believed that smart materials led to great achievement and have revolutionized the field of material science [53, 54].

Mechanofluorochromic behavior is achieved by physical or chemical structural changes in the material upon applying mechanical stress. Most commonly bond breaking or bond formation results in chemical structural changes taking place during a chemical reaction. For these changes to occur laborious conditions or high pressure is necessary, however during this chemical reaction frequently unsatisfactory conversion, loss of fluorescence, or irreversible reaction may occur. In contrary photophysical properties of the molecule in the solid state completely depend on conformational flexibility, molecular rearrangement, and intermolecular interactions occurring within the molecule. Due to this modification, alteration, and rearrangement in conformations, and molecular packing affect the HOMO-LUMO energy levels that alter the photoluminescence properties of the molecule. There are numerous compounds such as organometallic material, organic fluorophore, polymeric material, and dyes doped with polymeric substances shows mechanochromic properties that have a wide range of

applications. At present AIE material has opened a new opportunity in the field of mechanochromic. Therefore, by using this we utilized the molecules that were synthesized for sensing application [55,56,57].

Upon successful synthesis and characterization, the molecule was studied for change in photophysical properties on applying the mechanical stress on the molecule. This mechanical stress employed by process of grinding, fuming and heating. The following changes are observed as shown in **Figure 4.7** The compound **1** shows strong golden yellow fluorescence and the fluorescence quantum yield was measured and found to be $\Phi_F = 62.10$. It can be concluded that the molecular packing in solid state exhibit the strong fluorescence via restriction of non-radiative relaxation pathway. When the compound **1** was grinded the color of the compound changes from golden yellow to bright yellow fluorescence, this accounted for reduction in the crystalline size of the compound **1** upon grinding. After grinding the compound was subjected to fuming in which the acetone was used as the solvent. Herein it was observed that upon fuming the compound does not revert to its original color intensity. Further upon heating the compound the bright yellow fluorescence disappears to give yellow color compound.

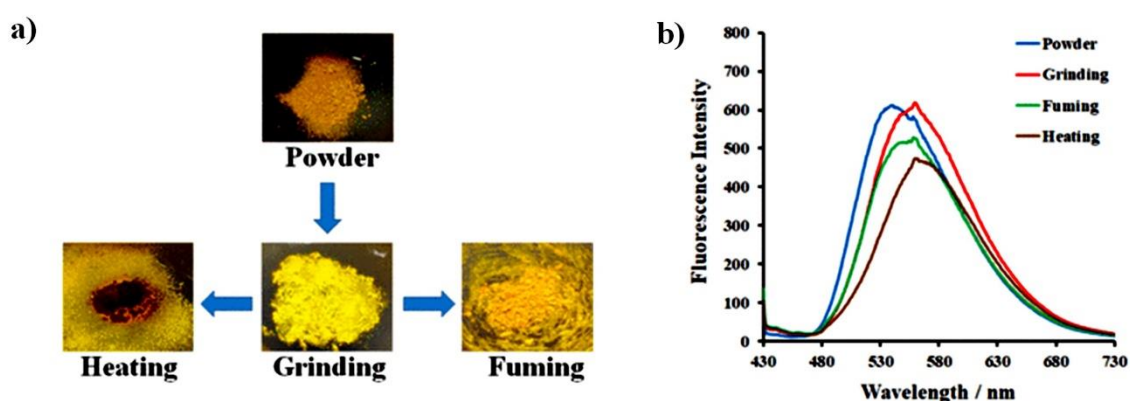


Figure 4.7 (a). Photograph representing the color changes upon grinding fuming and heating. **b)** represents the fluorescence emission recorded for compound upon grinding, fuming and heating.

Therefore, it can be concluded that the compound **1** shows significant mechanochromic behaviour after subjecting to various mechanical stress. The emission changes were recorded by fluorescence spectrometer at each stage of grinding, fuming and heating as shown in figure.

4.4.2 Solvent study

The rate and equilibrium of most of the chemical reactions that determines the peak intensity and absorption band in UV/vis/near-IR, NMR, ESR and IR are solvent dependent which are well known to every chemist. Therefore, nowadays appropriate and careful selection of solvent for analysis of every reaction and absorption study is considered as an important task. The absorption spectra of many chemical compounds are influenced by surrounding medium and solvent which brings about change in its absorption intensity, position and shape of band which is termed as *solvatochromism* [58,59]. There two kinds of solvatochromism i.e., negative solvatochromism which arises mainly due to a hypsochromic shift (blue shift) of UV/Vis/near-IR absorption as solvent polarity increases. However, “positive solvatochromism” appears through bathochromic (red shift) shift with increase in solvent polarity. The reason for solvatochromism is due to differential solvation of ground and excited state of light absorbing chromophore. Since our chromophore is highly fluorescent and soluble in organic solvents, we study the effect of solvent solute interaction by performing the solvent study [60].

Solvent study was performed for the compound before analysing it for sensing application. The compound **1** was highly soluble in organic solvent such as THF, acetonitrile (ACN), and dimethyl sulfoxide (DMSO). The absorption and emission spectra for compound was recorded in aforementioned solvents. The obtained results depicted that the absorption peaks were observed at 410 nm, 430, and 425 in in THF, ACN and DMSO solvent respectively while the emission peaks were appearing at 565, 567 and 628 nm for the THF, ACN, and DMSO when compound is excited at 410 nm. from solvent study as shown in figure that in THF compound showed very weak fluorescence in comparison to ACN and DMSO. Thus, in conclusion from

UV-Vis and emission spectral study depicts these solvent plays very crucial role and attributes to solvophobic effect. **Figure 4.8.**

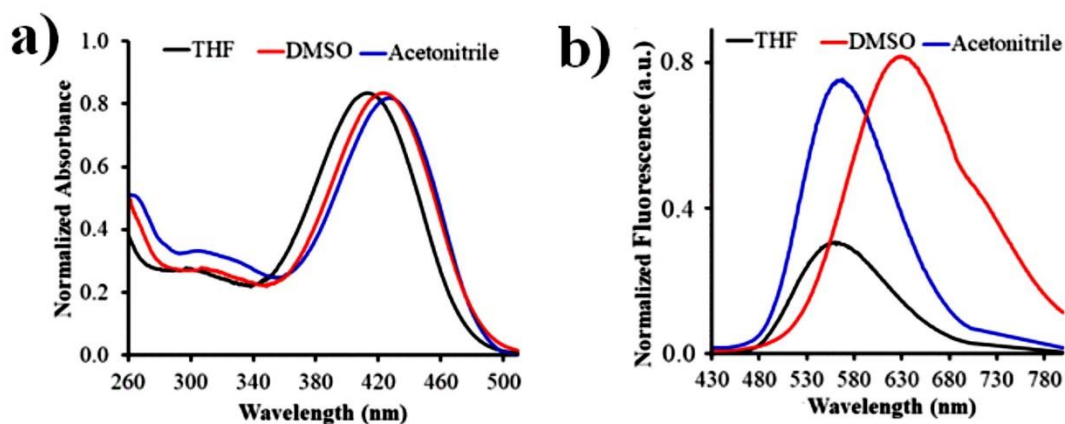


Figure 4.8. Solvent study performed for the compound 1 in ACN, THF and DMSO (a) Absorption spectra (b) Emission spectra.

4.4.3. Aggregation induced emission (AIE) study

Aggregation-induced emission (AIE) is an important abnormal photophysical phenomenon developed by the Tang and group in 2001 in HAKUST University. In AIE active process non planar molecules undergoes strong emission of light in the solid aggregated state. During AIE initially, the fluorogen is non-emissive in dilute solution state but becomes highly emissive in the aggregated state. The AIE process was developed over another detrimental process called as aggregation caused quenching (ACQ) in which fluorogens are emissive in dilute solution and become non-emissive in the aggregated state which just reverse phenomenon to AIE. Amongst ACQ and AIE, ACQ is determined as detrimental which led to the finding of AIE which is the most important and very useful in the today's scientific era. The discovery of AIE has unlocked a new way for traditional thinking and has brought up new ideas in designing and synthesizing the novel luminophore [61]. **Figure 4.9.**

It was observed that most of the fluorophores suffer from ACQ effect produced due to π - π stacking interaction. AIE another photophysical phenomenon which exactly opposite to ACQ

where luminophore becomes non-emissive in dilute solution and becomes highly emissive in a solid aggregate state in poor solvents. This phenomenon observed in any fluorophore is termed as AIE and the fluorophore with AIE property termed as AIEgens. The AIEgens are widely used as a turn-on fluorescent probe for biosensor because of strong sensitivity, high selectivity, rapid response, and low background noise. These AIEgens are not only limited for sensing application but it has inspired the AIEgens to design new fluorophore towards utilization in diverse field [62,63].

During the formation of aggregate the molecular rotation is restricted which results in radiative decay and the emission of light takes place in aggregative state. AIEgens are not only useful in vitro but these fluorogens are utilized for biological imaging of the molecules, cell, tissues, and various components of organism. The AIE active molecules are extensively used as optical sensors for accurate sensing of explosive. AIEgens can be used in the assay of proteins, peptides, and amino acids and can be also utilized for monitoring the conformational changes. Moreover, the recent progress in the scope of AIEgens application has expanded in the various scientific field.

Nowadays many scientists have increasingly exploited this concept for developing various luminescent material for potential practical application. Because of the continuous research and efforts by several groups have developed various kinds of stimuli-responsive AIE active materials such as fluorescent organic molecules, nanoparticles, different molecular rotors, polymer-based nanogels these AIE active molecules can be used to study the responses to various environmental changes such as light, temperature, pressure, pH, and viscosity. Amongst all these parameters temperature, pH and viscosity are the major factors responsible for biological activities occurring in the living system [64].

Most common examples of AIE property can be well explained with TPE based molecule,

hexaphenylsilole (HPS), whereas perylene and fluorescein explain describe about the phenomenon of ACQ. As shown in figure

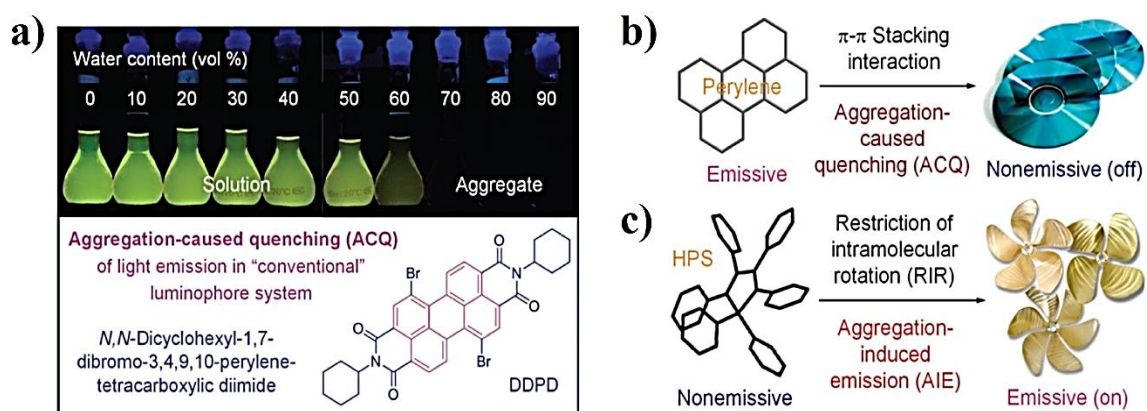


Figure 4. 9. Representative examples for AIE and ACQ (a and b; ACQ phenomenon) Hexaphenylsilole an example of AIE phenomenon.

By utilizing the deepest insight into AIE we performed the AIE activity for compound 1 as TPE is donor system which shows high AIE property. The AIE for the compound was performed in THF and water system. As shown in **Figure 4.10**. When the compound 1 was added to THF solvent the fluorescence was very low initially at 0% water fraction. But as the water fraction was increased from 10 to 99% with solution containing the compound there was increase in the fluorescence. This is ascribed as per the principle of AIE i.e., as the poor solvent fraction increases there is formation of aggregate resulting in to restriction of intramolecular rotation of the free phenyl groups present at the periphery resulting in to radiative decay.

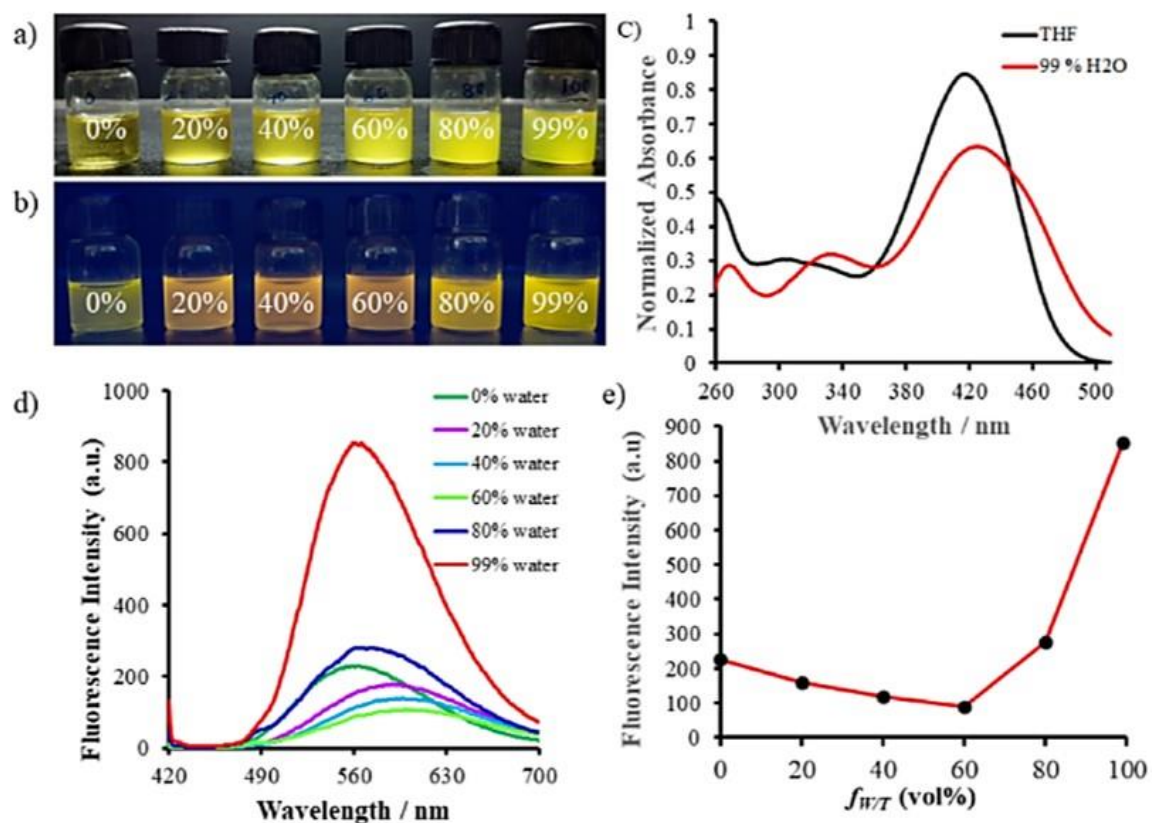


Figure 4.10. Aggregation induced emission study performed for the compound 1 in which (a) represents formation of aggregate as the water fraction is increased from 0 to 99%. (b) the solution after addition were placed under UV light illumination.

4.4.4 Sensing performance

The sensing performance was performed for compound 1 by reacting it with various analyte especially anions such as (Cl^- , I^- , F^- , Br^- , HSO_4^- , H_2PO_4^- , HCO_3^- , NO_3^- , ClO_4^-) and (CN^-) in its tetrabutylammonium salts. The series of anion solution was prepared and added to the solution containing ($2 \times 10^{-5} \text{M}$) of probe 1. When various anions were added the color of the solution containing probe 1 changes which was observed under day light as well as when placed under UV-Vis (365nm) illumination. It was observed that in presence of various anions only cyanide showed appreciable colour change from yellow to red color which was observed under day light as well as at 365nm (**Figure 4.11. a,b**) respectively. The figure below shows the sensing

capability of compound 1 solution to cyanide by resulting in to color change from yellow to red indicating that the compound 1 is highly selective towards CN^- .

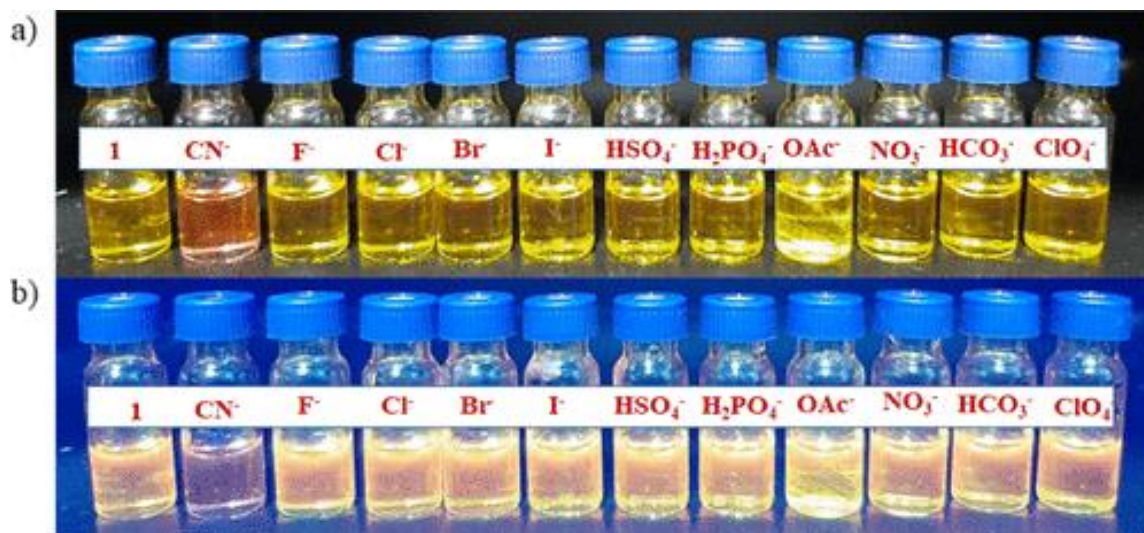


Figure 4.11. (a) Photograph of solution containing compound 1 with addition of various anions the color change was observed for solution with the addition of cyanide. (b) The fluorescence color change from yellow resulting in to quenching of fluorescence with the addition of CN^- .

4.4.5 UV-Vis study

From sensing performance, it was confirmed that the molecule was highly selective to CN^- anion. Therefore, it was further proved by studying its photophysical changes by using UV-Vis absorption and emission study. The solution containing probe 1 was subjected to UV-Vis study and strong absorption peak at 425 nm was observed. The absorption spectra were recorded for probe 1 containing various anions as shown in **Figure 4.12** It is observed that the probe 1 showed shift in the absorption with the addition of CN^- but not change observed with addition other anions. The probe 1 showed absorption maxima at 425 nm but with the addition of CN^- a new absorption peak appeared at 345 nm with shoulder peak at 302 nm. The change in absorption shift was further investigated with the incremental addition of CN^- anion. The following absorption titration revealed that as cyanide content increase the shift in the

absorption with isosbestic point 360nm. Thus, from the absorption analysis it can be predicted that the shift in the absorption may appear due to simple nucleophilic addition reaction taking place at the vinylic bond of the probe **1**. The following change in its photophysical characteristics is mainly due to its interruption of intramolecular charge transfer process. Therefore, the probe **1** can be utilized for selective detection of cyanide anion.

4.4.6 Fluorescence Emission Study

After absorption study the solution of probe **1** was subjected for fluorescence study. the emission study revealed that the molecule showed excellent emission band at 628nm in DMSO solvent. To the solution of the probe **1** various anions were added such as (Cl^- , I^- , F^- , Br^- , HSO_4^- , H_2PO_4^- , HCO_3^- , NO_3^- , ClO_4^-) and (CN^-). **Figure 4.13 (a)** It was observed that with addition of various anion there was no change observed in the emission band at 628nm. but when CN^- anion was added there was abrupt decrease in the fluorescence intensity which results in to quenching of fluorescence. Further followed by emission titration study representing that with the incremental addition from 0 -4 equiv. quenching of fluorescence was observed. **Figure 4.13 (b)** the complete disappearance of emission intensity at 628 due to breaking of ICT process in probe **1**.

4.4.7. Stoichiometry and Binding constant

The binding mode between probe **1** and CN^- ion was determined by using the Job's method of continuous variation. and binding constant was determined via Benesi-Hildebrand plot [65]. Plot for Binding constant and Stoichiometry study (Jobs plot) is given in **Figure 4.14**. below the plot of changes in fluorescence emission intensity (y-axis) against the molecular fraction of $[\text{1}]/[\text{1}+\text{CN}^-]$ From Job's plot it is very clearly indicate that the probe **1** when it reacted with CN^- forms 1:1 stoichiometric complexation reaction between probe **1** and CN^- . While the binding constant was determined by the Benesi-Hildebrand plot was employed to determine the binding constant (K) between probe **1** and CN^- ions. The linear relationship of fluorescence

emission intensity as a function of $[\text{CN}^-]$ from 0 to 4 equiv ($R = 0.9831$) was found graphically.

The binding constant (K_a) of **1** with CN^- was found to be $4.78 \times 10^6 \text{ M}^{-1}$.

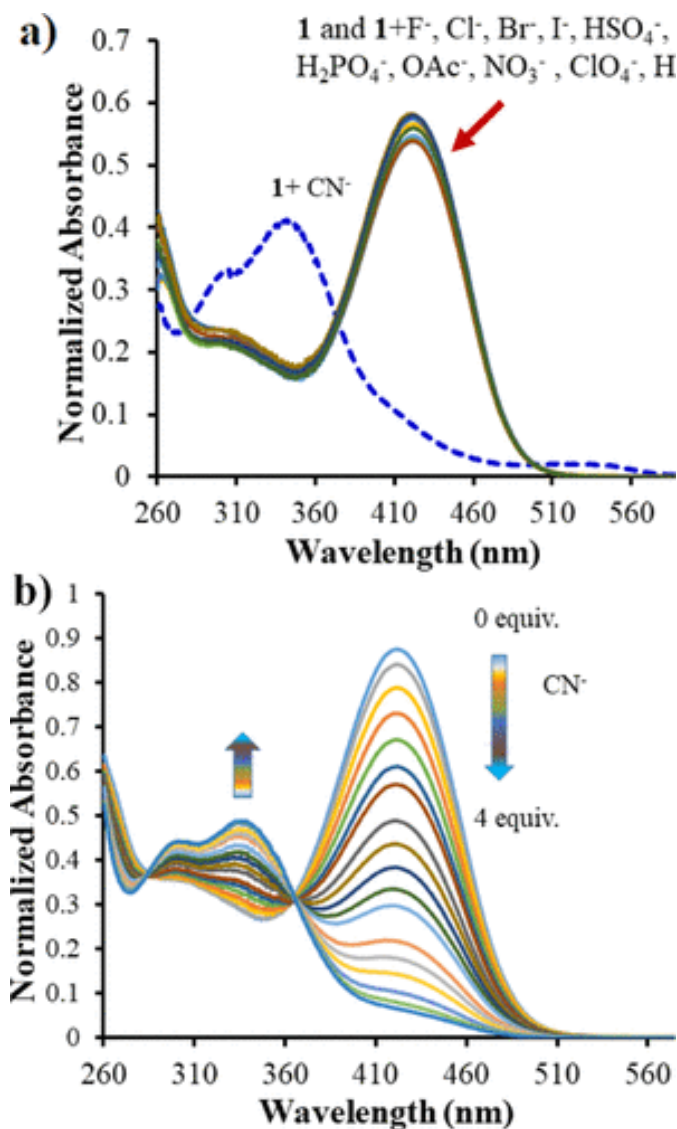


Figure 4.12. (a) UV-Vis absorption spectra recorded with the addition of various anions (b) UV-Vis absorption titration performed with the incremental addition of CN^- anion (0-4 equiv.).

4.4.8 Limit of Detection

The calculated limit of detection ($LOD = 3\sigma/S$), where σ is the standard deviation of the blank sample and S is the absolute value of the slope between fluorescence emission intensity and concentration of CN^- of the probe **1** is 67 nM, which is very low as compared to the maximum permissible level of CN^- . According to WHO (1.9 mM) and Environmental protection agency guidelines. This concludes that probe **1** can be successfully employed as a sensitive fluorescent probe for the quantitative detection of CN^- at nanomolar levels. **Figure 4.15**

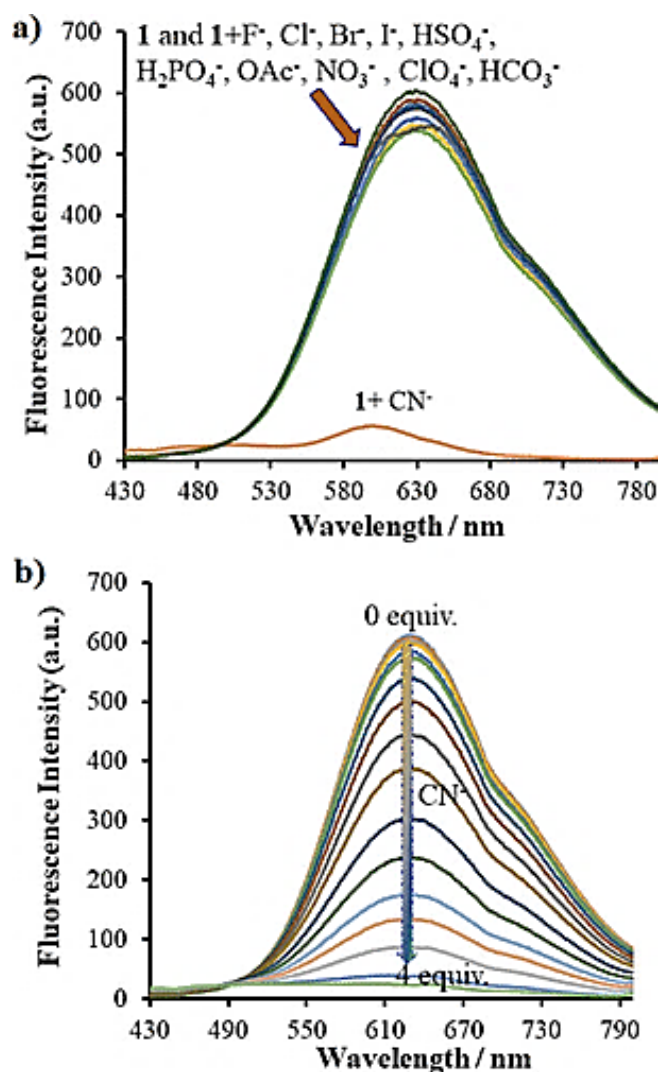


Figure 4.13. (a) Plot representing the quenching of fluorescence with the addition of CN^- in presence over other anions (b) Emission titration performed with incremental addition of CN^- (0-4equiv.).

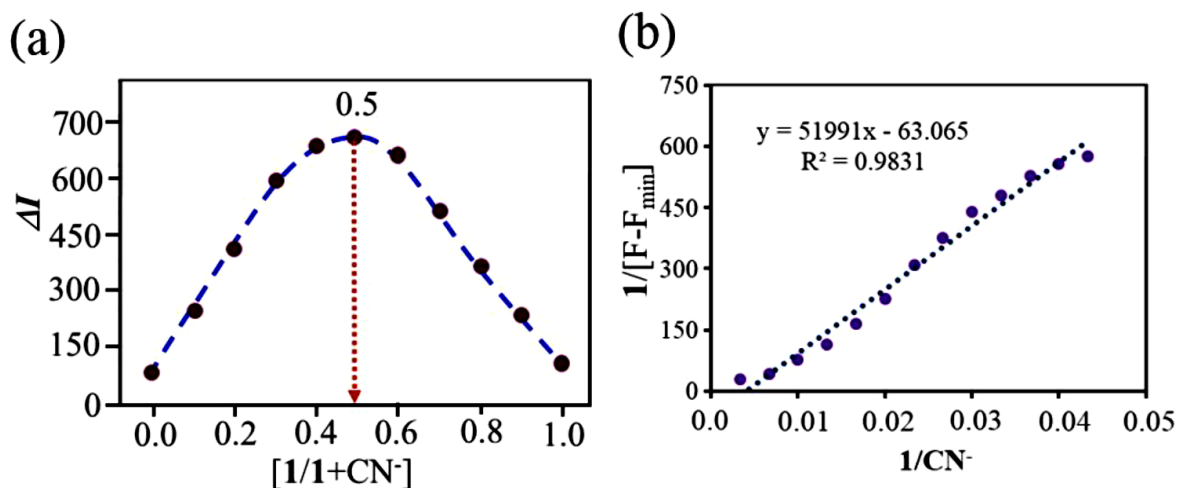


Figure 4.14. (a) the Jobs plot representing 1:1 stoichiometry (b) Benesi-Hildebrand plot for receptor 1 with CN^- .

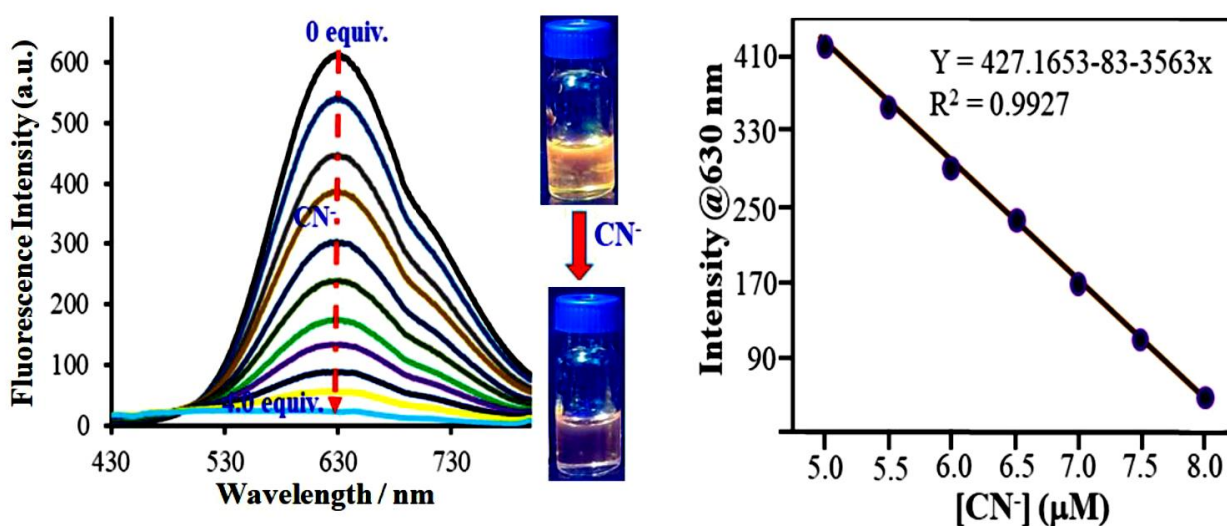


Figure 4.15. Emission spectra with incremental addition of CN^- (0-4 equiv.) with limit of detection plot (right).

4.4.9. The mechanism for CN^- detection by 1H NMR Study

The binding mechanism was studied for the probe **1** by performing 1H NMR experiment in DMSO- d_6 solvent. From **Figure 4.16** it illustrated that probe **1** showed a characteristic peak at δ 8.55 ppm which corresponds to vinylidene proton labelled as H_1 **Figure 4.16 (a)** To the same solution when TEACN was added (1.2 equiv.) the peak appearing at δ 8.55 ppm disappeared entirely with the appearance of the new peak at 5.09 ppm the proton labelled as H_2 in **Figure**

4.16.(b). In addition, the thiophene proton shifted to a higher frequency resulting in an alteration in the molecular structure of probe **1**. Therefore, it is evident that with the addition of CN^- a strong nucleophile undergoes addition at vinylidene bond ($\text{C}=\text{C}$) of the receptor which breaks the ICT process between the electron acceptor and donor TPE of the probe **1**.

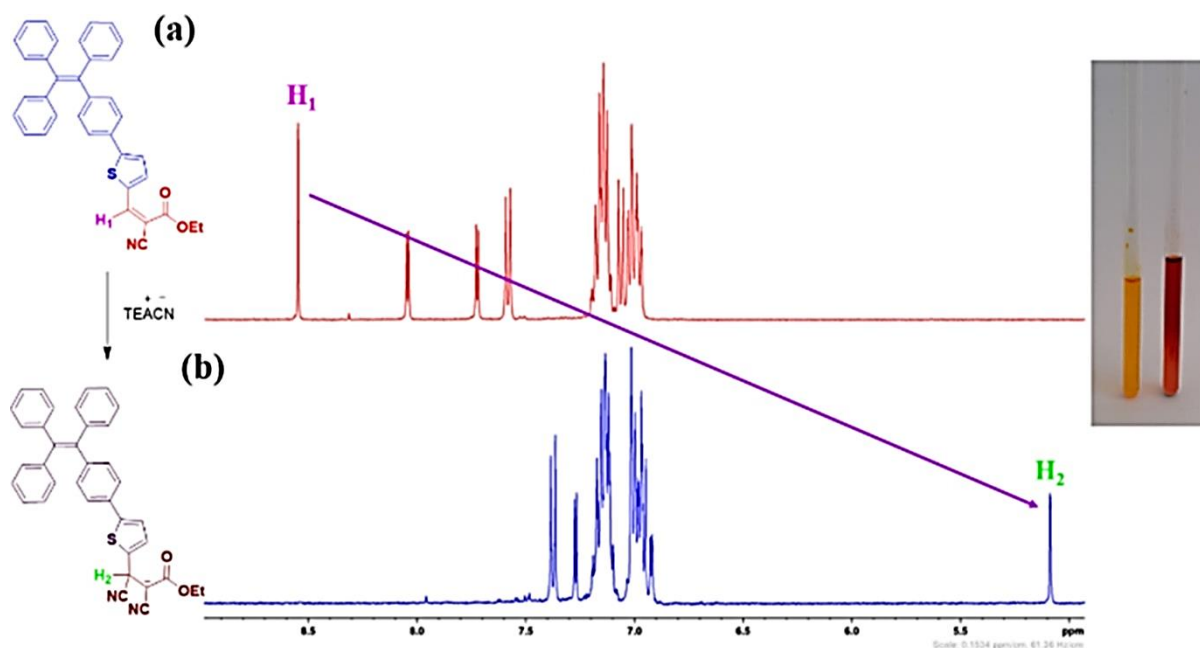


Figure 4.16. ^1H NMR study performed for the probe **1** (a) without addition of CN^- (labelled as H_1) (b) Represents the chemical shift with addition of CN^- (labelled as H_2).

4.5. Density Functional Theoretical calculations (DFT)

To further confirm the sensing properties of probe **1** towards CN^- by theoretical studies which was performed by Density Functional Theory (DFT) and time dependent DFT (TD-DFT) calculations. The results were obtained by using Gaussian 09 ab initio/DFT quantum chemical simulation package [66]. The geometry of the molecule was optimized in the series **1** and **1-CN** by B3LYP/6-31G* level of theory in addition the frequency calculations were performed to confirm the minima. Further the frontiers molecular orbitals (FMOs) of **1** and **1-CN** were produced by using Avogadro [67]. As shown in **Figure 4.17**. The highest occupied molecular orbitals of probe **1** shows delocalization mainly on the donor TPE and the thiophene moiety.

But the lowest unoccupied molecular orbital (LUMO) is distributed on the phenyl group of TPE, nitrile group and thiophene moiety. On contrary the HOMO of 1-CN⁻ is localized on ethyl cyanoacetate along with new cyanide moiety while the LUMO is delocalized especially on donor TPE and thiophene group. Thus, the charge transition properties of the probe **1** changes with addition of CN⁻. The experimental data was in agreement DFT calculation obtained which signify that with addition of CN⁻ there is nucleophilic addition reaction at C=C bond inhibiting the ICT process. The geometries obtained for probe **1** and 1-CN⁻ are studied using B3LYP/6-31G*. TD-DFT results were analysed by using Gauss-Sum 2.2.5 program, [68] obtained results are shown in **Table 4.2** The HOMO and LUMO without and with addition of CN⁻ was also confirmed by cyclic voltammetry study as shown in **Figure 4.18** and calculated values are denoted in **Table 4.1**

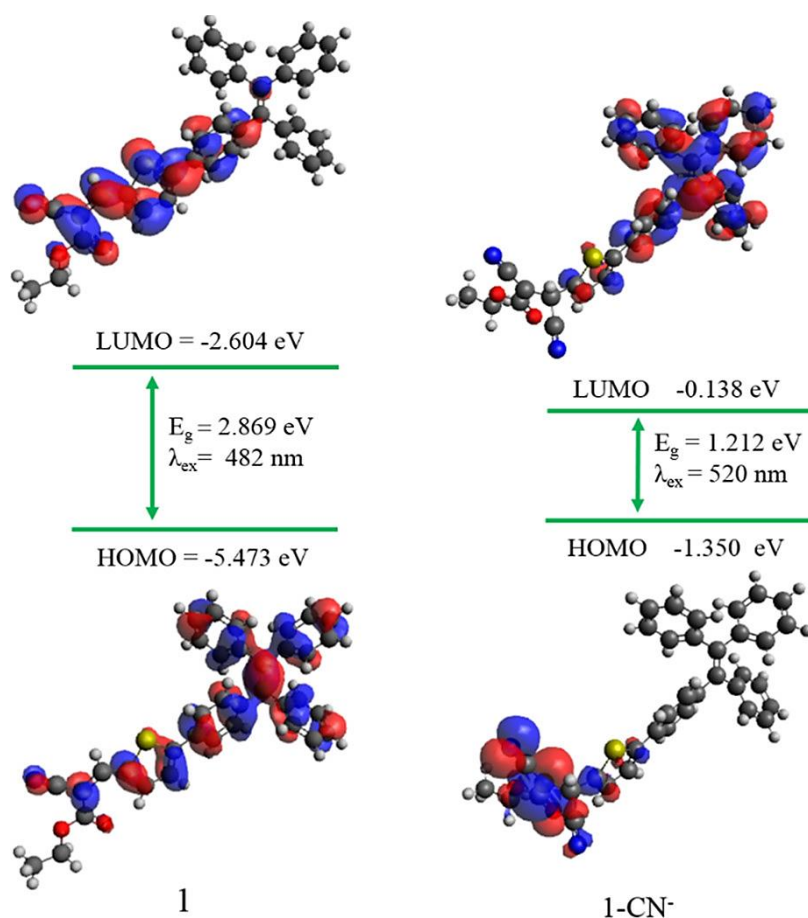


Figure 4.17. Represents the optimized geometries of the structure without and with presence of CN⁻.

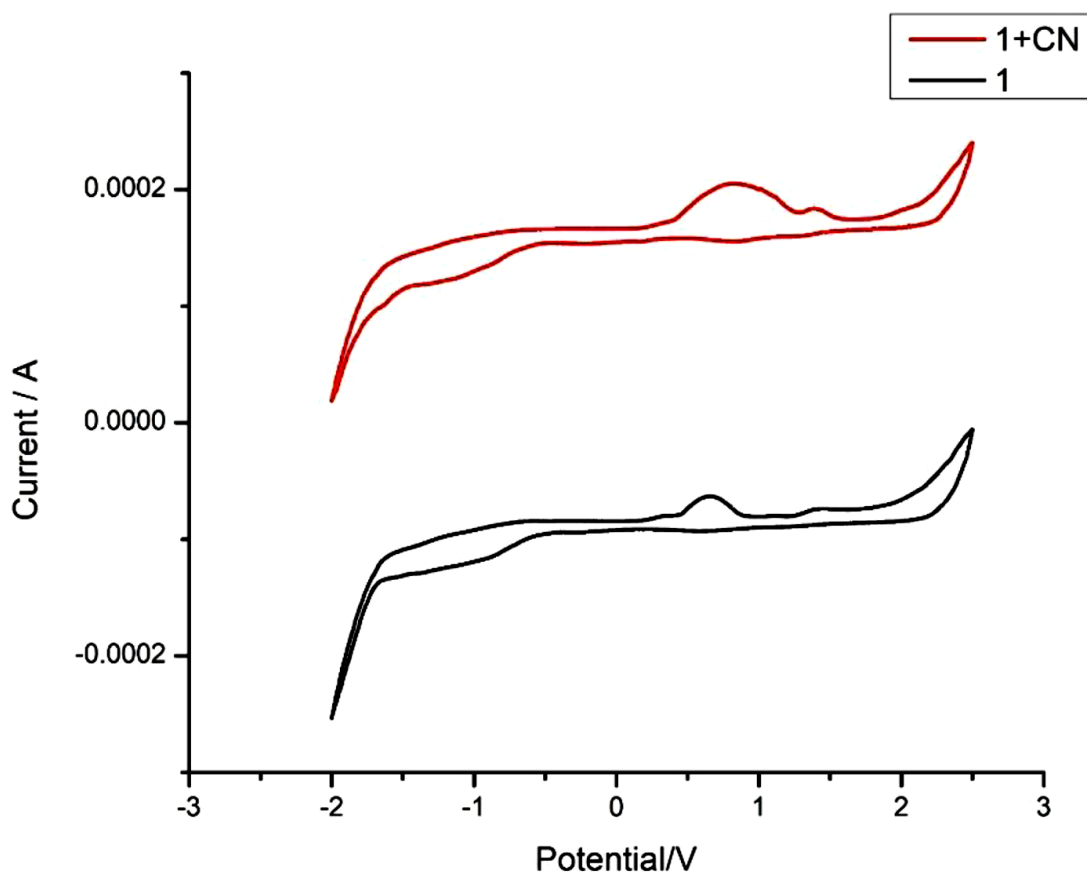


Figure 4.18. Cyclic voltammogram in presence and absence of CN^- added to probe 1

Molecular Code	1	1+CN
$E^{\text{ox}}_{\text{onset}}$ (V)	0.482	0.400
$E^{\text{red}}_{\text{onset}}$ (V)	-0.660	-0.799
HOMO (eV)	-5.182	-5.10
LUMO (eV)	-4.04	-3.901
E^{elg} (eV) ^c	1.142	1.19

Table 4.1. Calculated values for HOMO and LUMO with and without addition of CN^-

4.6 Competitive study

The specificity and selectivity study can be well explored by performing the competitive study with addition of various anions in presence of the CN^- . As can be seen from the blue bar represents probe 1+ tested anions such as (Cl^- , I^- , F^- , Br^- , HSO_4^- , H_2PO_4^- , HCO_3^- , NO_3^- , ClO_4^- , OAc^-) while the red bar represents the probe 1 + tested anion+ CN^- . From graph it is very clear that with addition of CN^- along with the tested anion shows complete quenching and blue bar diminishes with CN^- . Therefore, the probe 1 can be employed successfully for recognition of CN^- anion with excellent selectivity and good anti-interference property. **Figure 4.19.**

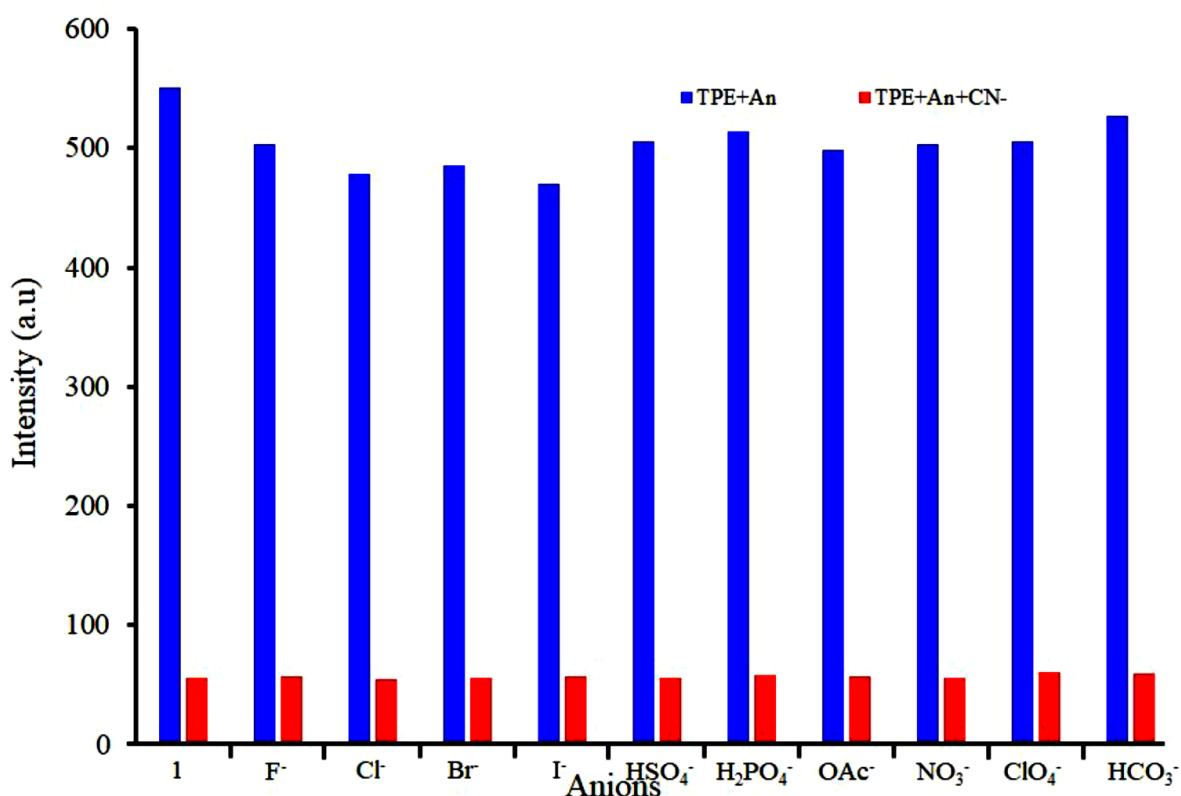


Figure 4.19. Competitive study performed for the probe with addition of various anion along with CN^- anion.

4.7 Practical Application

4.7.1. Strip sensing

After confirmation by various characterization techniques and confirmation its selectivity towards CN^- the molecule was employed for practical use in test strip sensing application and in food assay. To employ the probe 1 for strip sensing the molecule was adsorbed on the strips of the Whatman paper by dissolving the **probe 1** in chloroform. The strips prepared were used for detection of CN^- anion. In **Figure 4.20** it is observed that initially the strips were yellow in colour in day light. To the strips were tested for various anions and it was observed that the probe showed complete disappearance of yellow color with addition of CN^- while no color change was observed in presence of other anions. The test strips were observed in day light as well as under 365 nm. At 365 nm it was observed that there was complete quenching of fluorescence with the addition of CN^- .

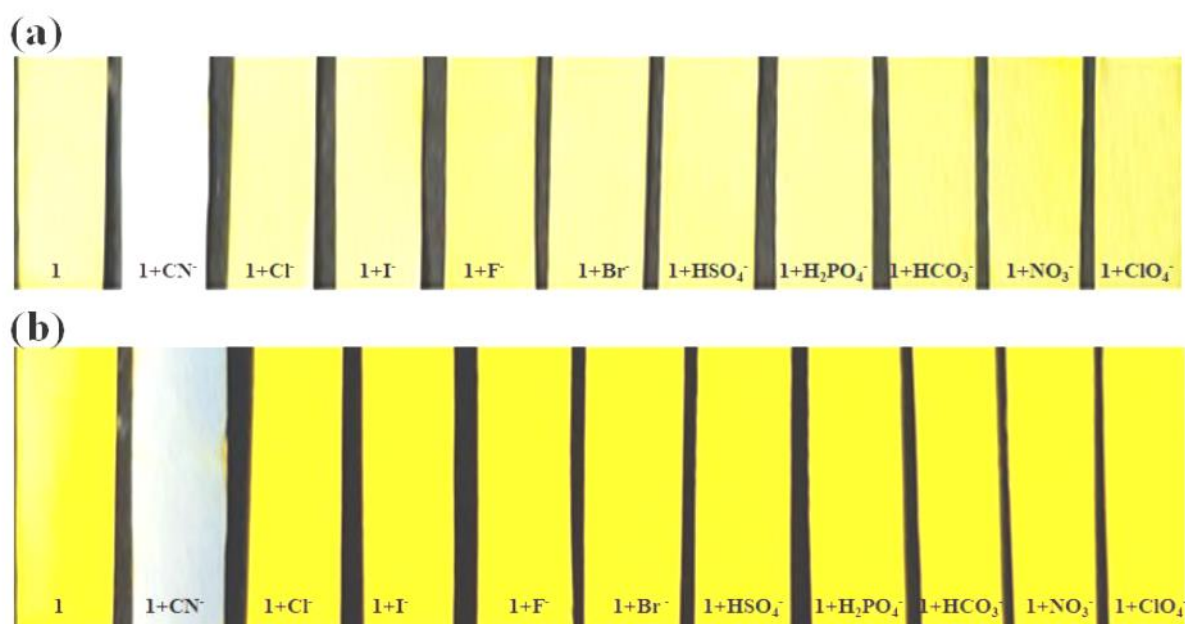


Figure 4.20. Test strip representing the color change with the addition of various anions observed under (a) day light (b) under UV light at 365 nm.

4.7.2 Application of probe 1 in live cell imaging

4.7.2. Cell Toxicity

Cell toxicity study was performed on HeLa cells by using the synthesized probe **1**. MTT assay revealed that the cells were stable up to 30nM while showed 100% viability in 10 nM concentration even after 24 hours of incubation.

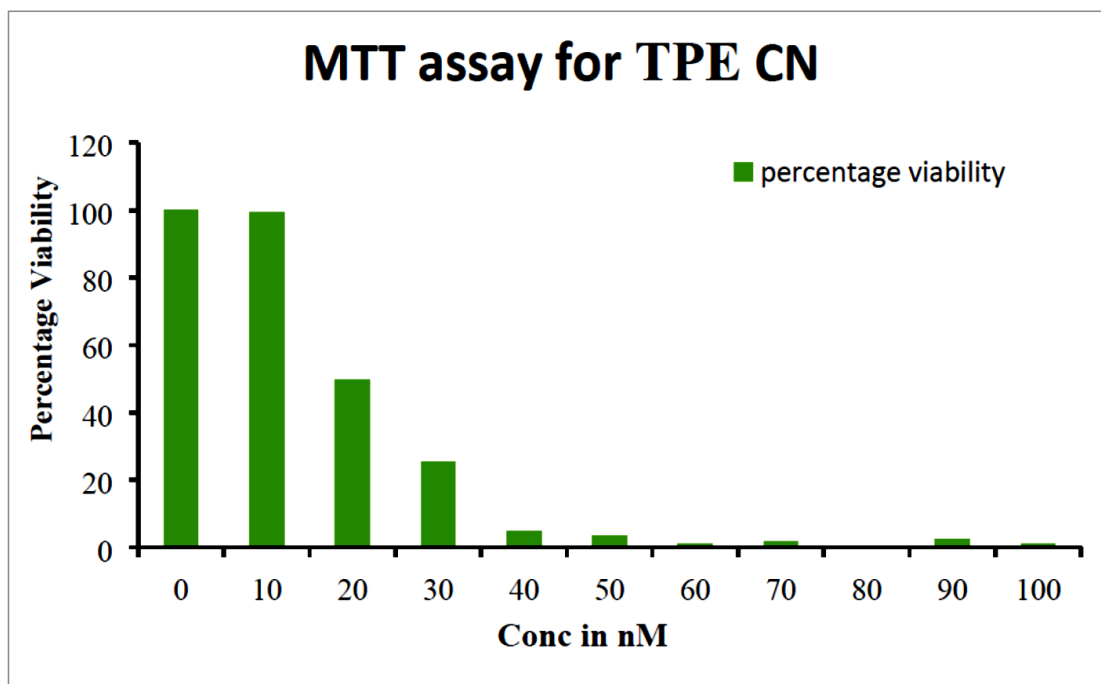


Figure 4.21. MTT Assay performed for probe **1** to determine the toxicity.

From the experimental data it was analysed that when the HeLa cells were incubated with 10nM it doesnot show toxicity with 100% viability compared to control. Since it is not toxic 10nM concentration can be used further for fluorescence cell imaging applictiaion. The cells were studied under confocal laser microscopy by placing the HeLa Cells under bright field and FITC fluorescence filter as shown in **Figure 4.21**. In this study the the HeLa cells were incubated with 10 nM concentration of probe 1 and was observed under bright field and again the same concentration was placed under FITC fluorescence filter which showed green fluorescence indicating that the cells haven taken up the probe **1** and remains viable. Further when CN^- anion was added to the HeLa cells incubated with probe **1** it was observed that the

in presence of cyanide there was complete quenching of green fluorescence when the incubated cells were placed under bright field and fluorescence FITC filter. The complete fluorescence disappeared mainly due to reaction between the probe incubated intracellularly and cyanide added. thus these represents that probe 1 upon incubation penetrate intracellular deeply in to HeLa cells which helps to detect CN^- in live cells. as shown in **Figure 4.22**.

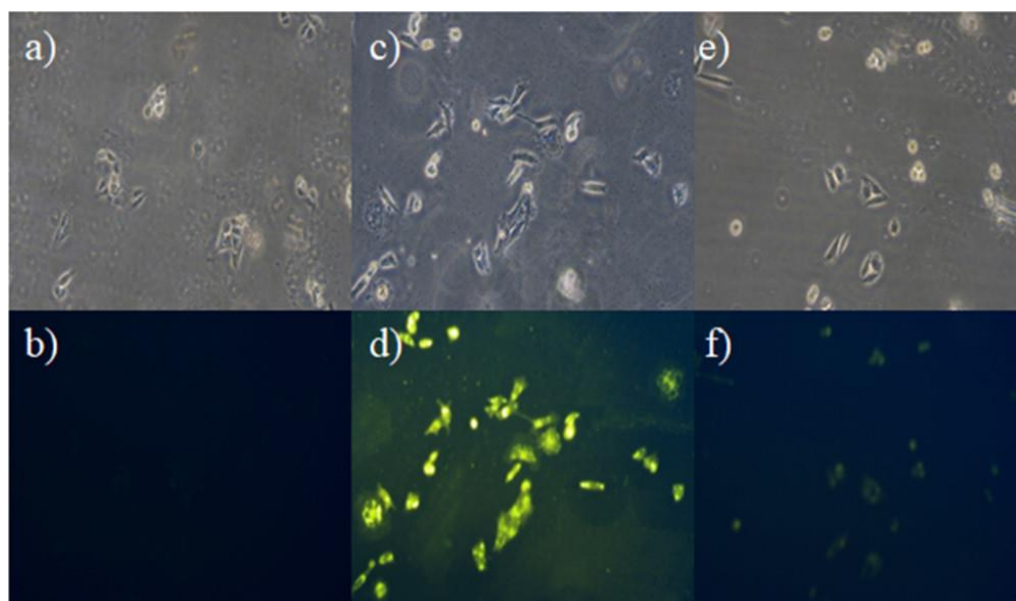


Figure 4.22. Cell imaging study performed for probe 1. **(a)** HeLa Cells focussed under bright field **(b)** no fluorescence observed in HeLa cells without incubation with probe 1 under FITC filter. **(c)** image depicts the HeLa cells incubated with probe 1 under bright field **(d)** image depicts the HeLa cells incubated with probe 1 under showing green fluorescence in FITC filter. **(e)** image capture under bright field with addition of CN^- when cells incubated with probe 1. **(f)** HeLa Cells placed under FITC filter with addition of CN^- .

4.7.3. Food Assay

In addition to food analysis further the molecule was investigated for application of probe 1 in food samples containing cyanogenic glycoside such as bitter almonds, sweet potato and sprouted potato. To check the endogenous cyanide content in food sample the selected food samples were crushed and pulverize by using mortar and pestle. After that the 10 ml water was added with 5 mg of NaOH under constant stirring for 10 mins the clear solution was obtained by centrifugation for 20 mins. The obtained clear solution was used for sensing application in

which a cyanide containing solution was added to the probe **1**. Upon addition of cyanide there was distinct quenching of fluorescence observed for probe as shown in **Figure 4.23**

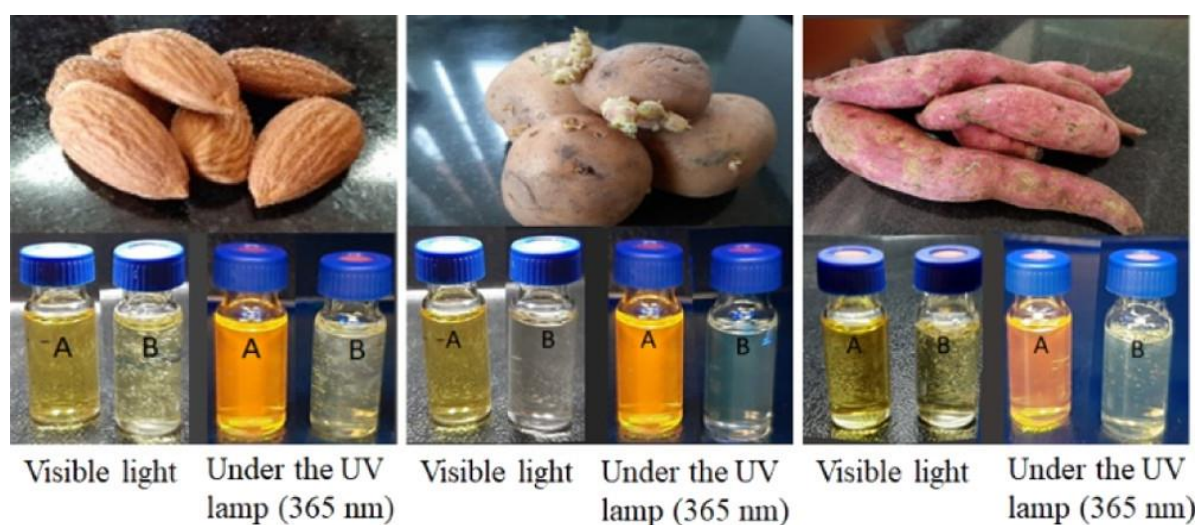
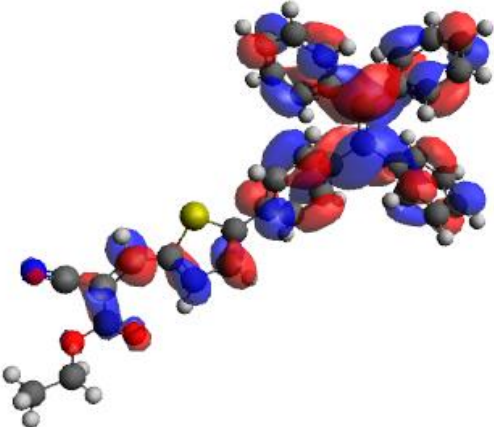
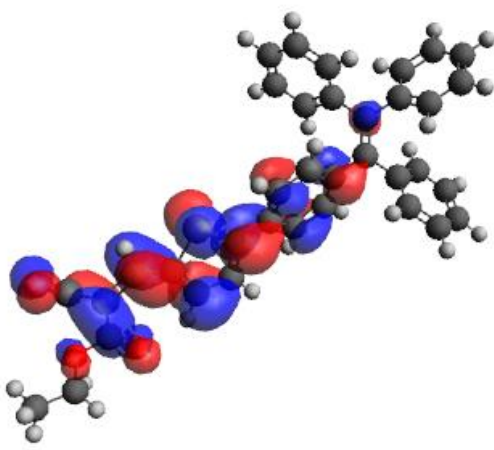
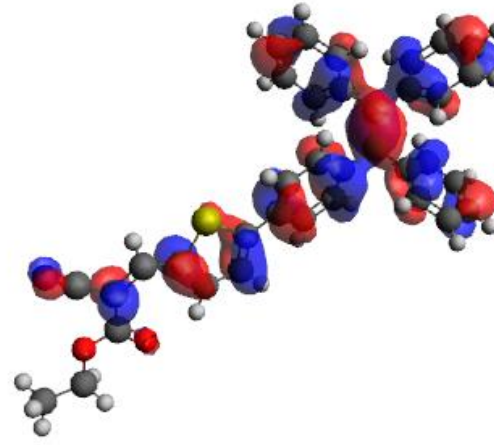


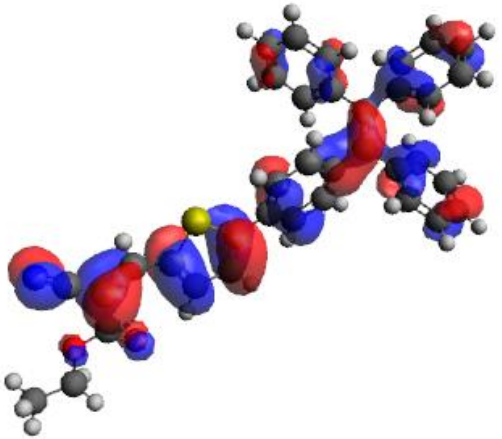
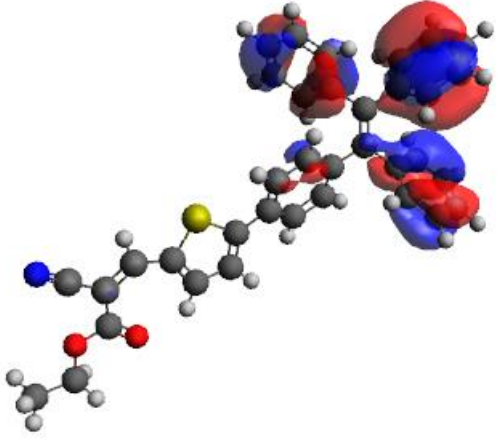
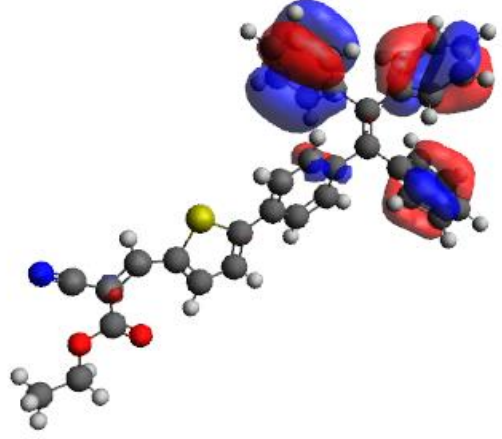
Figure 4.23. The probe **1** was utilized for detection of CN^- in food analysis.

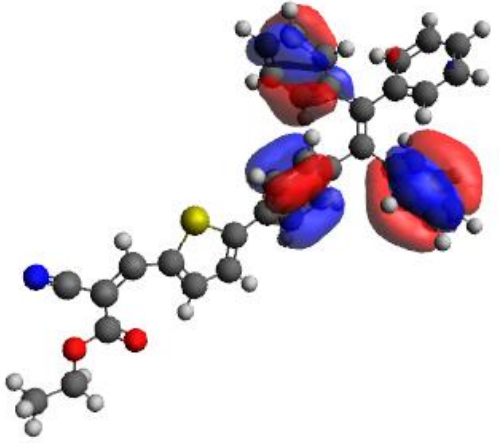
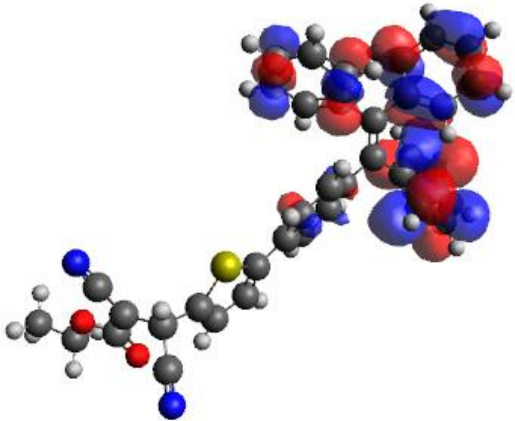
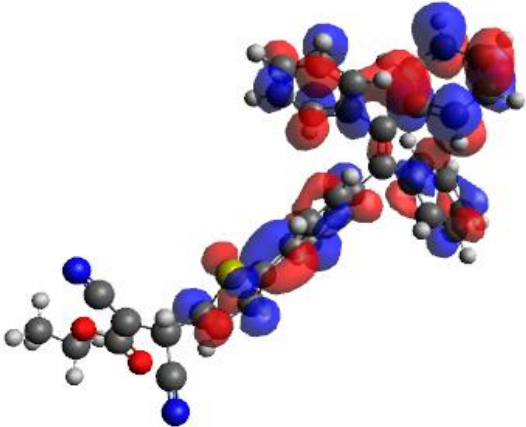
Table 4.2: Calculated TD-DFT excitation properties of probe **1** and **1:CN⁻**

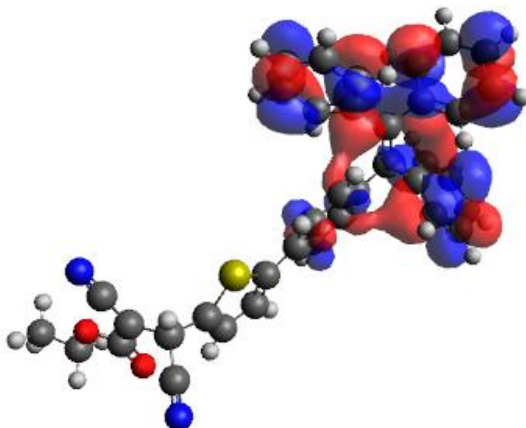
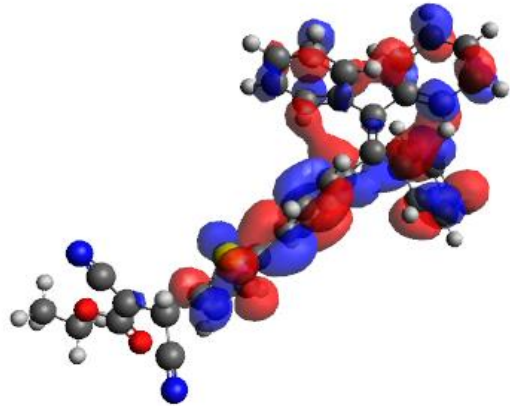
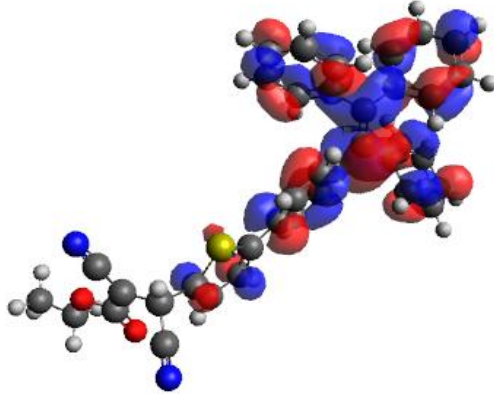
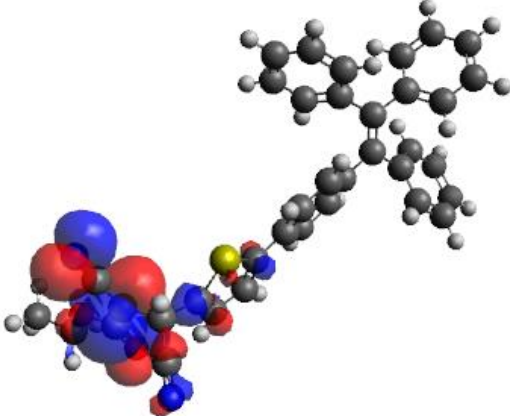
Molecules	Excitation Energy (eV)	Excitation Wavelength (nm)	Oscillator Strength (f)	Excitations	Percentage contribution for transition		
Probe 1	2.5735	481.76	0.6332	141 ->142	HOMO->LUMO (99%)		
	3.3004	375.67	0.8477	140 ->142	H-1->LUMO (89%)		
				141 ->143	HOMO->L+1 (9%)		
	3.6006	344.34	0.1745	139 ->142	H-2->LUMO (3%),		
				140 ->142	H-1->LUMO (7%)		
	3.7809	327.92	0.0459	141 ->143	HOMO->L+1 (85%)		
				137 ->142	H-4->LUMO (10%),		
				138 ->142	H-3->LUMO (6%),		
				139 ->142	H-2->LUMO (75%)		
				141 ->143	HOMO->L+1 (3%)		
	3.8158	324.93	0.0076	137 ->142	H-4->LUMO (15%),		
				138 ->142	H-3->LUMO (66%),		
				139 ->142	H-2->LUMO (15%)		
1:CN ⁻	1.2094	1025.18	0.0368	148 ->149	HOMO->LUMO (99%)		
2.0195	613.94	0.0392	148 ->150	HOMO->L+1 (92%)			
			148 ->152	HOMO->L+3 (6%)			
			2.2412	553.20	0.0001	148 ->151	HOMO->L+2 (99%)
			2.3637	524.53	0.0035	148 ->150	HOMO->L+1 (7%)
						148 ->152	HOMO->L+3 (92%)
			2.6094	475.14	0.0012	148 ->153	HOMO->L+4 (98%)

Table 4.3. Frontier molecular orbitals of probe **1** and **1+CN⁻** with energy in eV.

Probe 1			
Orbital	Orbital number	Energy (eV)	Orbital Picture
LUMO+1	143	-1.491eV	
LUMO	142	-2.604eV	
HOMO	141	-5.473eV	

H-1	140	-6.113eV	
H-2	139	-6.714eV	
H-3	138	-6.779eV	

H-4	137	-6.853eV	 A 3D ball-and-stick model of a molecule with red and blue isosurfaces representing the H-4 orbital. The molecule consists of a central chain with a sulfur atom (yellow) and a nitrogen atom (blue). The orbitals are concentrated on the right side of the molecule.
1-CN⁻			
LUMO+4	153	-1.503eV	 A 3D ball-and-stick model of a molecule with red and blue isosurfaces representing the LUMO+4 orbital. The molecule is similar to the one above. The orbitals are distributed across the right side of the molecule.
LUMO+3	152	-1.287eV	 A 3D ball-and-stick model of a molecule with red and blue isosurfaces representing the LUMO+3 orbital. The molecule is similar to the one above. The orbitals are distributed across the right side of the molecule.

LUMO+2	151	-1.141eV	
LUMO+1	150	-1.034eV	
LUMO	149	-0.138eV	
HOMO	148	-1.350eV	

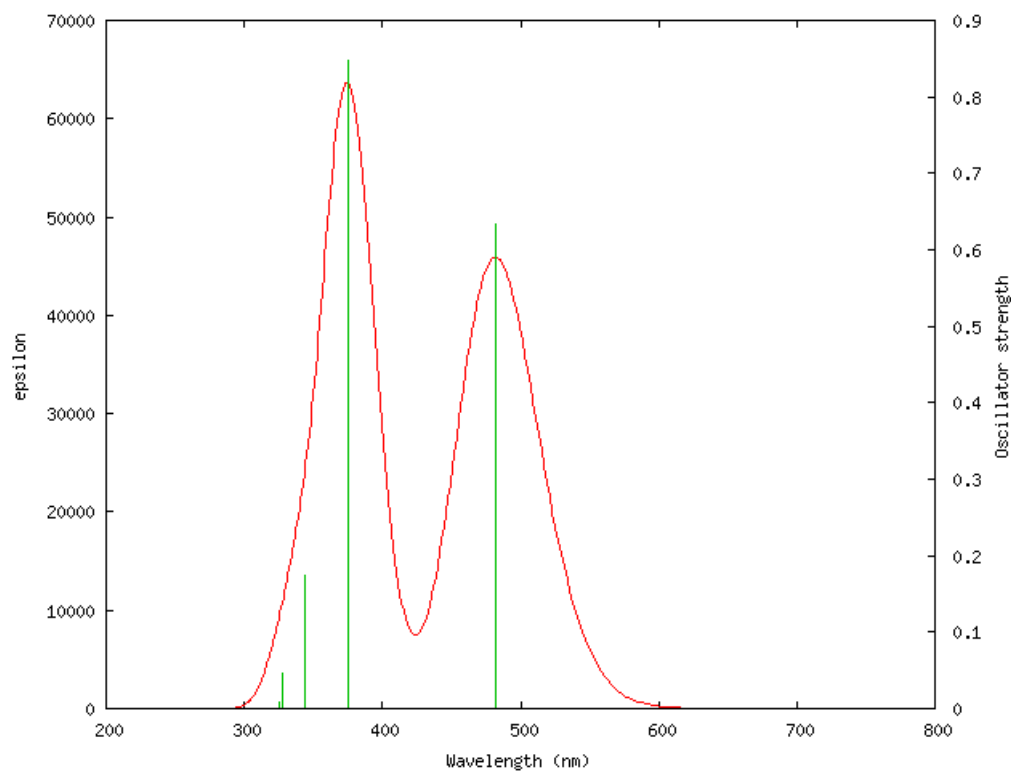


Figure 4.24. Theoretical UV-vis absorption spectra of probe **1**.

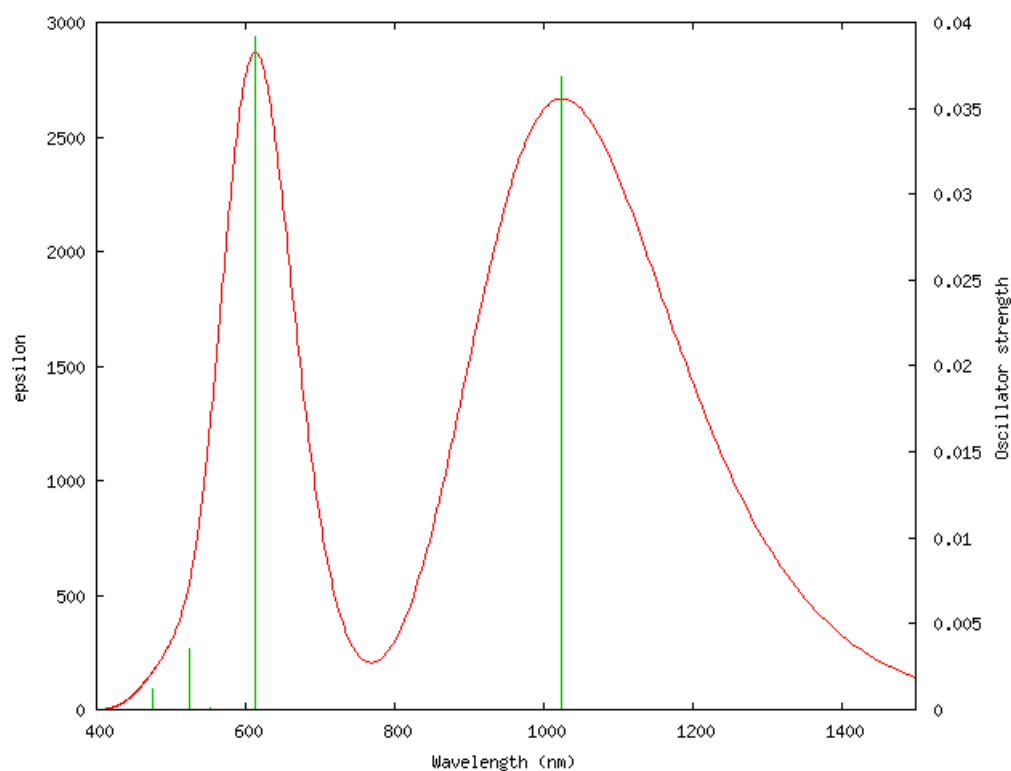
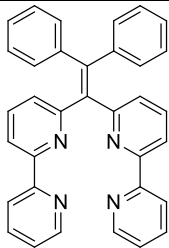
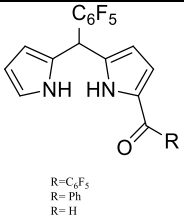
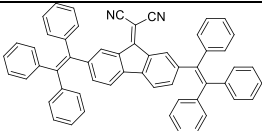
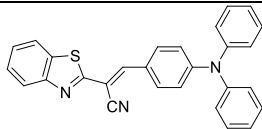
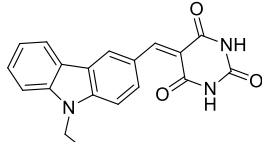
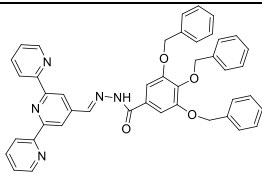
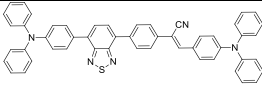
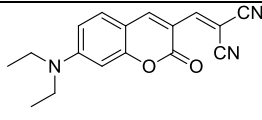
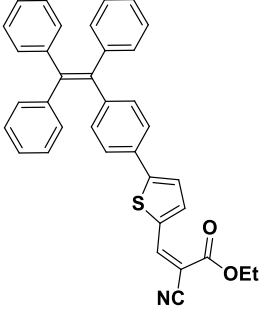


Figure 4.25. Theoretical UV-vis absorption spectra of probe **1:CN⁻**.

4.8. Comparison table for various fluorescent molecule for CN⁻ sensingTable 4.4: Comparison of CN⁻ sensing with literature.

Compound	Sensing method	AIE	H ₂ O %	LOD (μM)	pH range	Test strip	Cell Imaging	Ref.
	Fluorescence turn-on	Yes	0	0.59	No data	No	No	¹
 R=C ₆ F ₅ R=Ph R=H	Colorimetric sensing	No	0	0.3	No data	No	No	²
	Fluorescence Turn-on	Yes	0	-	No data	Yes	No	³
	Fluorescence Turn-off	Yes	0	0.2	No data	Yes	Yes	⁴
	Naked eye and colorimetric sensing	Yes	100	64.4 nM	No data	Yes	No	⁵
	Fluorescence turn-on	Yes	-	1.09	No data	No	No	⁶
	Fluorescence turn-on	Yes	-	0.35	No data	Yes	Yes	⁷
	Colorimetric Probe	No	-	1.5	6-8	No	Yes	⁸

	Naked eye, colorimetric, Fluorescence turn-Off	Yes	-	0.85		Yes	Yes	Our Work
---	---	-----	---	------	--	-----	-----	-------------

4.9. Conclusion

The Aggregation induced emission active molecule based on tetraphenylethene was synthesized ethyl-2-cyano-3-(5-(4-(1,2,2-triphenylvinyl)phenyl)thiophen-2-yl)acrylate (1). The molecule was synthesized three steps by reacting diphenylmethane and benzophenone in presence of n-butyl lithium and PTSA, toluene under refluxing condition to yield mono-bromo tetraphenylethene (1-(4-bromophenyl)-1,2,2-triphenylethene (4)) which further undergoes Suzuki coupling in presence of thiophene boronic acid in Pd(PPh₃)₄, DME and Na₂CO₃ to give 5-(4-(1,2,2-triphenylvinyl)phenyl)thiophene-2-carbaldehyde (6). Then the compound 6 undergoes Knoevenagel condensation to yield ethyl-2-cyano-3-(5-(4-(1,2,2-triphenylvinyl)phenyl)thiophen-2-yl)acrylate (1). The probe was characterized successfully by ¹H NMR, ¹³C NMR, ESI-Mass, elemental analysis DFT study. In addition, the molecule was investigated for its photophysical properties by UV-Vis absorption study and fluorescence emission study by spectrofluorometer.

The synthesized probe 1 was employed for selective and sensitive detection of CN⁻ anion in presence over other competing anions. The limit of detection for the CN⁻ by using the probe 1 was found to be 67nM which is very low compared to the guideline provided by environmental protection agency (EPA) and WHO (1.9μM). The binding mode for sensing of CN⁻ over vinylic bond of the receptor was confirmed by ¹H NMR study. The molecule was used for practical application in strip sensing. Another most important application of fluorescent molecule was

utilized for sensing of CN^- in food sample such as potato, sweet potato and almonds. In addition the fluorescent probe was employed in biological cell imaging application. Thus, this proves that the probe can be used for selective and sensitive detection of cyanide in various systems and in future this probe can be successfully employed for practical applications in environmental remediation and food analysis.

4.10. References

- (1) Way, J. L. Cyanide Intoxication and Its Mechanism of Antagonism. *Annu. Rev. Pharmacol. Toxicol.* **1984**, VOL. 24, 451–481. <https://doi.org/10.1146/annurev.pharmtox.24.1.451>.
- (2) Chmielewski, M. J.; Charon, M.; Jurczak, J. Supramolecular Chemistry of Anions. *J. Coord. Chem. Rev.* **2003**, 240 (2), 1647–1654.
- (3) Zhou, X.; Mu, W.; Lv, X.; Liu, D. Ratiometric Fluorescent Detection of CN^- -Based on CN^- -Promoted Interruption of π -Conjugation of a Coumarin-Bearing Michael Receptor. *RSC Adv.* **2013**, 3 (44), 22150–22154. <https://doi.org/10.1039/c3ra44245d>.
- (4) Chen, C. L.; Chen, Y. H.; Chen, C. Y.; Sun, S. S. Dipyrrole Carboxamide Derived Selective Ratiometric Probes for Cyanide Ion. *Org. Lett.* **2006**, 8 (22), 5053–5056. <https://doi.org/10.1021/ol061969g>.
- (5) Nicoletti, C. R.; Nandi, L. G.; Machado, V. G. Chromogenic Chemodosimeter for Highly Selective Detection of Cyanide in Water and Blood Plasma Based on Si-O Cleavage in the Micellar System. *Anal. Chem.* **2015**, 87 (1), 362–366. <https://doi.org/10.1021/ac504037v>.
- (6) Tayfur, G.; Kirer, T.; Baba, A. Groundwater Quality and Hydrogeochemical Properties of Torbali Region, Izmir, Turkey. *Environ. Monit. Assess.* **2008**, 146 (1–3), 157–169. <https://doi.org/10.1007/s10661-007-0068-6>.
- (7) Kulig, K. W.; Ballantyne, B.; Becker, C.; Borak, J.; Cannella, J.; Goldstein, B.; Hall, A.; Jackson, R. J.; Rodnick, J.; Wheeler, R.; Wummer, B. Cyanide Toxicity. *Am. Fam. Physician* **1993**, 48 (1), 107–109. https://doi.org/10.1007/978-3-642-00418-6_817.
- (8) Services, H. Toxicological Profile for Cyanide. *ATSDR's Toxicol. Profiles* **2002**, No. July. https://doi.org/10.1201/9781420061888_ch68.
- (9) Liu, D.; Wang, Z.; Jiang, X. Gold Nanoparticles for the Colorimetric and Fluorescent

- Detection of Ions and Small Organic Molecules. *Nanoscale* **2011**, 3 (4), 1421–1433. <https://doi.org/10.1039/c0nr00887g>.
- (10) Finlayson, B. A.; Finlayson, B. A.; Engineering, C. Ullmann ' s Encyclopedia of Industrial Chemistry. **2016**, No. October. <https://doi.org/10.1002/14356007.b01>.
- (11) Long, L.; Wang, L.; Wu, Y. A Fluorescence Ratiometric Probe for Detection of Cyanide in Water Sample and Living Cells. *Adv. Mater. Phys. Chem.* **2013**, 03 (08), 307–313. <https://doi.org/10.4236/ampc.2013.38042>.
- (12) Bolarinwa, I. F.; Orfila, C.; Morgan, M. R. A. Determination of Amygdalin in Apple Seeds, Fresh Apples and Processed Apple Juices. *Food Chem.* **2015**, 170, 437–442. <https://doi.org/10.1016/j.foodchem.2014.08.083>.
- (13) Herschy, R. W. Water Quality for Drinking: WHO Guidelines. *Encycl. Earth Sci. Ser.* **2012**, 876–883. https://doi.org/10.1007/978-1-4020-4410-6_184.
- (14) Xu, Z.; Chen, X.; Kim, H. N.; Yoon, J. Sensors for the Optical Detection of Cyanide Ion. *Chem. Soc. Rev.* **2010**, 39 (1), 127–137. <https://doi.org/10.1039/b907368j>.
- (15) Li, X.; Gao, X.; Shi, W.; Ma, H. Design Strategies for Water-Soluble Small Molecular Chromogenic and Fluorogenic Probes. *Chem. Rev.* **2014**, 114 (1), 590–659. <https://doi.org/10.1021/cr300508p>.
- (16) Lee, M. H.; Kim, J. S.; Sessler, J. L. Small Molecule-Based Ratiometric Fluorescence Probes for Cations, Anions, and Biomolecules. *Chem. Soc. Rev.* **2015**, 44 (13), 4185–4191. <https://doi.org/10.1039/c4cs00280f>.
- (17) Zeng, Q.; Cai, P.; Li, Z.; Qin, J.; Tang, B. Z. An Imidazole-Functionalized Polyacetylene: Convenient Synthesis and Selective Chemosensor for Metal Ions and Cyanide. *Chem. Commun.* **2008**, No. 9, 1094–1096. <https://doi.org/10.1039/b717764j>.
- (18) Chung, Y.; Lee, H.; Kyo, H. A. N-Acyl Triazenes as Tunable and Selective Chemodosimeters toward Cyanide Ion. *J. Org. Chem.* **2006**, 71 (25), 9470–9474. <https://doi.org/10.1021/jo061798t>.
- (19) Miyaji, H.; Sessler, J. L. Off-the-Shelf Colorimetric Anion Sensors. *Angew. Chemie - Int. Ed.* **2001**, 40 (1), 154–157. [https://doi.org/10.1002/1521-3773\(20010105\)40:1<154::AID-ANIE154>3.0.CO;2-G](https://doi.org/10.1002/1521-3773(20010105)40:1<154::AID-ANIE154>3.0.CO;2-G).
- (20) Sun, S. S.; Lees, A. J. Anion Recognition through Hydrogen Bonding: A Simple, yet Highly Sensitive, Luminescent Metal-Complex Receptor. *Chem. Commun.* **2000**, No. 17, 1687–1688. <https://doi.org/10.1039/b004541l>.
- (21) Anzenbacher, P.; Tyson, D. S.; Jursíková, K.; Castellano, F. N. Luminescence Lifetime-Based Sensor for Cyanide and Related Anions. *J. Am. Chem. Soc.* **2002**, 124 (22), 6232–

6233. <https://doi.org/10.1021/ja0259180>.
- (22) Gimeno, N.; Li, X.; Durrant, J. R.; Vilar, R. Cyanide Sensing with Organic Dyes: Studies in Solution and on Nanostructured Al₂O₃ Surfaces. *Chem. - A Eur. J.* **2008**, *14* (10), 3006–3012. <https://doi.org/10.1002/chem.200700412>.
- (23) Zou, Q.; Tao, F.; Xu, Z.; Ding, Y.; Tian, Y.; Cui, Y. A New Dibenzothiophene-Based Dual-Channel Chemosensor for Cyanide with Aggregation Induced Emission. *Anal. Methods* **2019**, *11* (43), 5553–5561. <https://doi.org/10.1039/c9ay01806a>.
- (24) Padghan, S. D.; Wang, L. C.; Lin, W. C.; Hu, J. W.; Liu, W. C.; Chen, K. Y. Rational Design of an ICT-Based Chemodosimeter with Aggregation-Induced Emission for Colorimetric and Ratiometric Fluorescent Detection of Cyanide in a Wide PH Range. *ACS Omega* **2021**, *6* (8), 5287–5296. <https://doi.org/10.1021/acsomega.0c05409>.
- (25) Lee, K. S.; Kim, H. J.; Kim, G. H.; Shin, I.; Hong, J. I. Fluorescent Chemodosimeter for Selective Detection of Cyanide in Water. *Org. Lett.* **2008**, *10* (1), 49–51. <https://doi.org/10.1021/ol7025763>.
- (26) Tomasulo, M.; Sortino, S.; White, A. J. P.; Raymo, F. M. Chromogenic Oxazines for Cyanide Detection. *J. Org. Chem.* **2006**, *71* (2), 744–753. <https://doi.org/10.1021/jo052096r>.
- (27) García, F.; García, J. M.; García-Acosta, B.; Martínez-Mañez, R.; Sancenón, F.; Soto, J. Pyrylium-Containing Polymers as Sensory Materials for the Colorimetric Sensing of Cyanide in Water. *Chem. Commun.* **2005**, No. 22, 2790–2792. <https://doi.org/10.1039/b502374b>.
- (28) Yang, Y. K.; Tae, J. Acridinium Salt Based Fluorescent and Colorimetric Chemosensor for the Detection of Cyanide in Water. *Org. Lett.* **2006**, *8* (25), 5721–5723. <https://doi.org/10.1021/ol062323r>.
- (29) Sancenón, F.; Martínez-Mañez, R.; Soto, J. A Selective Chromogenic Reagent for Nitrate. *Angew. Chemie - Int. Ed.* **2002**, *41* (8), 1416–1419. [https://doi.org/10.1002/1521-3773\(20020415\)41:8<1416::AID-ANIE1416>3.0.CO;2-2](https://doi.org/10.1002/1521-3773(20020415)41:8<1416::AID-ANIE1416>3.0.CO;2-2).
- (30) Kim, Y. K.; Lee, Y. H.; Lee, H. Y.; Kim, M. K.; Cha, G. S.; Ahn, K. H. Molecular Recognition of Anions through Hydrogen Bonding Stabilization of Anion-Ionophore Adducts: A Novel Trifluoroacetophenone-Based Binding Motif. *Org. Lett.* **2003**, *5* (21), 4003–4006. <https://doi.org/10.1021/ol035624z>.
- (31) Sun, Y.; Liu, Y.; Chen, M.; Guo, W. A Novel Fluorescent and Chromogenic Probe for Cyanide Detection in Water Based on the Nucleophilic Addition of Cyanide to Imine

- Group. *Talanta* **2009**, *80* (2), 996–1000. <https://doi.org/10.1016/j.talanta.2009.08.026>.
- (32) Peng, L.; Wang, M.; Zhang, G.; Zhang, D.; Zhu, D. A Fluorescence Turn-on Detection of Cyanide in Aqueous Solution Based on the Aggregation-Induced Emission. *Org. Lett.* **2009**, *11* (9), 1943–1946. <https://doi.org/10.1021/ol900376r>.
- (33) Zelder, F. H.; Männel-Croisé, C. Recent Advances in the Colorimetric Detection of Cyanide. *Chimia (Aarau)*. **2009**, *63* (1–2), 58–62. <https://doi.org/10.2533/chimia.2009.58>.
- (34) Wang, F.; Wang, L.; Chen, X.; Yoon, J. Recent Progress in the Development of Fluorometric and Colorimetric Chemosensors for Detection of Cyanide Ions. *Chem. Soc. Rev.* **2014**, *43* (13), 4312–4324. <https://doi.org/10.1039/c4cs00008k>.
- (35) Pati, P. B. Organic Chemodosimeter for Cyanide: A Nucleophilic Approach. *Sensors Actuators, B Chem.* **2016**, *222*, 374–390. <https://doi.org/10.1016/j.snb.2015.08.044>.
- (36) Padghan, S. D.; Wang, C. Y.; Liu, W. C.; Sun, S. S.; Liu, K. M.; Chen, K. Y. A Naphthalene-Based Colorimetric and Fluorometric Dual-Channel Chemodosimeter for Sensing Cyanide in a Wide PH Range. *Dye. Pigment.* **2020**, *183* (August), 108724. <https://doi.org/10.1016/j.dyepig.2020.108724>.
- (37) Luo, J.; Xie, Z.; Xie, Z.; Lam, J. W. Y.; Cheng, L.; Chen, H.; Qiu, C.; Kwok, H. S.; Zhan, X.; Liu, Y.; Zhu, D.; Tang, B. Z. Aggregation-Induced Emission of 1-Methyl-1,2,3,4,5-Pentaphenylsilole. *Chem. Commun.* **2001**, *18*, 1740–1741. <https://doi.org/10.1039/b105159h>.
- (38) He, Z.; Ke, C.; Tang, B. Z. Journey of Aggregation-Induced Emission Research. *ACS Omega* **2018**, *3* (3), 3267–3277. <https://doi.org/10.1021/acsomega.8b00062>.
- (39) Hong, Y.; Lam, J. W. Y.; Tang, B. Z. Aggregation-Induced Emission: Phenomenon, Mechanism and Applications. *Chem. Commun.* **2009**, No. 29, 4332–4353. <https://doi.org/10.1039/b904665h>.
- (40) Hong, Y.; Lam, J. W. Y.; Tang, B. Z. Aggregation-Induced Emission. *Chem. Soc. Rev.* **2011**, *40* (11), 5361–5388. <https://doi.org/10.1039/c1cs15113d>.
- (41) Zhang, Y.; Li, D.; Li, Y.; Yu, J. Solvatochromic AIE Luminogens as Supersensitive Water Detectors in Organic Solvents and Highly Efficient Cyanide Chemosensors in Water. *Chem. Sci.* **2014**, *5* (7), 2710–2716. <https://doi.org/10.1039/c4sc00721b>.
- (42) Deng, K.; Wang, L.; Xia, Q.; Liu, R.; Qu, J. A Turn-on Fluorescent Chemosensor Based on Aggregation-Induced Emission for Cyanide Detection and Its Bioimaging Applications. *Sensors Actuators, B Chem.* **2019**, *296* (June), 126645. <https://doi.org/10.1016/j.snb.2019.126645>.

- (43) Chen, X.; Wang, L.; Yang, X.; Tang, L.; Zhou, Y.; Liu, R.; Qu, J. A New Aggregation-Induced Emission Active Fluorescent Probe for Sensitive Detection of Cyanide. *Sensors Actuators, B Chem.* **2017**, *241*, 1043–1049. <https://doi.org/10.1016/j.snb.2016.10.040>.
- (44) Chua, M. H.; Zhou, H.; Lin, T. T.; Wu, J.; Xu, J. Triphenylethylenyl-Based Donor-Acceptor-Donor Molecules: Studies on Structural and Optical Properties and AIE Properties for Cyanide Detection. *J. Mater. Chem. C* **2017**, *5* (46), 12194–12203. <https://doi.org/10.1039/c7tc04400c>.
- (45) Gao, M.; Tang, B. Z. Fluorescent Sensors Based on Aggregation-Induced Emission: Recent Advances and Perspectives. *ACS Sensors* **2017**, *2* (10), 1382–1399. <https://doi.org/10.1021/acssensors.7b00551>.
- (46) Huang, X.; Gu, X.; Zhang, G.; Zhang, D. A Highly Selective Fluorescence Turn-on Detection of Cyanide Based on the Aggregation of Tetraphenylethylene Molecules Induced by Chemical Reaction. *Chem. Commun.* **2012**, *48* (100), 12195–12197. <https://doi.org/10.1039/c2cc37094h>.
- (47) Mei, J.; Hong, Y.; Lam, J. W. Y.; Qin, A.; Tang, Y.; Tang, B. Z. Aggregation-Induced Emission: The Whole Is More Brilliant than the Parts. *Adv. Mater.* **2014**, *26* (31), 5429–5479. <https://doi.org/10.1002/adma.201401356>.
- (48) Yang, X.; Chen, X.; Lu, X.; Yan, C.; Xu, Y.; Hang, X.; Qu, J.; Liu, R. A Highly Selective and Sensitive Fluorescent Chemosensor for Detection of CN^- , SO_3^{2-} and Fe^{3+} Based on Aggregation-Induced Emission. *J. Mater. Chem. C* **2016**, *4* (2), 383–390. <https://doi.org/10.1039/c5tc02865e>.
- (49) Aljabri, M. D.; Jadhav, R. W.; Al Kobaisi, M.; Jones, L. A.; Bhosale, S. V.; Bhosale, S. V. Antenna-like Ring Structures via Self-Assembly of Octaphosphonate Tetraphenyl Porphyrin with Nucleobases. *ACS Omega* **2019**, *4* (7), 11408–11413. <https://doi.org/10.1021/acsomega.9b00909>.
- (50) Wang, C.; Li, Z. Molecular Conformation and Packing: Their Critical Roles in the Emission Performance of Mechanochromic Fluorescence Materials. *Mater. Chem. Front.* **2017**, *1* (11), 2174–2194. <https://doi.org/10.1039/c7qm00201g>.
- (51) Wang, L.; Liu, L.; Xu, B.; Tian, W. Recent Advances in Mechanism of AIE Mechanochromic Materials. *Chem. Res. Chinese Univ.* **2021**, *37* (1), 100–109. <https://doi.org/10.1007/s40242-021-0431-0>.
- (52) Zhu, H.; Zhang, S.; Yang, J.; Wu, M.; Wu, Q.; Liu, J.; Zhang, J.; Kong, L.; Yang, J. Tunable Aggregation-Induced Emission, Solid-State Fluorescence, and Mechanochromic Behaviors of Tetraphenylethylene-Based Luminophores by Slight

- Modulation of Substituent Structure. *J. Solid State Chem.* **2022**, *305* (September 2021), 122706. <https://doi.org/10.1016/j.jssc.2021.122706>.
- (53) Zhang, H.; Zhang, H.; Huang, G.; Li, B. S. Two Tetraphenylethene-Pyrene Isomers: Distinct Fluorescence and Mechanochromic Properties. *Dye. Pigment.* **2021**, *185*, 108947. <https://doi.org/10.1016/j.dyepig.2020.108947>.
- (54) Dong, Y. Q.; Lam, J. W. Y.; Tang, B. Z. Mechanochromic Luminescence of Aggregation-Induced Emission Luminogens. *J. Phys. Chem. Lett.* **2015**, *6* (17), 3429–3436. <https://doi.org/10.1021/acs.jpcllett.5b01090>.
- (55) Liu, J. J.; Yang, J.; Wang, J. L.; Chang, Z. F.; Li, B.; Song, W. T.; Zhao, Z.; Lou, X.; Dai, J.; Xia, F. Tetrathienylethene Based Red Aggregation-Enhanced Emission Probes: Super Red-Shifted Mechanochromic Behavior and Highly Photostable Cell Membrane Imaging. *Mater. Chem. Front.* **2018**, *2* (6), 1126–1136. <https://doi.org/10.1039/c8qm00008e>.
- (56) Todres, Z. V. Recent Advances in the Study of Mechanochromic Transitions of Organic Compounds. *J. Chem. Res.* **2004**, No. 2, 89–93. <https://doi.org/10.3184/030823404323000332>.
- (57) Rao, C. N. R.; Singh, S.; Senthilnathan, V. P. Spectroscopic Studies of Solute-Solvent Interactions. *Chem. Soc. Rev.* **1976**, *5*, 297–316. <https://doi.org/10.1039/CS9760500297>.
- (58) Reichardt, C. Solvatochromic Dyes as Solvent Polarity Indicators. *Chem. Rev.* **1994**, *94* (8), 2319–2358. <https://doi.org/10.1021/cr00032a005>.
- (59) Reichardt, C. Solvents and Solvent Effects: An Introduction. *Org. Process Res. Dev.* **2007**, *11* (1), 105–113. <https://doi.org/10.1021/op0680082>.
- (60) Chen, Y.; Lam, J. W. Y.; Kwok, R. T. K.; Liu, B.; Tang, B. Z. Aggregation-Induced Emission: Fundamental Understanding and Future Developments. *Mater. Horizons* **2019**, *6* (3), 428–433. <https://doi.org/10.1039/c8mh01331d>.
- (61) Cai X.; Liu, B. Aggregation induced Emission: recent advances in material and biomedical applications. *Angewandte Chemie International Edition*, **2020**. *59* (25), 9868–9886. <https://doi.org/10.1002/anie.202000845>.
- (62) Liu, B.; Tang, B. Z. Aggregation-Induced Emission: More Is Different. *Angew. Chemie - Int. Ed.* **2020**, *59* (25), 9788–9789. <https://doi.org/10.1002/anie.202005345>.
- (63) Singh, V.; Bhosale, R. Advances in Aggregation Induced Emission Materials in Biosensing and Imaging for Biomedical Applications-Part A; Progress in molecular biology and translationla Science, *Volume 1084*, **2021**.

-
- (64) Benesi, H. A.; Hildebrand, J. H. Spectrophotometry of Iodine with Aromatic Hydrocarbons. *J. Am. Chem. Soc.* **1949**, *71* (8), 2703–2707.
- (65) Kuntz, I. D.; Gasparro, F. P.; Johnston, M. D.; Taylor, R. P. Molecular Interactions and the Benesi-Hildebrand Equation. *J. Am. Chem. Soc.* **1968**, *90* (18), 4778–4781. <https://doi.org/10.1021/ja01020a004>.
- (66) Frisch, M. J.; Trucks, G. W.; Schlegel, H. B.; Scuseria, G. E.; Robb, M. A.; Cheeseman, J. R.; Scalmani, G.; Barone, V.; Mennucci, B.; Petersson, G. A.; Nakatsuji, H.; Caricato, M.; Li, X.; Hratchian, H. P.; Izmaylov, A. F.; Bloino, J.; Zheng, G.; Sonnenberg, J. L.; Hada, M.; Ehara, M.; Toyota, K.; Fukuda, R.; Hasegawa, J.; Ishida, M.; Nakajima, T.; Honda, Y.; Kitao, O.; Nakai, H.; Vreven, T.; Montgomery, J. A.; Peralta, J. E.; Ogliaro, F.; Bearpark, M.; Heyd, J. J.; Brothers, E.; Kudin, K. N.; Staroverov, V. N.; Kobayashi, R.; Normand, J.; Raghavachari, K.; Rendell, A.; Burant, J. C.; Iyengar, S. S.; Tomasi, J.; Cossi, M.; Rega, N.; Millam, J. M.; Klene, M.; Knox, J. E.; Cross, J. B.; Bakken, V.; Adamo, C.; Jaramillo, J.; Gomperts, R.; Stratmann, R. E.; Yazyev, O.; Austin, A. J.; Cammi, R.; Pomelli, C.; Ochterski, J. W.; Martin, R. L.; Morokuma, K.; Zakrzewski, V. G.; Voth, G. A.; Salvador, P.; Dannenberg, J. J.; Dapprich, S.; Daniels, A. D.; Farkas, Foresman, J. B.; Ortiz, J. V.; Cioslowski, J.; Fox, D. J. *Gaussian 09, Revision B.01. Gaussian 09, Revis. B.01, Gaussian, Inc., Wallingford CT 2009*, 1–20.
- (67) López, R. Capillary Surfaces with Free Boundary in a Wedge. *Adv. Math. (N. Y.)* **2014**, *262*, 476–483. <https://doi.org/10.1016/j.aim.2014.05.019>.
- (68) Allouche, A. Software News and Updates Gabedit — A Graphical User Interface for Computational Chemistry Softwares. *J. Comput. Chem.* **2012**, *32*, 174–182. <https://doi.org/10.1002/jcc>.

CHAPTER 5

CHAPTER 5

5.1 Introduction

A wide range of biological and physiological processes are governed by various cations and anions. Many efforts have been devoted by the researchers for studying and developing the fluorescent molecules for sensing application. One such organic fluorescent derivative was synthesized and used for selective and sensitive detection of fluoride [1]. Recently selective anion sensing and recognition has gained lot of attention and extended immense research widely in the field of supramolecular chemistry because anions play very crucial role in our daily life with regards to various physiological, biological and industrial process. Consequently, the anions can be very essential as well as can act dangerous/harmful pollutants. Therefore, detection and monitoring these species is actively focussed area of research [2].

Anion sensors have been introduced with simple hydrocarbons-based chromophores/fluorophores, with one or more charged or charge neutral recognition moieties. But now a days more advance research in anion species has focussed more on the development of specific and potent sensor that are highly selective towards the specific anion to detect anion in competing media in aqueous, environmental, biological and medical application [3] In addition, researchers have also identified the more economical sensors which can be synthesized via simple synthetic methods and by using less expensive starting materials. However, capability of absorbing and emitting nature of fluorophore at longer wavelength makes it more permissible to facilitate naked eye detection with long lived excited state and high quantum yield [4].

The fluorescent chemosensors comprises of optically signalling unit linked covalently to neutral receptor such as urea, phenols, pyrroles, imidazolium salt, triazole, azide, quinoxaline. [5,6,7]. Fluoride ion (F^-) is very important in dental health and in osteoporosis treatment, while the excessive ingestion results in urolithiosis and can also cause cancer therefore there is need

of developing the receptor system showing high selectivity and good sensitivity with rapid response to F^- ion. In addition, as mentioned earlier naked eye detection, specific receptor with low-cost development, along with application in real sample such as water analysis. The most common strategies that are involved in developing F^- ion sensor is based on three kinds of molecular interactions i.e., F^- induced deprotonation via hydrogen bond interaction [8], B-F complexation [9, 10, 11] and F^- mediated desilylation of Si-O/Si-C bonds [12-16]. Amongst all the three interaction B-F complexation and desilylation reaction has limitation with respect to its formation of different fluoroborates and excessive fluoride is needed to reach that particular signal respectively, sometimes it shows unsatisfactory response time [17,18].

So far fluorescent receptors based on hydrogen bond interactions have attracted attention of many researchers. Even after enormous research most of the hydrogen bonded F^- sensors shows poor selectivity as they sometimes represent interference from other anions such as AcO^- , $H_2PO_4^-$, CN^- , and OH^- ions [19, 20, 21]. Keeping aforementioned criteria for developing fluorescent receptor we designed colorimetric and fluorometric receptor 1-(p-tolyl)-4,9-dihydro-3Hpyrido[3,4-b]indole which shows remarkable fluorescence change with ratiometric changes in absorption and emission spectra upon addition of fluoride and cyanide. The molecules containing polarized N-H fragments are considered as a good hydrogen donor that can be used for sensing and recognition of analyte [22].

Our group have already worked on cyclic urea-based compound for selective detection of fluoride by using AIE active tetraphenylethene donor molecule [23]. Another naphthalenediimide molecule was developed by Bhosale *et al.* for fluoride sensing application [24]. Herein we have developed iodine-DMSO catalysed fluorescent molecule containing N-H bond. As described, most of the N-H bond containing molecules are highly selective towards F^- ion. Thus, by using the approach we utilized the molecule for fluorescent sensing fluoride anion. The molecule was synthesized successfully, characterized by 1H NMR, ^{13}C NMR,

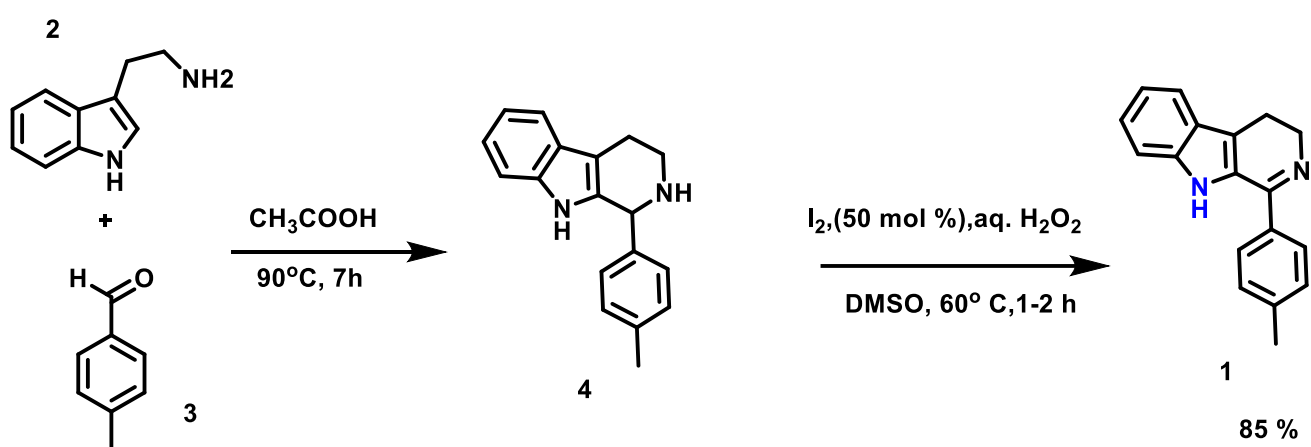
HRMS, followed by study of photophysical properties by UV Vis and fluorescence emission study.

5.2. Experimental

5.2.1. Methods and Materials

2-(1*H*-indol-3-yl)ethan-1-amine (tryptamine), 4-methylbenzaldehyde, Acetic acid, Dimethyl sulphoxide (DMSO) were purchased from TCI and Sigma Aldrich. Tetraethyl ammonium salts of all anions such as F⁻, Cl⁻, NO₃⁻, Br⁻, I⁻, SO₄²⁻, HPO₄²⁻, OAc⁻, tetraethyl ammonium cyanide (TEACN⁻). The compound **1** was successfully characterized on by ¹H NMR (400 MHz) and ¹³C NMR (100 MHz) Bruker spectrometer by using Tetramethylsilane (TMS) as an internal standard. A deuterated solvent DMSO-*d*₆ were used as solvent. Mass spectrometric data were obtained by high resolution mass spectrometer positive electron spray ionization (HRMS) technique on an Agilent Technologies 1100 Series (Agilent Chemstation Software) mass spectrometer. UV-vis absorption spectra were recorded by UV-vis-1800 Shimadzu spectrophotometer and fluorescence emission measured on RF-6000 (Shimadzu, Japan) Spectrofluorometer.

5.2.2. Synthetic route for synthesis of compound **1** 1-(*p*-tolyl)-4,9-dihydro-3*H*pyrido[3,4-*b*]indole



Scheme 5.1. Schematic pathway for synthesis of compound **1** 1-(*p*-tolyl)-4,9-dihydro-3*H*pyrido[3,4-*b*]indole.

The compound **4** was synthesized from the reported literature [24] by reacting 100mg of 2-(1*H*-indol-3-yl)ethan-1-amine (tryptamine) to react with 4-methylbenzaldehyde 100mg in presence of glacial acetic acid. the reaction was refluxed for 7 hours and temperature was maintained to 90° C. The obtained compound **4** was further filtered and purified by column chromatography. Further compound **4** undergoes oxidation under optimized condition using I₂ (50mol%), aq. H₂O₂, DMSO, 60°C, refluxed for 1-2 h to yield compound **1** the compound was purified by column chromatography and yellowish solid was obtained with Yield 85% yield. Further the compound was characterized by ¹H NMR, ¹³C NMR and HRMS.

5.3. Characterization

5.3.1. ¹H NMR spectra of receptor **1** 1-(p-tolyl)-4,9-dihydro-3*H*pyrido[3,4-*b*]indole

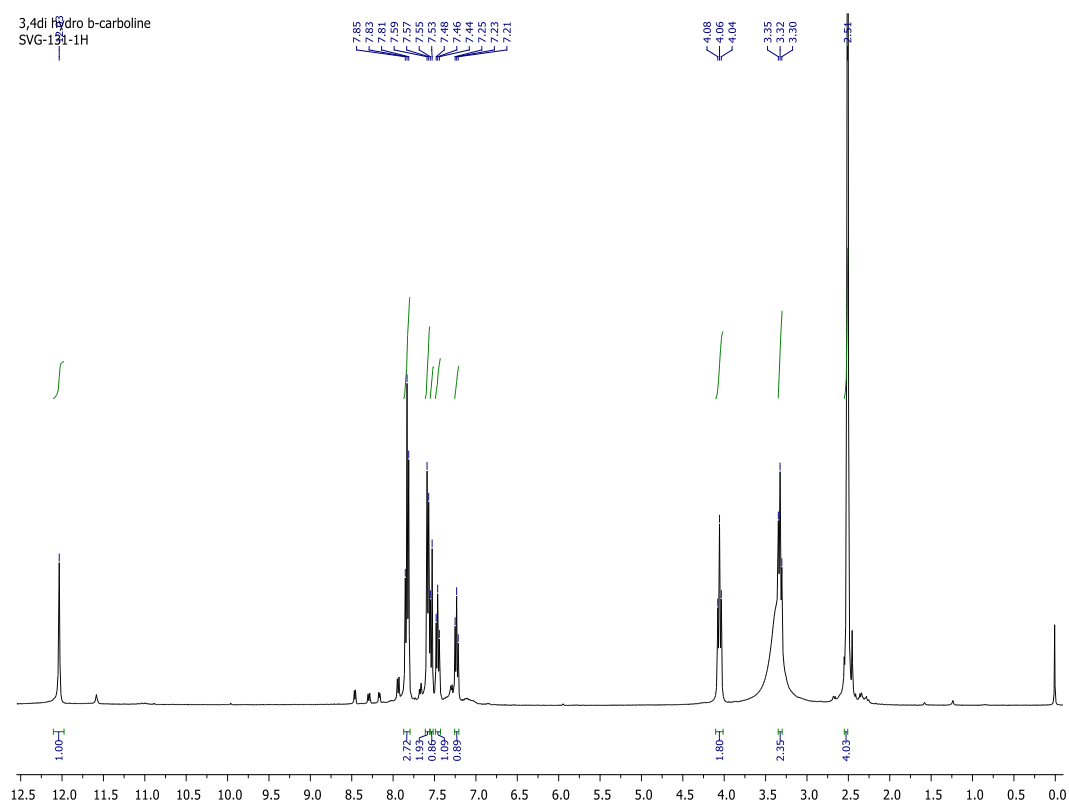


Figure 5.1. ¹H NMR spectra of receptor **1** 1-(p-tolyl)-4,9-dihydro-3*H*pyrido[3,4-*b*]indole.

5.3.2. ^{13}C NMR spectra of receptor **1** 1-(p-tolyl)-4,9-dihydro-3*H*pyrido[3,4-*b*]indole.

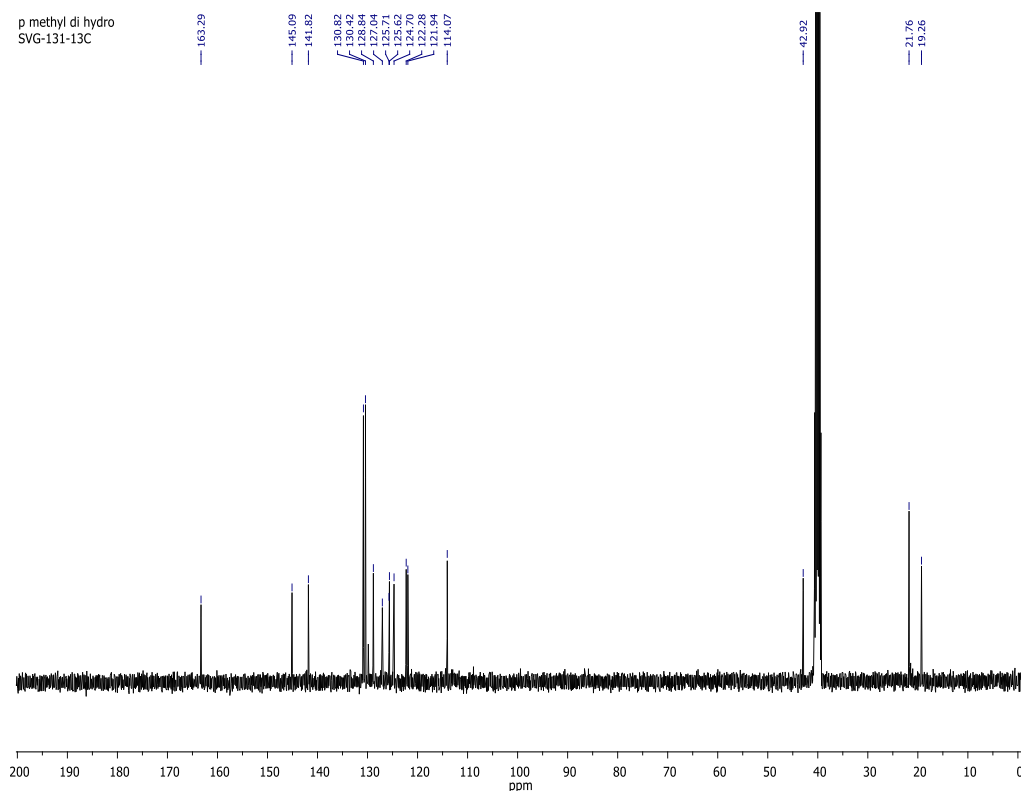


Figure 5.2. ^{13}C NMR spectra of receptor **1** (1-(p-tolyl)-4,9-dihydro-3*H*pyrido[3,4-*b*]indole).

5.3.3. HRMS positive mode for receptor **1** (1-(p-tolyl)-4,9-dihydro-3*H*pyrido[3,4-*b*]indole).

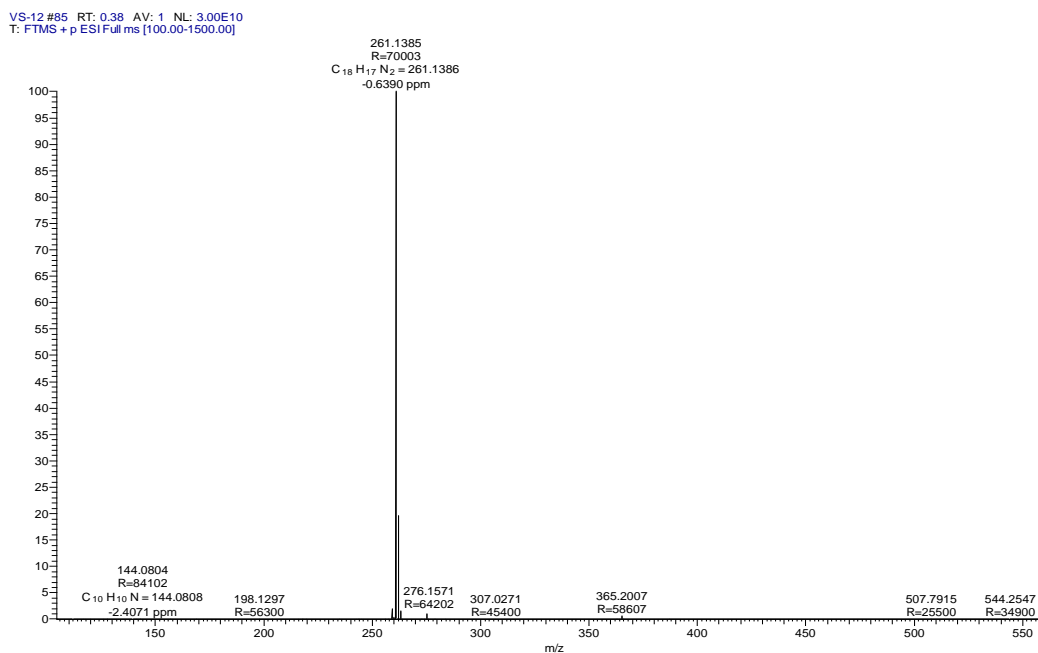


Figure 5.3. HRMS positive mode for receptor **1** 1-(p-tolyl)-4,9-dihydro-3*H*pyrido[3,4-*b*]indole.

5.4. Results and Discussion

5.4.1. Solvent Study

In chemistry solubility is important parameter to be considered whenever we start with the other experimental analysis. Solubility in various solvent and its effect of solvent on the resulting solute is very crucial and study of this effect on solute in presence of various solvent is called as “*solvatochromism*”. In other words, the solvatochromic effect can be define as the change in the spectrum of the solute when dissolved in various solvents. Thus, in solvatochromic effect hydrogen bonding capacity and dielectric constant of solute with solvent are considered important characteristics. This occurs mainly due to effect on the electronic ground and excited state of solute as the solvent changes which further results on the absorption and emission spectra of the solute. Due to this shape, intensity and position of the spectroscopic band appears in the spectrum with the change in the color. Therefore, we performed the solvatochromic effect study on receptor **1** in order to observe whether our molecule shows any spectral or color changes which can help to determine the suitable solvent for further analysis. The studies revealed that the molecule was highly soluble in organic solvent such as DMSO, ACN, THF, CHCl₃, MeOH, and H₂O. As can be seen from **Figure 5.4 a**. The receptor **1** showed following absorption and emission changes. It is noted from absorption spectra that DMSO exhibits intense absorption peak as 365nm and 300nm, while for other solvents the intensity was much lower than the DMSO. Further simultaneously we recorded the emission spectra as shown in **Figure 5.4 b**. and it is observed that CHCl₃ showed high intensity peak 530nm while in THF showed decrease in fluorescence intensity. In addition, MeOH and ACN showed decrease in fluorescence intensity along with light shift in emission wavelength at 550nm. The emission spectrum exhibited shift in the absorption with decrease in fluorescence intensity in DMSO solvent which is observed at 558 nm. But abrupt change in emission intensity as well as shift of absorption band towards shorter wavelength was observed when the receptor was

dissolved in water system. This indicates that the receptor shows solvatochromic effect and thus we predicted that ACN, DMSO and THF can be used for further analysis.

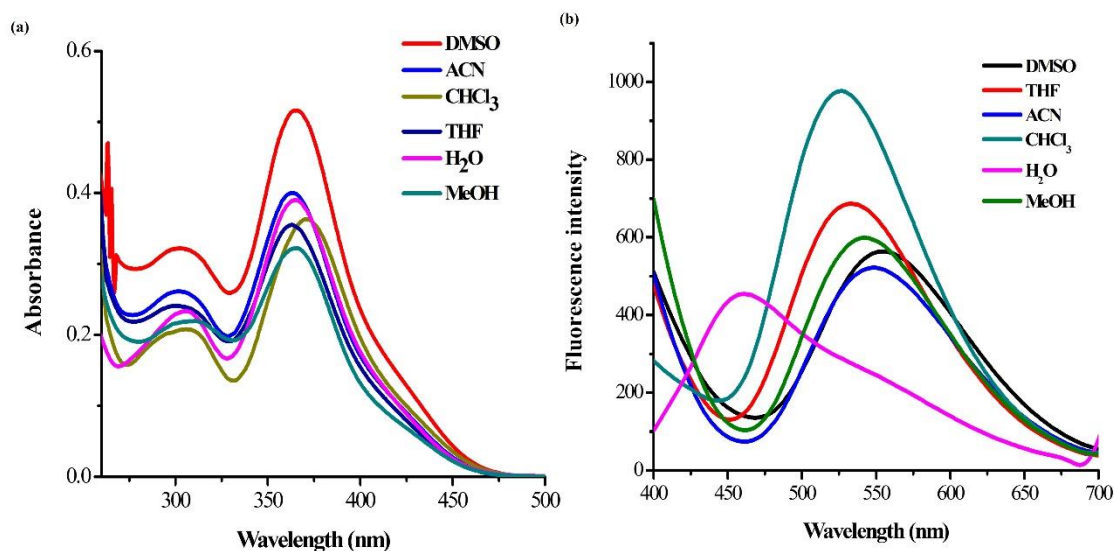


Figure 5.4. Solvatochromism study for receptor **1** in various solvents (a) Absorption spectra (b) Emission spectra

5.4.2. Sensing Performance

After solvent the receptor **1** was investigated for sensing of various anions such as F⁻, Cl⁻, NO₃⁻, Br⁻, I⁻, HSO₄⁻, HPO₄²⁻, OAC⁻, CN⁻. The ACN solvent was used for sensing performance. In the given **Figure 5.5.** below it can be concluded that receptor **1** showed high selectivity towards F⁻ in presence over other anions. The anions chosen for the study are tetra butyl ammonium salt except CN⁻ which is tetraethyl ammonium Cyanide (TEACN). This shows that the molecule was highly selective towards F⁻ anion and CN⁻ anion. For this sensing performance study 1mM stock solution of receptor was prepared and series of 50 μM of receptor **1** was taken in vial. In each vial 10 equivalent of each anion was added and it was observed that there was complete color change from yellow to colorless under visible light while when same solution with various anion were placed under UV light at 365 nm there was complete quenching of fluorescence observed with F⁻ and CN⁻. Further the same series of solution containing anions

were investigated on UV-Vis and fluorescence spectrometer.



Figure 5.5. Photograph exhibiting fluorescence color change with addition of Fluoride anion in presence over other anions such as (F^- , Cl^- , NO_3^- , Br^- , I^- , HSO_4^- , HPO_4^{2-} , OAc^- , CN^-) in solution containing receptor **1** 1-(p-tolyl)-4,9-dihydro-3Hpyrido[3,4-b]indole.

5.4.3. Absorption and fluorescence emission with various anions

The interaction of receptor **1** with various analyte (F^- , Cl^- , NO_3^- , Br^- , I^- , HSO_4^- , HPO_4^{2-} , OAc^- , CN^-) was investigated in ACN solvent by UV-Vis absorption spectroscopy. Various anions used for analysis were tetrabutyl ammonium salt. The absorption study showed that when 10 equivalents of anions were added only fluoride and cyanide showed shift in absorption while no change was observed with other anions. Initially for receptor **1** there are two absorption peaks appeared at 365 nm and 300 nm. When anions were added there is decrease in absorption intensity with shift of absorption intensity anions such as Cl^- , NO_3^- , Br^- , I^- , HSO_4^- , HPO_4^{2-} , OAc^- , while it is noted that the receptor **1** shows blue shift of the absorption from 365 nm to 320 nm. **Figure 5.6. (a)** This blue shift clearly shows that in presence over other anions only fluoride and CN^- shows prominent change and excellent selectivity. Further the emission properties of the receptor **1** was investigated. It is noted that the receptor **1** showed two emission peaks at 562 nm and 400 nm. When the solution of the receptor was reacted with various anions it is observed that the emission peak appearing at 562 nm disappeared completely with increasing emission intensity at 400 nm. As shown in **Figure. 5.6. (b)**

5.4.4. Absorption and Fluorescence titration Study for CN⁻ anion

To study its binding capacity titration was performed by addition of CN⁻ from 0 to 10 equiv. of analyte to receptor **1**. Nearly 0.001 M stock solution was prepared and from this 200 μ L solution of the receptor **1** was taken in 2 ml of acetonitrile solvent (1×10^{-4} M). Initially the absorption study was performed it was observed that when CN⁻ anion was added with incremental addition the absorption goes on decreasing with blue shift in absorption. From UV absorption plot it is very clear that the new isosbestic point is observed at 330 nm which indicates the formation new species. The reason may be due to the anion induced deprotonation reaction at the N-H group. The fluorescence study was performed simultaneously with incremental addition of CN⁻ **Figure 5.7. (a)**.

When the solution of the receptor **1** was subjected to emission study in absence and presence of various anions along with the incremental addition of CN⁻ with excitation wavelength at 360 nm. It is observed that with incremental addition of CN⁻ from 0 to 10 equivalent the peak appearing at 550 nm decreases with enhancement in the emission intensity at 400 nm. This occurs due to intramolecular charge transfer reaction between the NH and aromatic carboline system (N-H...A⁻). Thus, the clear shift of absorption towards blue shift indicates clearly deprotonation of proton of N-H group of the receptor **1**. The emission spectra as shown in **Figure 5.7. (b)**

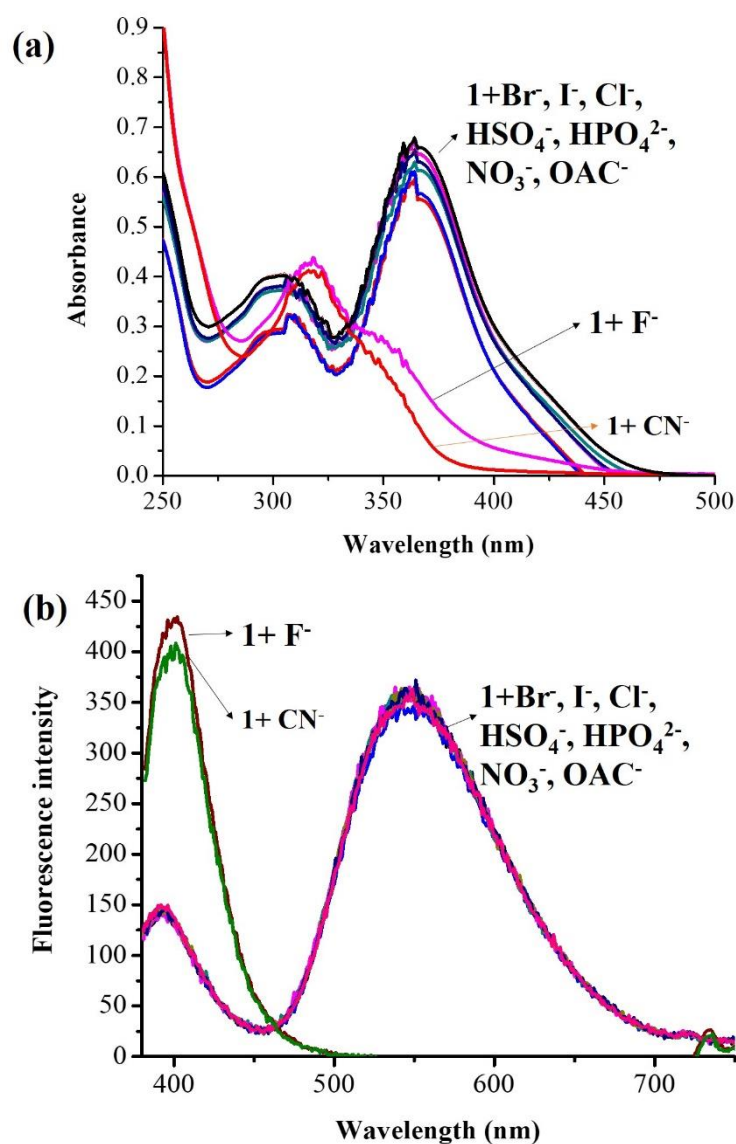


Figure 5.6. (a) The plot represents the absorption spectra in presence of various anions such as F^- , Cl^- , NO_3^- , Br^- , I^- , HSO_4^- , HPO_4^{2-} , OAc^- , CN^- . (b) Absorption titration performed for probe 1 with addition of 10 equivalent of fluoride anion.

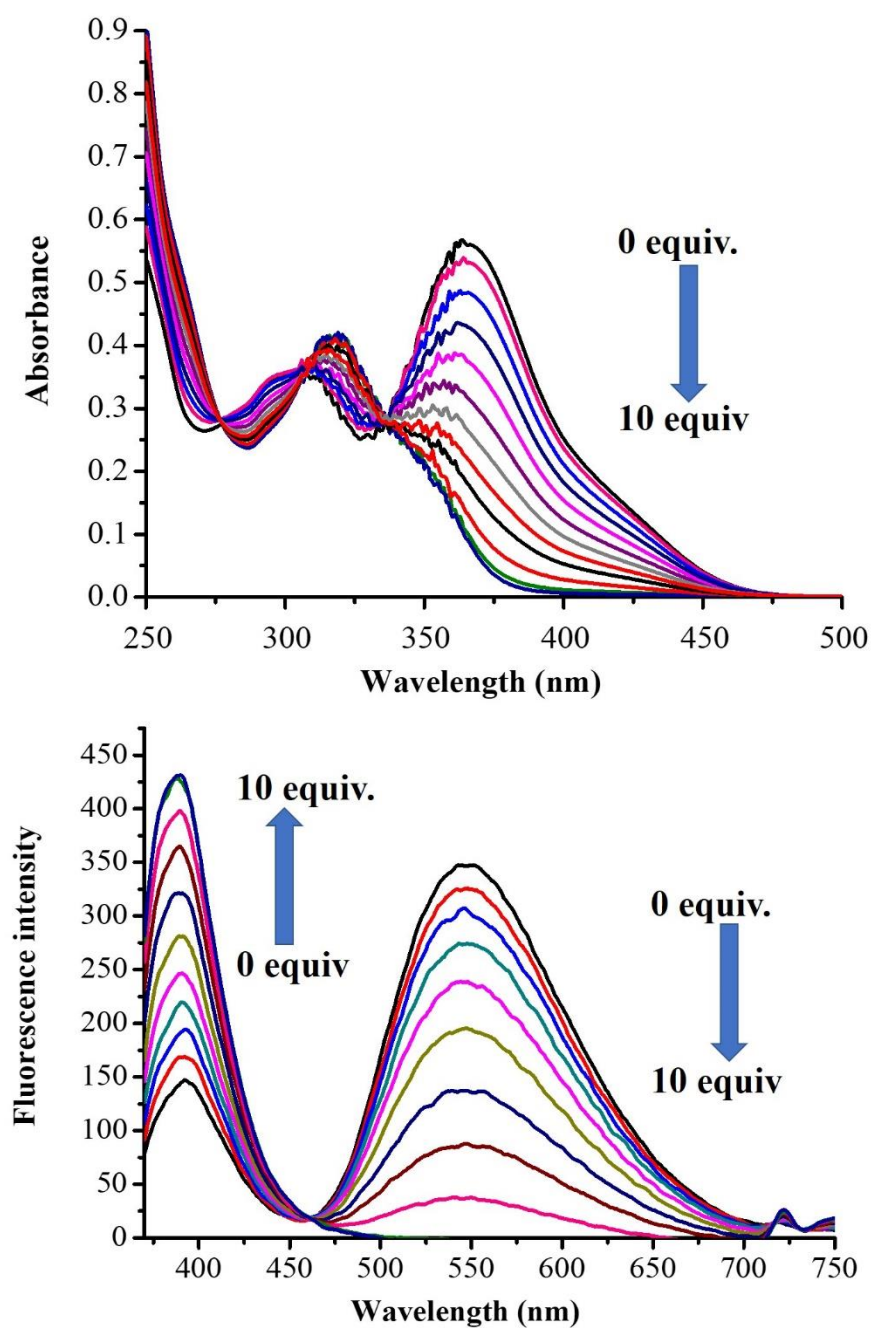


Figure 5.7. (a) Emission spectra recorded for the receptor **1** in presence various anions (b) Fluorescence titration performed for receptor **1** in presence of CN^- (0 to 10 equivalent).

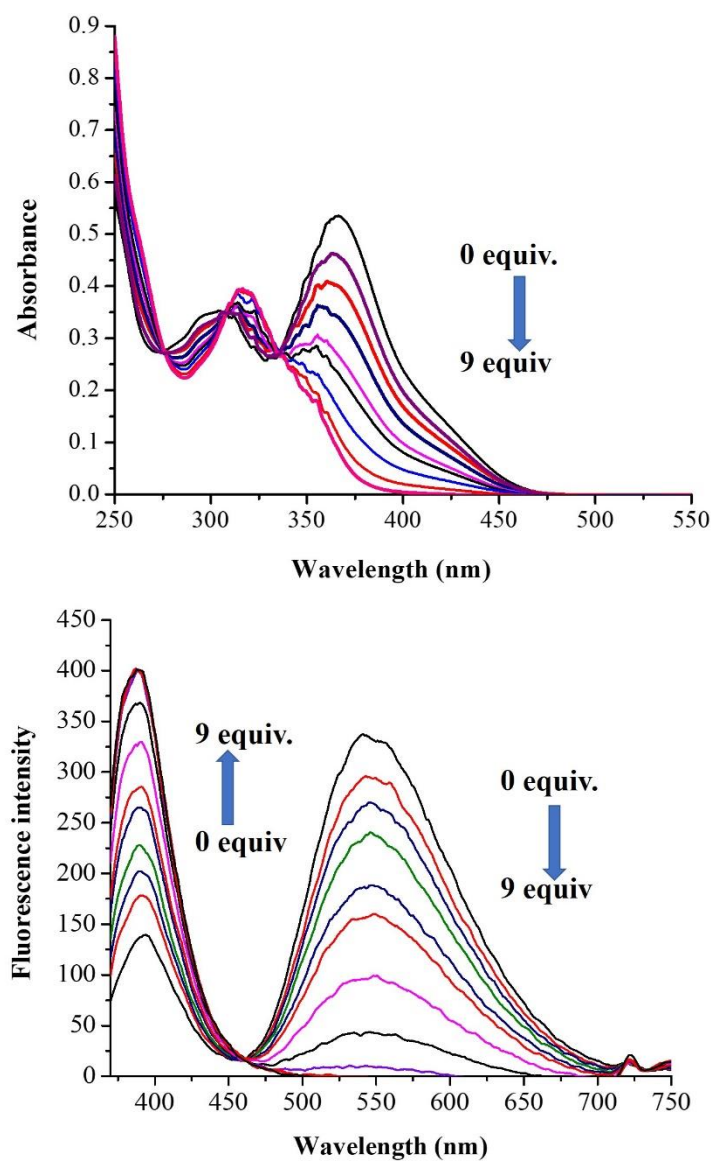
5.4.5. Absorption and Fluorescence titration study for F⁻ anion

Figure 5.8. (a) Emission spectra recorded for the receptor **1** in presence various anions (b) fluorescence titration performed for receptor **1** in presence of fluoride (0 to 2 equivalent).

Since the receptor **1** showed high selectivity towards CN⁻ and F⁻ further the molecule was investigated for fluoride anion. The absorption and emission study were performed with the incremental addition of F from 0 to 9 equiv⁻. The stock solution of (0.001M) was prepared and analyte solution is approximately 0.001M was prepared in ACN solvent. To the solution

containing receptor **1** (1×10^{-4} M) was taken and to that increasing amount of analyte F^- anion was added. It is observed that as the F^- anion is added quenching of fluorescence was at 550 nm with increasing fluorescence intensity at 400 nm. **Figure 5.8 (a)** represents the absorption spectra with incremental addition of F^- anion and **Figure 5.8. (b)** represents emission spectra with the incremental addition of CN^- .

5.5. Limit of detection for CN^-

The limit of detection was calculated by using ($LOD = 3\sigma/S$), where σ is the standard deviation of the blank sample and S is the absolute value of the slope between fluorescence emission intensity and concentration of CN^- of the probe **1** is 61.5 nM, which is very low as compared to the maximum permissible level of CN^- . According to the environmental protection agency and WHO the permissible limit of CN^- is (1.9 mM).

5.6. Limit of detection for F^-

The limit of detection was calculated by using ($LOD = 3\sigma/S$), where σ is the standard deviation of the blank sample and S is the absolute value of the slope between fluorescence emission intensity and concentration of F^- of the probe **1** is 75 nM, which is very low as compared to the maximum permissible level of F^- . According to the environmental protection agency and WHO the permissible limit of F^- 270 μ M.

5.7. Conclusion

In conclusion 1-(p-tolyl)-4,9-dihydro-3Hpyrido[3,4-*b*]indole was successfully synthesized and characterized by 1H NMR, ^{13}C NMR, HRMS. The molecule was utilized for sensing of F^- anion and CN^- anion. The molecule was further investigated for its photophysical properties by UV-Vis absorption, fluorescence emission properties. The fluorescent molecule was successfully utilized for sensing of F^- and CN^- in presence of various anions. The limit of detection was observed to be 61.5 nM for CN^- whereas for fluoride the detection limit was observed to be 75 nM. The complete work on the molecule will be continued in future.

5.8. References

- (1) Gale, P. A.; Caltagirone, C. Anion Sensing by Small Molecules and Molecular Ensembles. *Chem. Soc. Rev.* **2015**, *44* (13), 4212–4227. <https://doi.org/10.1039/c4cs00179f>.
- (2) Duke, R. M.; Veale, E. B.; Pfeffer, F. M.; Kruger, P. E.; Gunnlaugsson, T. Colorimetric and Fluorescent Anion Sensors: An Overview of Recent Developments in the Use of 1,8-Naphthalimide-Based Chemosensors. *Chem. Soc. Rev.* **2010**, *39* (10), 3936–3953. <https://doi.org/10.1039/b910560n>.
- (3) Busschaert, N.; Caltagirone, C.; Van Rossom, W.; Gale, P. A. Applications of Supramolecular Anion Recognition. *Chem. Rev.* **2015**, *115* (15), 8038–8155. <https://doi.org/10.1021/acs.chemrev.5b00099>.
- (4) Basu, A.; Dey, S. K.; Das, G. Amidothiourea Based Colorimetric Receptors for Basic Anions: Evidence of Anion Induced Deprotonation of Amide -NH Proton and Hydroxide Induced Anion $\cdots\pi$ Interaction with the Deprotonated Receptors. *RSC Adv.* **2013**, *3* (18), 6596–6605. <https://doi.org/10.1039/c3ra23123b>.
- (5) Nadimetla, D. N.; Zalmi, G. A.; Bhosale, S. V. An AIE-Active Tetraphenylethylene-Based Cyclic Urea as a Selective and Efficient Optical and Colorimetric Chemosensor for Fluoride Ions. *ChemistrySelect* **2020**, *5* (28), 8566–8571. <https://doi.org/10.1002/slct.202002126>.
- (6) Chen, X.; Liu, Y. C.; Bai, J.; Fang, H.; Wu, F. Y.; Xiao, Q. A “Turn-on” Fluorescent Probe Based on BODIPY Dyes for Highly Selective Detection of Fluoride Ions. *Dye. Pigment.* **2021**, *190* (January), 109347. <https://doi.org/10.1016/j.dyepig.2021.109347>.
- (7) Dey, S. K.; Al Kobaisi, M.; Bhosale, S. V. Functionalized Quinoxaline for Chromogenic and Fluorogenic Anion Sensing. *ChemistryOpen* **2018**, *7* (12), 934–952. <https://doi.org/10.1002/open.201800163>.
- (8) Zheng, X.; Zhu, W.; Liu, D.; Ai, H.; Huang, Y.; Lu, Z. Highly Selective Colorimetric/Fluorometric Dual-Channel Fluoride Ion Probe, and Its Capability of Differentiating Cancer Cells. *ACS Appl. Mater. Interfaces* **2014**, *6* (11), 7996–8000. <https://doi.org/10.1021/am501546h>.
- (9) Chen, C. H.; Gabbai, F. P. Exploiting the Strong Hydrogen Bond Donor Properties of a Borinic Acid Functionality for Fluoride Anion Recognition. *Angew. Chemie - Int. Ed.* **2018**, *57* (2), 521–525. <https://doi.org/10.1002/anie.201709494>.
- (10) Zhao, H.; Leamer, L. A.; Gabbai, F. P. Anion Capture and Sensing with Cationic

- Boranes: On the Synergy of Coulombic Effects and Onium Ion-Centred Lewis Acidity. *Dalt. Trans.* **2013**, 42 (23), 8164–8178. <https://doi.org/10.1039/c3dt50491c>.
- (11) Hirai, M.; Gabbai, F. P. Squeezing Fluoride out of Water with a Neutral Bidentate Antimony(V) Lewis Acid. *Angew. Chemie* **2015**, 127 (4), 1221–1225. <https://doi.org/10.1002/ange.201410085>.
- (12) Du, M.; Huo, B.; Liu, J.; Li, M.; Fang, L.; Yang, Y. A Near-Infrared Fluorescent Probe for Selective and Quantitative Detection of Fluoride Ions Based on Si-Rhodamine. *Anal. Chim. Acta* **2018**, 1030, 172–182. <https://doi.org/10.1016/j.aca.2018.05.013>.
- (13) Roy, A.; Kand, D.; Saha, T.; Talukdar, P. A Cascade Reaction Based Fluorescent Probe for Rapid and Selective Fluoride Ion Detection. *Chem. Commun.* **2014**, 50 (41), 5510–5513. <https://doi.org/10.1039/c4cc01665c>.
- (14) Cao, J.; Zhao, C.; Zhu, W. A Near-Infrared Fluorescence Chemodosimeter for Fluoride via Specific Si-O Cleavage. *Tetrahedron Lett.* **2012**, 53 (16), 2107–2110. <https://doi.org/10.1016/j.tetlet.2012.02.051>.
- (15) Yang, Q.; Jia, C.; Chen, Q.; Du, W.; Wang, Y.; Zhang, Q. A NIR Fluorescent Probe for the Detection of Fluoride Ions and Its Application in in Vivo Bioimaging. *J. Mater. Chem. B* **2017**, 5 (10), 2002–2009. <https://doi.org/10.1039/C6TB03193E>.
- (16) Zhang, J. F.; Lim, C. S.; Bhuniya, S.; Cho, B. R.; Kim, J. S. A Highly Selective Colorimetric and Ratiometric Two-Photon Fluorescent Probe for Fluoride Ion Detection. *Org. Lett.* **2011**, 13 (5), 1190–1193. <https://doi.org/10.1021/ol200072e>.
- (17) Han, J.; Zhang, J.; Gao, M.; Hao, H.; Xu, X. Recent Advances in Chromo-Fluorogenic Probes for Fluoride Detection. *Dye. Pigment.* **2019**, 162, 412–439. <https://doi.org/10.1016/j.dyepig.2018.10.047>.
- (18) Qi, Y.; Cao, X.; Zou, Y.; Yang, C. Multi-Resonance Organoboron-Based Fluorescent Probe for Ultra-Sensitive, Selective and Reversible Detection of Fluoride Ions. *J. Mater. Chem. C* **2021**, 9 (5), 1567–1571. <https://doi.org/10.1039/d0tc05496h>.
- (19) Bhosale, S. V.; Bhosale, S. V.; Kalyankar, M. B.; Langford, S. J. A Core-Substituted Naphthalene Diimide Fluoride Sensor. *Org. Lett.* **2009**, 11 (23), 5418–5421. <https://doi.org/10.1021/ol9022722>.
- (20) Zhu, H.; Huang, J.; Zhou, Q.; Lv, Z.; Li, C.; Hu, G. Enhanced Luminescence of NH₂-UiO-66 for Selectively Sensing Fluoride Anion in Water Medium. *J. Lumin.* **2019**, 208 (December 2018), 67–74. <https://doi.org/10.1016/j.jlumin.2018.12.007>.
- (21) Chowdhury, A. R.; Ghosh, P.; Roy, B. G.; Mukhopadhyay, S. K.; Murmu, N. C.; Banerjee, P. Cell Permeable Fluorescent Colorimetric Schiff Base Chemoreceptor for

-
- Detecting F⁻ in Aqueous Solvent. *Sensors Actuators, B Chem.* **2015**, 220, 347–355. <https://doi.org/10.1016/j.snb.2015.05.044>.
- (22) Suman, G. R.; Pandey, M.; Chakravarthy, A. S. J. Review on New Horizons of Aggregation Induced Emission: From Design to Development. *Mater. Chem. Front.* **2021**, 5 (4), 1541–1584. <https://doi.org/10.1039/d0qm00825g>.
- (23) Gaikwad, S. V; Nadimetla, D. N.; Kobaisi, A.; Devkate, M. Iodine-DMSO-Catalyzed Chemoselective Biomimetic Aromatization of Tetrahydro- β -Carbolines-3-Carboxylic Acid: Mechanism Study with DFT-Calculation. **2019**, No. Figure 2, 10054–10059. <https://doi.org/10.1002/slct.201902419>.
- (24) Ali, R.; Dwivedi, S. K.; Mishra, H.; Misra, A. Dyes and Pigments Imidazole-Coumarin Containing D – A Type Fluorescent Probe: Synthesis Photophysical Properties and Sensing Behavior for F⁻ and CN⁻ Anion. *Dye. Pigment.* **2020**, 175 (December 2019), 108163. <https://doi.org/10.1016/j.dyepig.2019.108163>.

Chapter 6

Chapter 6

6.1 Conclusion

In conclusion there are number of organic fluorescent molecules which have been successfully synthesized and characterized. The fluorescent sensors are the powerful analytical tool for studying the various analyte in biological processes. The fluorescent material plays various roles in biology, environment and scientific development. The fluorescent molecules have extended its wide application in sensing, food and drug industry, forensic science, biological cell imaging application, drug delivery system and fluorescent material can be used in optical light emitting diode. Overall thesis covers the different organic fluorescent molecules that can be used for sensing of various cations such as Fe^{3+} , Cu^{2+} ions and anions such as F^- , CN^- . The synthesized molecules were successfully characterized by various instrumental techniques such as ^1H NMR, ^{13}C NMR, ESI-MS, Elemental analysis, Single Crystal XRD, UV-Vis Spectrophotometer and Fluorescence Spectrophotometer and by theoretical calculations DFT. The binding of the receptor was well characterized by density functional theoretical calculations. Chapter 1 represents use of fluorescent molecules in sensing of cations, anions and neutral molecule. In addition fluorescent molecule can be also used for sensing of pH, temperature and intracellular viscosity sensing.

In Chapter 2 the molecule **DFPDA 1** was successfully synthesized and characterized by ^1H NMR, ^{13}C NMR, ESI- Mass, elemental analysis, single crystal XRD, UV-Vis spectrophotometry and fluorescence spectrometry. The molecule was further employed for fluorescent sensing of metal ions. The DFPDA 1 is highly sensitive and selective to Fe^{3+} metal ion in presence over other ions such as Cu^{2+} , K^+ , Cd^{2+} , Co^{2+} , Mn^{2+} , Ni^{2+} , Ba^{2+} , Hg^{2+} , Al^{3+} , Pb^{2+} , Zn^{2+} , Ca^{2+} , Fe^{2+} salts. The synthesized **DFPDA 1** showed lowest detection limit (LOD) of 52 nM. However, the stoichiometry of the complex formed between **DFPDA 1** and metal

ion (1: Fe³⁺) is 2:1. The compound **4** and the **DFPDA 1** was crystallized in methanol/chloroform by diffusion method and characterized by SXRD. The reusability and reversibility study were performed by using simple NaOH base, and found to be reversible for 3 cycles resulting in to formation of Fe (OH)₃. Thus, we conclude that the molecule shows reversible nature and is highly selective and sensitive towards Fe⁺³.

In chapter 3 the molecule **DTBPA 1** was synthesized by two steps via aldol condensation and second step by Michael addition of pyridine salt. The intermediate formed was further reacted to give DTBPA 1 by Krohnke pyridine synthesis where pyridine was formed by insitu reaction in presence of ammonium hydroxide ammonium acetate and acetic acid under refluxing condition. Further molecule was purified column chromatography and characterized successfully by ¹H NMR, ¹³C NMR, elemental analysis, single crystal XRD, ESI mass spectrometry. After characterization the molecule was investigated for its photophysical properties in which the molecule was completely analysed by using UV-Vis and fluorescence spectroscopy. The reported the fluorescent **DTBPA 1** molecule was applied for sensing application. The molecule showed good response towards Cu²⁺ ion in a solution in presence of various cations. Further to study the interaction of molecule to Cu²⁺ theoretically the DFT calculation were performed by using ab initio gaussian software Gaussian 16 *ab initio*/DFT quantum chemical simulation. The fluorescent sensor reached lower detection limit of 0.789µM very low given by environmental protection agency. The developed molecule was successfully utilized for determination of copper in water sample which showed good recovery percentage of 98% to 104% .

In conclusion chapter 4 ethyl-2-cyano-3-(5-(4-(1,2,2-triphenylvinyl)phenyl)thiophen-2-yl)acrylate (**1**) probe **1** was successfully synthesized and employed for sensing of anions. The probe 1 showed to excellent colorimetric and fluorescent receptor for sensing of CN⁻ anion in presence over various competing anions such as Cl⁻, I⁻, F⁻, Br⁻, HSO₄⁻, H₂PO₄⁻, NO₃⁻, HCO₃⁻,

and ClO_4^- in DMSO solvent. The synthesized probe was highly selective and sensitive towards CN^- ion. The limit of detection (LOD) for probe **1** was found to be 67 nM. Further probe **1** was employed for real practical application in strip sensing, biological cell imaging, and food analysis application for determination of cyanide ion. This result shows that the probe was highly selective and sensitive towards CN^- anion as well as can be successfully employed for real world application in food analysis as well as in live cell imaging.

Chapter 5 includes the synthesis and characterization of 1-(p-tolyl)-4,9-dihydro-3Hpyrido[3,4-b]indole. The molecule was successfully synthesized and characterized by ^1H NMR, ^{13}C NMR HRMS mass spectrometry. The molecule was utilized for sensing of F^- anion and CN^- anion. The photophysical properties by UV-Vis absorption, Fluorescence emission was investigated. The fluorescent molecule was successfully utilized for sensing of F^- and CN^- in presence of various anions. The limit of detection was observed to be 61.5 nM for CN^- whereas for Fluoride the detection limit was observed to be 75 nM. Still the experimental work on the molecule will be continued.

In conclusion overall thesis describes different small organic fluorescent molecule for sensing of various analytes such as essential, non-essentials elements, toxic cation, anion, biomolecule/neutral molecule sensing. Thesis also covers the brief strategies for synthesis of organic fluorescent molecule for sensing various parameters such as pH, temperature and viscosity of biological cell intracellularly. Therefore, synthesis of organic fluorescent molecule is of great interest and very important in various field of Science and Technology. Now a days there is need of developing and designing such organic fluorescent molecules in order to detect the toxic pollutants and further to undergo remediation. In the name of industrialization and development there is extreme toxication and pollution observed in to the environment in turn harming various biological system, polluting the various water bodies, resulting in to harmful effect on ecosystem, animal and major impact on human health.

Therefore, there is need of developing simple, easy, cost effective and handheld method for detecting these toxic pollutants. Although there are various techniques for detection of toxic contaminant but due to their high sophistication and high cost limits its application. Thus, fluorescent molecule plays significant role in detection of toxic pollutants. As the fluorescent method of sensing is simple, easy synthesis, naked eye detection, hand held method, cost effective, high selectivity and high sensitivity. The organic fluorescent molecules are not only useful for sensing of toxic pollutant or essential elements but it plays significant role in theranostic application in drug delivery, cancer cell study. In future much more applications can be explored by the use of organic fluorescent molecule in to the field of Supramolecular Chemistry.

Appendix

List of publications

Appended to thesis

- (1) **Zalmi, G. A.**; Nadimetla, D. N.; Kotharkar, P.; Puyad, A. L.; Kowshik, M.; Bhosale, S. V. Aggregation-Induced Emission-Based Material for Selective and Sensitive Recognition of Cyanide Anions in Solution and Biological Assays. *ACS Omega* **2021**, *6* (26), 16704–16713. <https://doi.org/10.1021/acsomega.0c06080>.
- (2) **Zalmi, G. A.**; Nadimetla, D. N.; Harmalkar, S. S.; Narvekar, K. U.; Bhosale, S. V. A Receptor Based on Diphenylaniline Donor Connected with Difuran and Pyridine as Acceptors: Synthesis, Crystal Structure and Selective Detection of Iron Ion. *ChemistrySelect* **2022**, *7* (33). <https://doi.org/10.1002/slct.202202276>.
- (3) **Zalmi, G. A.**; Jadhav, R. W.; Mirgane, H. A.; Bhosale, S. V. Recent Advances in Aggregation-Induced Emission Active Materials for Sensing of Biologically Important Molecules and Drug Delivery System. *Molecules* **2022**, *27* (1). <https://doi.org/10.3390/molecules27010150>.
- (4) **Zalmi, G. A.**; Gawade, V. K.; Nadimetla, D. N.; Bhosale, S. V. Aggregation Induced Emissive Luminogens for Sensing of Toxic Elements. *ChemistryOpen* **2021**, *10* (7), 681–696. <https://doi.org/10.1002/open.202100082>.

Other publications

- (1) Nadimetla, D. N.; **Zalmi, G. A.**; Bhosale, S. V. An AIE-Active Tetraphenylethylene-Based Cyclic Urea as a Selective and Efficient Optical and Colorimetric Chemosensor for Fluoride Ions. *ChemistrySelect* **2020**, 5 (28), 8566–8571. <https://doi.org/10.1002/slct.202002126>.
- (2) **Zalmi, G. A.**; Jadhav, S. E.; Mirgane, H. A.; Madje, B. R.; Bhosale, S. V. A Phenolic Schiff Based AIE-Active Quinoxaline-Based Receptor for Selective Sensing of Fluoride Ions. *ChemistrySelect* **2023**, 8 (5). <https://doi.org/10.1002/slct.202203380>.
- (3) More, V. G.; Nadimetla, D. N.; **Zalmi, G. A.**; Gawade, V. K.; Jadhav, R. W.; Mane, Y. D.; Bhosale, S. V. A New "Off-on" system Based on Core-Substituted Naphthalene Diimide with Dimethylamine for Reversible Acid-Base Sensing. *ChemistryOpen* **2022**, 11 (5). <https://doi.org/10.1002/open.202200060>.

Manuscript under preparation

1. **Zalmi, G. A.**; Gaikwad S. and Bhosale, S. V. "Indole based fluorescent molecule for sensing of fluoride and cyanide anion". *Manuscript under preparation*

Manuscript Communicated

1. **Zalmi, G. A.**; Puyad, A.; and Bhosale, S. V. "AIE active molecules for selective Cu²⁺ detections".

Book chapter

1. Zalimi G.A., Bhosale S.V. Aggregation Induced Emission (AIE) molecules for measurement intracellular pH, temperature and viscosity sensing. *Progress in Molecular biology and Translational Science*, Elsevier, 2021, 184, 1877-1173, doi: <https://doi.org/10.1016/bs.pmbts.2021.07.004>
2. Optical Sensors for Glucose Sensing.
Zalimi, G. A.; Mirgane, H. A.; Bhosale, S. V. (Accepted in Nova Publisher)

Participation and presentation at National & International conferences

1. Participated in three days workshop on “X-rays Crystallography” held on 21st - 23rd July 2022 organized by School of Chemical Sciences and School of Physical and Applied Sciences, Goa University, Goa
2. Participated and Secured first place in One Day Virtual National Conference on “*Role of Women Chemists and Technologists for Sustainable Future*” held on 8th March 2022 on the occasion of International Women’s Day, organized by The Department of Chemistry (Research Centre) in association with Rotary Club of Miramar, Panji, Goa.
3. Participated and Secured 3rd place in Oral Presentation in 2 days virtual international conference organized by Dyanprassarak Mandal’s College and Research Centre with Syngenta Biosciences Private Limited on “Advances in Green Chemistry and sustainable Technology”
4. Participated in 2 days workshop on Material Science between University of Porto, University of Coimbra and Goa University organized by Directorate of International Cooperation and Exchange (DICE) and Directorate of Research Mobilization (DRDRM) held on November 18th and 19th at Goa University

-
5. Participated in oral presentation at National Conference (Virtual) on “Nanomaterials for Environmental Applications” organised by Post Graduate Department of Chemistry, P.E. S’s R.S.N. College of Arts and Science Farmagudi Ponda Goa 28th and 29th December 2020.
 6. Participated in 3 days International conference on Aggregation Induced Emission from Fundamental to Application and recognized as best oral presenter award from ACS Omega organized by Department of Chemistry and BITS Pilani University, BITS Pilani K.K Birla Goa Campus, India on December 16th to 18th 2022